

Fall 2012

Synthesis of Bicyclic Thieno[2,3-d]Pyrimidines, Tricyclic Thieno[2,3-d]Pyrimidines and Thieno[3,2-d]Pyrimidines as Classical and Nonclassical Antifolates

Xilin Zhou

Follow this and additional works at: <https://dsc.duq.edu/etd>

Recommended Citation

Zhou, X. (2012). Synthesis of Bicyclic Thieno[2,3-d]Pyrimidines, Tricyclic Thieno[2,3-d]Pyrimidines and Thieno[3,2-d]Pyrimidines as Classical and Nonclassical Antifolates (Master's thesis, Duquesne University). Retrieved from <https://dsc.duq.edu/etd/1413>

This Immediate Access is brought to you for free and open access by Duquesne Scholarship Collection. It has been accepted for inclusion in Electronic Theses and Dissertations by an authorized administrator of Duquesne Scholarship Collection. For more information, please contact phillips@duq.edu.

SYNTHESIS OF BICYCLIC THIENO[2,3-*d*]PYRIMIDINES, TRICYCLIC
THIENO[2,3-*d*]PYRIMIDINES AND THIENO[3,2-*d*]PYRIMIDINES AS CLASSICAL
AND NONCLASSICAL ANTIFOLATES

A Thesis

Submitted to the Mylan School of Pharmacy

Duquesne University

In partial fulfillment of the requirements for
the degree of Master of Science

By

Xilin Zhou

December 2012

SYNTHESIS OF BICYCLIC THIENO[2,3-*d*]PYRIMIDINES, TRICYCLIC
THIENO[2,3-*d*]PYRIMIDINES AND THIENO[3,2-*d*]PYRIMIDINES AS CLASSICAL
AND NONCLASSICAL ANTIFOLATES

By

Xilin Zhou

Approved September 6, 2012

Aleem Gangjee, Ph. D.
Professor of Medicinal Chemistry
(Committee Chair)

Patrick T. Flaherty, Ph. D.
Associate Professor of Medicinal
Chemistry
(Committee Member)

David J. Lapinsky, Ph.D.
Assistant Professor of Medicinal
Chemistry
(Committee Member)

Douglas J. Bricker, Ph.D.
Dean, Mylan School of Pharmacy
Associate Professor of Pharmacology

ABSTRACT

SYNTHESIS OF BICYCLIC THIENO[2,3-*d*]PYRIMIDINES, TRICYCLIC THIENO[2,3-*d*]PYRIMIDINES AND THIENO[3,2-*d*]PYRIMIDINES AS CLASSICAL AND NONCLASSICAL ANTIFOLATES

By

Xilin Zhou

December 2012

Thesis Supervised by Dr. Aleem Gangjee, PhD

An introduction, background and research progress in the areas of antifolates and antimetabolic agents has been reviewed and discussed. Thymidylate synthase (TS), dihydrofolate reductase (DHFR) and glycinamide ribonucleotide formyltransferase (GARFTase) are important folate dependent enzymes that are targets for cancer chemotherapy and the treatment of infectious diseases. As a part of this study, thirty-five novel compounds were designed and synthesized on the basis of existing clinically active compounds and their crystal structures. These compounds were synthesized and evaluated as single and/or multiple targeted classical and nonclassical antifolates to decrease toxicity and improve the antitumor activity and selectivity of existing therapeutic agents.

In addition, bicyclic substituted thieno[2,3-d]- and theino[3,2-d]pyrimidines were synthesized as antimitotic agents. These compounds allowed potent inhibition of tumor cells in culture and extended the structure-activity relationship in the antimitotic area.

TABLE OF CONTENTS

	Page
Abstract	iv
List of Figures	vii
List of Schemes	x
List of Tables	xii
List of Abbreviations	xiv
I. Biochemical Review	1
II. Chemical Review	46
III. Statement of the Problem	71
IV. Chemical Discussion	103
V. Summary	138
VI. Experimental	144
VII. Bibliography	203
Appendix	258

LIST OF FIGURES

	Page
Figure 1. Chemical structure of folic acid	1
Figure 2. The reduction pathway of folic acid	2
Figure 3. The <i>de novo</i> synthesis of dTMP from dUMP	2
Figure 4. The <i>de novo</i> synthesis of purines	4
Figure 5. Representative examples of classical antifolates and their principal target(s)	6
Figure 6. Representative examples of nonclassical antifolates and their principal target	7
Figure 7. Proposed catalytic mechanism of human TS. (Adapted from Ref. 59)	11
Figure 8. X-ray crystal structure of <i>E. coli</i> TS with inhibitor PDDF (CB3717)	13
Figure 9. The structures of 5-FU and FdUMP	15
Figure 10. The structure of PDDF (CB3717) and its analogues	16
Figure 11. The structure of Raltitrexed (ZD1694)	17
Figure 12. The structure of 10 (ZD9331)	18
Figure 13. The structure of 11 and 12	19
Figure 14. The structures of DDATHF and pemetrexed	19
Figure 15. The structures of 13-17	20
Figure 16. The structure of 18	21
Figure 17. The structures of 19-22	22
Figure 18. The structure of BW1843 (OSI-7904)	22
Figure 19. The structure of 23	23
Figure 20. The structure of 24-27	24
Figure 21. The structures of 28-31	25
Figure 22. Proposed catalytic mechanism of DHFR	26
Figure 23. Pyrrolo [2,3- <i>d</i>]pyrimidine analogues 32 and 33	29
Figure 24. Pyrrolo [2,3- <i>d</i>]pyrimidine analogues 34-41	30
Figure 25. Pyrrolo[2,3- <i>d</i>]pyrimidine analogue 42	30
Figure 26. The structures of 43-51	31

Figure 27.	The structures of Pyrimethamine, Methoprin and DAMP	34
Figure 28.	The structures of MZPES and Methylbenzoprim	34
Figure 29.	The structures of TMQ and 55-57	35
Figure 30.	Tetrahydroquinazoline analogues 58-60	35
Figure 31.	The structure of PTX and 61 and 62	36
Figure 32.	Pyrrolo and thieno[2,3- <i>d</i>]pyrimidine analogues 63-66	36
Figure 33.	Furo[2,3- <i>d</i>]pyrimidine analogues 67-69	37
Figure 34.	Tricyclic thieno and furo[2,3- <i>d</i>]pyrimidines 70-73 and 74-78	38
Figure 35.	Tricyclic DHFR inhibitors 79-82	38
Figure 36.	Mechanism of polyglutamylation by FPGS	40
Figure 37.	Proposed mechanism of GARFTase	41
Figure 38.	The structure of DDATHF	43
Figure 39.	The structure of 89	43
Figure 40.	The structure of 90	44
Figure 41.	The structure of 91 and 92	44
Figure 42.	The structure of 93	45
Figure 43.	Structures of antifolates	71
Figure 44.	Superimposition of a 6-5 thieno[2,3- <i>d</i>]pyrimidine ring system (red) on to a 6-5 pyrrolo[2,3- <i>d</i>]pyrimidine ring system (gray)	73
Figure 45.	Antifolates	77
Figure 46.	Stereoview compound 297 superimposed on pemetrexed (not shown) in human TS (PDB1JU6395), indicating the interaction of the 6-CH ₃ with Trp109	79
Figure 47.	Target classical antifolates with the tricyclic benzo[4,5]thieno[2,3- <i>d</i>]pyrimidine scaffold	80
Figure 48.	Superimposition of benzo[4,5]thieno[2,3- <i>d</i>]pyrimidine (red), pyrrolo[2,3- <i>d</i>]pyrimidine (green) and benzo[<i>f</i>]quinazoline (cyan)	81
Figure 49.	Stereoview of compound 298 (blue) superimposed on 296 (purple) in ecTS (green). Figure prepared with MOE 2008.10	82
Figure 50.	Proposed binding mode with DHFR. The “Normal mode” is defined as the binding mode of folic acid (a 2-amino-4-oxo pyrimidine system) to human DHFR. The “flipped” mode is defined as the binding mode when the molecule is rotated about the C ₂ -NH ₂ bond by 180°	83
Figure 51.	The structure of Nolatrexed	84
Figure 52.	The structure of thieno[2,3- <i>d</i>]pyrimidine antifolates 302-313	85

Figure 53.	Stereoview: Docking structure of 304 (gray) in the X-ray crystal structure of 302 (blue) with double mutant human DHFR (PDB : 3GHC), generated by MOE 2008.10	87
Figure 54.	Stereoview: compound 304 (isopropyl) bound to human DHFR in “normal” mode (violet), in “flipped” mode (green) (PDB :3GHW), generated by MOE 2008.10	88
Figure 55.	The structure of thieno[2,3- <i>d</i>]pyrimidine antifolates 314-323	89
Figure 56.	Stereoview: compound 314 bound to human DHFR in “normal” mode (PDB : 3GHW), generated by MOE 2008.10.	89
Figure 57.	The structure of antifolates 324-330	93
Figure 58.	The structure of antifolates 331-334	94
Figure 59.	A: Structural alignment between 2,5-disubstituted thiophene (purple) and <i>para</i> -disubstituted benzene (green), B: tructural alignment between 2,5-disubstituted furan (purple) and 1,3- <i>meta</i> -disubstituted benzene (green)generated by MOE 2008.10	96
Figure 60.	The structure of antifolates 335-339	97
Figure 61.	The structures of microtubule targeting agents	99
Figure 62.	The structures of antimitotic agent 340-344	101
Figure 63.	Proposed mechanism of aromatization of 351 and 359	114

LIST OF SCHEMES

		Page
Scheme 1.	Retro-synthetic analysis of thieno[2,3- <i>d</i>]pyrimidines	46
Scheme 2.	Synthesis of thiophene 103 and 104	47
Scheme 3.	Synthesis of thieno[2,3- <i>d</i>]pyrimidine 109	47
Scheme 4.	Synthesis of thieno[2,3- <i>d</i>]pyrimidine 114	48
Scheme 5.	Synthesis of thieno[2,3- <i>d</i>]pyrimidine 117	48
Scheme 6.	Synthesis of thieno[2,3- <i>d</i>]pyrimidine 120	49
Scheme 7.	Synthesis of thieno[2,3- <i>d</i>]pyrimidine 123	49
Scheme 8.	Synthesis of thieno[2,3- <i>d</i>]pyrimidine 127	50
Scheme 9.	Synthesis of thieno[2,3- <i>d</i>]pyrimidine 131	51
Scheme 10.	Synthesis of thieno[2,3- <i>d</i>]pyrimidine 134	51
Scheme 11.	Synthesis of thieno[2,3- <i>d</i>]pyrimidine 134	52
Scheme 12.	Synthesis of thieno[2,3- <i>d</i>]pyrimidine 142	52
Scheme 13.	Synthesis of thieno[2,3- <i>d</i>]pyrimidine 146	52
Scheme 14.	Synthesis of thieno[2,3- <i>d</i>]pyrimidine 149	53
Scheme 15.	Synthesis of thieno[2,3- <i>d</i>]pyrimidine 155	53
Scheme 16.	Synthesis of thieno[2,3- <i>d</i>]pyrimidine 158	54
Scheme 17.	Synthesis of thieno[2,3- <i>d</i>]pyrimidine 162	54
Scheme 18.	Synthesis of thieno[2,3- <i>d</i>]pyrimidine 166	55
Scheme 19.	Synthesis of thieno[2,3- <i>d</i>]pyrimidine 170	55
Scheme 20.	Synthesis of thieno[2,3- <i>d</i>]pyrimidine 173	56
Scheme 21.	Synthesis of thieno[2,3- <i>d</i>]pyrimidine 176	56
Scheme 22.	Synthesis of thieno[2,3- <i>d</i>]pyrimidine 180	56
Scheme 23.	Synthesis of thieno[2,3- <i>d</i>]pyrimidine 188	57
Scheme 24.	Synthesis of thieno[2,3- <i>d</i>]pyrimidine 196	57
Scheme 25.	Retro-synthetic analysis of thieno[3,2- <i>d</i>]pyrimidines	58
Scheme 26.	General routes for the synthesis of thieno[3,2- <i>d</i>]pyrimidines from key thiophene intermediate 202	58
Scheme 27.	Synthesis of key thiophene intermediate 207	59
Scheme 28.	Synthesis of key thiophene intermediate 210	59

Scheme 29.	Synthesis of key thiophene intermediate 215	60
Scheme 30.	Synthesis of thieno[3,2- <i>d</i>]pyrimidine 220	60
Scheme 31.	Synthesis of thieno[3,2- <i>d</i>]pyrimidine 224	61
Scheme 32.	Synthesis of thieno[3,2- <i>d</i>]pyrimidine 229	61
Scheme 33.	Synthesis of pyrimidothieno[3,2- <i>d</i>]pyrimidine 234	62
Scheme 34.	Corey-Fuchs reacton and Seyferth-Gilbert reaction	62
Scheme 35.	Bestmann-Ohira modification	63
Scheme 36.	proposed mechanism for Seyferth-Gilbert reaction	64
Scheme 37.	Preparation of the Bestmann-Ohira reagent	64
Scheme 38.	Proposed mechanism for the Bestmann-Ohira reagent preparation	65
Scheme 39.	Improved one-pot reaction	66
Scheme 40.	A general model for the Ullmann coupling	67
Scheme 41.	Ullmann coupling	67
Scheme 42.	Ullmann coupling	68
Scheme 43.	Microwave assisted Ullmann coupling	68
Scheme 44.	A general model for Sonogashira coupling	68
Scheme 45.	Example of Sonogashira coupling	69
Scheme 46.	Example of Sonogashira coupling	69
Scheme 47.	Microwave assisted Sonogashira coupling	70
Scheme 48.	The synthesis of nonclassical analogues 285-295	103
Scheme 49.	Retro synthetic analysis to classical analogue (2 <i>S</i>)-2-(5-{(2-amino-4-oxo-3,4-dihydro[1]benzothieno[2,3- <i>d</i>]pyrimidin-5-yl)methyl}amino)-1-oxo-1,3-dihydro-2 <i>H</i> -isoindol-2-yl)pentanedioic acid 301	105
Scheme 50.	Synthesis of tricyclic thieno[2,3- <i>d</i>]pyrimidine 357	106
Scheme 51.	Attempted synthesis of key intermediate 350	107
Scheme 52.	Synthesis of side-chain of 355	116
Scheme 53.	Synthesis of classical analogue 301	117
Scheme 54.	Synthesis of thieno[2,3- <i>d</i>]pyrimidine 373	118
Scheme 55.	Synthesis of thieno[2,3- <i>d</i>]pyrimidine 305	118
Scheme 56.	Attempted synthesis of key intermediates 374 or 375	119
Scheme 57.	Synthesis of key intermediate 375	120

Scheme 58.	The synthesis of thio ester 381	120
Scheme 59.	Synthesis of classical analogue 304 <i>via</i> Buchward coupling	121
Scheme 60.	Synthesis of nonclassical analogues 305-313 <i>via</i> Ullmann coupling	123
Scheme 61.	Synthesis of nonclassical analogues 317-319 and 323	123
Scheme 62.	Synthesis of thieno[2,3- <i>d</i>]pyrimidines 324-330	124
Scheme 63.	Attempted synthesis of key intermediate 440	126
Scheme 64.	Synthesis of key intermediate 448	126
Scheme 65.	Synthesis of intermediate 451	127
Scheme 66.	Synthesis of thieno[2,3- <i>d</i>]pyrimidine 457	129
Scheme 67.	Synthesis of thieno[2,3- <i>d</i>]pyrimidine 333	132
Scheme 68.	Synthesis of thieno[2,3- <i>d</i>]pyrimidines 335-338	133
Scheme 69.	Synthesis of thieno[3,2- <i>d</i>]pyrimidines 342-344	134
Scheme 70.	Synthesis of thieno[3,2- <i>d</i>]pyrimidine 471	136
Scheme 71.	Synthesis of thieno[3,2- <i>d</i>]pyrimidine 472	137
Scheme 72.	Synthesis of thieno[3,2- <i>d</i>]pyrimidine 474	137

LIST OF TABLES

		Page
Table 1.	Folate transports in mammalian cells	8
Table 2.	Tricyclic classical analogues	32
Table 3.	The angle of aryl disubstitutions	95
Table 4.	Strategy I: Aromatization of tricyclic thieno[2,3- <i>d</i>]pyrimidine 352	107
Table 5.	Strategy I: Aromatization of tricyclic thieno[2,3- <i>d</i>]pyrimidine 358	109
Table 6.	Strategy II: Aromatization of bicyclic intermediate 351	111
Table 7.	Strategy II: Aromatization of bicyclic intermediate 359	111
Table 8.	Strategy II: Aromatization of bicyclic intermediate 351	113
Table 9.	Application of Pd-C in aromatization of tricyclic thieno[2,3- <i>d</i>]pyrimidines 352 and 358	115
Table 10.	Application of Pd-C condition in aromatization of bicyclic thieno[2,3- <i>d</i>]pyrimidines 364 and 365	115
Table 11.	Attempted synthesis of aldehyde 452	128
Table 12.	Comparison of hydrogenation with different intermediates	130
Table 13.	Inhibition concentration (IC ₅₀ , μM) against isolated TS and DHFR ^a of 285-294	258
Table 14.	Inhibitory concentrations (IC ₅₀ , μM) against isolated DHFR ^a and selectivity ratios ^b of 285-294	259
Table 15.	Inhibitory Concentrations of 301 (IC ₅₀ in μM) against TS and DHFR	260
Table 16.	Inhibition concentration (IC ₅₀ , μM) against isolated TS and DHFR ^a of 304-311	261
Table 17.	Inhibition concentration (IC ₅₀ , μM) against isolated TS and DHFR ^a of 317- 319	262
Table 18.	Inhibition concentration (IC ₅₀ in μM) against TS and DHFR ^a of 324-330	263
Table 19.	IC ₅₀ s (nM) for thienopyrimidine compounds 324 to 330 in cell proliferation inhibition of RFC- and FR-expressing cell lines	264
Table 20.	Inhibition concentration (IC ₅₀ in μM) against TS and DHFR ^a of 335-38	265
Table 21.	FRα binding percentages and IC ₅₀ s (nM) for thienopyrimidine compounds 335-338 in cell proliferation inhibition of RFC- , PCFT- and FR-expressing cell lines	266
Table 22.	Inhibition concentration (IC ₅₀ in μM) against TS and DHFR ^a of 333	267
Table 23.	FRα binding percentages and IC ₅₀ s (nM) for thienopyrimidine compounds 1-4 in cell proliferation inhibition of RFC- , PCFT- and FR-expressing cell lines	268

LIST OF ABBREVIATIONS

5-FU	5-Fluorouracil
AICAR	Aminoimidazole-4-carboxamide ribosyl-5-phosphate
AICARFTase	Amino-imidazole-carboxamide-ribonucleotide formyl transferase
AIDS	Acquired immunodeficiency syndrome
AMT	Aminopterin
ATP	Adenosine-5'-triphosphate
Bz ₂ O ₂	Benzoyl peroxide
CA4	combretastatin A-4
CA4P	combretastatin A-4 phosphate
CML	chronic myelogenous leukemia
CRD	cysteine-rich domain
dATP	2'-Deoxyadenosine-5'-triphosphate
DDATHF	5,10-dideazatetrahydrofolic acid
dGTP	2'-deoxyguanosine-5'-triphosphate
dGTP	2'-Deoxyguanosine-5'-triphosphate
DHFR	dihydrofolate reductase
DNA	Deoxyribonucleic acid
dTDP	thymidine-5'-diphosphate
dTMP	2'-Deoxythymidylate-5'-monophosphate
dTTP	Deoxythymidine-triphosphate
dTTP	Deoxythymidine-triphosphate
dUMP	2'-Deoxyuridylate-5'-monophosphate
dUTP	2'-deoxyuridine-5'-triphosphate
<i>E. coli</i>	<i>Escherichia coli</i>
FA	Folic acid
fAICAR	formyl-amino-imidazolecarboxamide ribosyl-5-phosphate
FdUMP	5-fluoro-2'-deoxyuridine-5'-monophosphate
FdUTP	5-fluoro-2'-deoxyuridine-5'-triphosphate
fGAR	Formyl-glycinamide ribosyl-5-phosphate
FGFR	fibroblast growth factor receptor
FH ₂	7,8-Dihydrofolate
FH ₄	5,6,7,8-Tetrahydrofolate
FPGH	Folylpolyglutamate hydrolase
FPGS	folylpoly-γ-glutamate synthetase
FR	folate receptor
FR	Folate receptor
GAR	Glycinamide ribosyl-5-phosphate
GARFTase	Glycinamide-ribonucleotide transformylase
GISTs	gastrointestinal stromal tumors
GPI	glycosyl phosphatidylinositol
GTP	guanosine-5'-triphosphate
IFN	Interferon
IMP	inosine-5'- monophosphate
InsR	insulin receptor

<i>L. casei</i>	<i>Lactobacillus casei</i>
<i>L. major</i>	<i>Leishmania major</i>
leucovorin	LV
LMX	lometrexol
<i>M. avium</i>	<i>Mycobacterium avium</i>
MDR	multiple drug resistance
MOE	Molecular Operating Environment
MRP	multidrug resistance protein
MRPs	multidrug-resistance-proteins
MTHFR	methylenetetrahydrofolate reductase
MTX	Methotrexate
<i>Mycobacterium</i>	
<i>avium</i>	<i>M. avium</i>
N^{10} -CHO-FH ₄	10-Formyltetrahydrofolate
N^5, N^{10} -CH ₂ -FH ₄	5,10-Methylenetetrahydrofolate
N^5 -CH=NH-FH ₄	5-formiminotetrahydrofolate
N^5 -CH ₃ -FH ₄	5-Methyltetrahydrofolate
N^5 -CHO-FH ₄	5-Formyltetrahydrofolate
NADPH	Nicotinamide adenine dinucleotide phosphate
NBS	<i>N</i> -bromosuccinimide
NGFR	nerve growth factor receptor
<i>P. carinii</i>	<i>Pneumocystis carinii</i>
PABA	<i>p</i> -Aminobenzoic acid
PCFT	proton coupled folate transporter
PCP	<i>P. carinii pneumonia</i>
PDDF	N^{10} -propargyl-5,8-dideazafolate
Piv	Pivaloyl (trimethyl acetyl)
PMX	pemetrexed
<i>Pneumocystis</i>	
<i>jirovecii</i>	<i>P. jirovecii</i>
PteGlu	Pteroylglutamic acid
PTX	piritrexim
RFC	reduced folate carrier
rh GARFTase	recombinant human GARFTase
rl	rat liver
RNA	ribonucleic acid
Rr	resistance index
RTK	Receptor tyrosine kinase
RTKs	receptor tyrosine kinases
RTX	raltitrexed
<i>T. gondii</i>	<i>Toxoplasma gondii</i>
<i>T. gondii</i>	<i>Toxoplasma gondii</i>
TLC	Thin layer chromatography
TMP	trimethoprim

TMQ
TS

trimetrexate
Thymidylate synthase

I. BIOCHEMICAL REVIEW

More than twenty interrelated enzymatic reactions in cellular metabolism require folate coenzymes. These reactions are essential to maintain *de novo* synthesis of deoxyribonucleic acid (DNA) and some important amino acids.¹ Folate metabolism has long been considered as an attractive target for cancer chemotherapy because of its crucial role in the biosynthesis of nucleic acid precursors. Antifolates interfere with metabolism pathway of nucleotides. They are clinically used as antimicrobial, antifungal, antiprotozoal, and antitumor agents.² Hitchings, G. A. Folate Antagonists as Antibacterial and Antiprotozoal Agents. *Ann. N. Y. Acad. Sci.* **1971**, *186*, 444-451.

1. An overview of the folate pathway

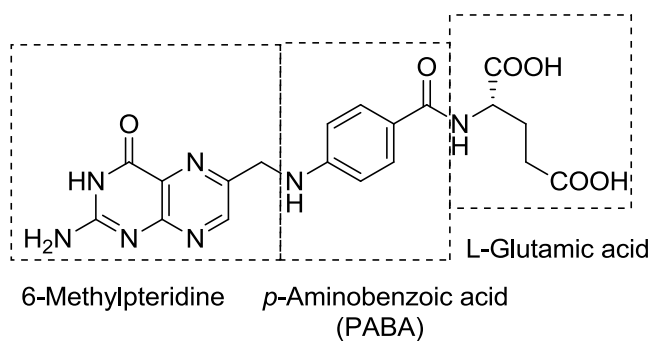


Figure 1. Chemical structure of folic acid

Folic acid (FA) (Figure 1) is a water-soluble vitamin of the B-complex group. It was first reported more than 70 years ago as an anti-anemia agent in animals and as a growth factor in bacteria. The chemical structure of the vitamin is composed of three distinct chemical moieties: a hetero-bicyclic pteridine, a *p*-aminobenzoic acid (PABA) and a glutamic acid (Figure 1). Folic acid plays a crucial role in the biosynthesis of nucleic acid precursors and hence in DNA synthesis and cell replication.^{1,4-6}

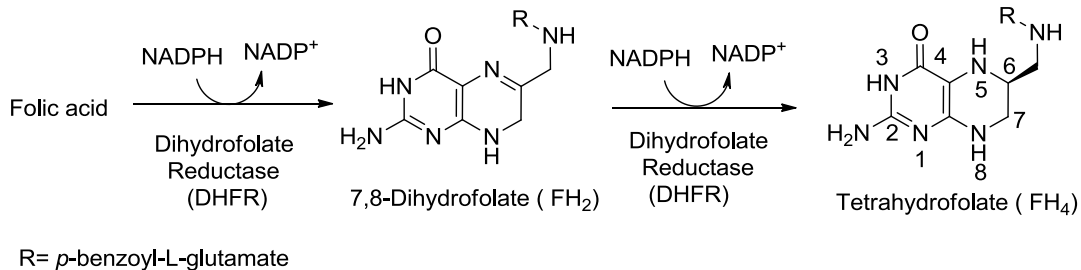


Figure 2. The reduction pathway of folic acid

In eukaryotes and prokaryotes, folates are obtained through two different pathways. Prokaryotes can *de novo* synthesize 7,8-dihydropteroate (FH₂) from *p*-aminobenzoic acid, which is then reduced to 5,6,7,8-tetrahydrofolate (FH₄) catalyzed by dihydrofolate reductase (DHFR) (Figure 2).^{7,8} However, mammalian cells (including human) are incapable of synthesizing FA and acquire it from the diet.

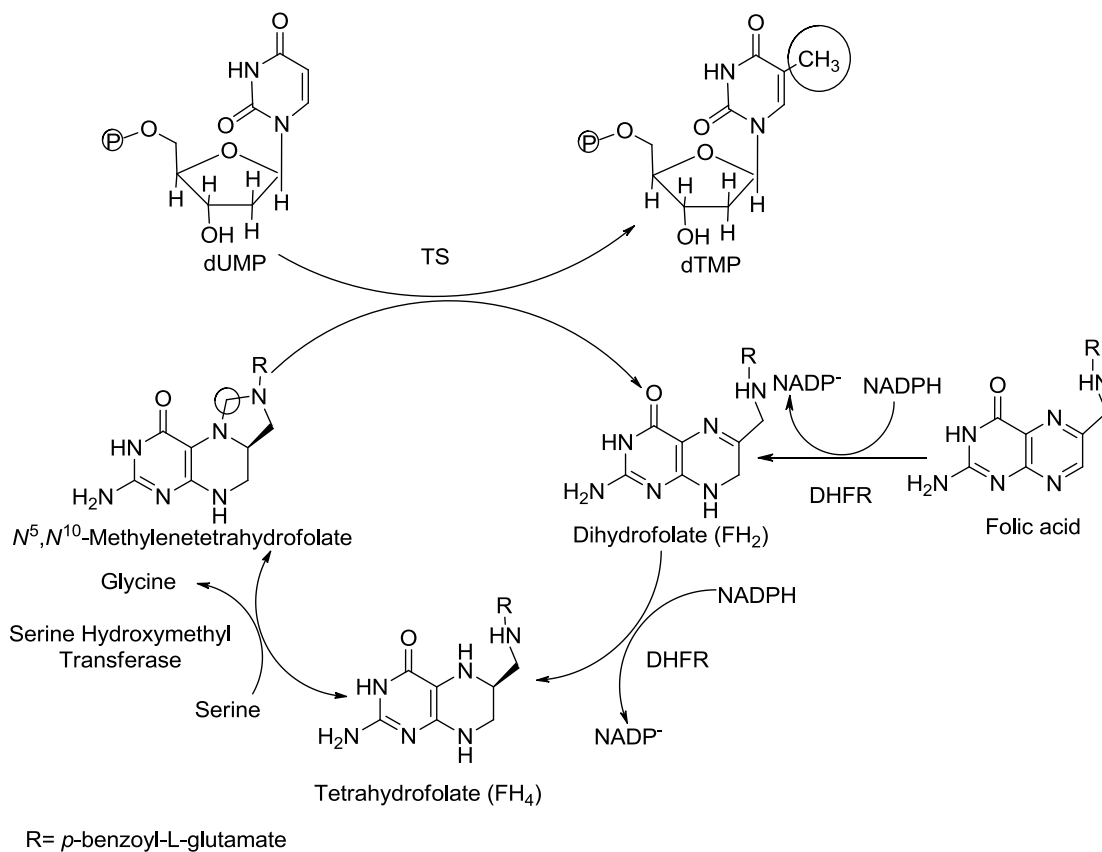


Figure 3. The *de novo* synthesis of dTMP from dUMP

Folic acid exists in several oxidative states, each of which is an essential cofactor in metabolism. In order to work as cofactors, folates must be reduced to FH₄, and is catalyzed by dihydrofolate reductase (DHFR) in two steps: first to FH₂ and then to FH₄ (Figure 2).

Folates are especially important in the *de novo* synthesis of 2'-deoxythymidylate-5'-monophosphate (dTMP) from 2'-deoxyuridylate-5'- monophosphate (dUMP), which is catalyzed by the enzyme, thymidylate synthase (TS) (Figure 3).

During this process, N⁵, N¹⁰- methylene -FH₄ works as a one-carbon unit donor and a reductant. It is a cofactor in this conversion and its one-carbon unit is transferred to the 5-position of dUMP to form the 5-methyl group of dTMP (Figure 3).

This process represents the only *de novo* source of dTMP. Hence, inhibition of TS leads to “thymineless death” in the absence of salvage.^{10, 11} “Thymineless death” is usually observed in mammalian cells when severe deoxythymidine-triphosphate (dTTP) depletion takes place due to methotrexate (MTX) or 5-fluorouracil (5-FU) treatment. This effect is unusual in that deprivation of many other nutritional requirements has a biostatic, but not lethal effect.¹²⁻¹⁶ DHFR then completes the cycle by regenerating FH₄ from FH₂. DHFR thus controls the overall intracellular concentration of FH₄, which is crucial for cell proliferation.^{17, 18} Thus inhibition of DHFR leads to a partial depletion of the intracellular reduced folate pool, which consequently limits cell growth.¹⁹⁻²¹ Because of the essential role in DNA replication, inhibition of these folate dependent enzymes (TS and DHFR) are important strategies for chemotherapy, typified by antitumor agent 5-fluorouracil (5-FU), antimicrobial agent trimethoprim (TMP) and antiprotozoal agent pyrimethamine.^{4, 22}

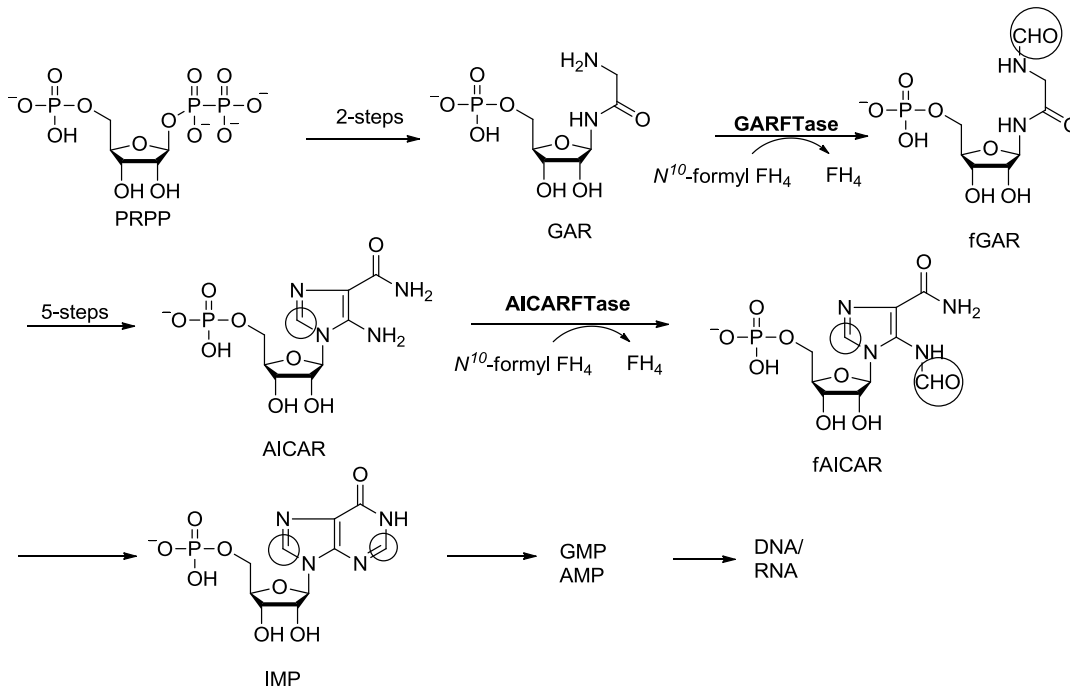


Figure 4. The *de novo* synthesis of purines

The *de novo* synthesis of purines occurs primarily in proliferating cells such as liver and bone marrow and also to some extent, in mononuclear cells and lymphocytes. N^{10} -Formyl tetrahydrofolate (N^{10} -formyl FH₄) is a cofactor that transfers one carbon units in the *de novo* biosynthesis of purine nucleotides (Figure 4). Glycinamide-ribonucleotide transformylase (GARFTase) is the first folate-dependent enzyme in this pathway, which catalyzes the conversion of glycinamide ribosyl-5-phosphate (GAR) to formyl-glycinamide ribosyl-5-phosphate (fGAR), utilizing N^{10} -formyl-FH₄ (Figure 4). Amino-imidazolecarboxamide ribosyl-5-phosphate formyl transferase (AICARFTase) is another folate-dependent enzyme in the biosynthesis of purines. It utilizes N^{10} -CHO-FH₄ and converts amino-imidazolecarboxamide ribosyl-5-phosphate (AICAR) to formyl-amino-imidazolecarboxamide ribosyl-5-phosphate (fAICAR). These two folate-dependent enzymes are responsible for the insertion of carbon atoms at positions 2 and 8 in inosine-

5'-monophosphate (IMP) (Figure 4), the precursor of adenosine-5'-triphosphate (ATP) and guanosine-5'-triphosphate (GTP) for ribonucleic acid (RNA) synthesis and of 2'-deoxyadenosine-5'-triphosphate (dATP) and 2'-deoxyguanosine-5'-triphosphate (dGTP) necessary for DNA synthesis.^{20, 23}

Intracellularly, FA and derived coenzymes are converted to their polyglutamylated derivatives with additional glutamic acid residues to the γ -carboxylic acid via amide bonds by the enzyme folylpolyglutamate synthetase (FPGS).²⁴ The number of glutamate residues varies widely in naturally occurring folates. Usually 2-9 glutamate residues are added to the γ -carboxylic acid group of the FA. This is an important mechanism for trapping folates or classical antifolates within the cell.

Most folate enzymes have a higher affinity for polyglutamate forms than monoglutamate form. This polyglutamylation reaction has several biologically important consequences: (1) The hydrophilicity of the molecule is enhanced due to an increase in negative carboxylate groups by polyglutamylation together with a greater intracellular retention, which is enabled with a decreased cellular efflux. (2) In some cases, the polyglutamylated folate species are thought to have higher binding affinity to some folate dependent enzymes.²⁵ For example, after polyglutamylation, a classical TS inhibitor may also possess the ability to inhibit DHFR and vice versa.²⁵⁻²⁷ Antifolates are classified into two types: classical and nonclassical, on the basis of their mechanism of transport and the ability to be polyglutamylated.^{28, 29}

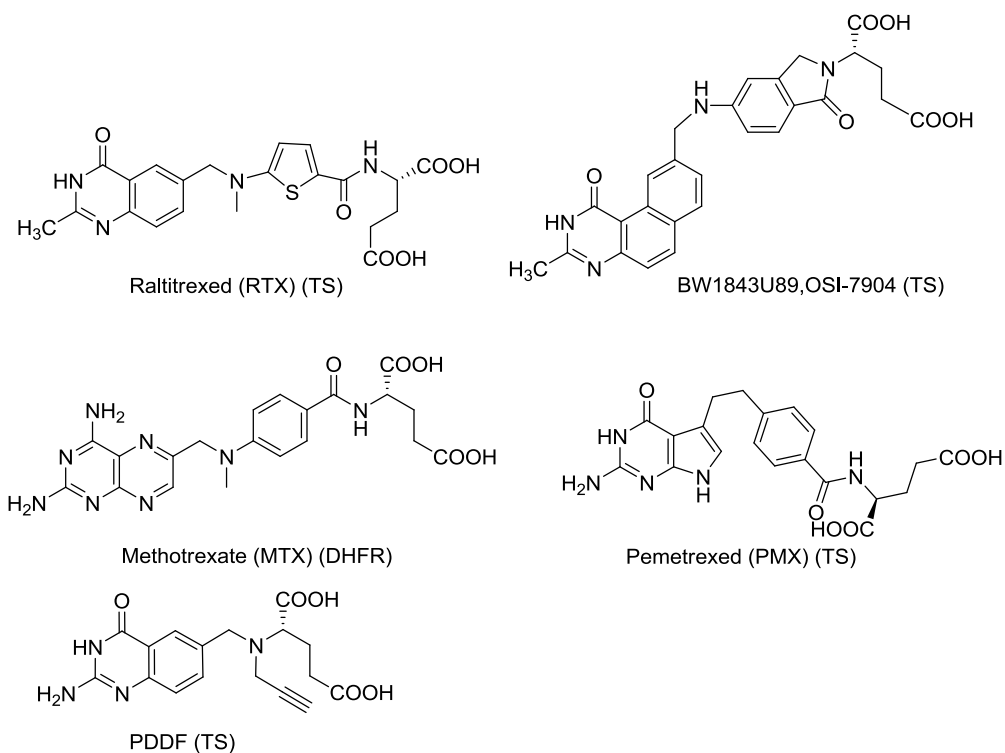


Figure 5. Representative examples of classical antifolates and their principal target(s)

The classical antifolates (Figure 5) are analogs that contains an L-glutamate side chain such as raltitrexed (ZD1694, Tomudex)(RTX), GW1843(OSI-7904), methotrexate (MTX), pemetrexed (LY231514, Alimta)(PMX) and PDDF (N^{10} -propargyl-5,8-dideazafolate). However, tumor cells may be resistant or develop resistance to classical folate-based antimetabolites through reduced expression of FPGS.³⁰ This fact has prompted the search for a complementary class of agents which would not be substrates for FPGS.

Lipophilic side chains instead of the L-glutamate is the characteristic feature of ‘non-classical’ antifolates.

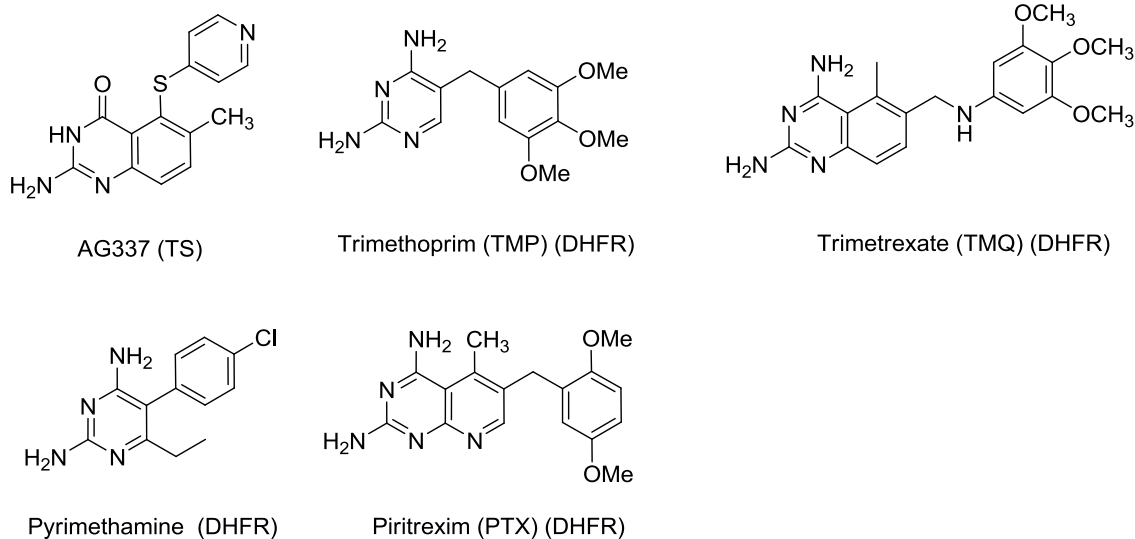


Figure 6. Representative examples of nonclassical antifolates and their principal target

These nonclassical analogues are represented by structures (Figure 6) such as AG337, trimethoprim (TMP), trimetrexate (TMQ), pyrimethamine, and piritrexim. Nonclassical antifolates cannot be polyglutamylated by FPGS and thus do not undergo prolonged retention within the cell as compared to the ‘classical’ analogues.

2. Folates and antifolates transport systems

It is necessary to maintain a high concentration of the folate pool for normal activity of the cell. Since animals and human lack the *de novo* biosynthesis of folates, cellular uptake of these derivatives is essential for tissue regeneration and cell growth. At physiological pH, the α - and γ -carboxyl groups of the glutamate side chain are negatively charged. Because of this, folates poorly pass biological membranes by diffusion alone. Folate transport is required not only for cellular uptake but also for intracellular compartmentation of the cofactors. Transport of folates and antifolates into the cell is usually accomplished by three carrier proteins present on the cell surface: the reduced folate carrier (RFC), the membrane folate receptor (FR) and the proton-coupled folate

transporter (PCFT).³¹ A summary of biochemical and functional properties of these transporters is provided in Table 1.

Table 1. Folate transports in mammalian cells

RFC	FR	PCFT
Integral protein	anchored in plasma membranes by a glycosyl phosphatidylinositol (GPI) anchor ^{32, 33}	A member of the superfamily of facilitative carriers ^{34, 35}
Anion exchange mechanism (driven by anion gradients) ³²	Endocytotic mechanism ³²	H ⁺ symporter
The primary transporter of folates and antifolates ³²		Transport a wide range of folates and antifolates
High affinity for reduced FA (K _m ~1-5 μM); Low affinity for FA (K _i ~200 μM)	High affinity for FA (1 nM) and reduced folates (5-10 nM)	
Ubiquitously expressed in normal tissues and tumor cells ³²	Most normal cells do not express FRα; over expression of the FRα on the surface of some tumor cells ³⁶	Wide but likely more restricted expression than hRFC ^{34, 35}

Optimum at physiological pH (~7.4) ²⁴		Optimum at acidic pH (5.5~6.5) ^{34, 35}
--	--	--

The functional properties for RFC were first documented in 1968 by Goldman³⁷ in murine leukemia cells. It is a member of the major facilitator superfamily of transporters with the characteristics of an anion exchanger. And is an integral transmembrane protein with high affinity for reduced folates ($K_m \sim 1-5 \mu\text{M}$) and a low affinity for FA ($K_i \sim 200 \mu\text{M}$) with a neutral pH optimum.³² RFC is ubiquitously expressed in normal tissues and tumor cells. It is the major transport system for folates in mammalian cells. And more importantly, it is the primary transporter of antifolate drugs used for the cancer chemotherapy, including MTX, PMX, RTX and others. The decrease of RFC level or its function is a common mode of antifolate resistance.^{38, 39} Impaired RFC function is an important mechanism of resistance to MTX and other antifolates *in vitro*.^{32, 39}

FRs are anchored in plasma membranes by a glycosyl phosphatidylinositol (GPI) anchor and mediate an endocytic mechanism. It shows high affinity for FA (1 nM) and reduced folates (5-10 nM). FRs are high affinity folate binding proteins encoded by three distinct genes (α , β and γ).⁴⁰ FR α is overexpressed in some epithelial tumors, especially the kidney, placenta and choroid plexus, and has a restricted distribution in normal tissues⁴¹⁻⁴³, which provides an opportunity for the development of antifolates specifically targeted at FR α overexpressing tumors.^{44, 45} Antifolate toxicity mainly occur in proliferating tissues such as bone marrow and gut.⁴⁶ This might be because: (1) Most antifolates are primarily transported into cells by the ubiquitously expressed RFC. (2) Proliferative tissues are highly dependent on the enzymes that antifolates target. Thus

antifolates that are specifically transported by FR α should show very low toxicity to normal tissues.

PCFT was recently identified as a third transporter for folates. It is a member of the superfamily of facilitative carriers and implicated as the major FA transport system at the acidic pH in the upper small intestine.^{34,35} PCFT is widely expressed, but has a likely more restricted expression than hRFC. PCFT is a proton-folate symporter that functions optimally at acidic pH (5.5~6.5)³⁵, which is one of the important aspects of PCFT in the treatment of cancer. It is known that acidic microenvironment is a characteristic of solid tumors.⁴⁷ Recently, Goldman reported that at pH 5.5, PCFT increased the inhibitory activity of PMX, which illustrated the unique property of PCFT as a transporter of antifolates.

3. Thymidylate Synthase (TS)

3.1 Enzyme description and Catalytic Mechanism

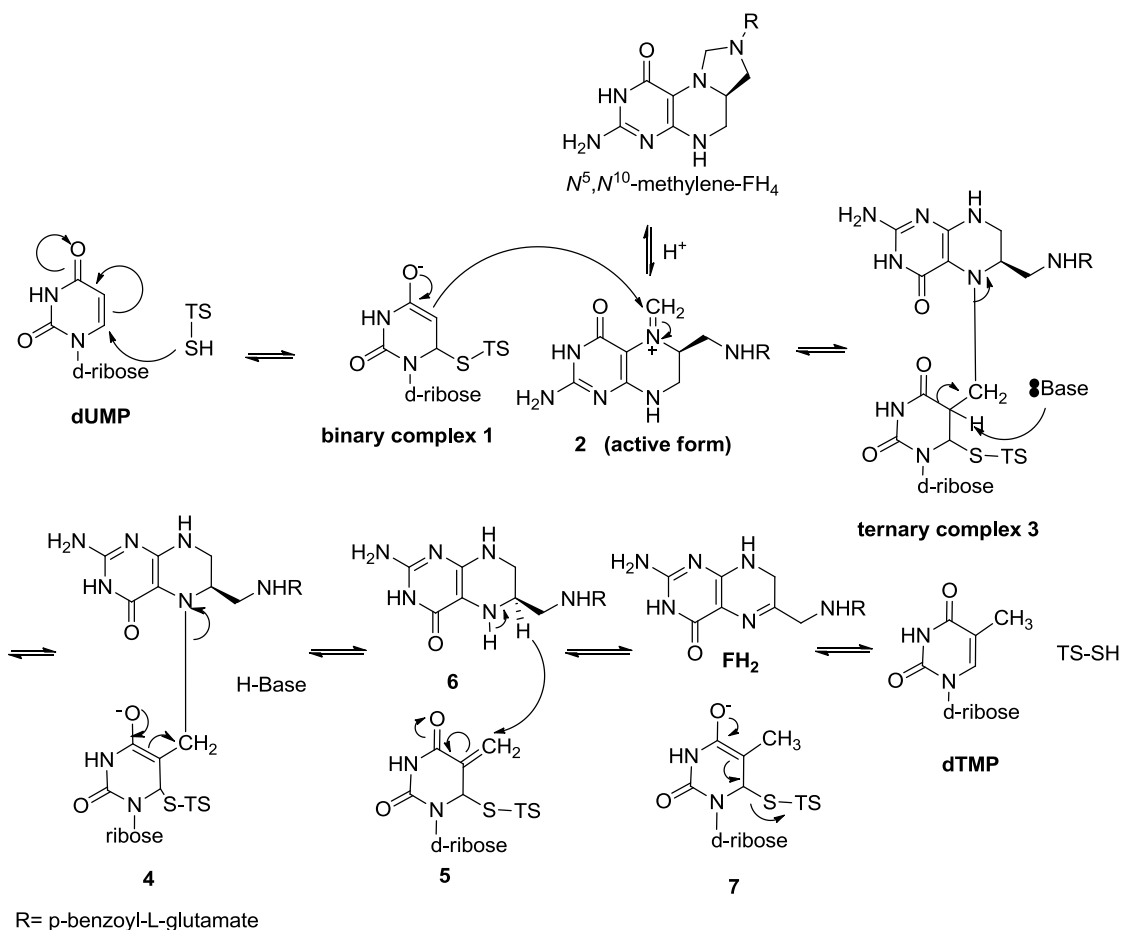


Figure 7. Proposed catalytic mechanism of human TS. (Adapted from Ref. 59)

TS (EC 2.1.1.45) is a two-substrate enzyme that accepts both dUMP and N^5, N^{10} -methylene -FH₄ to form a ternary complex and carries out the reductive methylation of dUMP, which is the only *de novo* biosynthesis of dTMP.⁷ TS inhibition results in a thymineless state, which prevents the growth of actively dividing cells.^{7, 48, 49} TS has long been considered a key target in anticancer chemotherapy.

The catalytic mechanism of TS has been reviewed extensively.^{22, 50-53} The detailed catalytic mechanism is described in Figure 7.

TS first forms a noncovalent binary complex **1** with dUMP (TS-dUMP), which then binds to the active form of cofactor N^5, N^{10} -methylene-FH₄ **2** to form the noncovalent

ternary complex **3** (TS-dUMP-cofactor). The protonation of the cofactor at the N^{10} position changes it from an inactive form to the active form **2** which is in an iminium ion at N^5 .²¹ dUMP is activated at the C5 position by a nucleophilic attack on the C6 of the uracil ring of dUMP by a catalytic thiol (Cys-195, human TS) which results in the formation of a Michael-type adduct **1** (Figure 7). The iminium ion of **2** is very reactive and rapidly allows the C5 of dUMP to attack to form ternary complex **3**. The proton at C5 of the uracil ring is abstracted by an unidentified base in the enzyme active site to form **4**, which is followed by double bond formation between the C5 of uracil and the carbon unit accompanied by its cleavage from the cofactor **5**. The resulting double bond in **5** is reduced through hydride transfer from C6 of the reduced cofactor **6**, which is simultaneously oxidized to form FH_2 ; at the same time, the enzymatic thiol group undergoes β -elimination to reform the double bond and affords dTMP and free TS.⁵⁴

3.2 The structure of TS

TS is a macromolecular homodimeric protein with a identical subunits of 30-35 kDa each and a primary sequence of approximately 316 amino acids long.⁵⁵⁻⁵⁷ TS from more than thirty species have been isolated, and contain about 316 amino acids. The primary structures of about 30 TS enzymes including those of humans, bacteriophages, and plants have been determined. TS is one of the most highly conserved enzymes known.⁵⁵ The primary structure of TS is highly conserved: approximately 27 amino acids are completely conserved and 165 amino acids (80%) are conserved in more than 60% of the organisms.⁵⁸ X-ray crystal structures of TS from *E. coli*,⁵⁵ *L. casei*,^{59, 60} *Leishmania major*,⁶¹ and *P. carinii*⁶² and human have been reported in the literature. In addition, many crystal structures of TS complexed with substrates and ligands are available as

well.⁶³⁻⁶⁷ A comparison of these structures indicates that the tertiary structure is well conserved.

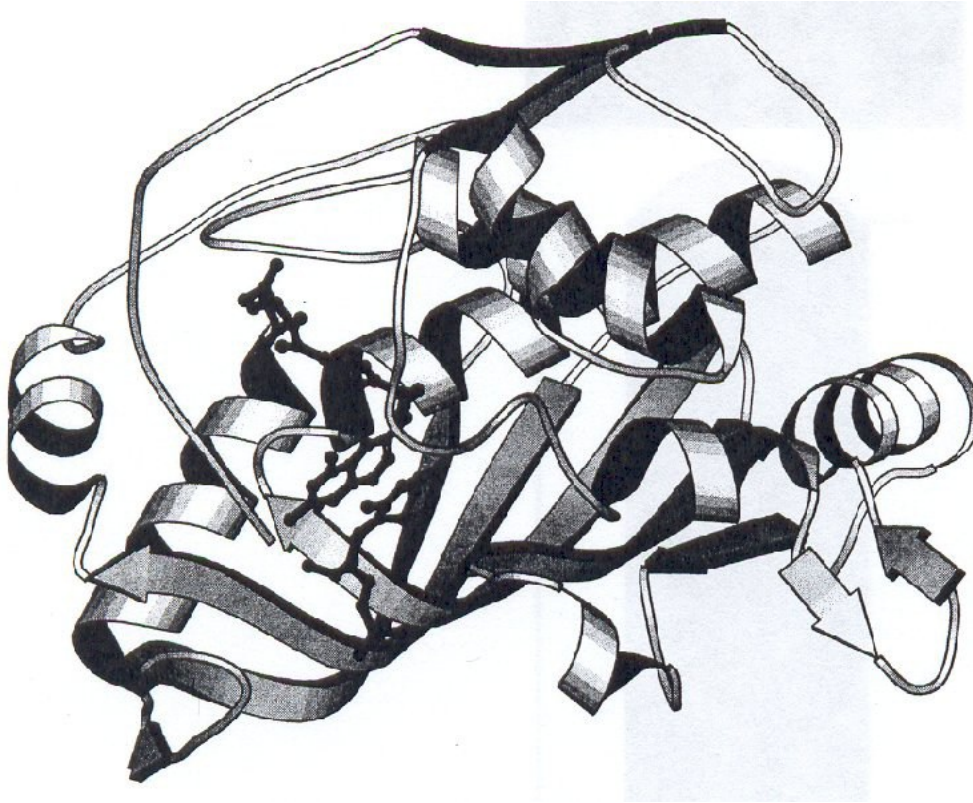


Figure 8. X-ray crystal structure of *E. coli* TS with inhibitor PDDF (CB3717)⁶⁸

The subunit interface is formed by a stranded twisted β -sheet composed of about twenty five residues that packs against the same sheet formed by the other subunit of the dimer. Each subunit has a deep active site cavity that contains a bound inorganic phosphate, which has been observed in all solved TS structures, in the absence of nucleotides.⁶⁸

The active site of dUMP is formed by 32 amino acids, of which 16 are conserved. The X-ray crystal structure of *E. coli* TS bound to dUMP and inhibitor PDDF (CB3717) showed that TS consists of a series of 8 α -helices, 10 strands of β -sheet, and several

segments of coil that join the secondary structural elements together. The subunit interface is formed by a stranded twisted β -sheet composed of about 25 residues that packs against the same sheet formed by the other subunit of the dimer. Each subunit has a deep active site cavity that contains a bound inorganic phosphate, which has been observed in all solved TS structures, in the absence of nucleotides (Figure 8). Cys198 is on the side of the cavity, and three Arg residues and Ser219 are at the base of the cavity coordinated to the bound phosphate.^{68,69}

The crystal structures of PMX and RTX with human TS have also been obtained in 2001.^{70,71} These structures are important for the understanding of both the mechanism and the inhibition of hTS. Several crystal structures of TS complexed with substrates and inhibitors have also been reported.⁶³⁻⁶⁷ These crystal structures allow a structure-based rational design of TS inhibitors.

3.2 Representative TS Inhibitors

These can be broadly divided into five categories:

1. Nucleotide Analogues
2. 6-6 Ring Fused Bicyclic Classical Analogues
3. 6-5 Ring Fused Bicyclic Classical Analogues
4. Tricyclic Classical Analogues
5. Nonclassical TS Inhibitors

3.2.1. Nucleotide Analogues

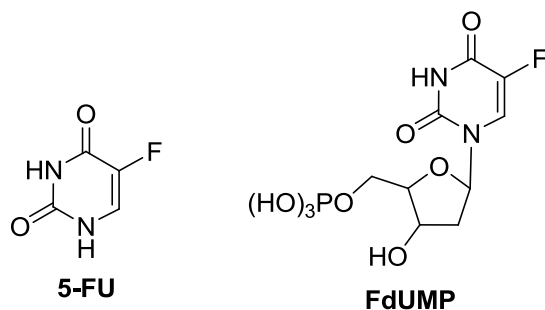


Figure 9. The structures of 5-FU and FdUMP

TS possesses two substrates: dUMP and N^5, N^{10} -methylene-FH₄, thus both dUMP and folate analogs can be designed as the inhibitors of this enzyme.⁷² The dUMP analogue 5-fluorouracil (5-FU) (Figure 9) belongs to the fluoropyrimidine class of antineoplastic agents and was first synthesized by Heidelberger and coworkers in 1957.⁷³

74

5-FU was rationally designed based on the postulation that a chemically modified uracil molecule might be effective in disrupting tumor DNA biosynthesis. Since its introduction some 55 years ago, 5-FU remains an active agent with broad-spectrum activity against many solid tumors, including colorectal, pancreas, breast, head and neck, gastric and ovarian cancers.⁷⁵ In the past few years, numerous efforts have been made to improve the efficacy of 5-FU. Biochemical modulation of 5-FU with other agents have been attempted in the clinic⁷⁶ including interferon (IFN), MTX, leucovorin (LV). LV has been the most successful thus far. For the past 15–20 years, the combination of 5-FU and LV has been considered the gold standard for treating patients with advanced colorectal cancer. LV is intracellularly metabolized to N^5, N^{10} -methylene-FH₄, which can form a ternary complex with FdUMP and TS to maintain the enzyme in a maximally inhibited state. This effect of maintaining the enzyme in an inhibited state is critical since the TS-

catalyzed reaction provides the essential nucleotide precursors for DNA biosynthesis. Subsequent work confirmed that 5-FU cytotoxicity was significantly enhanced upon addition of LV.⁷⁷

5-FU has several mechanisms of action including inhibition of TS, incorporation into DNA, and/or incorporation into RNA.⁷⁸ 5-FU is inactive in its original form and must be intracellularly converted to various nucleotide forms. For example, 5-fluoro-2'-deoxyuridine-5'-monophosphate (FdUMP) (Figure 9) is a critical nucleotide metabolite which forms a covalent ternary complex with TS in the presence of N^5, N^{10} -methylene-FH₄, resulting in inhibition of the enzyme. Nucleotide kinases phosphorylate FdUMP to 5-Fluoro-2'-deoxyuridine-5'-triphosphate (FdUTP), which incorporates into DNA leading to inhibition of DNA synthesis and function.

3.2.2. 6-6 Ring Fused Bicyclic Classical Analogues

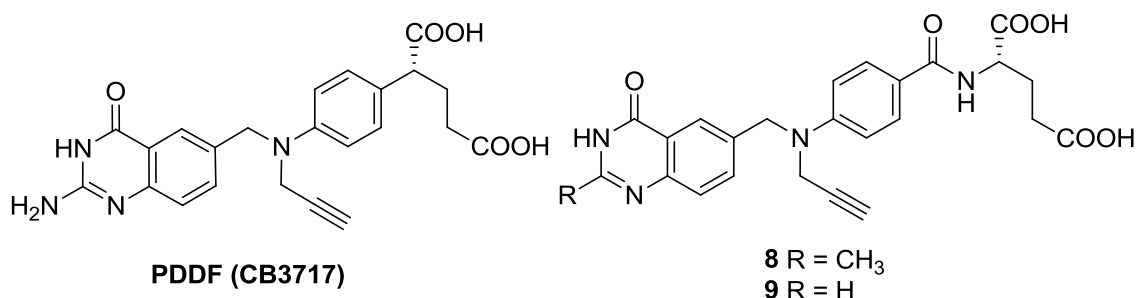
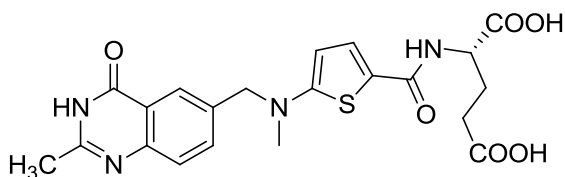


Figure 10. The structure of PDDF (CB3717) and its analogues

PDDF (CB3717) (Figure 10) is the first quinazoline-based antifolate analogue that was first investigated in the 1980s.^{79, 80} It is a potent TS inhibitor *in vitro* and shows broad-spectrum activity in patients with breast, liver, and cisplatin-refractory ovarian cancers in phase I studies. Unfortunately, unpredictable severe life-threatening renal- and hepatotoxicity observed in further clinical studies, which resulted in discontinuation of further clinical trial. The poor solubility, attributed to the presence of a 2-amino group in

PDDF, probably caused the drug to precipitate in the acidic pH of the renal tubules, thereby resulting in renal toxicity.⁷⁹ The metabolism of PDDF is typical of the classical antifolates: it is transported *via* RFC and polyglutamylated by FPGS inside the cell.

Structural alterations to the 2-substituent in pyrimidine *A* ring (Figure 10) with a 2- methyl substituent (**8**) or simply a proton (**9**) did not cause the drug to lose its TS inhibitory activity.



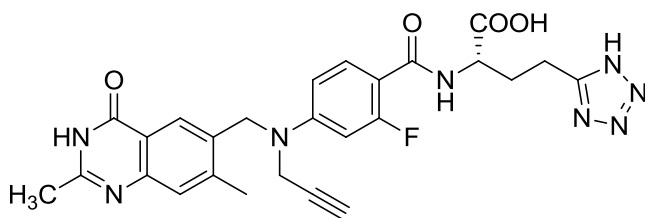
Raltitrexed (RTX) (ZD1694)

Figure 11. The structure of Raltitrexed (ZD1694)

Raltitrexed (RTX) (Figure 11) is a water-soluble analogue of PDDF and it does not cause renal toxicity due to its improved water solubility at low pH.⁸³ Like most classical antifolates, it is transported into cells by RFC and undergoes rapid polyglutamylation by FPGS. Although the activity of raltitrexed is 20-fold less than CB 3717, it is a good substrate for FPGS and once polyglutamylated, it is 60-fold more potent than the monoglutamylated form. The retention of polyglutamylated raltitrexed within cells is significantly prolonged compared to its monoglutamate form.⁸⁰

RTX was approved as first-line therapy for advanced colorectal cancer in several European countries, Australia, Canada, and Japan. Currently, much attention is focused on combination of raltitrexed with some other approved anticancer agents, such as topoisomerase I inhibitor irinotecan.^{84, 85} In a phase I study, the combination of raltitrexed with irinotecan was well tolerated.⁸⁵ In phase II studies, raltitrexed combined with

oxaliplatin for the treatment of patients with previously untreated metastatic colorectal carcinoma.⁸⁶ This combination showed a 47% response rate with a median overall survival of >14.5 months.



10 (ZD9331)

Figure 12. The structure of **10** (ZD9331)

Compound **10** (Figure 12) was rationally designed as TS inhibitor based on the X-ray crystal structure of *E. coli* TS enzyme ternary complexes of CB 3717 and its tetraglutamate derivative.^{87, 88} Unlike RTX, **10** does not require polyglutamylation by FPGS for activation and therefore retains cytotoxic activity in tumors expressing low levels of FPGS. Preclinical studies have shown **10** have a broad spectrum of antitumor activity in human cancer cell lines and tumor xenografts. In phase I studies, the dose-limiting toxicities were myelosuppression, nausea, vomiting, skin rash, and diarrhea.^{89, 90} In phase II trials, **10** has shown promising activity as second- and third-line therapy in patients with ovarian and colorectal cancer.^{91, 92} This agent is currently under investigation in other solid tumors, including non-small-cell lung, gastric, and pancreas cancer both as a single agent and in combination with other cytotoxic agents.

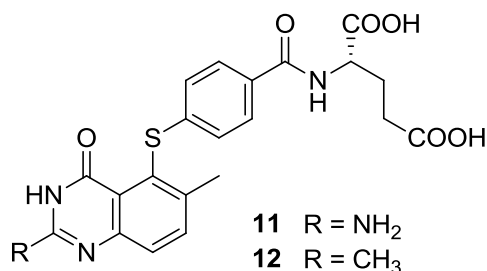


Figure 13. The structure of **11** and **12**

Webber and coworkers⁹³ designed another series of 5-arylthio quinazolinone analogues **11** and **12** (Figure 13) based on crystallographic analysis of protein-ligand structures. The binding site of the glutamic acid side-chain was from the 5-position instead of the 6-position. Moreover, a thio-bridge was utilized between the quinazolinone and the benzoylglutamate side-chain. Molecular modeling indicated that this transposition from the 6- to the 5-position of the side chain resulted in a void at the C6 position, originally occupied by the methylene moiety of PDDF, which interacts with Trp80 (hTS). Both **11** and **12** were excellent inhibitors of human recombinant TS ($K_i = 13$ nM and 0.124 nM respectively).⁹³ The cytotoxicity of the 2-amino derivative **11** was comparable to that of CB3717, whereas the 2-methyl version **12** was significantly less active than raltitrexed. The differences may be due to changes in active transport and/or polyglutamylation.

3.2.3. 6-5 Ring Fused Bicyclic Classical Analogues

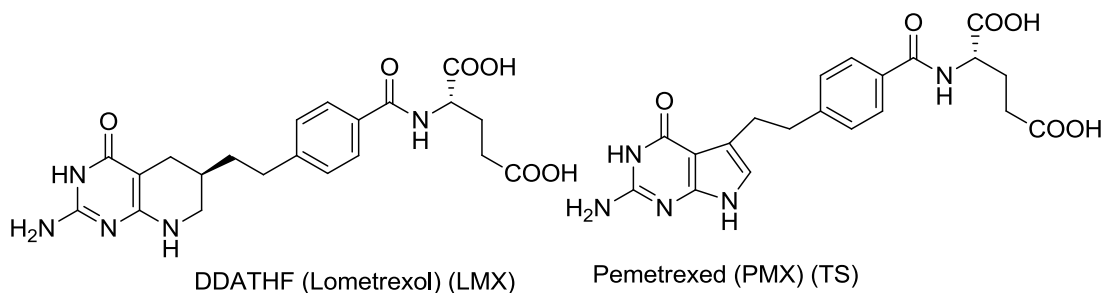


Figure 14. The structures of DDATHF and pemetrexed

In 1985, Taylor *et al.*⁹⁴ reported a novel “tight-binding” inhibitor, (6*R*)-5,10-dideazatetrahydrofolic acid LMX (Figure 14), of GARFTase with potent antitumor activity in a number of murine and human xenograft solid tumors. Taylor *et al.*⁹⁵ reported PMX, the B-ring contracted analogue of DDATHF, as a moderate inhibitor of mouse recombinant TS ($K_i = 0.34 \mu\text{M}$), but a potent cytotoxic agent with IC_{50} values of 22 nM and 16 nM against the growth of L1210 and CCRF-CEM cells in culture respectively.

PMX is a 6-5 fused pyrrolo[2,3-*d*]pyrimidine instead of the more common 6-6 fused pteridine or quinazoline ring structure. Preliminary studies⁹⁶ revealed that pemetrexed polyglutamates are multi-targeted antifolate (MTA): it is not only potent inhibitors of TS but also of DHFR and GARFTase and AICARFTase. PMX has been approved for the treatment of malignant pleural mesothelioma in combination with cisplatin in the United States and has provided a renewed interest in classical antifolates as antitumor agents. Like raltitrexed, it utilizes the RFC to gain entry into cells and requires polyglutamylation for maximal inhibitory effects on the various target enzymes. It has shown activity *in vitro* against colon, renal, liver, and lung cancers.⁹⁷

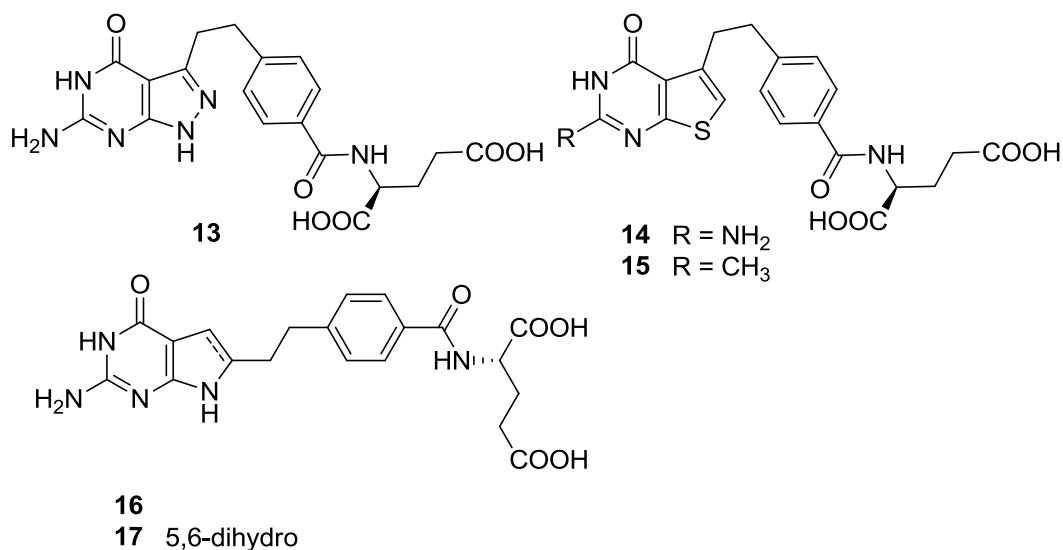


Figure 15. The structures of 13-17

Taylor *et al.*⁹⁸ further reported **13** in which the B-ring of PMX is replaced with a pyrazole (Figure 15) that abolished the cytotoxic activity of the drug. The replacement of B-ring of PMX with a thiophene ring resulted the design of **14** and **15**. Preliminary biological evaluation revealed that both **14** and **15** were inactive as inhibitors of the growth of tumor cells in culture.⁹⁹

The position of attachment of the side chain to the heterocycle is important for TS inhibitory activity. After moving the side chain of PMX from the 5- position to the 6- position, the resulting compound **16** (Figure 15) lost its TS activity completely. Interestingly, **17**, the 5,6-dihydro derivative of **16**, did show potent GARFT inhibitory activity.^{100, 101}

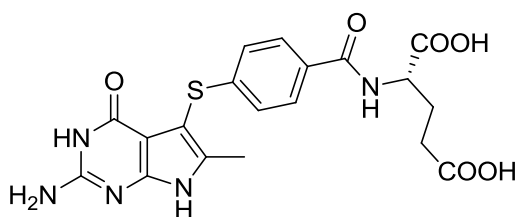


Figure 16. The structure of **18**

Gangjee *et al.*¹⁰² reported **18** (Figure 16), as a structural analogue of pemetrexed, in which a methyl group was introduced in the C6 position of pyrrolo[2,3-*d*]pyrimidine moiety and the bridge -CH₂-CH₂- was replaced with -S- moiety. This compound was a potent inhibitor of human TS (IC₅₀ = 42 nM) and *L. casei* TS (IC₅₀ = 21 nM). Further, it was more potent than PDDF in its inhibition of the growth of human CCRF-CEM cells in culture (EC₅₀ = 450 nM). The addition of a methyl group at the 6-position rendered the drug a non-substrate for FPGS.

3.2.4. Tricyclic Classical Analogues

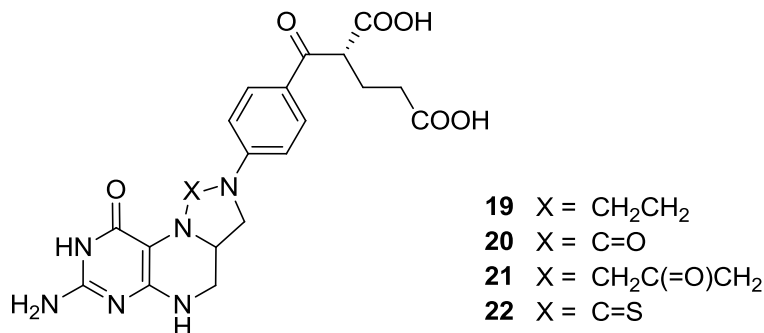


Figure 17. The structures of **19-22**

Tricyclic analogues of 5,10-methylene-tetrahydrofolate **19-22** were reported,^{103, 104} but none showed potent inhibitory activities against TS.

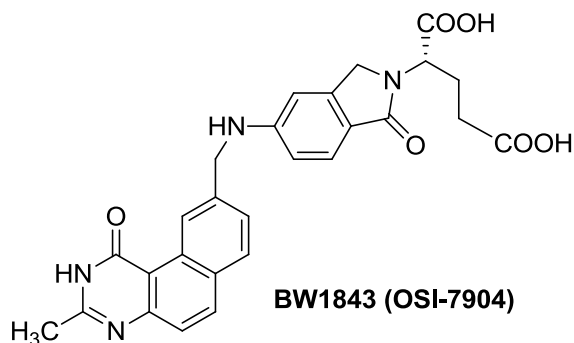


Figure 18. The structure of **BW1843 (OSI-7904)**

In 1993, Pendergast *et al.*¹⁰⁵ reported BW1843 in a series of benzo-quinazolines analogues. BW 1843 is an extremely potent noncompetitive inhibitor of TS ($K_i = 0.09$ nM). Although it is a good substrate for FPGS, the main cellular metabolite is the diglutamate rather than tri- or penta glutamate seen with most other antifolates. It has potent activity against human cancer cells in culture with IC_{50} values less than 1.0 nM.¹⁰⁶

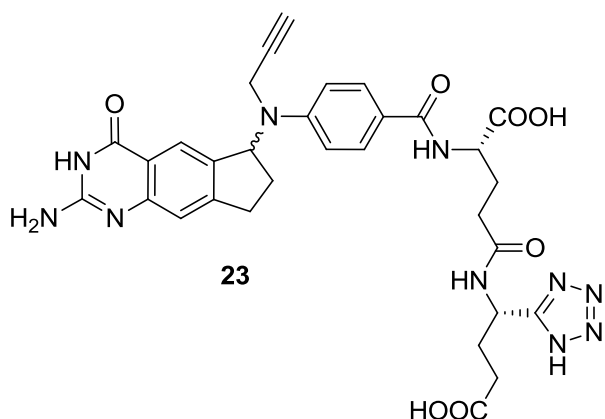


Figure 19. The structure of **23**

In 2002, Bavetsias *et al*¹⁰⁷ reported analogue **23** (Figure 19) as tricyclic tetrazole analogue of a potent TS inhibitor with K_i of 0.2 nM and IC_{50} of 0.44 μ M against L1210 TS.

3.2.5. Nonclassical TS Inhibitors

Classical compounds depend on folate transporter systems for their transportation into the cell. The impairment of the RFC can lead to drug resistance. Additionally, some classical antifolates depend on FPGS for polyglutamamylation, in part, for potent antitumor activity. The impairment of FPGS can also lead to drug resistance. Lipophilic nonclassical inhibitors of TS have been developed to overcome the problems mentioned above. Thus compounds that are not subject to metabolic activation through polyglutamamylation need to have high intrinsic potency against TS as well as tumor cells.

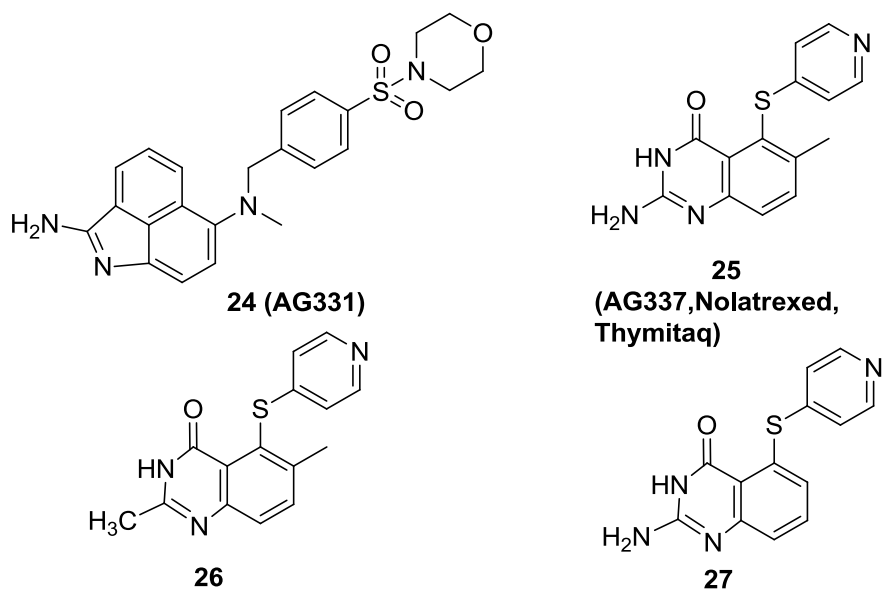


Figure 20. The structure of 24-27

Compounds **24** and **25** (Figure 20) were designed specifically on the basis of the crystal structure of ecTS as a surrogate for hTS. They enter cells *via* passive diffusion and are not dependent on the RFC or other specific transport systems to cross the cell membrane. Compound **24** was found to cause severe liver toxicity in phase I testing and further evaluation was subsequently terminated.^{108, 109} Compound **25** shows good inhibitory activities in both *E. coli* ($K_i = 490$ nM) as well as human TS inhibition ($K_i = 15$ nM). Compound **25** is well tolerated in the initial phase I, II and III studies, and shows promising activity against head and neck, pancreatic, and hepatocellular cancer. A phase II trial in patients with squamous cell cancer of the head and neck shows complete responses in 2 and partial responses in 2 of 22 patients to give an overall response rate of 18%.¹¹⁰ A large phase III randomized trial of **25** is currently ongoing in North America where patients with unresectable hepatocellular carcinoma are randomized to receive either nolatrexed or doxorubicin (the control arm). Replacing the 2-amino group of **25** with a methyl group (**26** in Figure 20) decreased the TS inhibitory activity.¹¹¹ Removal of

the 6-methyl group of **25** afforded **27** (Figure 20), which has a 10-20 fold decrease in human TS inhibition.

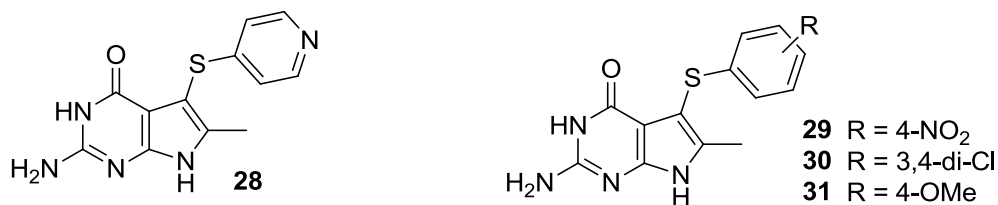


Figure 21. The structures of **28-31**

Gangjee *et al.*¹⁰² reported **28** (Figure 21) as a structural analogue of **25**. This analogue was a potent inhibitor of human TS ($IC_{50} = 340$ nM), but a weak inhibitor of *E. coli* TS and *S. faecium* TS. As an extension of this work, Gangjee *et al.*¹¹² reported a series of nonclassical analogues **29-31**, which also show potent inhibition of human TS.

4. Dihydrofolate Reductase (DHFR)

4.1 Enzyme description and Catalytic Mechanism

DHFR functions as a catalyst for the reduction of FH_2 to FH_4 by using nicotinamide adenine dinucleotide phosphate (NADPH) as the cofactor.¹¹³ The inhibition of DHFR leads to partial depletion of intracellular reduced folates with subsequent limitation of cell growth.¹⁹

DHFRs are relatively small, water-soluble, monomeric enzymes and possess 159-189 amino acid residues with a molecular weight of 18-22 kDa.¹¹⁴ The sequence of the bacterial DHFR is about 30 amino acid residues shorter than that of the vertebrate enzymes. The first crystal structure of a DHFR enzyme was reported by Matthews and coworkers in 1977.¹¹⁵ Since then, X-ray crystal structures and solution NMR structures have been reported for complexes of the protein from various species (bacteria, avian and

mammalian). These 3D-structures of DHFR are used in structure-based drug design and to acquire information on inhibitor binding, enzyme-inhibitor-cofactor complexes and in particular to determine differences in amino acid location between parasite and host DHFR.

DHFR structures from bacterial forms and higher organisms were established by X-ray diffraction analysis and NMR spectroscopy. Early in 2004, the RCSB protein data bank (PDB) contained 115 structures of DHFR from *Escherichia coli* (ec), *Lactobacillus casei* (lc), *Pneumocystis carinii* (pc), *Mycobacterium tuberculosis*, *Thermotoga maritime*, *Candida albicans*, and *Haloferax volcanii*, human DHFR, and the chicken liver (cl) enzyme. The homology among vertebrate DHFR is 75-90% while in bacterial DHFR it is only 25-40%. Homology is greatest at the N-terminal and least at the C-terminal.^{55, 116}

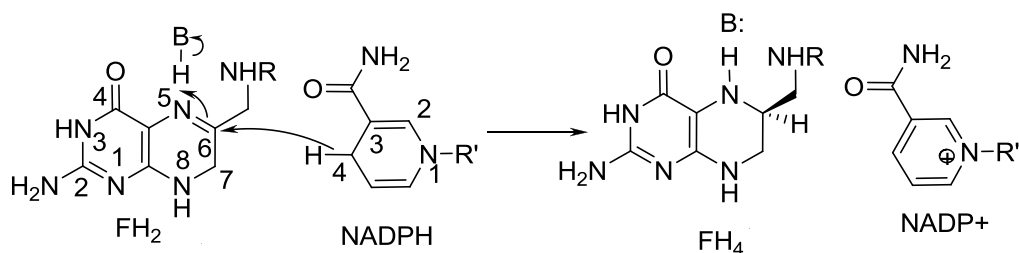


Figure 22. Proposed catalytic mechanism of DHFR

The mechanism of DHFR is not totally understood, although it has been extensively studied.¹¹⁷ DHFR catalyzes a hydride transfer from NADPH to the C6 of 7,8-FH₂, and at a much slower rate to the C7 of folate to form tetrahydrofolate.¹¹⁷⁻¹¹⁹ It is known that initial protonation of N5 followed by a hydride transfer from the C4 of the cofactor NADPH to the adjacent FH₂ C6, followed by the reduction of folate or FH₂ is accompanied by the transfer of the hydrogen atom located in the 4-*pro-R* position of NADPH to the C7 of folate or C6 of FH₂ (Figure 22).

4.2 Species-differences among DHFR

The species-differences among the DHFR¹²⁰ have been used to design discover compounds with particular selectivity. Three opportunistic pathogens that infect immunocompromised patients, especially those with acquired immune deficiency syndrome (AIDS), are *Pneumocystis jirovecii* (*P. jirovecii*), *Toxoplasma gondii* (*T. gondii*), and *Mycobacterium avium* (*M. avium*). The most notable differences between these pathogen DHFR and human (h) DHFR are discussed below.

The differences of the amino acid sequences among various DHFR in the active site has been exploited to design inhibitors that are selective for pathogen DHFR over human DHFR (that are lethal to pathogens but relatively harmless to mammals).

4.2.1 *Pneumocystis carinii* (*P. carinii*) DHFR and *Pneumocystis jirovecii* (*P. jirovecii*)

P. carinii DHFR is a small molecule with molecular weight of 26000 Dalton. It consists of 206 amino acid residues and is similar to rat liver (rl) DHFR in size. The enzyme's optimum pH was 7.0 and its K_m for FH₂ is four-fold higher ($17.6 \pm 3.9 \mu\text{M}$) than rat liver DHFR ($4.0 \pm 2.2 \mu\text{M}$).

The size of the cavity of *P. carinii* DHFR active site is smaller than that of human DHFR (L1210) but larger than that of bacterial (*E. coli*) DHFR. X-ray crystal structure¹²¹ have shown that most residues of DHFR involved in catalysis and binding are conserved in both human DHFR and *P. carinii* DHFR, while the polar Asn64 residue in human DHFR, located just outside the binding site, and is replaced by nonpolar Phe69 in *P. carinii* DHFR.

TMP (Figure 6) lacks the glutamic acid side-chain, which is the characteristic feature of the nonclassical antifolate. TMP possesses higher selectivity of binding to

bacterial DHFR ($IC_{50} = 7 \text{ nM}$ for *E. coli*) than human DHFR ($IC_{50} = 490000 \text{ nM}$) and is used for the treatment and prophylaxis of uncomplicated urinary tract infections and upper respiratory infections caused by pathogens such as *Proteus mirabilis*, *Escherichia coli*, and *Klebsiella* species;^{4, 113, 122, 123} It is also a first line drug for the treatment of *P. carinii pneumonia* (PCP) in combination with sulfamethoxazole,¹²⁴ which blocks the conversion of PABA to FH_2 through the inhibition of dihydropteroate synthase. The more potent *P. carinii* DHFR inhibitors like PTX ($IC_{50} = 19.3 \text{ nM}$) and TMQ ($IC_{50} = 42 \text{ nM}$) lack selectivity (Figure 6).¹²⁴⁻¹²⁶

Recent study showed that *P. jirovecii* is the real opportunistic pathogen that infects human, while *P. carinii* is the pathogen that is derived from and infects rats.⁶⁸ According to Cody *et al*⁶⁹, the recombinant human-derived pneumocystis DHFR (*P. jirovecii* DHFR) differs from rat-derived *P. carinii* DHFR by 38% in amino acid sequences.

4.2.2 *Toxoplasma gondii* (*T. gondii*) DHFR

T. gondii is a DHFR-TS bifunctional enzyme with the DHFR domain located at the N-terminus and the TS domain is at the C-terminus.¹²⁷ A junction polypeptide separates the two domains. The protozoan parasite *T. gondii* is a ubiquitous organism capable of infecting a wide range of vertebrate hosts, including man. Toxoplasmosis is a leading opportunistic pathogen associated with AIDS.^{128, 129} Although the crystal structures of *T. gondii* DHFR are not yet available, the primary structure of the DHFR-TS gene from *T. gondii* has been reported by Roos.¹³⁰

The K_m for *T. gondii* DHFR ($IC_{50} = 4.6 \pm 4.3 \text{ }\mu\text{M}$) is similar as that for rat liver DHFR ($IC_{50} = 20 \text{ }\mu\text{M}$). Several DHFR inhibitors such as TMQ ($IC_{50} = 10 \text{ nM}$), PTX

(IC₅₀ = 4.3 nM) and TMP (IC₅₀ = 2.8 μM) (Figure 6) are active against isolated *T. gondii* enzyme and against the growth of *T. gondii* cells in culture.¹²⁹

4.3 Representative DHFR Inhibitors

Some of the representative DHFR inhibitors have been reviewed and broadly divided into the following categories:

1. 6-5 Ring Fused Bicyclic Classical Analogues
2. Tricyclic Classical Analogues
3. Nonclassical DHFR Inhibitors

4.3.1. 6-5 Ring Fused Bicyclic Classical Analogues

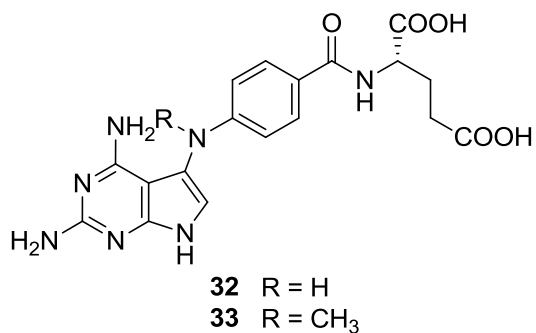


Figure 23. Pyrrolo [2,3-*d*]pyrimidine analogues **32** and **33**

Gangjee *et al.*^{151, 152} reported the pyrrolo[2,3-*d*]pyrimidine analogues of MTX (**32** and **33** in Figure 23). Both compounds inhibited the growth of CCRF-CEM human leukemia cell lines and showed potent inhibitory activities against *P. carinii* DHFR with IC₅₀ = 38 nM and 44 nM respectively

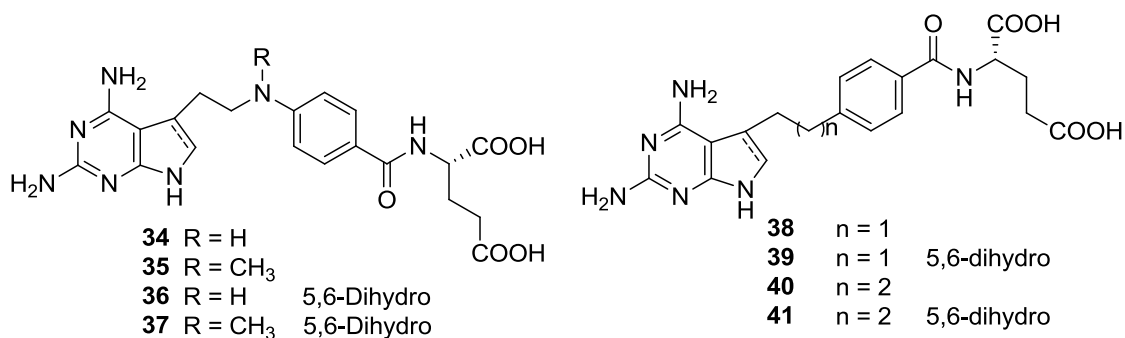


Figure 24. Pyrrolo [2,3-*d*]pyrimidine analogues **34-41**

Homologation of the methylene group of **32** and **33** in “bridge region” afforded **34** and **35** (Figure 24).¹⁵³ Both compounds are sub-micromolar inhibitors of human DHFR (IC₅₀ = 0.99 and 0.21 μM respectively). The reduced analogues **36** and **37** are 5-fold more potent than their 5,6-unsaturated counterparts (IC₅₀ = 0.20 and 0.049 μM).¹⁵³

The NH in the bridge region of **32** was replaced by a methylene group to afford compound **38**, which along with its 5,6-dihydro reduced analogue **39** (Figure 30) were potent cytotoxic agents in CCRF-CEM culture cell line (IC₅₀ = 1 ng/mL and 8 ng/mL respectively).¹⁵⁴⁻¹⁵⁶

Structural modifications of **34** and **36** afforded **40** and **41** (Figure 24).¹⁵⁷ Both compounds inhibited the growth of human epidermal carcinoma KB cells with IC₅₀ values of 0.27 ng/mL and 0.49 ng/mL, which were 18- and 10-fold lower than that of MTX (5.0 ng/mL) respectively.

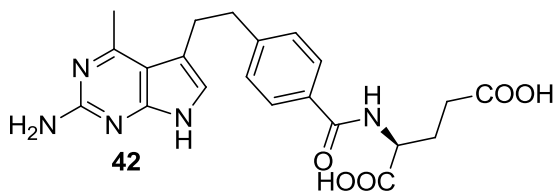


Figure 25. Pyrrolo[2,3-*d*]pyrimidine analogue **42**

As mentioned before, the 2,4-diaminopyrimidine structure is essential for potent DHFR inhibitory activity. However, the 4-methyl analogue of **42** (Figure 25) was found to be a potent dual TS-DHFR inhibitor.¹⁵⁸ This observation led to the postulation that **42** might bind to DHFR in a flipped model so that the pyrrole NH take the place of the 4-amino group of a regular DHFR inhibitor would have been (Figure 25).

This hypothesis was later confirmed by X-ray crystal structure of **42** (Figure 25) with *P. carinii* DHFR. Compound **42** binds to *P. carinii* DHFR in the proposed “2,4-diamino mode”. On the basis of molecular modeling, the 4- methyl group can increase hydrophobic interaction with Phe31 and Leu22 of human DHFR. Analog **42** inhibited the growth of CCRF-CEM and FaDu cells in culture with EC₅₀ values of 12.5 nM and 7.0 nM respectively. Metabolite protection studies indicated that **42** targets both TS and DHFR and that FPGS was essential for its activity.¹⁵⁸

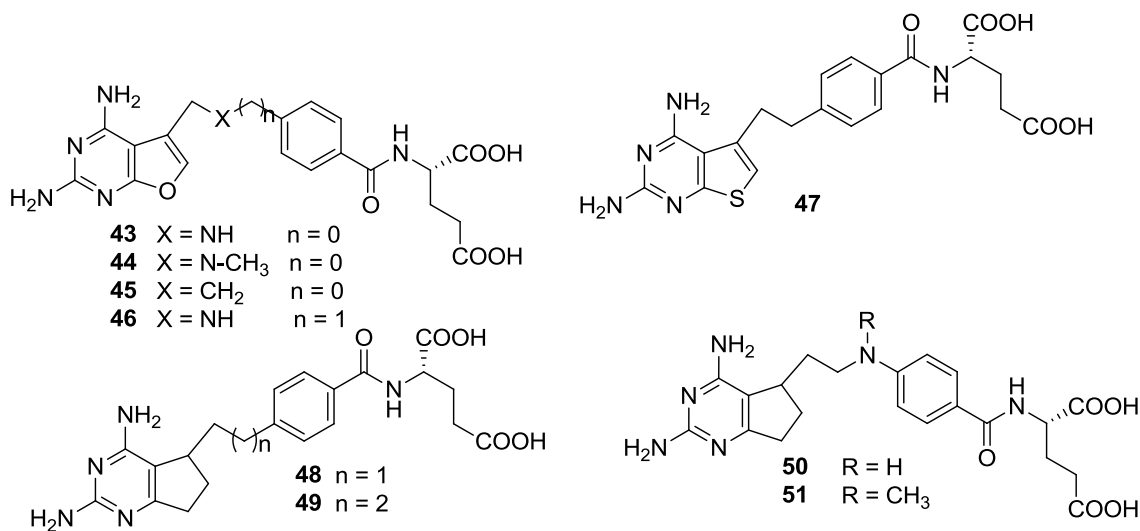


Figure 26. The structures of **43-51**

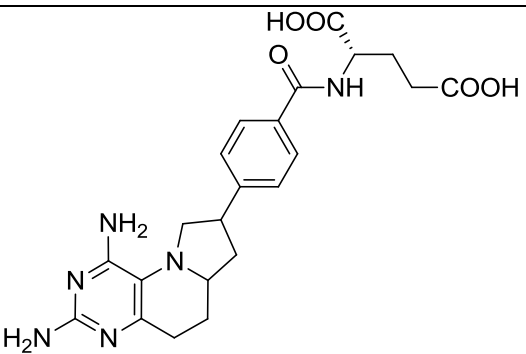
Gangjee *et al.*¹⁵⁹ reported the isosteric replacement of the pyrrole NH in **32**, **33** and **38** with an oxygen to afford classical furo[2,3-*d*]pyrimidine DHFR inhibitors **43-46**

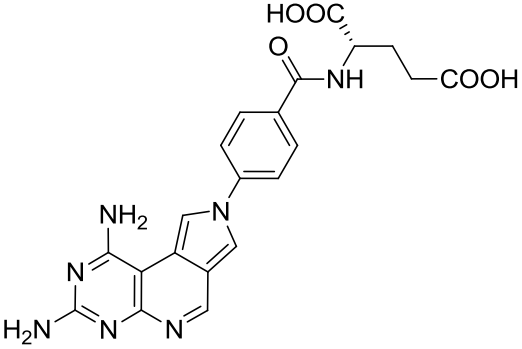
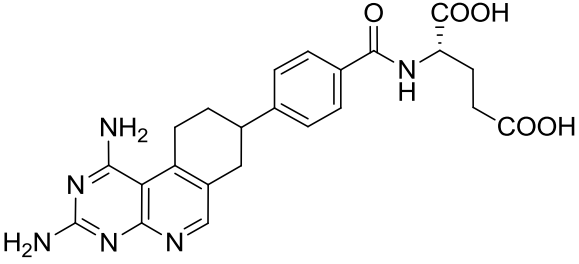
(Figure 26). Compounds **43** and **44** were moderate to good inhibitors of rh DHFR, ec DHFR and tg DHFR. The *N*-methyl analogue **44** was twice as potent as **43**. Compound **45** was much less potent than parent **38**. Addition of a methylene group in the bridge region of **43** afforded **46** (Figure 26).¹⁶⁰ This modification abolished the DHFR inhibitory activity.

Taylor *et al.*⁹⁹ reported the isosteric replacement of the pyrrole NH in **38** with a sulfur atom, and the resulting classical thieno[2,3-*d*]pyrimidine **47** (Figure 26) was inactive against tumor cell line growth in culture. Isosteric replacement of the pyrrole NH in **38** with a carbon atom, and the resulting classical dihydrocyclopenta[*d*]pyrimidine antifolates **48-51** (Figure 26) had bovine liver DHFR inhibitory activities comparable to that of MTX. Moreover, variation of the bridge region did not significantly affect the activities.^{161, 162}

4.3.4. Tricyclic Classical Analogues

Table 2. Tricyclic classical analogues

Compound and Structure	Activity	Ref.
 <p style="text-align: center;">52</p>	<p>IC₅₀ = 1.5 μM against lcDHFR Bovine DHFR and</p>	163

 <p style="text-align: center;">53</p>	<p>$IC_{50} = 39 \text{ nM}$ in Human leukemia cells (MTX: 12 nM)</p>	<p>164</p>
 <p style="text-align: center;">54</p>	<p>$K_i = 17 \text{ nM}$ against L1210 DHFR (MTX: 4.5 nM)</p>	<p>165</p>

4.3.5. Nonclassical DHFR Inhibitors

Some non-classical DHFR inhibitors show high potencies, which indicate that the *p*-aminobenzoylglutamic acid side chain is not essential for binding to DHFR. The discovery of TMQ and pyrimethamine as potential antibacterial and antimalarial agents has stimulated the research for new nonclassical antifolates. These agents can be used in anti-infective therapy since bacteria and protozoa synthesize folic acid *de novo* but do not utilize preformed folate. Moreover, these analogues are hydrophobic and do not utilize the folate active transport systems (such as FR or RFC). They are taken up by passive and/or facilitated diffusion and are not substrates for FPGS. Thus they overcome resistance encountered with classical inhibitors like PTX, which are associated with a defect in transport or FPGS activity. The main drawback of these new potent antifolates

is their lack of selectivity against DHFR derived from pathogens. Unfortunately, almost all the recently developed inhibitors follow this trend.

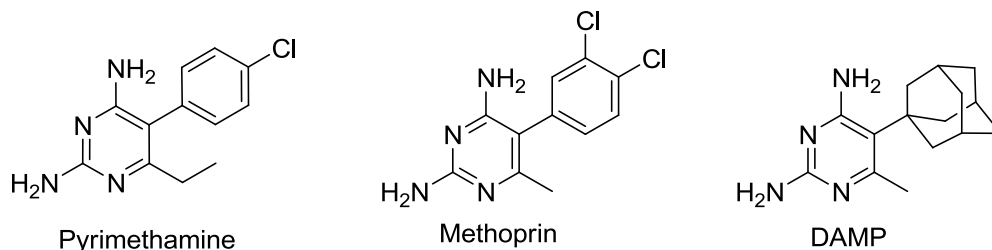


Figure 27. The structures of Pyrimethamine, Methoprin and DAMP

Pyrimethamine (Figure 27) is a potent selective inhibitor of plasmodia DHFR used in the treatment and prophylaxis of malarial.¹⁶⁶⁻¹⁶⁸ Two small structural changes to the pyrimethamine: changing the 6-ethyl group to a methyl group and introducing an additional chlorine substitution on the phenyl ring, led to Methoprin (Figure 27),¹⁶⁶ which is a potent vertebrate DHFR inhibitor and was clinically used to treat MTX resistant tumors along with the structurally related DAMP (Figure27)^{169, 170}

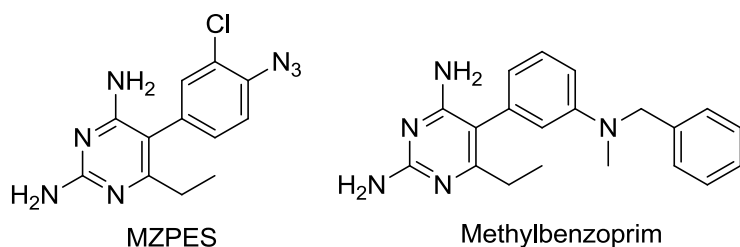


Figure 28. The structures of MZPES and Methylbenzoprim

Modifications of pyrimethamine in the 5-phenyl ring resulted in MZPES (Figure 28), which has completed Phase I clinical trial as an antitumor agent.¹⁷¹ Methylbenzoprim is one of the tightest binding nonclassical DHFR inhibitor ($K_i = 9$ pM against rat liver DHFR) known to date.¹⁷²

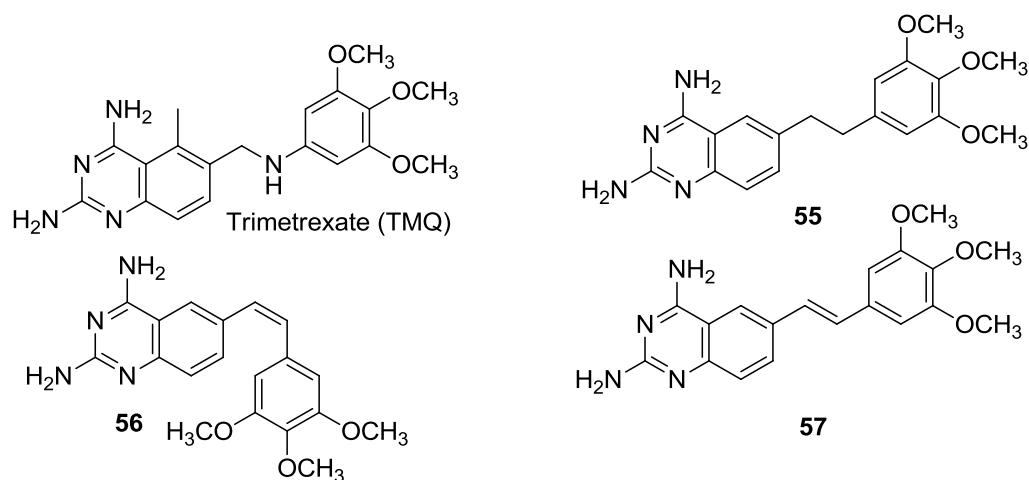


Figure 29. The structures of TMQ and **55-57**

Trimetrexate (TMQ) (Figure 29) is a potent inhibitor of human DHFR, displaying better antitumor activity than MTX.^{173, 174} It is also a potent inhibitor of *P. carinii* DHFR but is devoid of selectivity. TMQ (NeutrexinTM) has been approved for the treatment of *P. carinii* pneumonia. Replacing the nitrogen in the bridge region of TMQ with a carbon afford **55**¹⁷⁵ (Figure 29), which is a potent *ec* DHFR inhibitor. Harris *et al.*¹⁷⁵ reported the conformationally restrict analogues **56** and **57**. Compound **56** with the *Z*-configuration (cis) had better activity against *ec* DHFR than the *E*-isomer **57**.

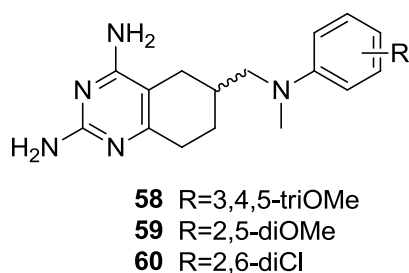


Figure 30. Tetrahydroquinazoline analogues **58-60**

Gangjee *et al.*¹⁷⁶ reported a series of 6-substituted tetrahydroquinazolines analogues of TMQ. Compounds **58-60** (Figure 30) were nanomolar inhibitors of *T. gondii* DHFR with 5-11 fold selectivity ratios as compared to *rl* DHFR.

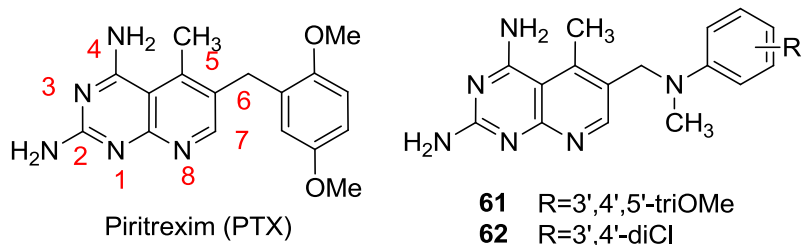


Figure 31. The structure of PTX and **61** and **62**

Piritrexim (PTX) is a potent inhibitor of *P. carinii* DHFR ($IC_{50} = 31$ nM) but is devoid of selectivity. It is now used as a second-line therapy in the clinic for moderate to severe PCP.¹⁷⁷ The 5-methyl group of PTX was important for high potency.¹⁷⁸ The removal of the 5-methyl group and/or the 2'5'-dimethoxy substituent both resulted in the decrease of activity.

Gangjee *et al.*¹⁷⁹ reported **61** and **62** which replaced the methylene bridge of PTX with CH_2NCH_3 (Figure 31). Compound **61** shows extremely potent inhibitory activity against *T. gondii* DHFR ($IC_{50} = 0.58$ nM) whereas **62** had excellent antitumor activity.

A large number of 6-5 bicyclic non-classical DHFR inhibitors including 2,4-diaminothieno[2,3-*d*]pyrimidines, 2,4-diaminopyrrolo[2,3-*d*] pyrimidines, and 2,4-diaminofuro[2,3-*d*]pyrimidines and purines have been reported in the literature.

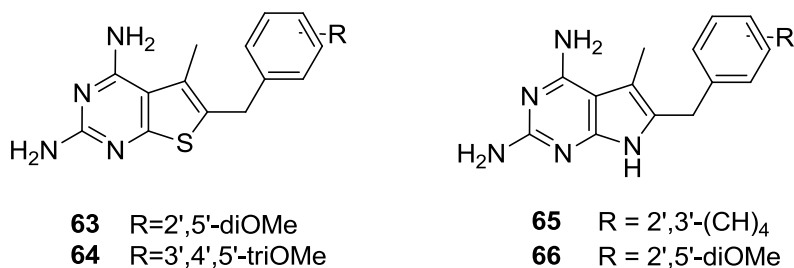


Figure 32. Pyrrolo and thieno[2,3-*d*]pyrimidine analogues **63-66**

Rosowsky *et al.*¹⁸⁰ reported a series of thieno analogs with a carbon atom bridge as bioisosteres of pyrido[2,3-*d*]pyrimidines (**63** and **64**) (Figure 32) as inhibitors of *P.*

carinii DHFR, *T. gondii* DHFR, and rat liver DHFR. Analogue **63** is the most potent in this series ($IC_{50} = 0.07\mu\text{M}$ against *T. gondii* DHFR) and **64** is the most selective for *T. gondii* DHFR (rl/tg = 81).

Gangjee *et al.*¹⁸¹ also reported a series of pyrrolo[2,3-*d*]pyrimidine analogues with different thiols substitution on the 6-position. Compounds **65** and **66** (Figure 32) are potent inhibitors of DHFR from opportunistic pathogens. It was found that disubstitution on the phenyl ring of the side chain was better for inhibiting *T. gondii* DHFR both in terms of potency and selectivity than the monosubstituted or unsubstituted phenyl analogues.¹⁸¹

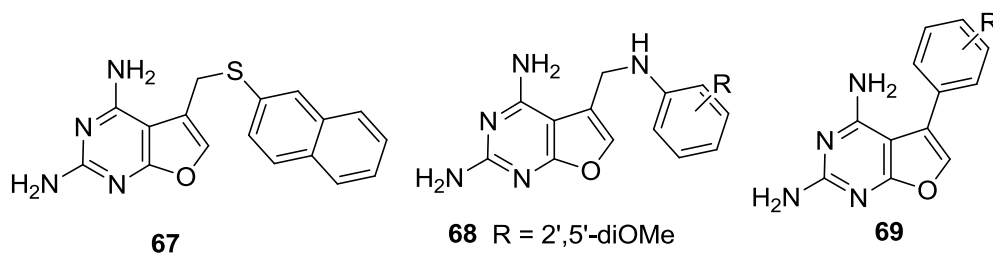


Figure 33. Furo[2,3-*d*]pyrimidine analogues **67-69**

Gangjee *et al.*^{182, 183} reported 2,4-diaminofuro[2,3-*d*]pyrimidines **67** and **68** (Figure 33) as potential DHFR inhibitors with good selectivity for both pcDHFR and tgDHFR compared to rat liver DHFR. Different analogues with variations in the bridge region indicate that a -CH₂-NH- or -CH₂-S- bridge connecting the lipophilic side chain were conducive for inhibiting *P. carinii* DHFR both for potency and selectivity. Analogue **67** is a potent inhibitor of *P. carinii* ($IC_{50} = 0.65\mu\text{M}$). In addition, compounds containing bicyclic moieties in the side chains were found to be conducive for *P. carinii* DHFR inhibition over analogues containing monocyclic or tricyclic moieties.

Dauzonne *et al.*¹⁸⁴ reported furo[2,3-*d*]pyrimidines **69** (Figure 33), in which the lipophilic side chains are attached directly at the 5-position, as inhibitors of DHFR from opportunistic pathogens. However, none of the analogs were found to have activity against *P. carinii* DHFR or *T.gondii* DHFR. Comparing their structures with **67** and **68** suggests that a direct phenyl substitution at 5-position decreased potency and selectivity for *T. gondii* DHFR.

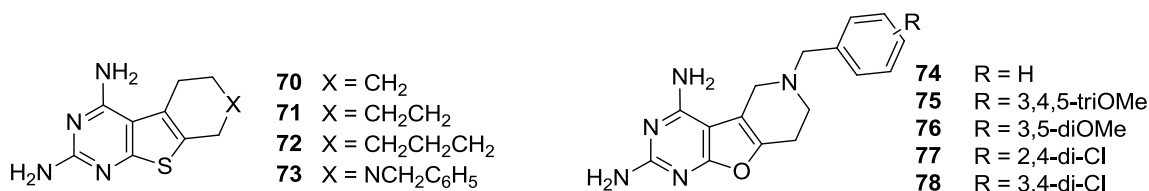


Figure 34. Tricyclic thieno and furo[2,3-*d*]pyrimidines **70-73** and **74-78**

Rosowsky *et al.*¹⁸⁰ reported tricyclic thieno[2,3-*d*]pyrimidines **70-73** (Figure 34) as inhibitors of *P. carinii* DHFR, *T. gondii* DHFR and rat liver DHFR. Although these analogues displayed potency in the micromolar range, they were non-selective. Gangjee *et al.*¹⁸⁵ also reported a series of moderately active tricyclic furo[2,3-*d*]pyrimidine DHFR inhibitors **74-78** (Figure 34).

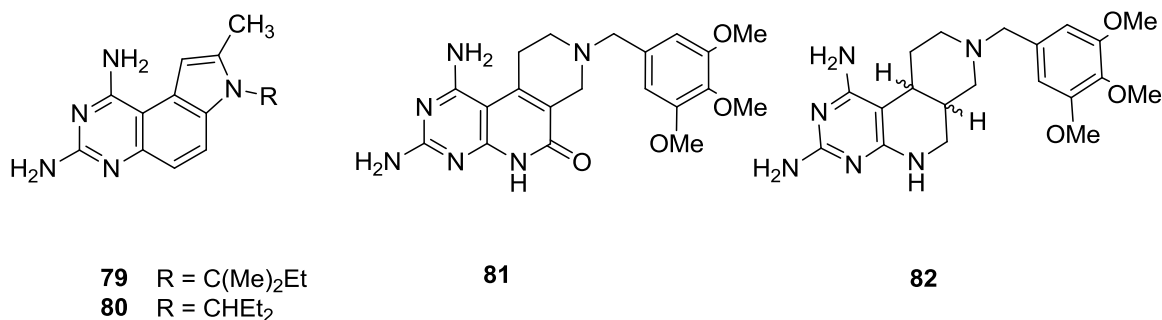


Figure 35. Tricyclic DHFR inhibitors **79-82**

A series of 7,8-dialkyl-1,3-diaminopyrrolo[3,2-*f*]quinazolines **79** and **80** (Figure 35) were reported by Kuyper *et al.*¹⁸⁶ as potential inhibitors of *P. carinii* DHFR, *T.*

Gondii DHFR and *C. albicans* DHFR. Compound **79** had a K_i of 0.0071 nM for *C. albicans* DHFR, while compound **80** had a K_i of 0.9 nM against *T. gondii* DHFR and an IC_{50} of 14 nM against *P. carinii* DHFR. Although they were extremely potent, they lacked selectivity for *P. carinii* DHFR or *T.gondii* DHFR. Gangjee *et al.*¹⁸⁷ reported a novel tricyclic pyrimido[4,5c][2,7] naphthyridone **81** (Figure 35) and the corresponding naphthyridines **82** as conformationally restricted inhibitors of DHFR. Although they displayed potency in the micromolar range, none of these were selective for *P. carinii* DHFR or *T.gondii* DHFR.

5. FOLYL POLY- γ -GLUTAMATE SYNTHETASE (FPGS)

FPGS is an ATP-dependent enzyme and has both cytosolic and mitochondrial forms. It catalyzes the addition of several equivalents of glutamic acid to the γ -carboxyl group of folate cofactors and classical antifolates containing the γ -carboxyl group, which leads to high intracellular concentration, utilizing ATP and magnesium.^{20, 25, 188} In cases of RTX and PMX, the inhibitory activity of the polyglutamylated form are 60-fold 130-fold more potent than their monoglutamate forms respectively.¹⁹¹⁻¹⁹⁴ FPGS has three functions in folate homeostasis *via* polyglutamation: (1) The polyglutamic acid chain is hydrophilic and anionic which prevents the efflux of folates and antifolates from the cell; (2) maintains high intracellular concentrations in most cases and increases its affinity for TS; (3) allows the accumulation of folates in the mitochondria that are required for glycine synthesis.¹⁸⁸

Tumor cells develop resistance to antifolates that depend on polyglutamylation for activation either for retention within tumor cells or to increase inhibitory activity against the target folate-dependent enzyme(s), both of which contribute to the antitumor activity

of the analogue.^{30, 195-199} Resistance to the antifolates can be manifested by reduction at the level of FPGS activity. Moreover, long retention of polyglutamate forms of antifolates within normal cells may cause toxicity, thus limiting the usefulness of such antifolates.^{72, 196, 200, 202}

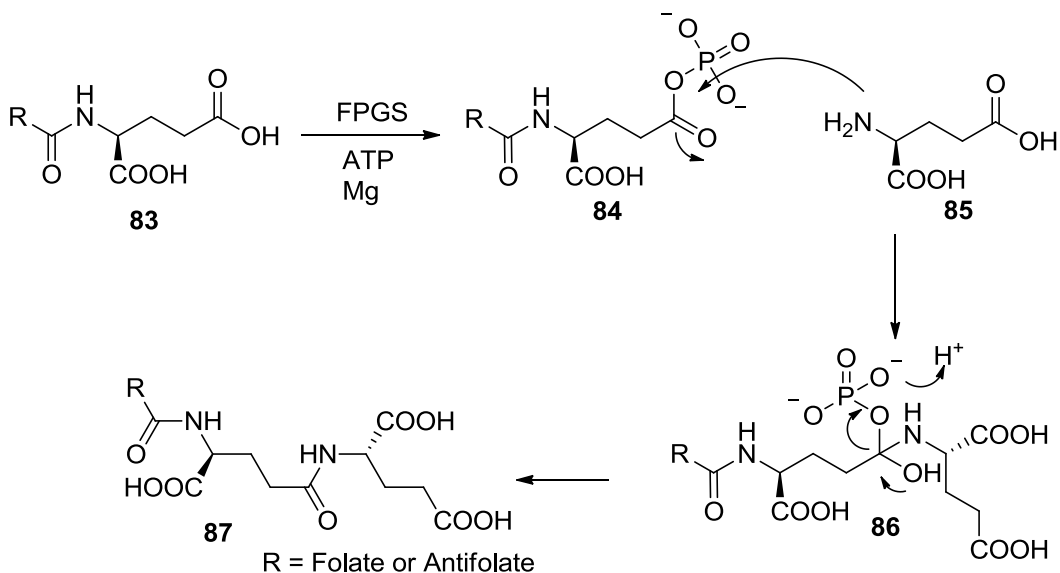


Figure 36. Mechanism of polyglutamylation by FPGS

The proposed catalytic mechanism of FPGS is shown in Figure 36. The mechanism involves the binding of the folate or antifolate to the protein followed by activation by Mg-ATP, and subsequent attachment of L-glutamate (Figure 36). FPGS catalyzes the formation of **84** as a result of an attack by the γ -COOH of folate or antifolates **83** by activation by Mg-ATP.²⁰³⁻²⁰⁵ Followed by the nucleophilic nitrogen of the L-glutamate **85** attacking the carbonyl group of **84**, resulting in a tetrahedral intermediate **86** which collapses to form **87** and inorganic phosphate.²⁰⁵⁻²⁰⁷

6. Glycinamide-ribonucleotide Formyltransferase (GARFTase)

6.1 Enzyme description and Catalytic Mechanism

Glycinamide-ribonucleotide formyltransferase (GARFTase) is a folate-dependent enzyme in the *de novo* purine biosynthetic pathway. It catalyzes the formyl transfer reaction that converts GAR to fGAR in the purine biosynthesis pathway, utilizing N^{10} -formyl FH₄ as the cofactor. Since purines are crucial components of DNA and RNA, inhibition of enzymes in the *de novo* biosynthesis of purine has been considered an effective approach for cancer chemotherapy.

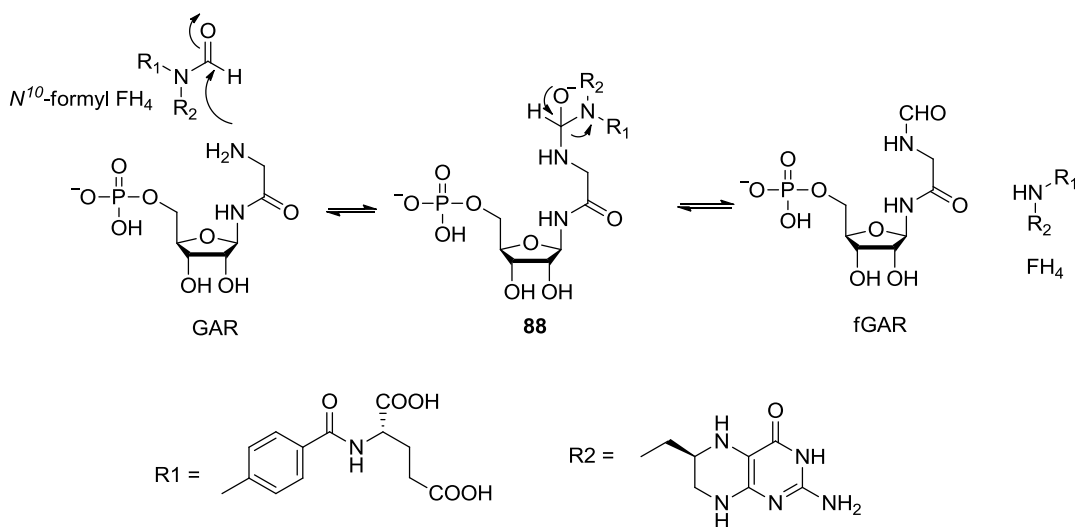


Figure 37. Proposed mechanism of GARFTase

The catalytic mechanism of GARFTase has been reported by Shim and co-workers (Figure 37).²⁰⁸ Nucleophilic attack by the amino group of GAR upon the formyl carbon of N^{10} -formyl FH₄ leads to the formation of the tetrahedral intermediate **88**, which converts to fGAR and FH₄, with the cleavage of the formyl carbon- N^{10} bond.

6.2 The structure of GARFTase

Human GARFTase is located at the C-terminus of a trifunctional enzyme human GART (*HsGART*) encoded by *purD-purM-purN* with a molecular weight of 108 kD (1010 amino acids).²⁰⁹ The trifunctional polypeptide encodes GAR synthase (GARS, PurD, E.C. 6.3.4.13) and aminoimidazole ribonucleotide synthetase (AIRS, PurM, E.C. 6.3.3.1) activities, in addition to GARFTase activity.²⁰⁹

The *E. coli* GARFTase structure was considered surrogate for its eukaryotic counterpart in the past, because *E. coli* and human GARFTase share a 38% sequence identity. However, recent kinetic and structural studies revealed a number of important differences between the human and *E. coli* enzymes.^{210,211} The human GARFTase domain of the trifunctional enzyme is readily available through cloning and overexpression.^{210, 212} In 2005, Smith and coworkers²¹¹ reported the three-dimensional structure of the GARTase domain from the human trifunctional enzyme which is useful for chemotherapeutic drug design. The structures of human GARFTase in complex with various ligands including β -GAR,²¹⁰ 10-trifluoroacetyl-5,10-dideaza-acyclic-5,6,7,8-tetrahydrofolic acid (10-CF₃CO-DDACTHF)²¹³, and a series of folate inhibitors²¹⁴ at different pH have also been reported.

Welin *et al.*²⁰⁹ recently reported the structures of two functional domains of *HsGART*: GARS and AIRS. Together with the previously reported the structures of the GARTase domain of *HsGART*,^{210,212} a complete structural characterization of the individual functional units of *HsGART* was achieved, which allows for a structural understanding of substrate specificity and catalytic mechanism, as well as for structure-based drug design. Although the construction of full-length *HsGART* *via* crystallization of the enzyme in its

intact trifunctional form was not successful, Welin and coworkers²⁰⁹ revealed the overall architecture of the trifunctional protein at low-resolution by combining small angle X-ray scattering (SAXS) data with the high-resolution crystal structures.

6.3 Representative GARFTase Inhibitors

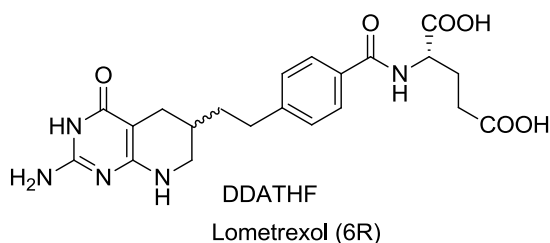


Figure 38. The structure of DDATHF

The discovery of 5,10-dideazatetrahydrofolic acid (DDATHF) (Figure 38), the first potent and selective GARFTase inhibitor and antitumor agent validated GARFTase as an anti-cancer drug target. DDATHF exhibits potent, broad-spectrum activity *in vivo* against solid murine and human tumors. As the first GARFTase inhibitor to be brought to clinical evaluation, lometrexol, the 6R diastereomer of DDATHF, exhibited promising preclinical activity *in vivo* against solid murine and human tumors. However, its clinical development was limited by serious cumulative toxicity,²¹³ which was attributed to accumulation of polyglutamate metabolites in normal tissues.

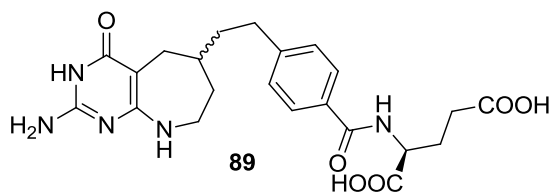


Figure 39. The structure of **89**

Compound **89** was reported by Taylor and coworkers²¹⁴ as an analogue of lometrexol. The addition of one methylene unit in the tetrahydropyridine ring of lometrexol provided additional conformational mobility in the bicyclic system.

Compound **89** had a K_i of 147 nM against murine trifunctional GARFTase and an IC_{50} of 47 nM *in vitro* cell growth inhibition assay.

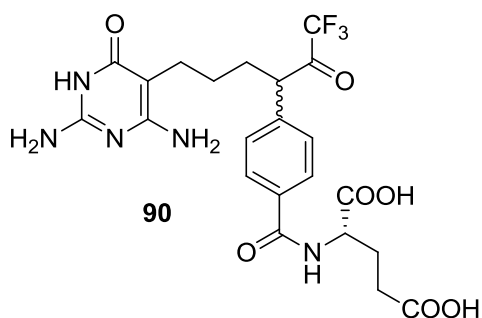


Figure 40. The structure of **90**

A novel GARFTase inhibitor **90** (Figure 40) was designed based on the crystal structure of rh GARFTase. Compound **90** shows potent inhibitory activity against recombinant human GARFTase ($K_i = 16$ nM). Moreover, in CCRF-CEM cell line, compound **90** ($IC_{50} = 16$ nM) shows 10-fold increase in potency than lometrexol. It was found that FPGS polyglutamylation of **90** caused its higher potency.²¹⁵

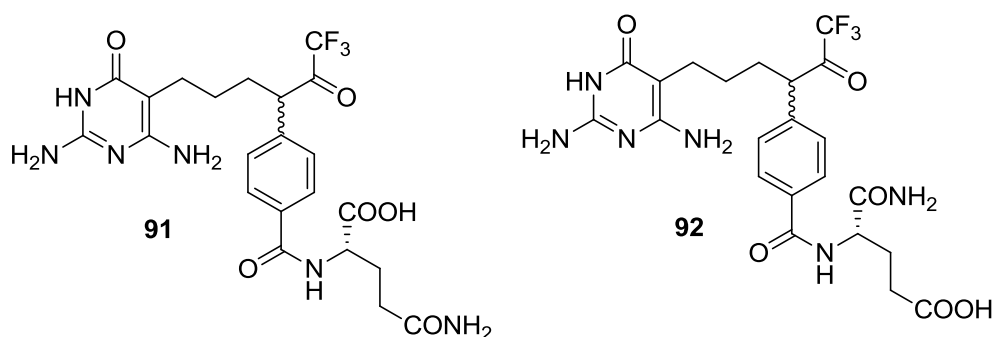


Figure 41. The structure of **91** and **92**

To further explore the role of side chain polyglutamation for activity, Demartino and coworkers²¹⁶ reported α - and γ -carboxamides **91** and **92** (Scheme 41) as analogues of **90**. Compound **91** was a potent and selective inhibitor of rhGARFTase ($K_i = 56$ nM) and active in cellular assays ($IC_{50} = 300$ nM), which indicated that incorporating the γ -carboxylic acid as a carboxamide had little effect on the enzyme inhibitory activity.

Moreover, the high potency of **91** suggested that selectivity and efficacy of GARFTase do not rely on FPGS polyglutamation. However, compound **92** was much less potent with K_i value 4.8 μM and inactive in cellular assays, which indicated that α -carboxylic acid was crucial for enzyme binding.

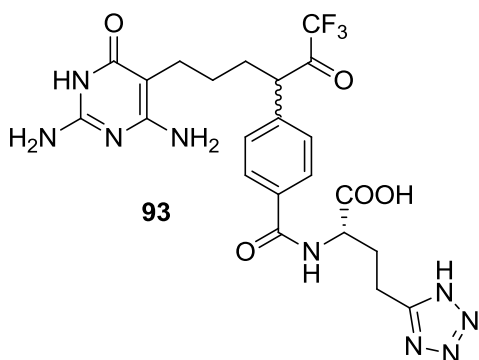


Figure 42. The structure of **93**

The replacement of the γ -carboxylic acid in **90** with a tetrazole afforded **93** (Figure 42),²¹⁷ which is a potent rhGARFTase inhibitor (rh GARFTase $K_i = 130$ nM) and is active *in vitro* ($IC_{50} = 40$ nM, CCRF-CEM). Although Compound **93** was 4-fold less potent against rhGARFTase and 2.5-fold less potent in cellular assays compared with **90**, the activity of **93** does not rely on FPGS polyglutamation and thus allowed its selection as a candidate for *in vivo* examination.

II. CHEMICAL REVIEW

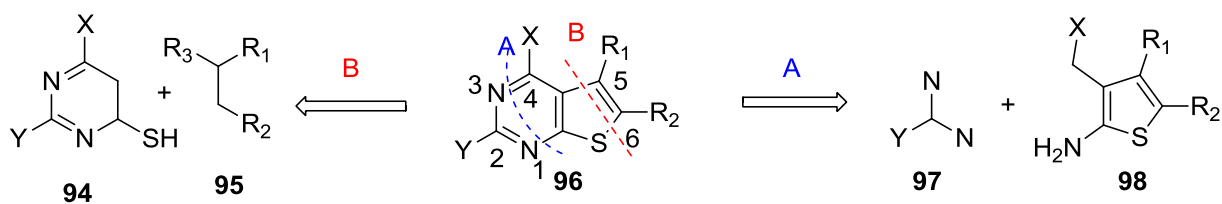
Isosteric replacement of the pyrrolo ring with a thieno ring provides an increase in ring size that more closely approximates the pteridine, 6-6 fused ring system of the natural folates cofactors. Thus, a series of thieno[2,3-*d*]pyrimidine derivatives have been designed and synthesized.

The chemistry related to the present work is reviewed and includes synthetic approaches to the following systems.

- A. Synthesis of thieno[2,3-*d*]pyrimidines
- B. Synthesis of thieno[3,2-*d*]pyrimidines
- C. Seyferth-Gilbert homologation and Bestmann's reagent
- D. Cross coupling reactions

A. Thieno[2,3-*d*]pyrimidines

Scheme 1. Retro-synthetic analysis of thieno[2,3-*d*]pyrimidines

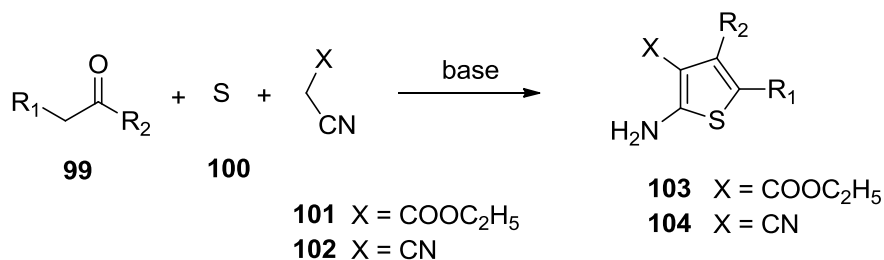


The synthetic strategy for the construction of thieno[2,3-*d*]pyrimidines includes two categories (Scheme 1):

1. From thiophene precursors (Route A)
2. From pyrimidine precursors (Route B)

1. From thiophene precursors (Route A)

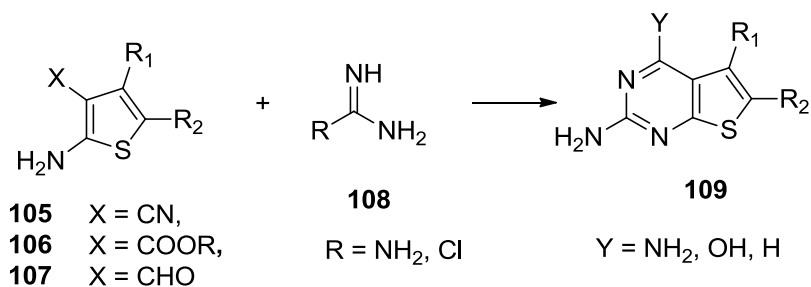
Scheme 2. Synthesis of thiophene **103** and **104**



The general method (Route A) involves the use of 2-amino thiophenes **103** and **104** (Scheme 2) has proven to be very fruitful and allowed synthetic entries into several thieno pyrimidine analogues with varying substitution patterns. The synthesis of derivatives *via* this general route is discussed below (Scheme 3-16). Reaction of ketones or aldehydes **99** with ethyl cyanoacetate **101** or malononitrile **102** and sulfur **100** in the presence of base (triethylamine or morpholine) under the general procedure of Gewald and coworkers²¹⁸ gave the expected 2-amino thiophenes **103** or **104**.

1.1 Condensation to obtain 2-amino-5,6-disubstituted thieno[2,3-*d*]pyrimidines

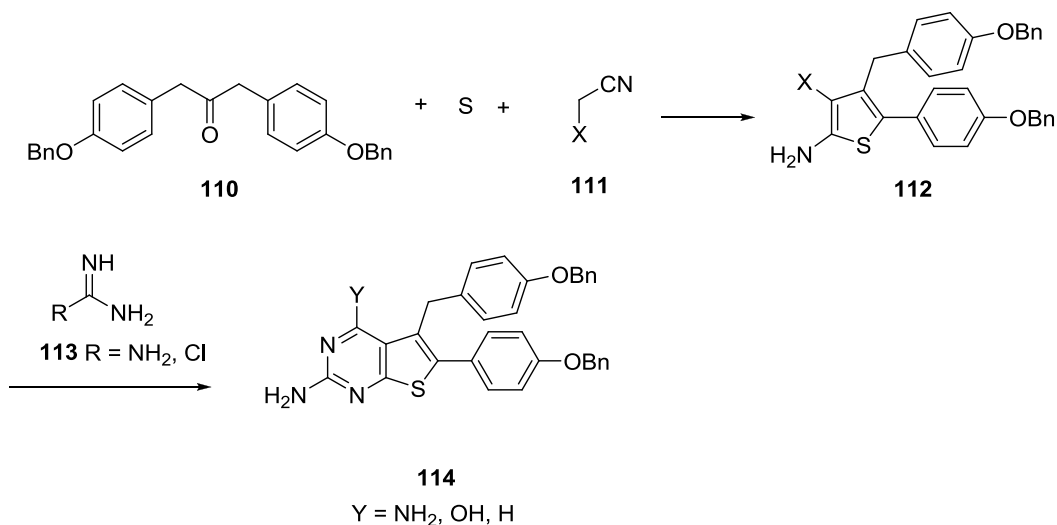
Scheme 3. Synthesis of thieno[2,3-*d*]pyrimidine **109**



2-Amino-5,6-disubstituted thieno[2,3-*d*]pyrimidines **109** (Scheme 3) were reported to be synthesized *via* cyclocondensation of appropriate thiophenes **105-107** with an amidine derivative **108**,^{219, 220} which can be guanidine (R = NH₂) or chloroformamidine

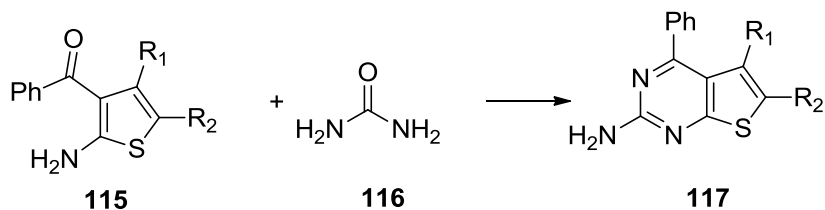
hydrochloride (R = Cl). The nature of the X substitution in thiophene **105-107** determines the substitution pattern at 4-position (Y at the C4-position) in **109**; when X = CN, COOR or CHO, the cycliation reaction affords **109** with Y = NH₂, OH or H respectively.

Scheme 4. Synthesis of thieno[2,3-*d*]pyrimidine **114**



Zhang and coworkers²²⁰ successfully utilized this strategy to synthesize 2-amino-4,5,6-trisubstituted thieno[2,3-*d*]pyrimidines **114** (Scheme 4). Thiophene intermediate **112** was synthesized from ketone **110**, sulfur and **111** *via* the Gewald reaction.²¹⁸ The target 2-amino-5,6-disubstituted thieno[2,3-*d*]pyrimidines **114** were obtained *via* the condensation of **112** with guanidine (R = NH₂) or chloroformamide hydrochloride (R = Cl).

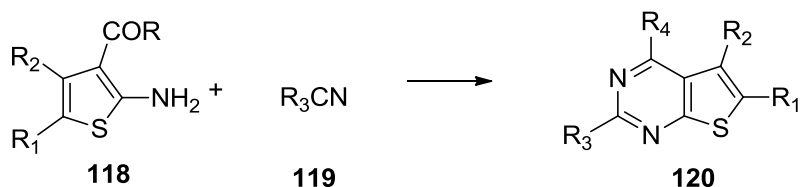
Scheme 5. Synthesis of thieno[2,3-*d*]pyrimidine **117**



In 1980, a novel synthesis of 2-amino-4-phenyl substituted thieno[2,3-*d*]-pyrimidines **117** was reported by Ishikawa and coworkers.²²¹ Urea **116** was utilized for condensation with aminocarbonyl thiophenes **115** to afford **117**.

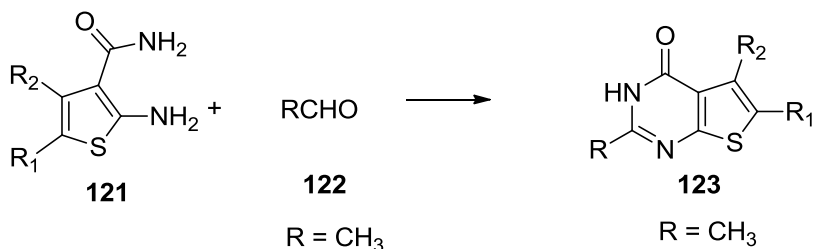
1.2 Condensation to obtain 2-methyl-5,6-disubstituted thieno[2,3-*d*]pyrimidines

Scheme 6. Synthesis of thieno[2,3-*d*]pyrimidine **120**



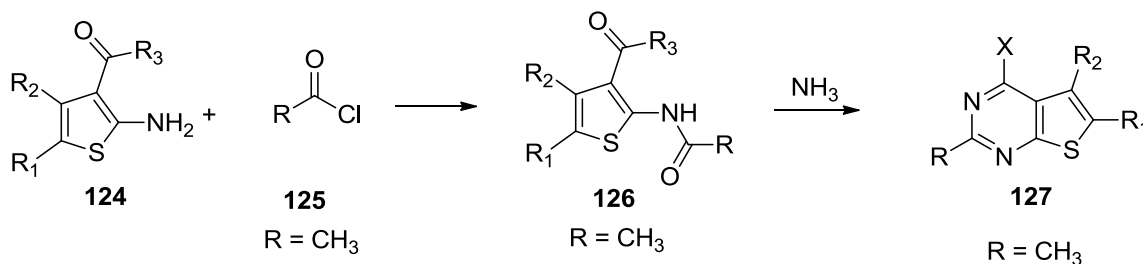
A novel facile method was reported by Dave and coworkers.²²² Substituted nitriles **119** as cyclization reagents reacted with 2-amino-4-carboxylate thiophenes **118** in the presence of HCl to afford thieno[2,3-*d*]pyrimidines **120** (Scheme 6). Different substitutions can be introduced in the 2-position depending on the substitution groups of the carbonitrile in **119**. For example, when acetonitrile was used in the reaction, 2-methyl-5,6-disubstituted thieno[2,3-*d*]pyrimidines was obtained. When the carboxylate substitution R of **118** is a good leaving group such as OR or NH₂, the cyclization product has an OH group at the 4-position.

Scheme 7. Synthesis of thieno[2,3-*d*]pyrimidine **123**



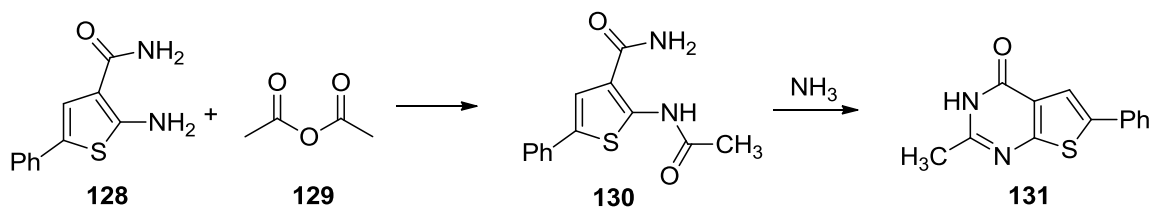
A novel approach for the synthesis of 2-substituted thieno[2,3-*d*]pyrimidines was reported by Cruceyra and coworkers.²²³ The 2-substituted-4-oxo- thieno[2,3-*d*]pyrimidines **123** (Scheme 7) were synthesized by the condensation of thiophene **121** and aldehyde **122**. The R group of **122** can be an alkyl or aromatic substitution. 2-Methyl-5,6-disubstituted thieno[2,3-*d*]pyrimidines **123** were obtained when the R group is a methyl group.

Scheme 8. Synthesis of thieno[2,3-*d*]pyrimidine **127**



A modified approach was reported by Corral and coworkers²²⁴ for the synthesis of thieno[2,3-*d*]pyrimidine in 1978, using acid chlorides as the cyclization reagent instead of an aldehyde (Scheme 8). The amino group of the thiophene **124** attacked the carbonyl group of acid chloride **125** to form the intermediate amide **126**, which cyclized with NH₃ to afford thieno[2,3-*d*]pyrimidines **127**. Good leaving groups, such as OCH₃, at R₃ position in **124** resulted in OH substitutions at the X position in **127**. When acetyl chloride was used as the reactant, 2-methyl-5,6-disubstituted thieno[2,3-*d*]pyrimidines **127** was obtained after cycliation.

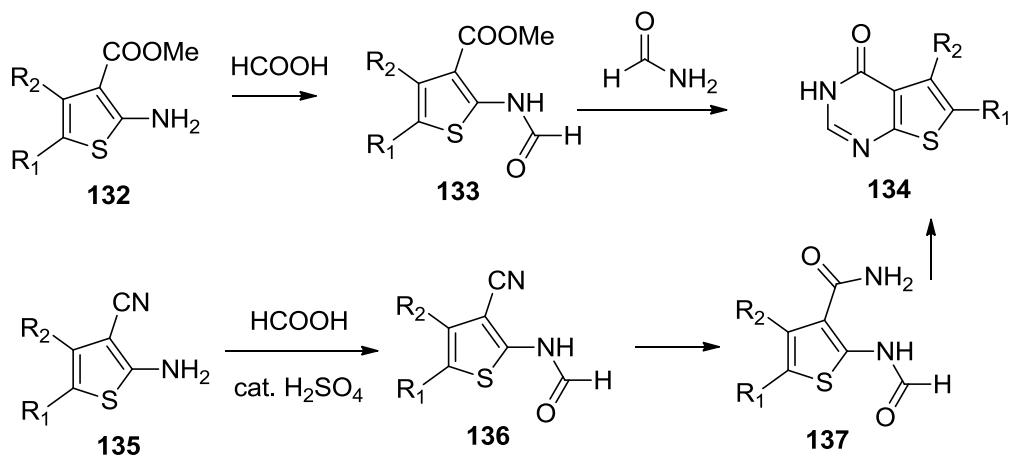
Scheme 9. Synthesis of thieno[2,3-*d*]pyrimidine **131**



Konno and coworkers²²⁵ reported the synthesis of **131**, 2-methyl-4-oxo-6-phenylthieno[2,3-*d*]pyrimidine, via the condensation of thiophene **128** with acetic anhydride **129**, followed by cyclization with NH_3 (Scheme 9).

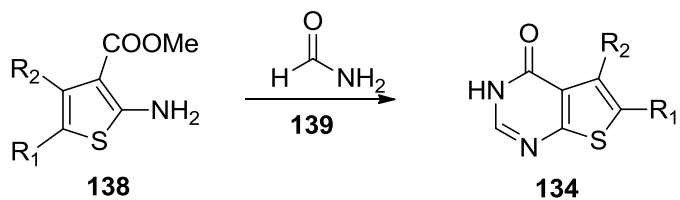
1.3 Condensation to obtain 2-unsubstituted-5,6-bisubstituted thieno[2,3-*d*]pyrimidines

Scheme 10. Synthesis of thieno[2,3-*d*]pyrimidine **134**



Hesse and coworkers²²⁶ reported the synthesis of thieno[2,3-*d*]pyrimidine **134**. The reaction of thiophene **132** and formic acid gave **133**, which cyclized with formamide to afford **134** (Scheme 10). Compound **134** was also obtained *via* the reaction of thiophene 4-carbonitrile **135** and formic acid in the presence of a catalytic amount of H_2SO_4 under microwave irradiation condition (Scheme 10).

Scheme 11. Synthesis of thieno[2,3-*d*]pyrimidine **134**

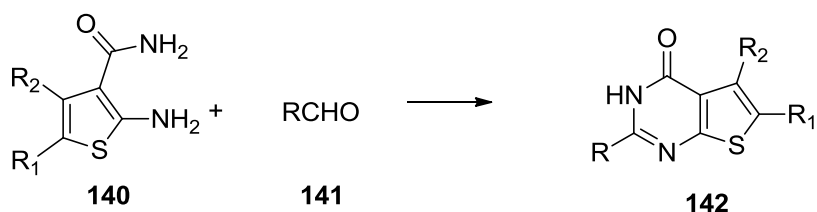


Recently, Horiuchi and coworkers²²⁷ reported the one-pot synthesis of **134**.

Thiophene **138** reacted with formamide afforded **134** in good yield (Scheme 11).

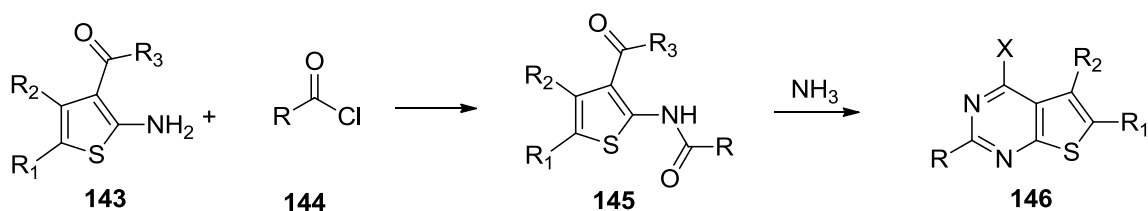
1.4 Condensation to obtain other 2-substituted thieno[2,3-*d*]pyrimidines

Scheme 12. Synthesis of thieno[2,3-*d*]pyrimidine **142**



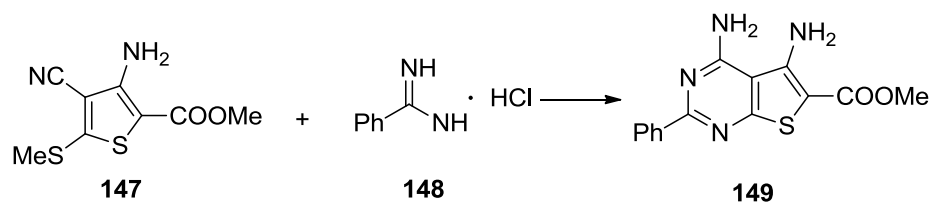
Cyclocondensation of **140** with various substituted aldehydes provided thieno[2,3-*d*]pyrimidines **142** with different substitutions at 2-position (Scheme 12). Depending on the nature of **141**, the R groups in **142** can be an alkyl or an aryl group.

Scheme 13. Synthesis of thieno[2,3-*d*]pyrimidine **146**



An acid chloride **144** was used instead of an aldehyde as the cyclization reagent in the cyclocondensation with **143** to afford various 2-substituted thieno[2,3-*d*]pyrimidines **146** (Scheme 13).

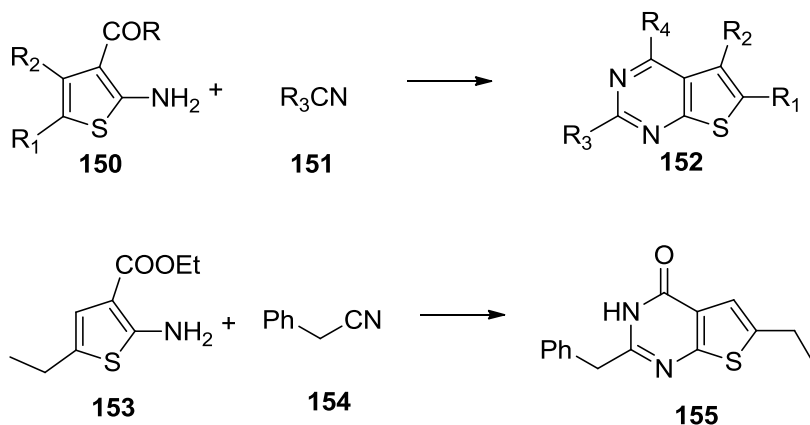
Scheme 14. Synthesis of thieno[2,3-*d*]pyrimidine **149**



In 1998, Briel and coworkers²²⁸ reported the synthesis of 2-phenyl substituted thieno[2,3-*d*]pyrimidine **149** via the condensation of thiophene **147** with benzamidine hydrochloride

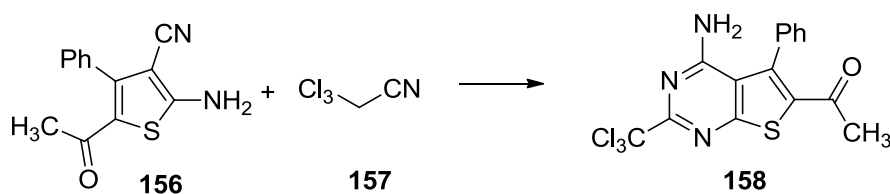
148 (Scheme 14).

Scheme 15. Synthesis of thieno[2,3-*d*]pyrimidine **155**



Scheme 15 shows the synthesis of 2-benzyl-4-oxo-6-substituted thieno[2,3-*d*]pyrimidine **155**, employing the same method as shown in scheme 6.²²²

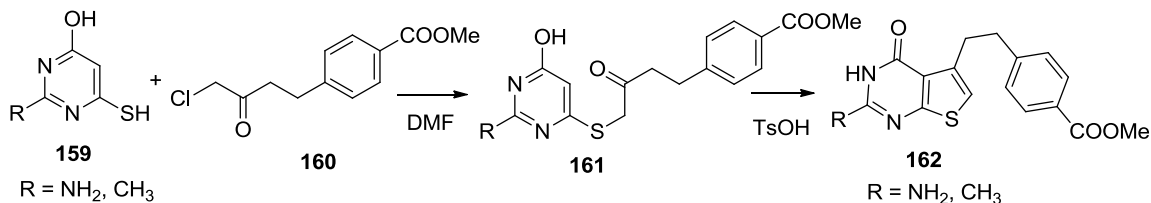
Scheme 16. Synthesis of thieno[2,3-*d*]pyrimidine **158**



Changing the thiophene 4-carboxylate **153** to the thiophene 4-carbonitrile **156** and condensation with trichloro-acetonitrile **157** affords 2-trichloromethyl-4-amino thieno[2,3-*d*]pyrimidine **158** (Scheme 16).²²²

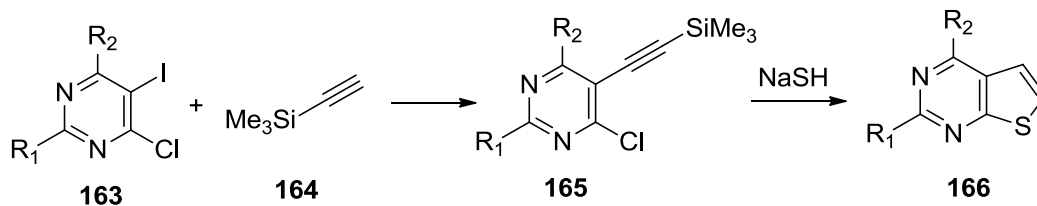
2. From pyrimidine precursors (Route B)

Scheme 17. Synthesis of thieno[2,3-*d*]pyrimidine **162**



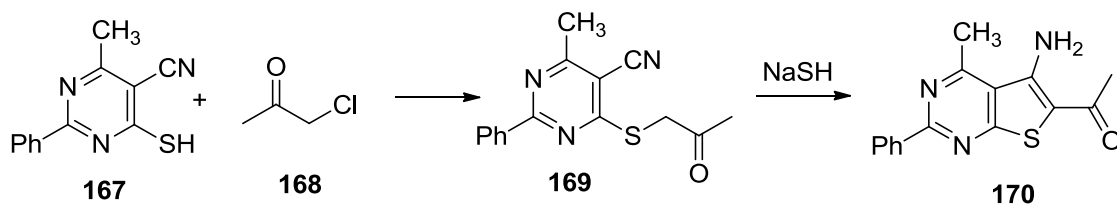
Taylor and coworkers²²⁹ reported the synthesis of the classical TS inhibitor **162** as an analogue of pemetrexed. Condensation of 2-substituted-4-hydroxy-6-mercaptopyrimidine **159** with the α -chloro ketone gave pyrimidine sulfide **161**, which cyclized to give **162**, in the presence of *p*-toluenesulfonic acid.

Scheme 18. Synthesis of thieno[2,3-*d*]pyrimidine **166**



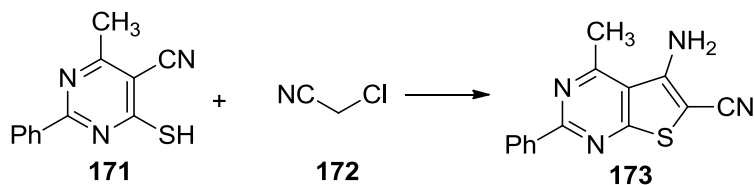
A novel approach for the synthesis of thieno[2,3-*d*]pyrimidine **166** was reported by Sakamoto and coworkers²³⁰ in 1986 (Scheme 18). The intermediate **165** was synthesized by Sonogashira coupling between iodopyrimidines **163** and ethynyltrimethylsilane **164**. Compound **165** then cyclized to give **166** in the presence of NaSH.

Scheme 19. Synthesis of thieno[2,3-*d*]pyrimidine **170**



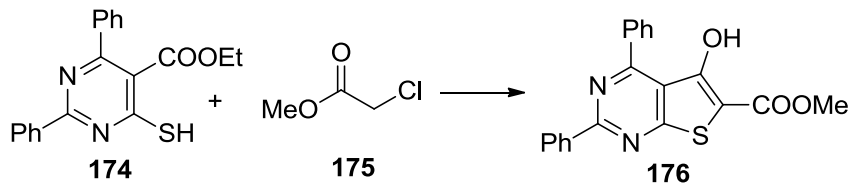
In 1988, a novel approach for the synthesis of the thieno[2,3-*d*]pyrimidine **170** via a cyclization reaction of 5-cyano-6-mercaptopyrimidines **167** and chloroacetone **168** (Scheme 19) was reported by Ried and coworkers.²³¹ Compound **169** was the key intermediate in the reaction, which was further cyclized in the presence of NaSH to give **17**

Scheme 20. Synthesis of thieno[2,3-*d*]pyrimidine **173**



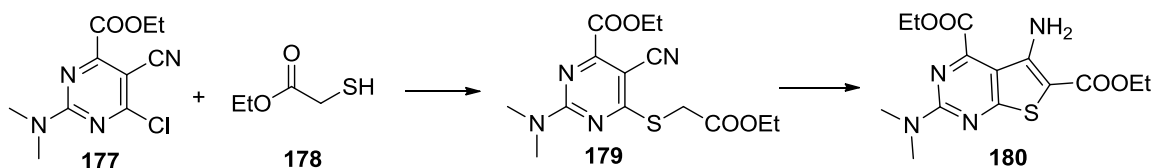
Similarly, El-Dean and coworkers²³² utilized chloro-acetonitrile **172**, instead of chloro-acetone **168**, with **171** to afford 5-amino-4-methyl-2-phenyl-thieno[2,3-*d*]pyrimidine-6-carbonitrile **173** (Scheme 20).

Scheme 21. Synthesis of thieno[2,3-*d*]pyrimidine **176**



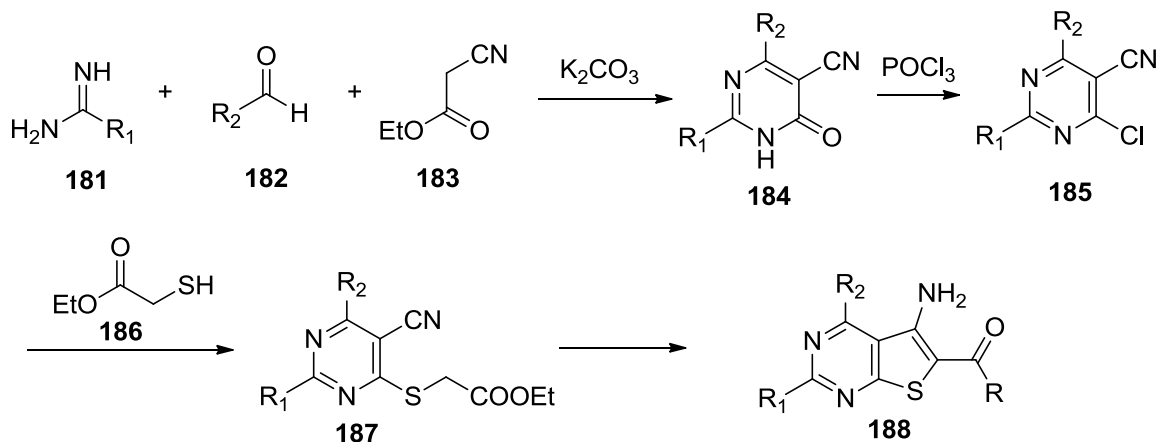
As shown in Scheme 21, Briel and coworkers²³³ reported a modified strategy to synthesize **176**. 5-Ethylester-6-mercaptopyrimidines **174** cyclized with chloroacetic acid methyl ester **175** to afford the thieno[2,3-*d*]pyrimidine **176** with a 5-hydroxy group instead of a 5-amino (Scheme 21).

Scheme 22. Synthesis of thieno[2,3-*d*]pyrimidine **180**



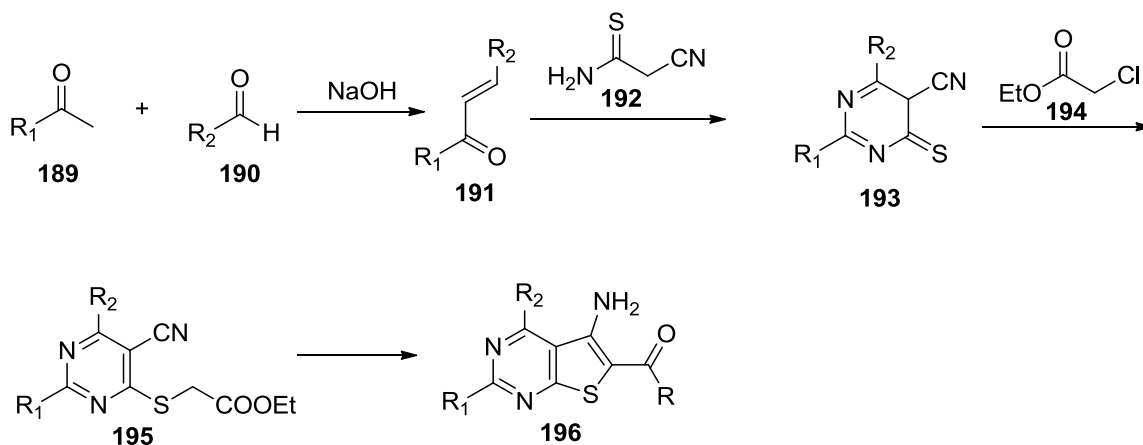
Based on the cyclization reaction shown in Scheme 19, a modified method was developed by Ried and coworkers (Scheme 22).²³⁴ 5-Carbonitrile-6-chloropyrimidine **177** reacted with ethyl 2-mercaptoacetate **178** to form intermediate **179**, which was further cyclized to afford **180**.

Scheme 23. Synthesis of thieno[2,3-*d*]pyrimidine **188**



Similarly, Van Straten and coworkers²³⁵ reported the synthesis of **188** (Scheme 22). Condensation of **181** with aldehyde **182** and ethyl cyanoacetate **183** in the presence of K_2CO_3 gave pyrimidone **184**, which was then treated with $POCl_3$ followed by base-mediated nucleophilic substitution and cyclization to afford **188** (Scheme 23).

Scheme 24. Synthesis of thieno[2,3-*d*]pyrimidine **196**

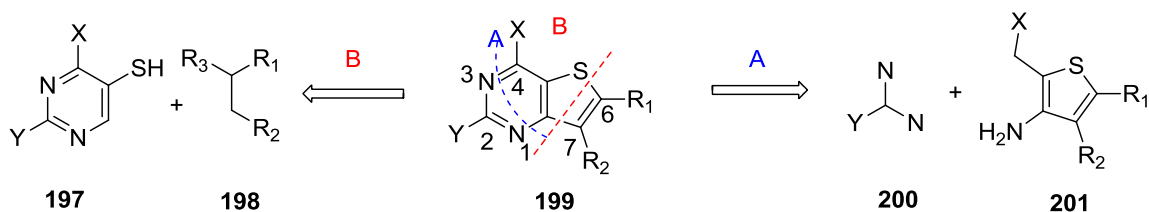


Van Straten and coworkers²³⁵ also reported the synthesis of **196** by the procedure depicted in Scheme 24. α,β -Unsaturated ketones, obtained by aldol condensations,

reacted with 2-cyanothioacetamide **192** to afford thiopyridones **193**, which underwent nucleophilic substitution and cyclization to afford **196** (Scheme 24).

B. Thieno[3,2-*d*]pyrimidines

Scheme 25. Retro-synthetic analysis of thieno[3,2-*d*]pyrimidines

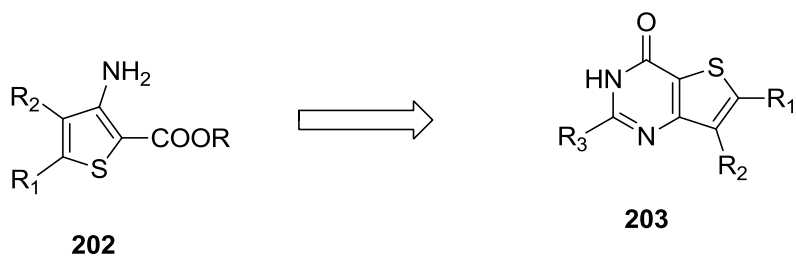


The synthetic strategy for the construction of thieno[3,2-*d*]pyrimidines includes two categories (Scheme 25):

1. From thiophene precursors (Route A)
2. From pyrimidine precursors (Route B)

1. From thiophene precursors (Route A)

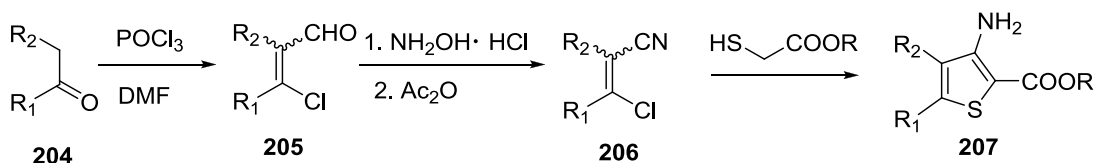
Scheme 26. General routes for the synthesis of thieno[3,2-*d*]pyrimidines from key thiophene intermediate **202**



$R_3 = \text{NH}_2, \text{SH}, \text{Alkyl}, \text{H}, \text{OH},$

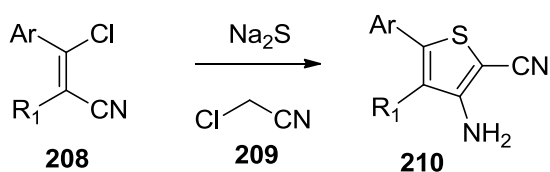
Route A: 3-amino-2-carboxyl-5,6-disubstituted thiophenes **202** (Scheme26) are the key intermediates for the synthesis of thieno[3,2-*d*]pyrimidines **203** with varying substitution patterns.

Scheme 27. Synthesis of key thiophene intermediate **207**



Migianu and Kirsch²³⁶ reported the synthesis of **207** from α -methylene ketones **204** by the procedure depicted in Scheme 27. α -Methylene ketones **204** were converted to β -chloroacroleins **205** via Vilsmeier-Haack-Arnold reaction. β -Chloroacrylonitriles **206** were prepared via the reaction of **205** and hydroxylamine and subsequent dehydration in acetic anhydride. Condensation of **206** with methyl or ethyl thioglycolate in base gave the key intermediate **207** (Scheme 27).

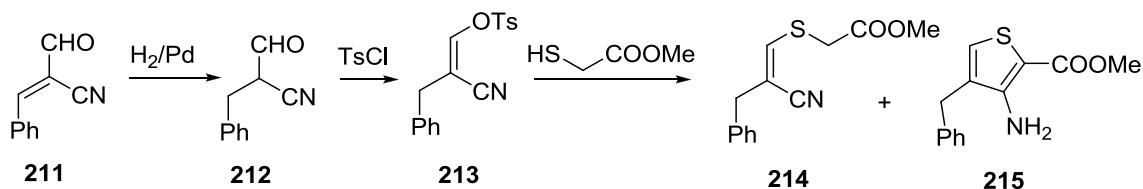
Scheme 28. Synthesis of key thiophene intermediate **210**



Recently, a similar method was reported by Thomae and coworkers.²³⁷ β -Chloroacrylonitriles **208** was synthesized by a previously described method (Scheme 27).

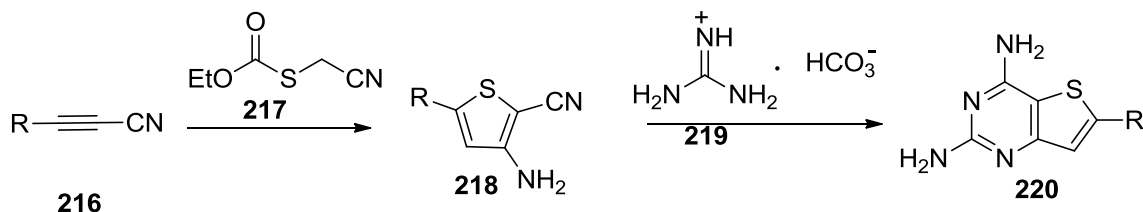
Condensation of **208** with Na₂S and β-chloroacrylonitrile afforded the key intermediate **210** (Scheme 28).

Scheme 29. Synthesis of key thiophene intermediate **215**



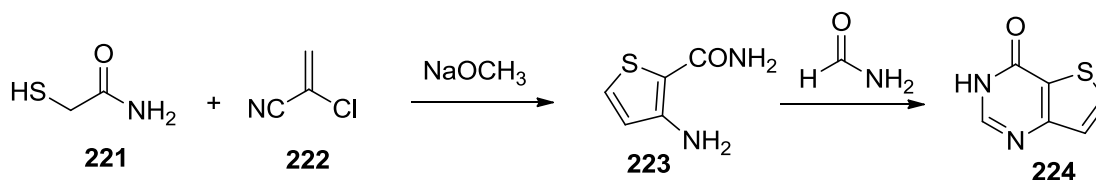
A novel approach to synthesize thiophenes **215** was reported by Ried and coworkers.²³⁸ The starting material **211** was reduced to **212**, which was treated with tosyl chloride to afford **213**. The tosyl group was displaced by methyl thioglycolate in methanol to give a mixture of **214** and **215** (Scheme 29). Cyclization of **215** similar to **207** afforded thieno[3,2-*d*]pyrimidines.

Scheme 30. Synthesis of thieno[3,2-*d*]pyrimidine **220**



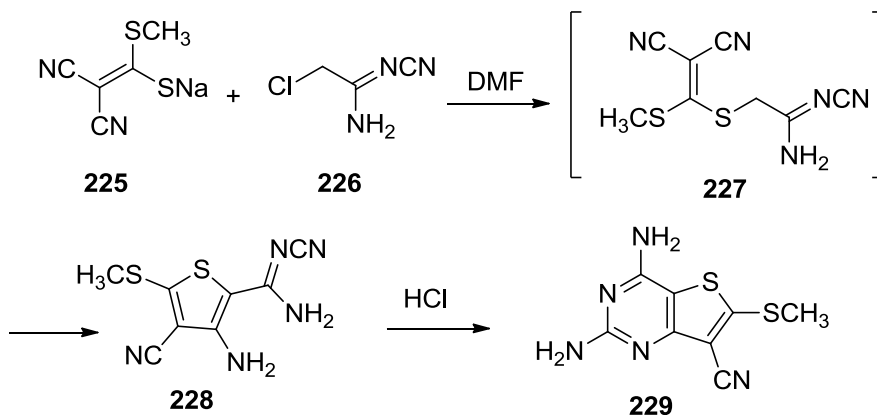
Ren and coworkers²³⁹ introduced an improved synthesis of **220** (Scheme 30). The *in situ* generated sodium mercaptoacetonitrile reacted with **216** to give thiophene **218**, which in turn reacted with guanidine carbonate to afford **220**. It is a general approach to convert *o*-aminonitriles to 2,4-diaminopyrimidines via the cyclization with guanidine.

Scheme 31. Synthesis of thieno[3,2-*d*]pyrimidine **224**



Peng and coworkers²⁴⁰ reported the synthesis of **224**. Cyclization of formamide and **223**, synthesized according to a literature procedure²⁴¹, afforded thieno[3,2-*d*]pyrimidine **224** (Scheme 31).

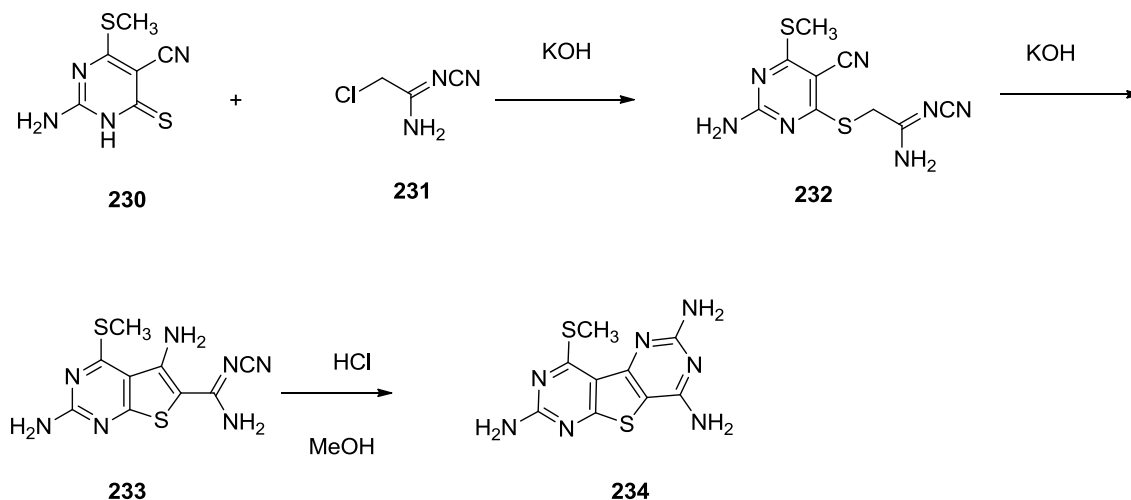
Scheme 32. Synthesis of thieno[3,2-*d*]pyrimidine **229**



Artyomov and coworkers²⁴² used *N*-cyanochloroacetamide **226** to synthesize fused pyrimidines. Regioselective alkylation of thiolate **225** at the S-atom afforded intermediate **227**, which then underwent a Thorpe cyclization to give aminothiophene **228**. Compound **228** under acid catalysis condition was converted to diaminopyrimidine **229** (Scheme 32).

2. From pyrimidine precursors (Route B)

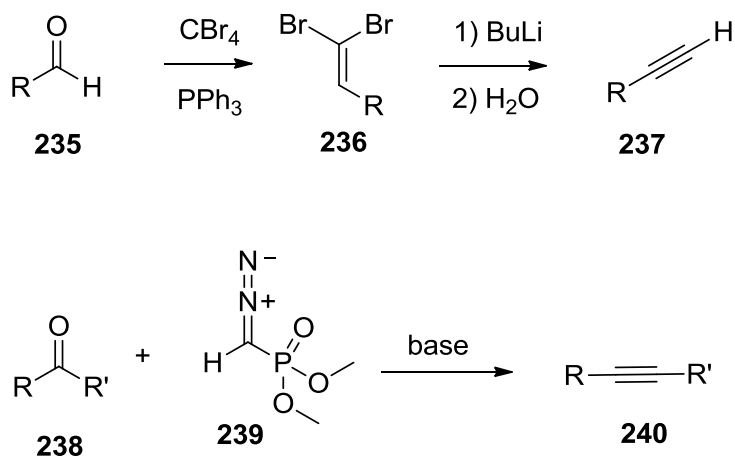
Scheme 33. Synthesis of pyrimidothieno[3,2-*d*]pyrimidine **234**



N-cyanochloroacetamide **231** was also used in the synthesis of a variety of substituted pyrimidines.²⁴² As shown in Scheme 33, **231** reacted with **230** to form **232**, which was cyclized to give the bicyclic thienopyrimidine **233** and then further cyclized to tricyclic pyrimidothienopyrimidine **234** (Scheme 33).

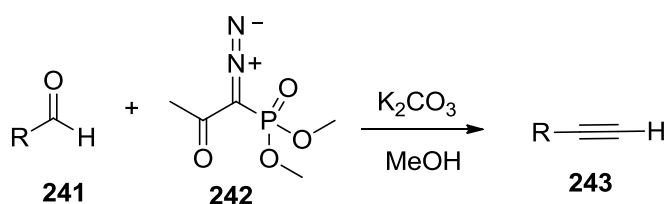
C. Seyferth-Gilbert homologation and Bestmann's reagent

Scheme 34. Corey-Fuchs reaction and Seyferth-Gilbert reaction



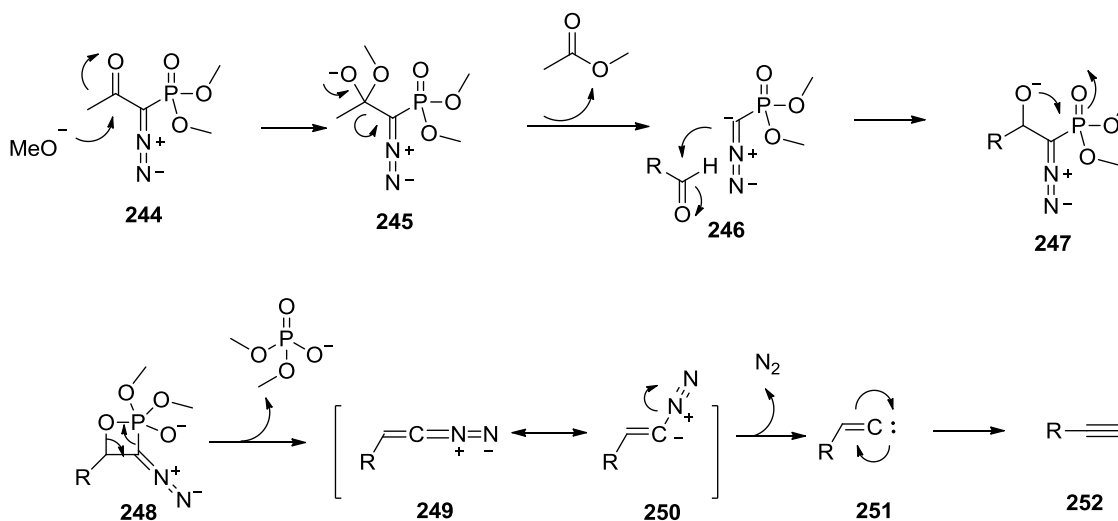
Terminal alkynes are extremely useful in organic transformations including Sonogashira couplings,²⁴³ Favorskii reaction,²⁴⁴ azide alkyne Huisgen cycloaddition to give triazoles.²⁴⁵ The Corey-Fuchs reaction²⁴⁶ and Seyferth-Gilbert reaction^{247, 248} have been employed in the conversion of aldehydes or ketones to alkynes that have one additional carbon than the starting material. However, the Corey-Fuchs reaction requires strong base for dehydrohalogenation of the intermediate **237** (Scheme 34) at low temperature, which limits its use. Seyferth-Gilbert reaction of a ketone or aldehyde with dimethyl (diazomethyl)phosphonate **239** in base affords alkynes (Scheme 34) in one step. Reagent **239** is often called the Seyferth-Gilbert reagent. It should be prepared freshly and isolated just prior to metalation.

Scheme 35. Bestmann-Ohira modification



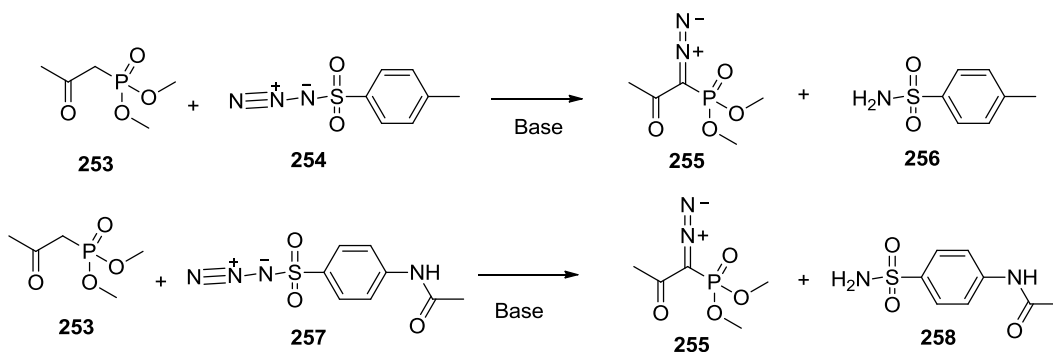
Recently, Bestmann²⁴⁹ and Ohira²⁵⁰ reported a modification to the Seyferth-Gilbert reaction. They utilized dimethyl 1-diazo-2-oxopropylphosphonate **242**, which is also called the Bestmann-Ohira reagent, instead of **239**. Under this mild reaction condition, reagent **242** *in situ* generated the anion of **239** by acyl cleavage and the aldehyde is converted to alkyne without the use of strong base.

Scheme 36. proposed mechanism for Seyferth-Gilbert reaction



Under base condition, the methoxy group attacks the carbonyl of the Bestmann-Ohira reagent **244** to form intermediate **245**, which cleaves to form methyl acetate and **246**. Anion **246** then reacts with aldehyde through a mechanism similar to the Wittig reaction to form oxaphosphatane **248**. Elimination of the phosphate anion gave the vinyl diazo-intermediate **249** and **250**. Elimination of nitrogen gas afforded the vinyl carbene **251**, which on rearrangement forms the desired alkyne **252** (Scheme 36).²⁵¹

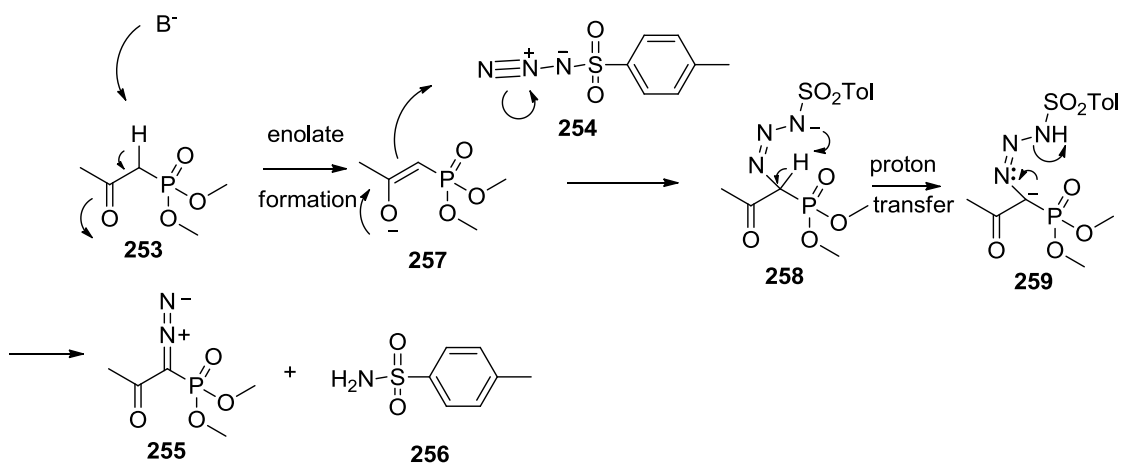
Scheme 37. Preparation of the Bestmann-Ohira reagent



Tosyl azide **254** is the most frequently used reagent for diazo transfer. Callant and coworkers²⁵² reported the synthesis of **255** *via* tosyl azide (Scheme 37). However, tosyl

azide was found to be most hazardous, of highest sensitivity and largest heat of decomposition.²⁵³ Recently, *p*-acetamidobenzenesulfonyl azide (*p*-ABSA) **255** (Scheme 37) has been used for the preparation of the diazo compounds.²⁵⁴ It is cheap, safe and ease of removal of the byproduct *p*-acetamidobenzenesulfonamide **258** through filtration. *p*-ABSA **257** reacted with **253** to afforded the Bestmann-Ohira Reagent in good yield.

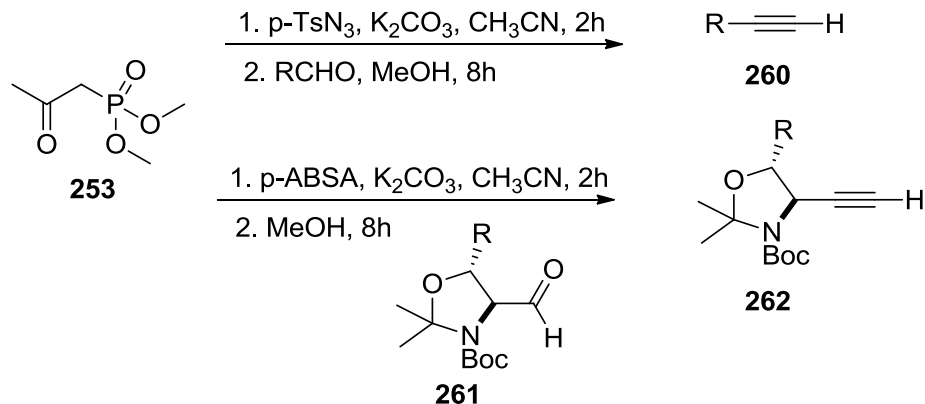
Scheme 38. Proposed mechanism for the Bestmann-Ohira reagent preparation



The proposed mechanism for Bestmann-Ohira reagent preparation reaction is listed in Scheme 38. The base picks up a proton from **253** to form an enolate **257**, which attacks the azide **254**. With the leaving of the sulfonyl amide **256**, the desired Bestmann-Ohira reagent is obtained.

Roth and coworkers,²⁵⁵ and Meffre and coworkers²⁵⁶ reported an improved one-pot reaction, which uses the *in situ* generation of the Bestmann-Ohira reagent for the reaction with the aldehyde.

Scheme 39. Improved one-pot reaction



Commercially available **253** and tosyl azide or *p*-ABSA are mixed in a suspension of K_2CO_3 in CH_3CN . After stirring for 2 h, the aldehyde, dissolved in methanol, was added to the above solution to afford the desired alkynes (Scheme 39).²⁵⁵ Meffre and coworkers applied this one-pot reaction to the compounds with stereogenic centers **261** without loss of optical purity in the resulting alkynes **262** (Scheme 39).²⁵⁶

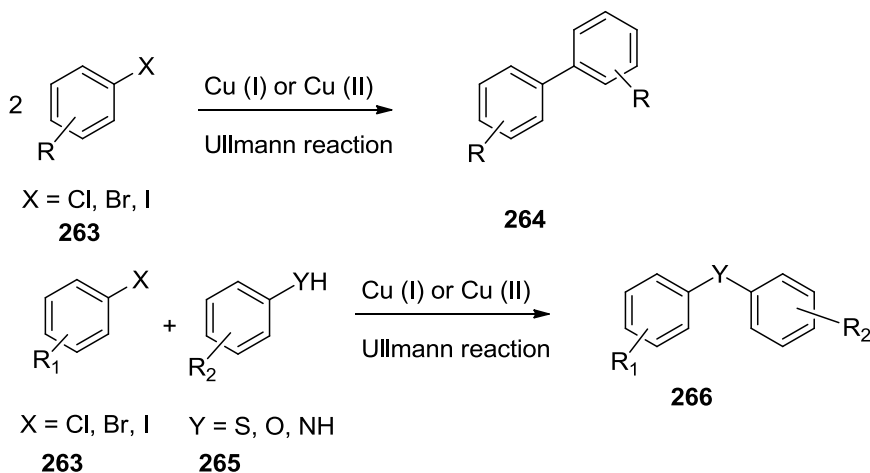
D. Cross coupling

Metal-catalyzed cross coupling reactions have been widely used in reactions involving C-C, C-H, C-N, C-S and C-P bonds formation.²⁵⁷⁻²⁵⁹ Various metal-catalyzed cross coupling reactions have been developed including Sonogashira coupling, Buchwald-Hartwig coupling, Suzuki coupling, Stille coupling, Ullmann coupling and others. Among the transition metals, palladium and copper are frequently used metal for organic synthesis.

1. Ullmann coupling
2. Sonogashira coupling
3. Buchwald type coupling

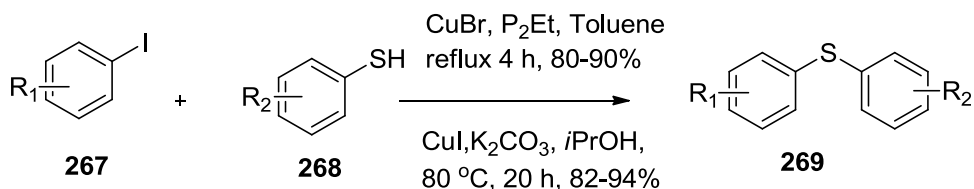
1. Ullmann coupling

Scheme 40. A general model for the Ullmann coupling



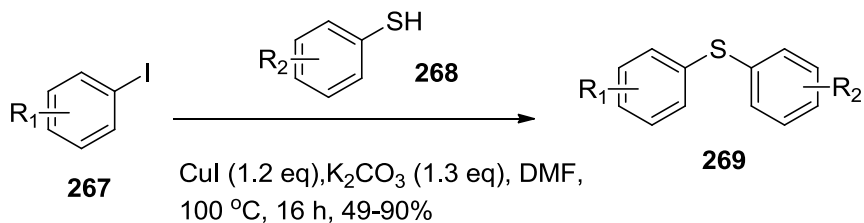
Ullmann coupling is a coupling reaction between aryl halides with copper (Scheme 40). The Ullmann coupling involves the formation of a C-O, C-N and C-S bond by the reaction between the aryl halide and phenol, aniline or thiophenol.²⁶⁰ The Ullmann coupling requires harsh reaction conditions, including high temperature (> 200 °C), strong bases, long reaction times. Cu (I) salts have been typically used as the metal source in Ullmann coupling.²⁶⁰ The bases used for this reaction can be K₂CO₃, Cs₂CO₃, NaOtBu.

Scheme 41. Ullmann coupling



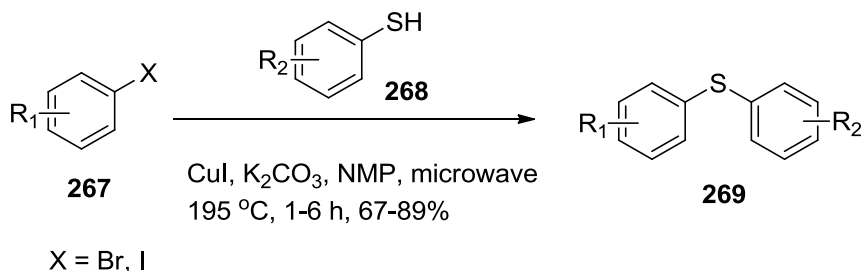
In 2003, Wu²⁶¹ and Miljanic²⁶² reported the formation of the C-S bond *via* Ullmann coupling (Scheme 41) at lower temperature (80-110 °C) with high yield.

Scheme 42. Ullmann coupling



Recently, Sperotto and coworkers²⁶³ reported a ligand free condition in Ullmann coupling (Scheme 42). Aryl iodides **267** reacted with aryl thiols using DMF or NMP as solvent, CuI (1.2 eq) and K₂CO₃ (1.3 eq) to afford **269** in high yield.

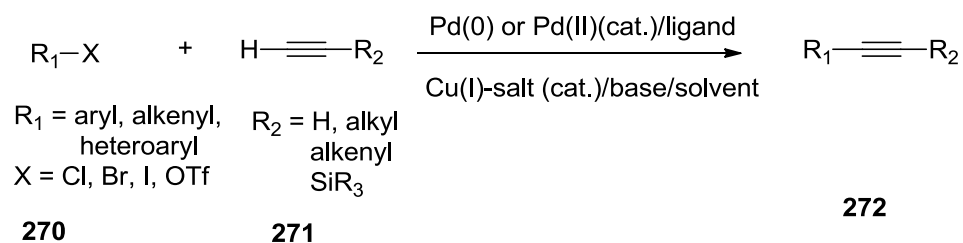
Scheme 43. Microwave assisted Ullmann coupling



Microwave assisted organic synthesis has been widely used in organic synthesis, resulting in faster and cleaner reactions. In 2002, Cherng and coworkers²⁶⁴ reported microwave assisted Ullmann coupling (Scheme 43). Substituted aryl bromides and iodides **267** reacted with aryl thiols in the presence of CuI, K₂CO₃ and NMP under microwave irradiation at 195 °C to afford **269** in 67-89% yield.

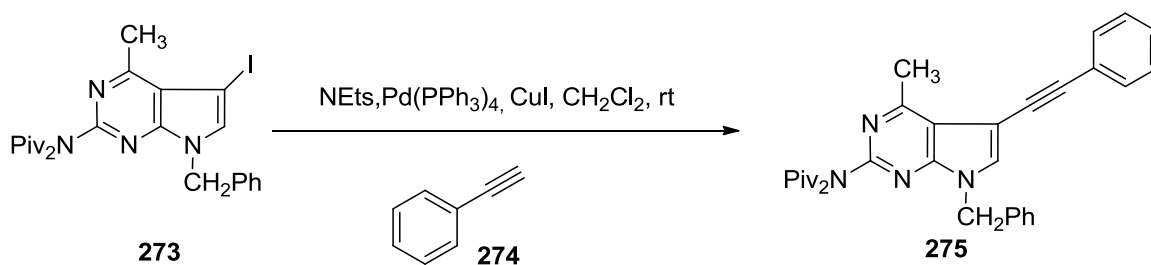
2. Sonogashira cross-coupling

Scheme 44. A general model for Sonogashira coupling



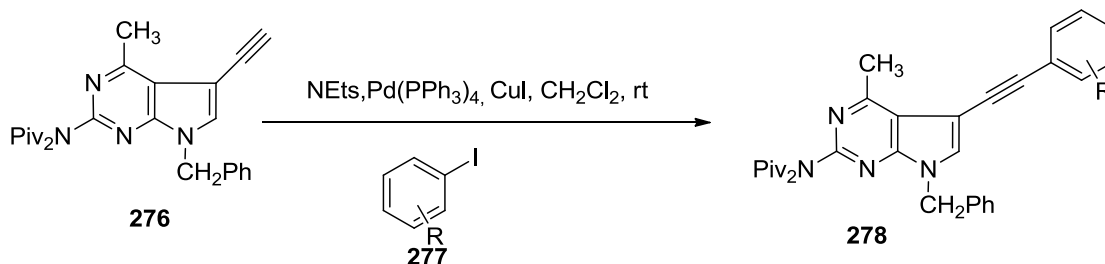
In 1975, Sonogashira *et al.*²⁶⁵ reported palladium catalyzed terminal alkynes in coupling reactions with aryl iodides or vinyl bromides (Scheme 44). The process of coupling involves oxidative addition, transmetallation and reductive elimination. Two catalysts, palladium (0) complex and copper (I) halide salt are required for this reaction, such as Pd(PPh₃)₄, Pd₂(dba)₃, Pd(OAc)₂. Base is necessary in this coupling reaction to neutralize the byproduct of this reaction. Base such as K₂CO₃, NEt₃, Cs₂CO₃ are generally used. The reactivity order aryl and vinyl halides is I ≈ OTf > Br >> Cl.²⁶⁶

Scheme 45. Example of Sonogashira coupling.



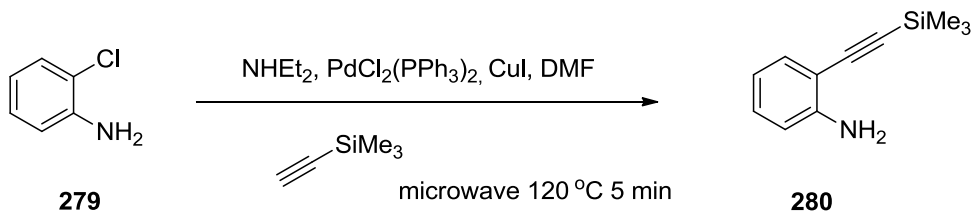
In 2007, Gangjee and coworkers²⁶⁷ reported the Sonogashira coupling of **273** with phenyl acetylene in the presence of Pd(PPh₃)₄ and CuI at room temperature over 12 h to afford **275** (Scheme 45).

Scheme 46. Example of Sonogashira coupling



In a similar trend, compound **278** was reported by Gangjee and coworkers²⁶⁸ and synthesized *via* a Sonogashira coupling of **276** with substituted aryl iodides (Scheme 46).

Scheme 47. Microwave assisted Sonogashira coupling



In 2002, Eedelyi and coworkers²⁶⁹ reported microwave assisted Sonogashira couplings between aryl iodides, bromides and chlorides with TMSA (trimethyl silyl alkyne). The reaction was carried out in the presence of DMF, DIEA, $\text{PdCl}_2(\text{PPh}_3)_2$ and CuI under microwave irradiation at $120\text{ }^\circ\text{C}$ for 5 min (Scheme 47).

III. STATEMENT OF THE PROBLEM

1. Synthesis of nonclassical analogues 5-methyl-6-substituted arylthio-thieno[2,3-*d*]pyrimidine-2,4-diamines 2-13 as DHFR inhibitors.

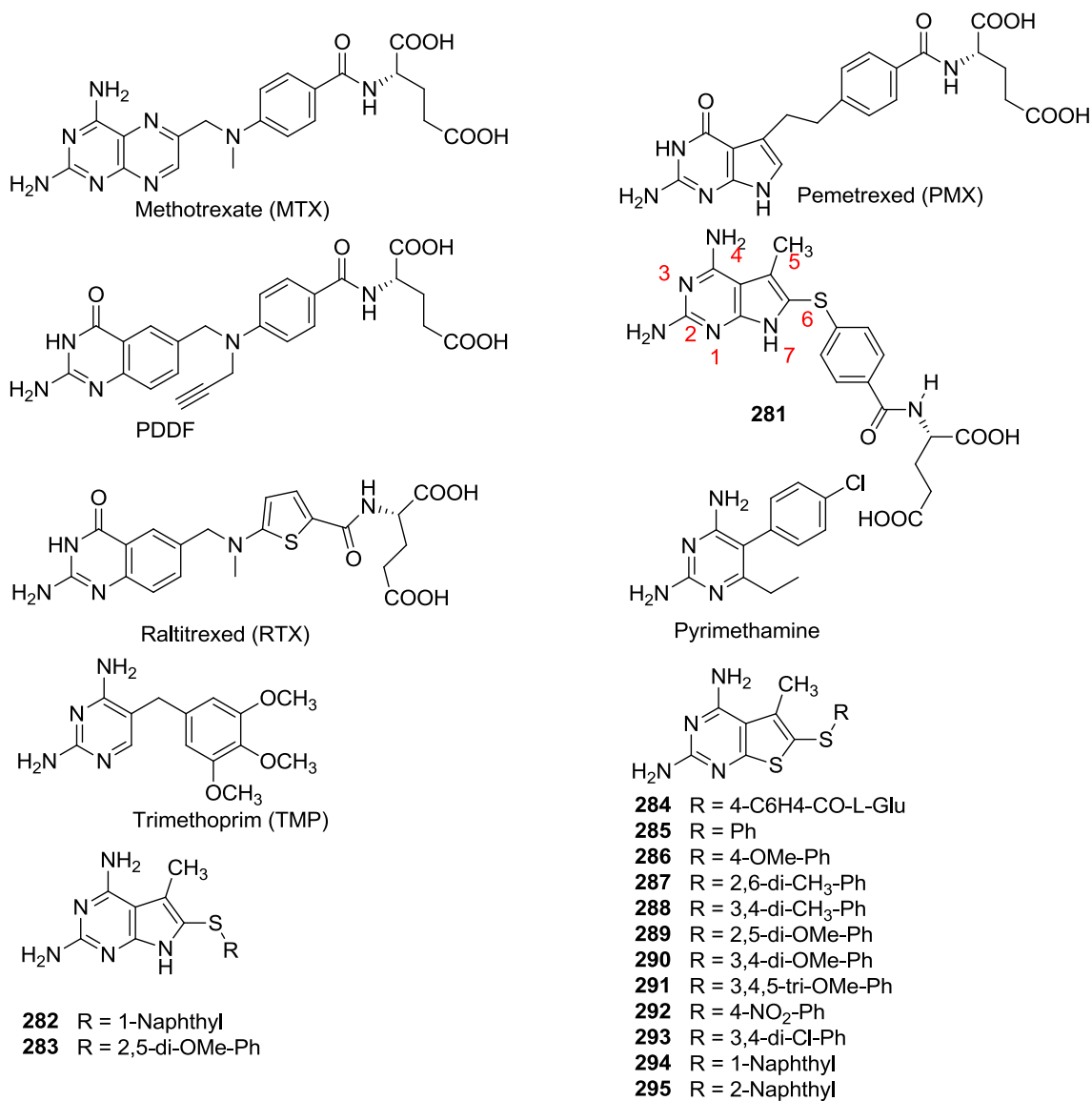


Figure 43. Structures of antifolates

Folate metabolism has long been recognized as an attractive target for cancer chemotherapy due to its indispensable role in the biosynthesis of nucleic acid precursors.

Within folate metabolism, the synthesis of 2'-deoxythymidine-5'-monophosphate

(dTMP) from 2'-deoxyuridine-5'-monophosphate (dUMP) is catalyzed by thymidylate synthase (TS). During this reductive methylation process, 5,10-methylenetetrahydrofolate is converted to dihydrofolate (DHF), which in turn is reduced to tetrahydrofolate (THF) *via* the enzyme DHFR. DHFR carries out the first step in the regeneration of 5,10-methylenetetrahydrofolate (5,10-MTHF) utilizing NADPH as the reductant. Thus, TS and DHFR are crucial for the synthesis of dTMP in DNA biosynthesis and cell proliferation. Inhibition of either enzyme leads to “thymineless death”. Because of this, both TS and DHFR represent attractive targets for developing antitumor agents, antibacterial, antifungal and antiopportunistic infection agents.¹⁻⁵

Several TS and DHFR inhibitors, as separate entities, have found clinical utility as antitumor agents. Figure 43 illustrates important examples of clinically used TS inhibitors such as raltitrexed and pemetrexed. Similarly, the DHFR inhibitor methotrexate (MTX) (Figure 43) has been used clinically for more than 50 years. Several TS and DHFR inhibitors which are analogues of folate have also shown antitumor activities *in vitro* and *in vivo* with some currently in clinical trials.

It has been observed, both in clinically available agents as well as in experimental agents, that TS inhibitors and DHFR inhibitors when used separately or in combination with other agents can provide successful antitumor therapy. In addition, synergism of two separate antifolates which inhibit TS and DHFR has been demonstrated in growth inhibitory studies against *Lactobacillus casei*, rat hepatoma cells, and human lymphoma cells. Thus it is of interesting to design a single agent with dual TS and DHFR inhibitory activity. Such dual inhibitors could act at two different sites (TS and DHFR) and might

be capable of providing “combination therapy” in a single agent without the pharmacokinetic disadvantages of two separate agents.²⁷⁰

As part of a continuing effort to develop novel classical antifolates as antitumor agents, Gangjee *et al.*²⁷¹ reported the synthesis of *N*-{4-[(2,4-diamino-5-methyl-7*H*-pyrrolo[2,3-*d*]-pyrimidin-6-yl)sulfanyl]benzoyl}-*L*-glutamic acid (**281**; Figure 43) as a potent dual inhibitor of DHFR and TS with IC₅₀ values in the 10⁻⁷ M range in its monoglutamate form, thus providing dual inhibition of human TS and human DHFR. Molecular modeling using SYBYL 7.0 indicated that **281** binds to human DHFR in the normal 2,4-diamino mode with the 5-methyl group interacting with Val115, while it could also bind to human TS in the flipped mode with the 5-methyl group forming hydrophobic interaction with Try109. Compound **281** also demonstrated potent inhibitory activity against the growth of several human tumor cell lines in the National Cancer Institute (NCI) preclinical in vitro screen, with GI₅₀ values of 10⁻⁷ to 10⁻⁸ M or lower. The DHFR inhibitory potency and tumor cell inhibitory activities of **281** were in part attributed to its C5-methyl group. Thus **281** is a promising lead compound which can be further structurally modified to optimize human TS, DHFR and tumor cells inhibitory activities.

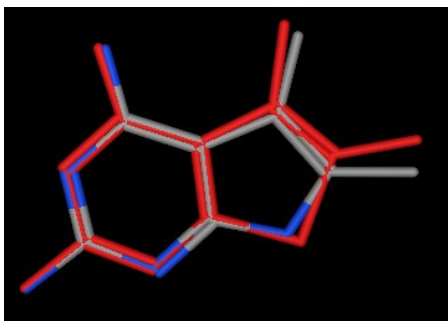


Figure 44. Superimposition of a 6-5 thieno[2,3-*d*]pyrimidine ring system (red) on to a 6-5 pyrrolo[2,3-*d*]pyrimidine ring system (gray)

In the course of structure-based drug design, the thieno[2,3-*d*]pyrimidine scaffold, which could be considered an isostere of the pyrrolo[2,3-*d*]pyrimidine system, was investigated to develop potential dual TS and DHFR inhibitors. Molecular modeling (Figure 44) using MOE indicated that the C5-methyl of thieno[2,3-*d*]pyrimidine (red) could mimic the C5-methyl of pyrrolo[2,3-*d*]pyrimidine (gray) in which the 5-methyl group was reported to have a conducive hydrophobic interaction with Val115 in human DHFR binding pocket. Thus, compound **284** (Figure 43) was designed as an isostere of **281** to determine the importance of the pyrrole 7-NH in **281** for binding to human TS and DHFR. The replacement of the NH of a pyrrolo[2,3-*d*]pyrimidine with a S to afford the thieno[2,3-*d*]pyrimidine was also anticipated to evaluate the importance of a hydrogen bond donor (NH) versus a hydrogen bond acceptor (S). In addition the larger size of the sulfur atom compared to the nitrogen allows the thieno[2,3-*d*]pyrimidines to more closely mimic the size of the 6-6 pteridine system of folates such as 5-methyl-5-deaza methotrexate or 5-methyl-5-deaza aminopterin, in which the 5-methyl group was reported previously to have a hydrophobic interaction with human DHFR.²⁸³ In addition to the classical analogue **284**, it was also of interest to synthesize nonclassical analogues **285-295** (Figure 43) with the thieno[2,3-*d*]pyrimidine scaffold as potential antitumor agents. An additional aspect of our interest in nonclassical dual TS-DHFR inhibitors lies in the treatment of opportunistic infections in immunocompromised patients such as those with acquired immunodeficiency syndrome (AIDS).²⁷² The principal cause of death in patients with AIDS is opportunistic infections caused by *Pneumocystis jirovecii* (*P. jirovecii*)²⁷³ and *Toxoplasma gondii* (*T. gondii*).²⁷⁴ *Mycobacterium avium* (ma) Complex can also adversely influence the quality of life of AIDS patients. Trimethoprim (TMP) and

pyrimethamine, which are nonclassical, lipophilic DHFR inhibitors, are currently used to treat *P. jirovecii* and *T. gondii* infections. However, both are weak inhibitors of *pj* DHFR and *tg* DHFR and must be used with sulfonamides to provide a synergistic effect.²⁷⁵ Unfortunately, combination therapy produce severe side effects in several cases. Gangjee *et al.*²⁷¹ have recently discovered the potent and selective DHFR inhibitory activity of a series of 2, 4-diamino-5-methyl-6-substituted pyrrolo[2,3-*d*]pyrimidines **282** and **283** in particular against *tg* DHFR. These are non-classical 6-5 bicyclic antifolates with 6-aryl substitutions. X-ray crystal structure,^{276, 277} multiple sequence alignment²⁷⁸ and molecular modeling (SYBYL 6.810) indicate that the 5-methyl group interacts with Ile123 in *pc* DHFR, Val151 in *tg* DHFR, and Ile102 in *ma* DHFR. The 5-methyl group in these compounds also influences the conformations of the 6- aryl side chain and could contribute to the potency of these compounds. Molecular modeling suggests that a 5-methyl group of a 6-5 bicyclic antifolate has similar interaction and conformational effects as a 5-methyl in a 6-6 ring system antifolate.²⁷⁶ Substituted thieno[2,3-*d*]pyrimidines **284-295** as sulfur isosteres of the lead pyrrolo[2,3-*d*]pyrimidines **282** and **283** were designed. It should be noted that the thieno[2,3-*d*]pyrimidine scaffold has been examined previously for antibacterial and antimalarial activity.²⁷⁹⁻²⁸³ Several nonclassical thieno[2,3-*d*]pyrimidine analogues have also been evaluated as inhibitors of *P. carinii* DHFR and *T. gondii* DHFR.²⁸⁰⁻²⁸³ Some of these analogues have been found to be selective for DHFR from these pathogens.^{281, 283}

2. 6,5,6-tricyclic Benzo[4,5]thieno[2,3-*d*]pyrimidines as Dual Thymidylate Synthase and Dihydrofolate Reductase Inhibitors

The TS reaction requires 5,10-methylenetetrahydrofolate (5,10-CH₂THF) as a cofactor for one carbon unit transfer and represents the only *de novo* pathway for intracellular dTMP synthesis. DHFR catalyzes the reduction of dihydrofolate to tetrahydrofolate, and is indirectly responsible for dTMP synthesis by maintaining the reduced folate pool.²⁸⁴

Raltitrexed (RTX),²⁸⁵ pemetrexed (PMX)²⁸⁶ and methotrexate (MTX)²⁸⁷ (Figure 43) are examples of TS and/or DHFR inhibitors used in the clinic. RTX, approved in several European countries, Australia, Canada, and Japan for the treatment of advanced colorectal cancer. RTX is a TS inhibitor that undergoes rapid polyglutamylation by the enzyme folylpolyglutamate synthetase (FPGS).^{288, 289} PMX, in combination with cisplatin, was approved for the treatment of malignant pleural mesothelioma and also for non-small cell lung cancer. With TS inhibition as the primary mechanism of action, PMX was reported to inhibit several other folate-dependent enzymes including DHFR, glycylamide ribonucleotide formyltransferase (GARFTase), and aminoimidazole carboxamideribonucleotide formyltransferase (AICARFTase).²⁸⁶ Similar to RTX, polyglutamyltion by FPGS is essential for the cytotoxicity of PMX.

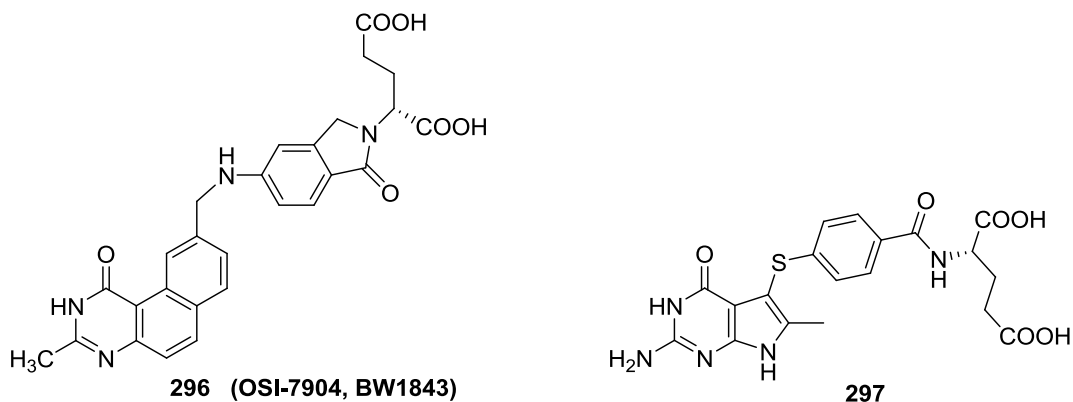


Figure 45. Antifolates

Classical antifolates, such as RTX and PMX, that have a *N*-benzoyl-L-glutamic acid side chain usually function as substrates for FPGS, which leads to high intracellular concentrations of these antitumor agents and increases TS inhibitory activity for some antifolates (RTX, 60-fold and PMX 130-fold) compared to their monoglutamate forms.²⁹⁰⁻²⁹³ Although polyglutamylation of certain antifolates (such as RTX and PMX) is necessary for their cytotoxic activity, it has also been implicated in toxicity to host cells, because of the longer cellular retention time of such polyanionic poly-glutamate metabolites.²⁹⁴ In addition, reduced expression of FPGS in tumor cells can lead to resistance to FPGS dependent classical antifolates such as PMX.²⁹⁵⁻²⁹⁷

To circumvent the potential tumor resistance problems associated with FPGS, classical antifolates should have high folate enzyme inhibitory potency as their monoglutamate forms and not require polyglutamylation by FPGS to exert their antitumor activity.^{298, 299} Typically, antifolates that contain a 2-methyl-4-oxo substitution in the pyrimidine ring (such as RTX) are TS inhibitors, while 2-amino-4-oxo substitution in the pyrimidine ring (such as PMX) may provide affinity for both TS and DHFR. 2,4-

Diamino substitutions on the pyrimidine ring of antifolates is usually associated with DHFR inhibitory activity.

In an attempt to prevent or minimize the potential problems associated with FPGS, including tumor resistance, and to develop dual TS and DHFR inhibitors, Gangjee *et al.*²⁹⁸ reported the synthesis of a classical antifolate *N*-{4-[(2-amino-6-methyl-4-oxo-4,7-dihydro-3*H*-pyrrolo[2,3-*d*]pyrimidin-5-yl)thio]benzoyl}-L-glutamic acid, **297** (Figure 45), as a potent inhibitor of isolated human (h) TS ($IC_{50} = 42$ nM) with moderate inhibition against human recombinant DHFR ($IC_{50} = 2.2$ μ M) in its monoglutamate form thus providing dual inhibitory activity of TS and DHFR.

Compound **297** was equipotent with **296** (Figure 45), a potent TS inhibitor, against hTS and was more potent than the clinically used RTX and PMX against isolated hTS in their monoglutamate forms. Molecular modeling (SYBYL 6.91)³⁰⁰ suggested that the 6-methyl group in **297** makes important hydrophobic contacts with Trp109 in hTS and also serves to lock the 5-position side chain into favorable, low energy conformations (Figure 46). Both these factors probably contribute to the high inhibitory activity of **297** in its monoglutamate form against hTS.

A potential advantage of compound **297** over RTX and PMX is that it is not a substrate for hFPGS, from CCRF-CEM cells, at concentrations up to 1045 μ M.²⁹⁸ The lack of hFPGS substrate activity of **297** was attributed, in part, to the presence of the 6-methyl group on the pyrrolo[2,3-*d*]pyrimidine of **297**. The 6-methyl group of **297** probably creates steric hindrance in its binding to the active site of hFPGS. Alternatively, the 6-methyl group of **297** may force the 5-position side chain into a conformation that is not conducive for binding to hFPGS. The fact that PMX, a pyrrolo[2,3-*d*]pyrimidine,

much like **297**, lacks a 6-methyl group and is a substrate for FPGS lends credence to the involvement of the 6-methyl moiety in preventing FPGS substrate activity in **297**.

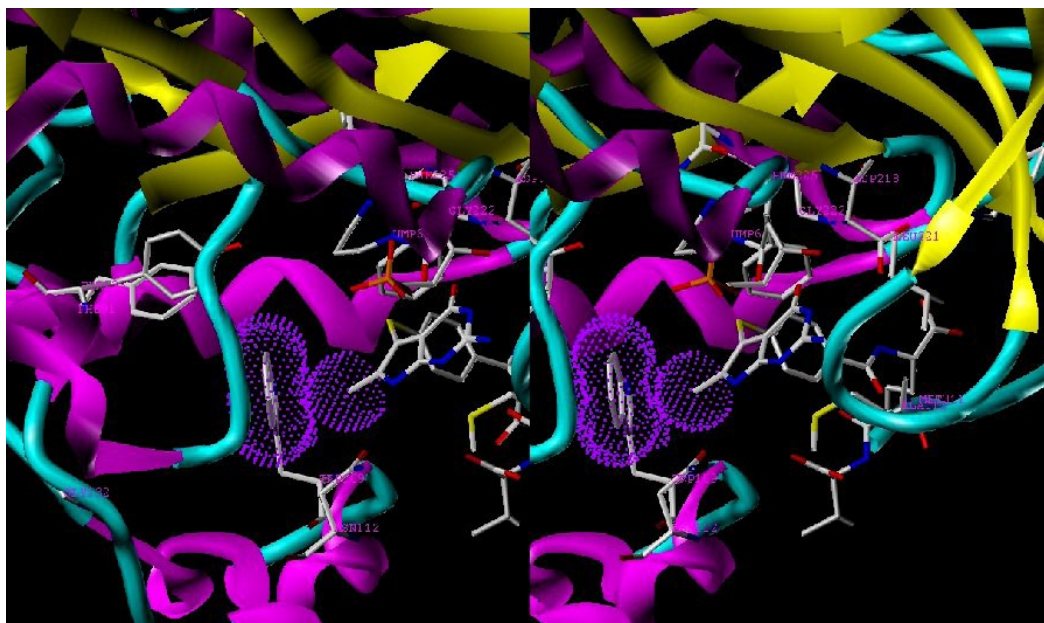


Figure 46. Stereoview compound **297** superimposed on pemetrexed (not shown) in human TS (PDB1JU6395), indicating the interaction of the 6-CH₃ with Trp109

Tricyclic **296** (Figure 45) is a classical TS inhibitor with $K_i = 0.09$ nM.²⁹⁸ Although this compound is an excellent substrate for FPGS, it is subject to the addition of only one additional glutamic acid. Moreover, the high potency of **296** does not rely on polyglutamation. The monoglutamate form is equi-potent with the diglutamate form.³⁰¹ Compound **296** is a noncompetitive TS inhibitor and its activity is not affected by the concentration of 5,10-CH₂THF.^{302, 303} In addition, it has been demonstrated that overexpression of the multidrug resistance proteins, MRP1 and MRP2, can confer tumor resistance to short term (4 h), but not long term (72 h), exposure of **296**.³⁰⁴

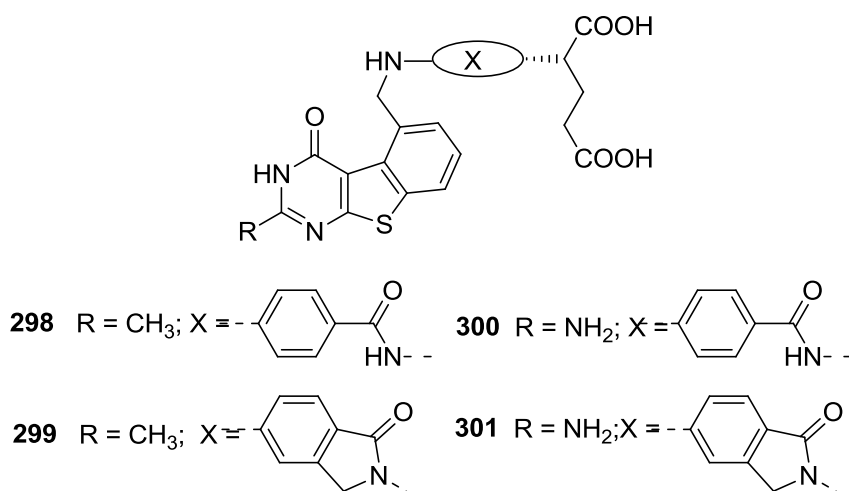


Figure 47. Target classical antifolates with the tricyclic benzo[4,5]thieno[2,3-*d*]pyrimidine scaffold.

In the course of our structure-based drug design program, it was of interest to synthesize classical antifolates **298-301** with a benzo[4,5]thieno[2,3-*d*]pyrimidine scaffold (Figure 47), as structural hybrids of **296** and **297**. Compounds **298** and **299**, similar to **296**, have a 2-methyl-4-oxo pyrimidine ring which is generally associated with TS inhibition. In contrast, **300** and **301** have a 2-amino-4-oxo substituent, which could afford dual TS and DHFR inhibition, as observed for **297** and PMX.

The 2-substitutions on **298-301** would access the importance of hydrogen-bonding at this position (**300**, **301**) versus hydrophobic binding (**298**, **299**) to biological activity. The size of a sulfur atom in **298-301** is larger than a nitrogen atom and smaller than two carbon atoms, thus the thiophene B-ring in benzo[4,5]thieno[2,3-*d*]pyrimidines **298-301** mimics both the smaller pyrrolo B-ring in **297** and the larger quinazoline B-ring in **298** (Figure 48).

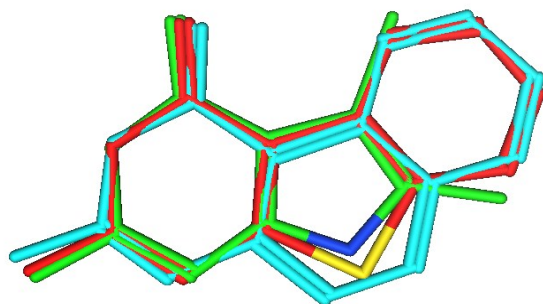


Figure 48. Superimposition of benzo[4,5]thieno[2,3-*d*]pyrimidine (red), pyrolo[2,3-*d*]pyrimidine (green) and benzo[*f*]quinazoline (cyan)

Similar to the C-ring in **296** and the 6-methyl group in **297**, the benzo C-ring in **398-301** makes hydrophobic contacts with Trp109 in hTS and restricts the side chain to a conformation conducive for potent TS activity but perhaps not for FPGS substrate activity.

To explore the effects of side chain flexibility on biological activity, compounds **298** and **300** have the same benzoylglutamate side chain as **297**, while **299** and **301** have a more conformationally restricted 2-isoindolinyll-L-glutamate side chain like **296**. Unlike other classical TS inhibitors, the glutamate side chain in **296** is part of an isoindolinone system, which restricts the side chain conformation. The crystal structure of the ternary complex TS-dUMP-**296** (PDB: 1SYN)³⁰⁵ revealed that the binding of **296** and the dUMP nucleotide induced a closed conformation of the TS protein, similar to other antifolates. Surprisingly, however, the binding surface of **296** includes a hydrophobic patch from Val 77 that is normally buried and not on the surface.³⁰⁵

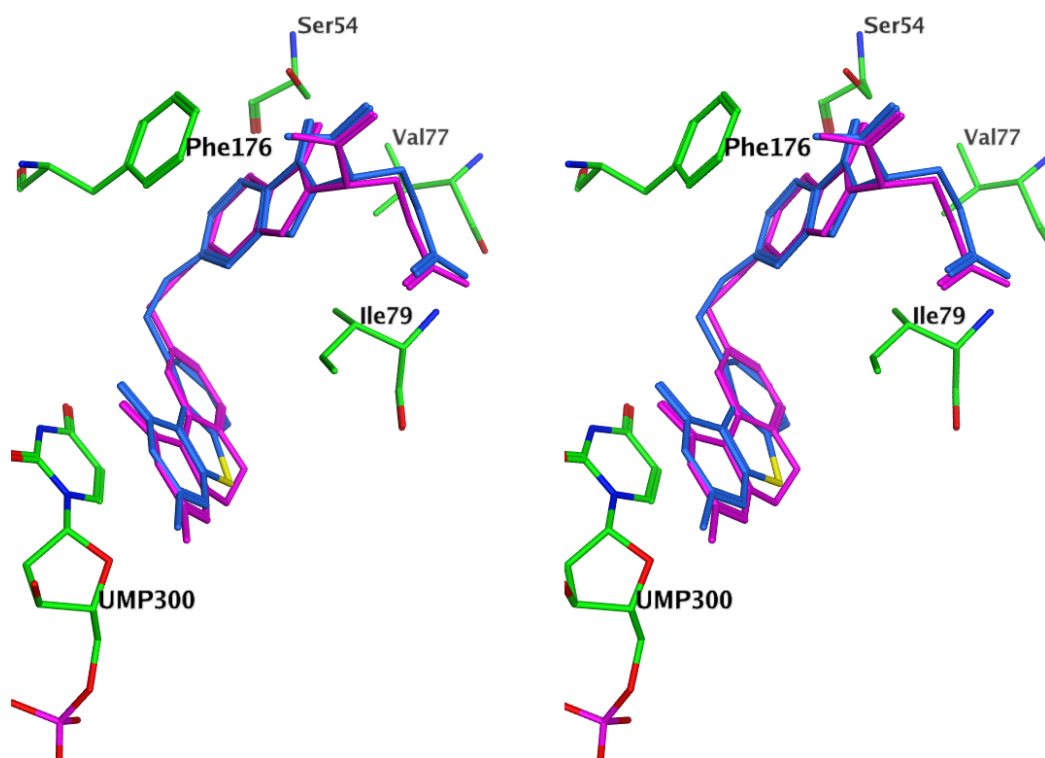


Figure 49. Stereoview of compound **298** (blue) superimposed on **296** (purple) in ecTS (green). Figure prepared with MOE 2008.10³⁰⁰

As shown in Figure 49, molecular modeling using MOE 2008.10³⁰⁰ revealed that when the central ring in **296** is truncated to a 5-member ring in the benzo[4,5]thieno[2,3-*d*]pyrimidine **298**, and the side chain substitution is moved from the 6-position to the 5-position, the resulting compound binds to TS in a manner similar to **296**.

Molecular modeling suggested that although 2-methyl substituted compounds **298** and **299** can not form a salt bridge with Glu30 of hDHFR at the N1 and 2NH₂, like MTX, the 2-amino compounds **300** and **301** (Figure 47) can bind just like folate (PDB: 1U72) in which the 2-amino-4-oxo group binds to the enzyme with hydrogen bonding and the

heterocycle and the benzoyl moieties bind to Phe31, Phe34 and Ile 60. The α -carboxylic acid of the glutamate makes ionic contact with Arg70.

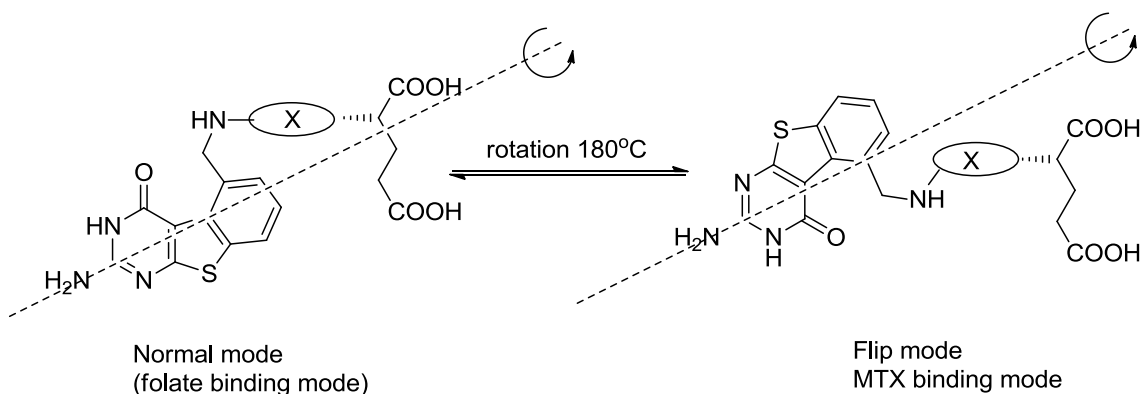
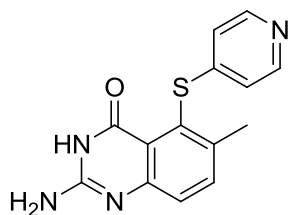


Figure 50. Proposed binding mode with DHFR. The “Normal mode” is defined as the binding mode of folic acid (a 2-amino-4-oxo pyrimidine system) to human DHFR. The “flipped” mode is defined as the binding mode when the molecule is rotated about the C₂-NH₂ bond by 180°

According to molecular modeling, a second mode of binding would involve a 180° rotation about the C-2, NH₂ bond (Figure 50), whereby the sulfur of the thiophene ring is now superimposed on the 4-oxo group of folate, with all other interactions being preserved. It is important to note that binding of **300** and **301** in the flipped mode (Figure 50) also allows the sulfur of the thiophene ring to mimic the 4-amino of MTX. To determine which of these two modes of binding the molecule adopts to bind hDHFR, **300** and **301** were each cocrystallized with isolated hDHFR (Dr. Vivian Cody).

3. Classical and Nonclassical 2-Amino-4-oxo-5-arylthio-substituted-6-isopropyl thieno[2,3-*d*]pyrimidines as Dual Thymidylate Synthase and Dihydrofolate Reductase Inhibitors and Potential Agent for *Toxoplasma gondii* Infection

The problem of resistance in tumors, due to low or defective FPGS, has placed limitations on the use of classical antifolates, which depend on polyglutamylation for their cytotoxicity. Classical antifolates also require carrier systems such as reduced folate carrier (RFC) to gain entry into the target cells. A decreased expression in folate transporter systems represents another mechanism for drug resistance.



Nolatrexed

Figure 51. The structure of Nolatrexed

Lipophilic nonclassical antifolates were designed to overcome the problem of tumor drug resistance associated with classical antifolates. These lipophilic nonclassical antifolates lack the polar glutamate side chain found in classical antifolates and hence do not depend on FPGS for their inhibitory activity of the target enzymes. Additionally, they also do not require the RFC system for active uptake into the cell since they are lipophilic and are passively transported into cells. Nolatrexed (Figure 51) is the first nonclassical TS inhibitor in clinical trials as an antitumor agents.^{306, 307}

Selective nonclassical dual TS and DHFR inhibitors have the potential to treat opportunistic infections in immunocompromised patients such as those with acquired

immunodeficiency syndrome (AIDS). The principal cause of death in patients with AIDS is opportunistic infections caused by *Pneumocystis jirovecii* (*P. jirovecii*) and *Toxoplasma gondii* (*T. gondii*).³⁰⁸⁻³¹⁰ Due to the limits of current therapies,³¹¹⁻³¹³ it is of considerable interest to incorporate selectivity and potency into single nonclassical antifolates that can be used alone to treat these infections.

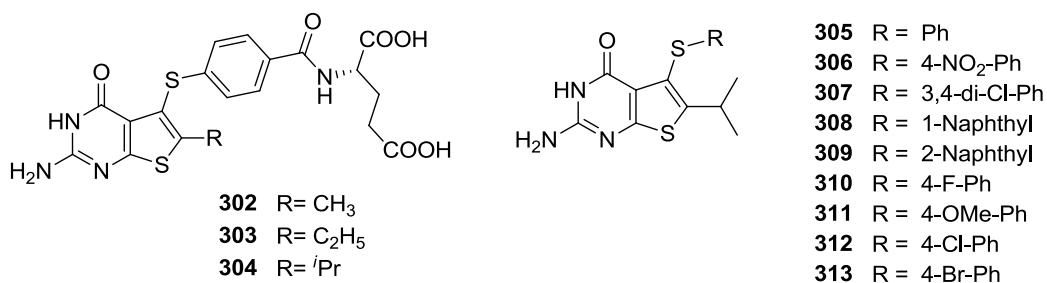


Figure 52. The structure of thieno[2,3-*d*]pyrimidine antifolates **302-313**

Gangjee *et al.*³¹⁴ discovered the potent TS inhibitory activity of a series of 2-amino-4-oxo-5-arylthio-substituted-6-ethylthieno[2,3-*d*]pyrimidine analogues.

Compound **303** (Figure 52) is a potent dual inhibitor of human TS (IC₅₀ = 54 nM) and human DHFR (IC₅₀ = 19 nM). Molecular modeling using (SYBYL 8.0)³⁰⁰ indicated that the 6-methyl group in **302** and the 6-ethyl group in **303** make important hydrophobic contacts with Trp109 in human TS and also sterically restrict the rotation of the 5-position side chain so that it adopts a favorable conformation for binding to human TS.

Gangjee *et al.*³¹⁴ previously reported the crystal structure of **302** and **303** bound to natural and mutant human DHFR (PDB: 3GHW and 3GHC). In both crystal structures, thieno[2,3-*d*]pyrimidine inhibitors were shown to bind with DHFR in the “normal” folate

orientation. The crystal structures also indicated that the 6-substituent interacted with a small hydrophobic pocket composed of Ile7, Thr56 and Val115.

To determine the optimum size of the 6-alkyl group for TS and DHFR inhibitory activity, classical 6-isopropyl substituted thieno[2,3-*d*]pyrimidines **304** (Figure 52) and nonclassical analogues **305-313** were also designed. The introduction of the bulky isopropyl substitution at 6-position was anticipated to further restrict the conformation of 5-position substitution thus affect the biological activities of the compounds. In addition, the hydrophobic interaction between the 6-isopropyl substitution and Trp 109 may be further enhanced compared to methyl and ethyl groups.

Gangjee *et al.* have previously shown that nonclassical analogues of **302** (Figure 52) with electron withdrawing groups in the phenyl ring of the side chain also enhance human TS inhibitory activity. SAR studies indicated that analogues with electron withdrawing groups at the 3- and/or 4-positions of the phenyl side chain provide optimum inhibitory potency against human TS. Some nonclassical analogues with electron withdrawing substitutions on the phenyl ring demonstrated greater potency against human TS than the clinically used RTX and PMX. In contrast to the requirements for human TS inhibition, electron donating substituents such as methoxy, methyl, and bulky substituents such as naphthyl are conducive for DHFR inhibition; hence nonclassical analogues containing these substituents were also designed in the 2-amino-4-oxo-5-arylthio-substituted-6-isopropyl thieno[2,3-*d*]pyrimidine series.

4. Classical and Nonclassical 2-Amino-4-oxo-5-arylthio-substituted-6-propyl thieno[2,3-*d*]pyrimidines as Dual Thymidylate Synthase and Dihydrofolate Reductase Inhibitors and Potential Agent for *Toxoplasma gondii* Infection

As introduced previously, Gangjee *et al.*³¹⁴ discovered the potent TS inhibitory activity of a series of 2-amino-4-oxo-5-arylthio-substituted-6-methylthieno[2,3-*d*]pyrimidine analogues. The 6-methyl group in **302** makes important hydrophobic contacts with Trp109 in human TS and also sterically restrict the rotation of the 5-position side chain so that it adopts a favorable conformation for binding to human TS.

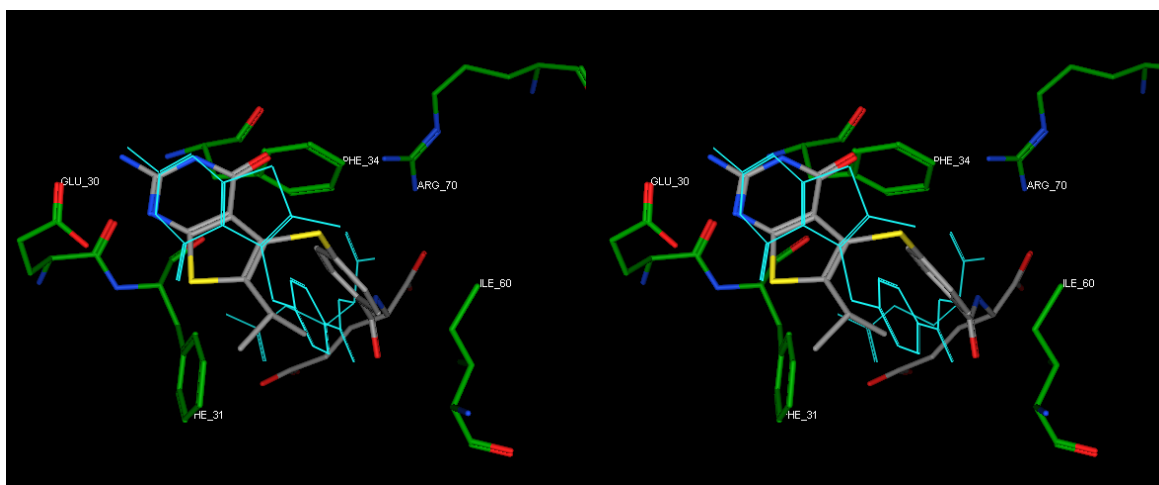


Figure 53. Stereoview: Docking structure of **304** (gray) in the X-ray crystal structure of **302** with double mutant human DHFR (PDB : 3GHC), generated by MOE 2008.10³¹⁵

In the crystal structures, **302** was shown to bind with DHFR in the “normal” folate orientation. The crystal structures also indicated that the 6-substituent interacted with a small hydrophobic pocket composed of Ile7, Thr56 and Val115 (Figure 53).

As mentioned above, to determine the optimum size of the 6-alkyl group for TS and DHFR inhibitory activity, classical 6-isopropyl substituted thieno[2,3-*d*]pyrimidines

304 (Figure 52) and nonclassical analogues **305-313** were also synthesized and evaluated. However, compound **304** showed poor DHFR inhibitory activity (fifty fold less potent than the methyl analog).

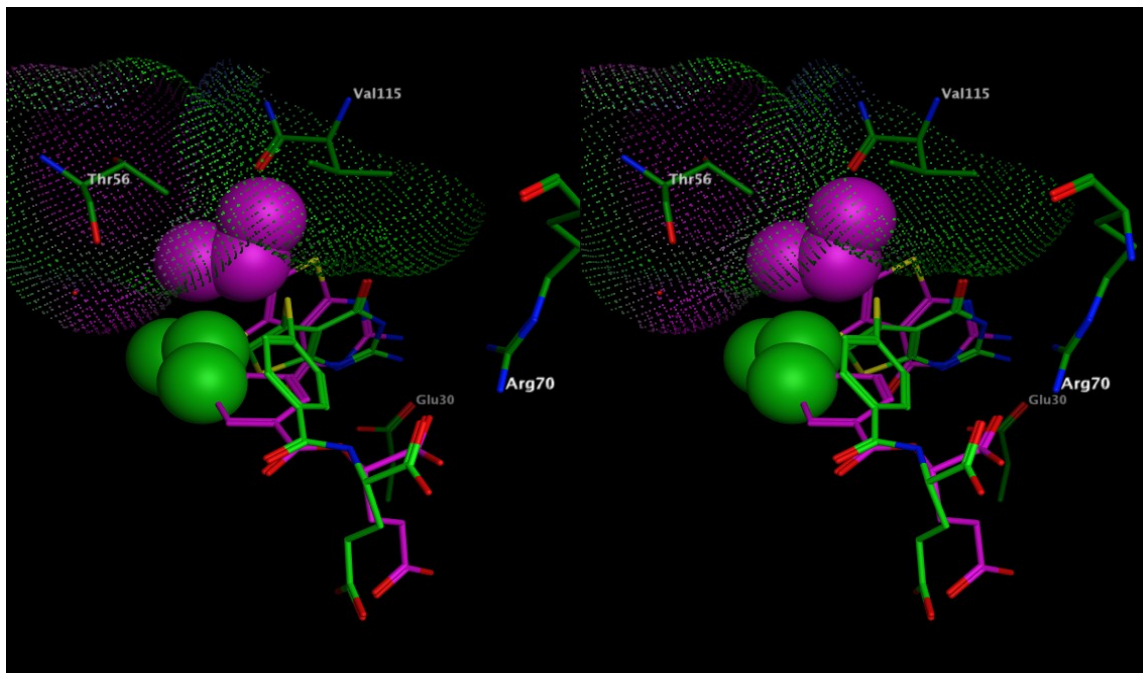


Figure 54. Stereoview: docking structure of **304** (isopropyl) bound to human DHFR in “normal” mode (violet), in “flipped” mode (green) (PDB :3GHW), generated by MOE 2008.10.³¹⁵

Molecular modeling revealed that compound **304** could not bind to human DHFR in the “normal” mode, because of the steric clash between the bulky 6-isopropyl group and the narrow hydrophobic pocket (Ile 7, Thr 56 and Val 115) (Figure 54). Instead, compound **304** adopts a “flipped” mode to bind with human DHFR compared to folic acid. Docking of **304** into the crystal structure of **302** (blue) in human DHFR (PDB : 3GHW) shows the sulfur atom of the thieno ring to be close to the 4-oxo group of **302** (Figure 53). In this binding mode, the Glu30 residue also interacts with the 2-NH₂ and N1 moieties of **304**. The *p*-aminobenzoyl ring along with thieno[2,3-*d*]pyrimidine ring makes

hydrophobic interactions with Phe31, Phe34, and Ile60, and the α -COOH forms an ionic bond with Arg70 just as compound **302** does with human DHFR in the “normal” binding mode. The flipped mode of **304** resulted in a 50-fold decrease in its activity compared with compounds (**302**, **303**) having a straight chain substitution at 6-position.

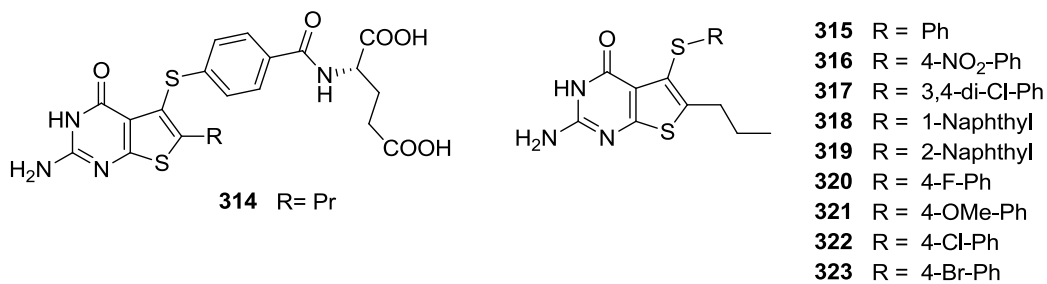


Figure 55. The structure of thieno[2,3-*d*]pyrimidine antifolates **314-323**

Thus it is proposed that a straight chain substitution at 6-position is more favorable for DHFR inhibition. To further explore the optimal substitution at the 6-position, classical and nonclassical 6-*n*-propyl straight chain substituted thieno[2,3-*d*]pyrimidines **314-323** (Figure 55) were designed.

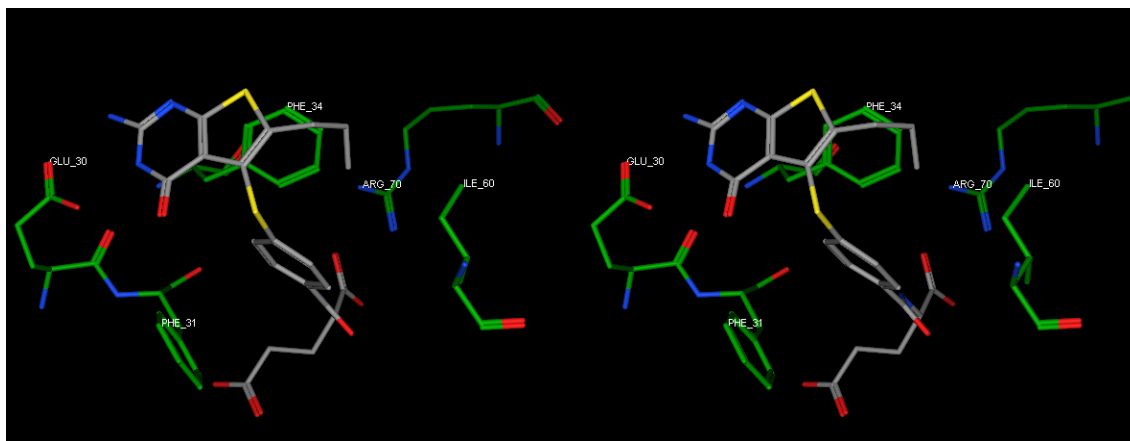


Figure 56. Stereoview: compound **314** bound to human DHFR in “normal” mode (PDB : 3GHW), generated by MOE 2008.10.³¹⁵

Molecular modeling also revealed that when the 6-substitution was a straight chain propyl group, the compounds retain the ability to bind the human DHFR in the “normal” binding mode and restore human DHFR inhibitory activity. In the “normal” binding mode (Figure 56), compound **314** binds just like folic acid (PDB : 1DRF), **302** (PDB : 3GHW) and **303** (PDB : 3GHC). In this binding mode, the 2-NH₂ and the N3 moieties form hydrogen bonds with Glu30. The α -carboxyl group of **314** interacts with Arg70 in an ionic bond and the thieno[2,3-*d*]pyrimidine and the phenyl ring make hydrophobic contacts with Phe31, Phe34, and Ile60 (Figure 56) in the binding pocket. The 6-propyl substitution contacts with Ile7 and Val115 in the hydrophobic pocket.

As mentioned above, Gangjee *et al.* have previously shown that nonclassical analogues of **302** (Figure 52) with electron withdrawing groups in the phenyl ring of the side chain also enhance human TS inhibitory activity. SAR studies indicated that analogues with electron withdrawing groups at the 3- and/or 4-positions of the phenyl side chain provide optimum inhibitory potency against human TS. Certain analogues with electron withdrawing substitutions on the phenyl ring demonstrated greater potency against human TS than the clinically used RTX and PMX. In contrast to the requirements for human TS inhibition, electron donating substituents such as methoxy, methyl, and bulky substituents such as naphthyl are conducive for DHFR inhibition; hence nonclassical analogues containing these substituents were also synthesized in the 2-amino-4-oxo-5-arylthio-substituted-6-propyl thieno[2,3-*d*]pyrimidine series. As indicated above for the classical analogue **314**, it was anticipated that the nonclassical analogues **315-323** would also provide dual inhibitory activity against human TS and human DHFR.

5. A novel series of 6-substituted thieno[2,3-d]pyrimidine antifolate inhibitors of purine biosynthesis with selectivity for high affinity folate receptors over reduced folate carrier for cellular entry

The biological importance of reduced folates derives from their essential roles in one-carbon transfer leading to thymidylate, purine nucleotides, serine, and methionine, and in biological methylation reactions from S-adenosylmethionine.³¹⁶ Antifolates, typified by MTX, PMX and RTX (Figure 43) are structurally similar to folic acid and typically bind to folate-dependent enzymes to inhibit folate-dependent pathways.³¹⁷ MTX continues to be an integral component of the chemotherapeutic arsenal for several cancers including pediatric acute lymphoblastic leukemia, osteogenic sarcoma, lymphoma, and breast cancer.³¹⁷ RTX is used throughout much of the world except USA for advanced colorectal cancer.³¹⁸ PMX was approved in 2004 for pleural mesothelioma in the US,³¹⁹ and subsequently, as a second line treatment for non-small cell lung cancer.³²⁰

MTX is a potent inhibitor of dihydrofolate reductase (DHFR), whereas PMX and RTX derive their primary cytotoxic effects by inhibiting thymidylate synthase (TS). Lometrexol (LMX) (Figure 43) was introduced in 1985³²¹ as a targeted antipurine antifolate. The notion of selectively targeting *de novo* purine nucleotide biosynthesis has roots in early studies of azaserine³²² or thiopurines³²³ and is based on the assumption that depletion of purine nucleotide pools can limit nucleotides for DNA synthesis and repair, while also impacting ATP and GTP stores important for cellular energetics.³²⁴ This effect could be even more acute in several cancer cells that lack enzymes involved in purine salvage.³²⁵ Although there have been reports that antipurine antifolates such as LMX

were cytostatic rather than cytotoxic,³²⁶ in other reports, antipurine antifolates were distinctly cytotoxic.^{327, 328}

While PMX, RTX, LMX and MTX the aforementioned antifolates are often considered to possess limited selectivity for tumor cells over normal proliferative tissues such as bone marrow and gastrointestinal mucosa, interest in the development of antifolates remains particularly high for agents that target high affinity folate receptors (FRs).³²⁹ This reflects the restricted patterns of tissue expression for FRs, including the vast majority of ovarian and endometrial cancers for FR α and myeloid leukemias for FR β .³³⁰ There are other factors that account for tumor selectivity of FR-targeted therapies, including the apical localization for FR α in normal epithelia such as renal tubules or choroid plexus where it is inaccessible to the circulation, and synthesis of non-functional FR β in normal hematopoietic cells.³³¹

Ample literature documents applications of FRs for tumor targeting with folic acid as the targeting agent. For instance, cytotoxins (e.g., mitomycin C), liposome-encapsulated drugs (e.g., doxorubicin), or radionuclides have been conjugated to folic acid for targeting FR-expressing tumors.³³²⁻³³⁴ There are at least two potential complications of this approach. These include: (i) instability in plasma versus that within tumor cells such that the folate conjugate may be prematurely cleaved and release the cytotoxic agent prior to reaching the tumor resulting in toxicity to normal cells, thus precluding selectivity; and (ii) the possibility that free folic acid released upon cleavage within the tumor could provide a growth-sustaining nutrient detrimental to tumor inhibition. Another approach involves a targeting ligand which itself is cytotoxic. Unfortunately, most folate-based therapeutics such as classical antifolates (including

RTX, PMX, and LMX) that are substrates for FRs are also substrates for the ubiquitously expressed reduced folate carrier (RFC) such that there is no tumor selectivity with these agents.³³⁵ Indeed, the discontinuation of continued clinical development of LMX can be directly traced to the severe myelosuppression encountered in a Phase 1 clinical trial,³³⁶ at least partly due to its excellent substrate activity for RFC uptake and polyglutamylation by normal tissues. Clearly, a specific FR-targeted agent that also possesses cytotoxic activity would circumvent the drawbacks of folic acid-conjugated cytotoxic agents and the lack of selectivity associated with clinically used antifolates MTX, PMX and RTX. Indeed, FR selective cytotoxic agents can be envisaged to provide highly selective antitumor agents against tumors expressing FR with little or no host toxicity.

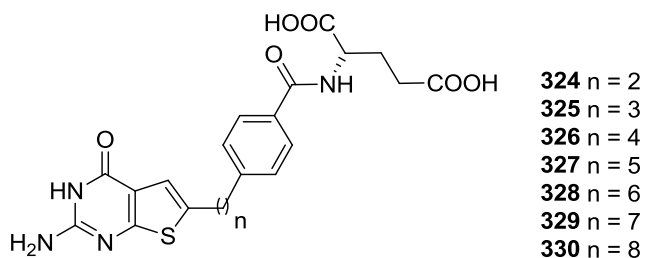


Figure 57. The structure of antifolates **324-330**

Deng *et al.*³²⁸ described a novel series of 6-substituted classical pyrrolo[2,3-*d*]pyrimidine antifolates, differing only in the lengths of the carbon bridge (3- to 6-carbons), characterized by potent and selective substrate activities for FR α and FR β , and negligible substrate activity for RFC. The intracellular enzyme target of the 6-substituted pyrrolo[2,3-*d*]pyrimidines was identified as glycylamide ribonucleotide formyltransferase (GARFTase), the first folate-dependent reaction in the *de novo* purine synthesis pathway. In this study, the focus was extended to a novel isosteric series of 6-substituted thieno[2,3-*d*]pyrimidine antifolates **324-330** (Figure 57), with a 2- to 8-carbon bridge

between the thieno[2,3-*d*]pyrimidine and the benzoyl moiety, respectively. Isosteric replacement of the pyrrolo ring with a thieno ring for this series provides an increase in ring size that more closely approximates the pteridine, 6-6 fused ring system of the natural cofactor. In addition, replacement of the NH of the pyrrole with a S also allows for comparison of the relative importance of a hydrogen bond donor (NH) with a hydrogen bond acceptor(s).

6. Importance of the Side Chain Aryl Group for Folate Receptor Targeting and GARFTase Inhibitory Activity in Classical Thieno[2,3-*d*]pyrimidine Antifolates

6-Substituted thieno[2,3-*d*]pyrimidine antifolates **324-330** were found to be potent and selective inhibitors of cells that express FR α and FR β . The thieno[2,3-*d*]pyrimidines **324-330** are unique and distinct from all other clinically used classical antifolates, including the pyrrolo[2,3-*d*]pyrimidine (PMX), quinazoline (RTX), and pteridine (MTX) antifolates, in that they are neither substrates for RFC nor PCFT. In this series, **326** with a four carbon bridge is the most potent inhibitor of cells expressing FRs α and β , and this activity is directly related to intracellular GARFTase inhibition.³³⁷

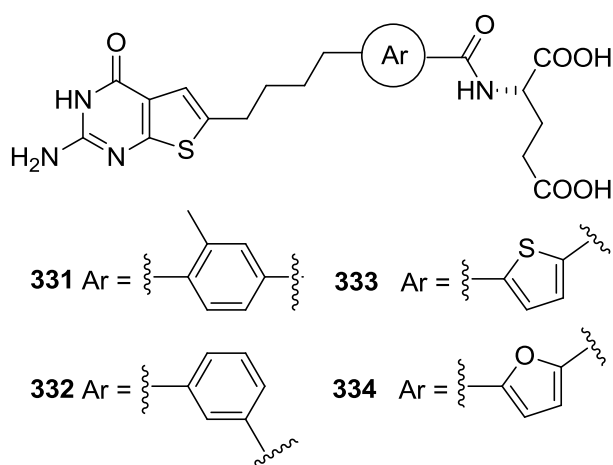
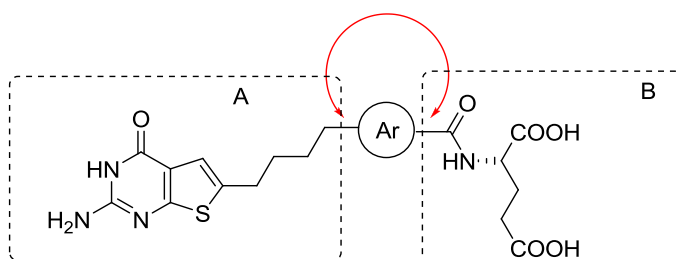


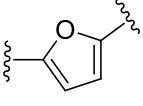
Figure 58. The structure of antifolates **331-334**

To further investigate the structural requirements of the thieno[2,3-*d*]pyrimidine antifolates for FR transport and GARFTase inhibition, particularly the importance of the aromatic ring in the side-chain, a series of compounds **331-334** (Figure 58) with positional isomer phenyl different aryl substitutions were designed, synthesized and evaluated. The aryl group in side-chain is believed not only to allow the appropriate relative orientation of the thieno[2,3-*d*]pyrimidine scaffold (part A) and the glutamate portion (part B), but also provides important interactions with the transporter and the target enzyme.

Table 3. The angle of aryl disubstitutions



Compound	Ar	angle
326		180°
331		180°
332		120°
333		147.4°

334		125.5°
------------	---	--------

As shown in Table 3, the angle between part A and part B is a measurement of the relative spatial orientation of A and B. For **331**, although A and B substitutions have the same angle (180°) as the parent **326**, the existence of an extra CH₃ in **331** *ortho* to the alkyl chain in part A may restrict the free rotation of the otherwise flexible alkyl linker. Moreover, this methyl group could provide extra hydrophobic binding with the transporter FR and/or the enzyme GARFTase.

Depending on the angle, the overall distance between A and B in **332**, **333** and **334** are slightly different (measured as the distance from the 6-CH₂ on the thieno[2,3-*d*]pyrimidine and the carbonyl on the aryl side chain), which may also affect the binding affinity of the compounds with the transporter and/or target enzyme.

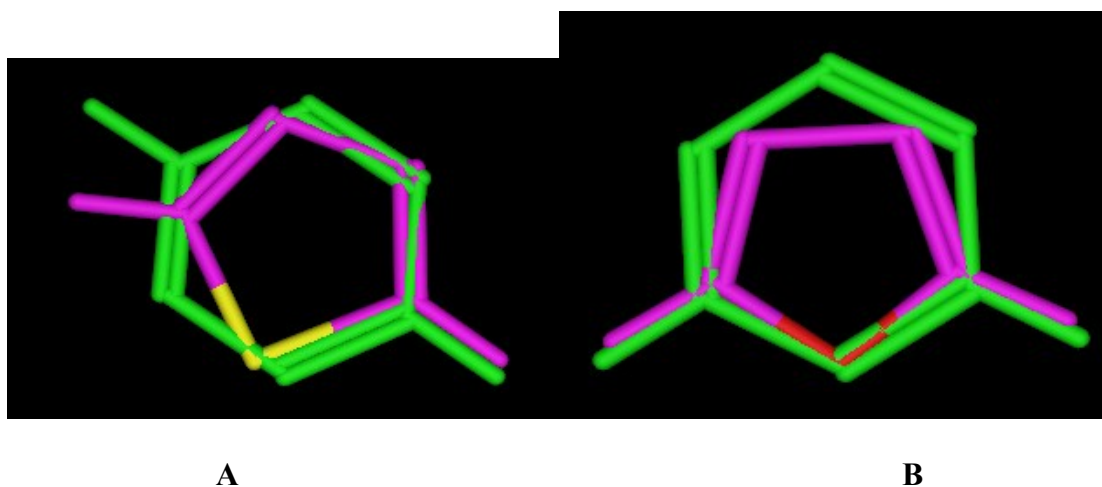


Figure 59. A: Structural alignment between 2,5-disubstituted thiophene (purple) and *para*-disubstituted benzene (green), B: structural alignment between 2,5-disubstituted furan (purple) and 1,3-*meta*-disubstituted benzene (green) generated by MOE 2008.10.

In **332**, a *meta* substitution pattern was adopted such that the angle between the two parts A and B is 120°. 2,5-Disubstituted thiophene can mimic *para*-substituted benzene (Figure 59), while 2,5-disubstituted furan can mimic *meta*-substituted benzene (Figure 59). Thus, the benzoyl ring in **326** was bioisoterically replaced by a thienoyl ring or a furoyl ring, the resulting compounds **333** and **334** have different 147.4° and 125.5° angles respectively (Table 3) as well as the potential interactions between the hetero atoms in the aryl ring and the transporter and/or enzyme.

7. Importance of the Glutamate Moiety for Folate Receptor Targeting and GARFTase Inhibitory Activity in Classical Thieno[2,3-*d*]pyrimidine Antifolates

As mentioned above, a series of thieno[2,3-*d*]pyrimidines **324-330** (Figure 57) were prepared as potent and selective inhibitors of tumor cells that express FRs α and β .³³⁷ This series of thieno[2,3-*d*]pyrimidine antifolates **324-330** are neither substrates for RFC nor PCFT, which is unique from all the other clinically used classical antifolates evaluated, including the pyrrolo[2,3-*d*]pyrimidine PMX, the quinazoline RTX, and the pteridine MTX antifolates. In this series, compounds **325** and **326** with a 3- or 4-methylene bridge were consistently the most potent inhibitors of cells expressing FRs α and β , and this was associated with potent inhibition of GARFTase.

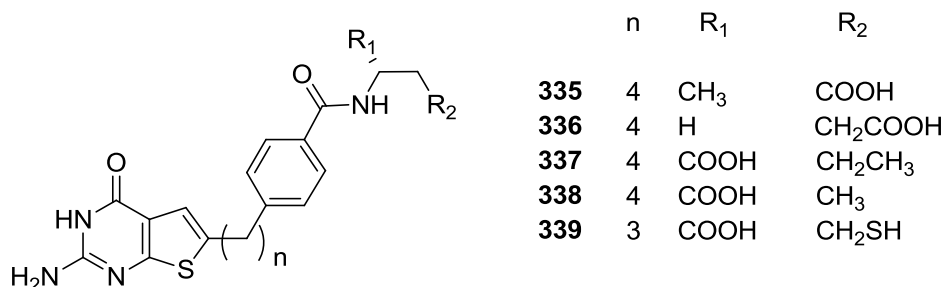


Figure 60. The structure of antifolates **335-339**

To further investigate the structural requirements of the thieno[2,3-*d*]pyrimidine antifolates for GARFTase inhibition and selective FR binding, particularly the importance of the carboxylic acid moieties in the glutamate, a series of analogues **335-339** (Figure 60) with variation in the carboxylic acids of the L-glutamate moiety were designed, synthesized and evaluated. Compounds **335** and **336** have a CH₃ or H at the α -position instead of a carboxylic acid group to explore the importance of glutamate α -carboxylic acid. Compounds **337-339** maintain the α -carboxylic acid but have variations (CH₃ in **337**, H in **338** and SH in **339**) at the γ -carboxylic acid position.

8. The synthesis of substituted thieno[3,2-*d*]pyrimidin-4-amine as antimetabolic anticancer agents.

Tubulin binding agents belong to a very important class of antitumor agents and are widely used in the clinic for cancer chemotherapy.³³⁸ Based on their binding sites on tubulin, most antimicrotubule agents can be divided into three classes, taxoids, the vinca alkaloids and colchicine site inhibitors.^{339, 340}

The first group includes paclitaxel (Taxol) and docetaxel (Taxotere), as well as the epothilones (Figure 61). Paclitaxel and other taxoids (and the epothilones) bind to the interior of the microtubule,^{341, 342} and the tubulin β -subunit. Unlike the other two classes of antimicrotubule agents, the taxoids stimulate tubulin polymerization and are designated microtubule-stabilizing agents. They are useful in the treatment of breast, lung, ovarian, head and neck and prostate carcinomas among others.

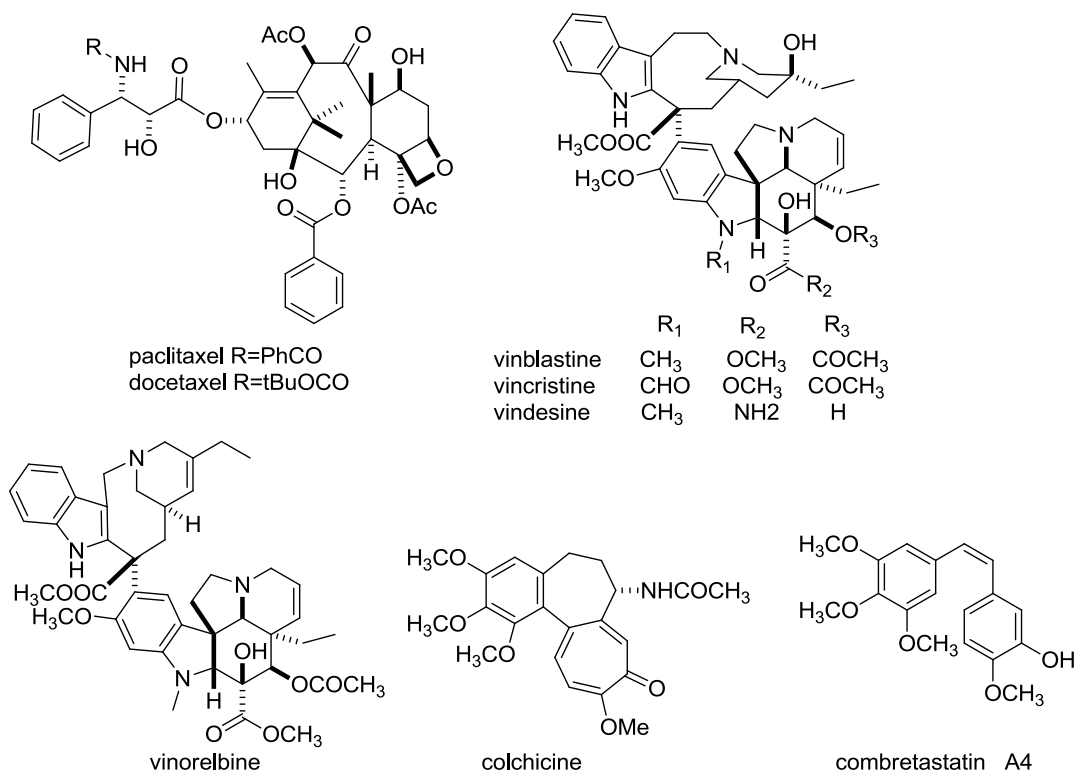


Figure 61. The structures of microtubule targeting agents

The second class are the vinca alkaloids including vincristine, vinblastine, vindesine and vinorelbine (Figure 61). The vinca alkaloids also bind at the β -tubulin but is distinct from that of taxoids. The vinca alkaloids are important in the treatment of leukemias, lymphomas, non-small cell lung cancer and other cancers. A diverse collection of small molecules, including colchicine and combrestatins, bind to the colchicine site on β -tubulin at its interface with α -tubulin, distinct from the vinca site. Similar to the vinca alkaloids, colchicine site agents inhibit tubulin polymerization. Colchicine itself is not used as an antitumor agent but is used in the treatment of gout and familial Mediterranean fever. Although there are no clinically approved antitumor agents that bind to the colchicine site, several of these agents are currently in clinical trials.^{343,}

³⁴⁴ Combretastatins, as exemplified by combretastatin A-4 (CA4) and its phosphorylated

prodrug combretastatin A-4 phosphate (CA4P) are currently in clinical trials,³⁴⁵ which demonstrates the importance of developing colchicine site agents as antitumor agents.

Multidrug resistance (MDR) is a major limitation of cancer chemotherapy, and MDR tumors are usually resistant to microtubule disrupting agents. Overexpression of P-glycoprotein (Pgp) represents one of the major mechanisms of tumor resistance. An elevated Pgp level has been reported in the clinical setting in a number of tumor types, particularly after patients have received chemotherapy.^{346, 347} In addition, Pgp expression has also been reported to be a prognostic indicator in certain cancers and is associated with poor response to chemotherapy.^{348, 349} Due to the overwhelming lack of success of Pgp inhibitors in the clinic, new microtubule targeting agents not susceptible to Pgp-mediated resistance are desired.^{347, 350} Such agents will fill an unmet need in the clinic for patients that develop resistance due to Pgp overexpression. The expression of β III-tubulin is involved in clinical resistance to taxoids and vinca alkaloids in multiple tumor types including non small cell lung,³⁵¹⁻³⁵³ breast,³⁵⁴ and ovarian cancers.^{355, 356} Stengel *et al.*³⁵⁷ and Lee *et al.*³⁵⁸ showed that colchicine site agents circumvent β III-tubulin resistance, which indicated the critical importance of developing new agents that bind to the colchicine site as an alternative to the taxoids for the treatment of refractory cancers.

Poor water solubility is an additional problem associated with several of the currently used antitubulin agents, particularly the taxoids. It is necessary to formulate such drugs in Cremophor or polysorbate, which can cause hypersensitivity reactions and require long administration times. Thus the development of water soluble microtubule targeted agents are highly coveted, and have attracted enormous research effort.

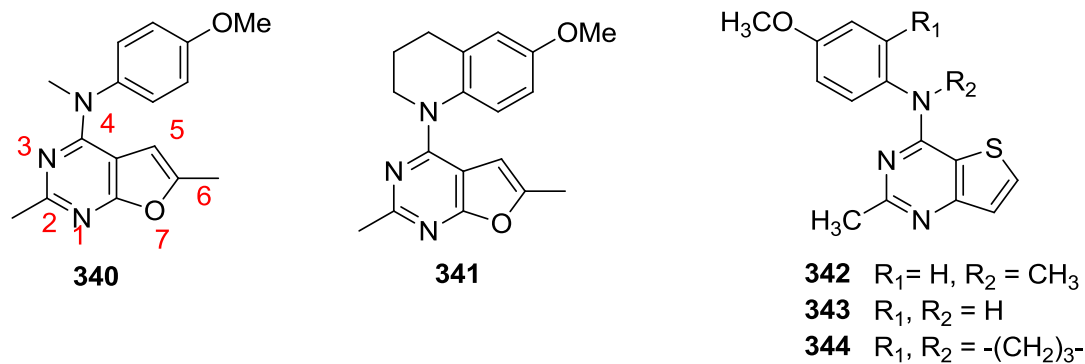


Figure 62. The structures of antimitotic agent **340-344**

Gangjee recently discovered that furo[2,3-*d*]pyrimidine **340** showed antiproliferative activity against the NCI-60 panel of tumor cells at low nanomolar levels and was active in taxol resistant tumor cell lines that over express Pgp. Compound **340** has additional advantages over clinical antimitotic agents, such as taxol, in that it is easily synthesized and is readily converted to the water soluble HCl salt form. Microtubule depolymerization through the binding at the colchicine site was determined to be the primary mechanism of action for **340**.

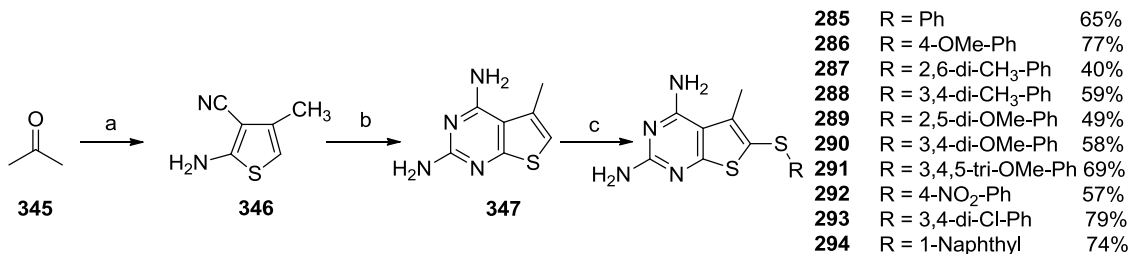
Compared to the 4-NH analogue, the 4-N-methylated compound **340** showed spectacular antimitotic antitumor activity, which could be attributed, in part, to conformational restriction. A structure-activity relationship study revealed that the conformationally restricted analogue **341** (Figure 62) showed potent antiproliferative activity against the NCI-60 tumor cells. Compound **341** was equipotent with CA4P and twice as potent as **340** as an inhibitor of tubulin assembly in a quantitative study. Compound **341** also inhibited the binding of [^3H]colchicine to tubulin as potently as CA4P. The quantitative study suggested that **341** is a more potent inhibitor than **340**.

The thieno[3,2-*d*]pyrimidine scaffold in this study was of interest to further explore the SAR of lead compounds **340** and **341**. This scaffold can be explored to determine the importance of the furan oxygen in the furo[2,3-*d*]pyrimidine for binding to tubulin. The larger size of the sulfur atom compared to the oxygen allows the thieno[3,2-*d*]pyrimidines to more closely mimic the size of a 6-6-ring system, which may influence the conformation of the 4'-methoxy aniline substitution. In addition, the replacement of the O of a furo[2,3-*d*]pyrimidine with a C in the thieno[3,2-*d*]pyrimidine was also anticipated to evaluate the importance of electron distribution in the ring system as well as the importance of hydrogen bonding abilities of O in the furo[2,3-*d*]pyrimidine scaffold.

IV. CHEMICAL DISCUSSION

1. Synthesis of nonclassical analogues 5-methyl-6-substituted arylthio-thieno[2,3-d]pyrimidine-2,4-diamines **285-295** as DHFR inhibitors.

Scheme 48. The synthesis of nonclassical analogues **285-295**



Reagents and conditions:

(a) sulfur, malononitrile, morpholine, rt, 24 h; (b) guanidine, DMSO, 190 °C, 2 h; (c) I₂/EtOH/H₂O, reflux or microwave (180 °C, 30 min)

The synthesis of **285-295** were accomplished as shown in Scheme 48. The key intermediate **347** was synthesized following a 2-step procedure (Scheme 48). Reaction of acetone with malononitrile and sulfur in the presence of morpholine was carried out according to the general procedure of Gewald and coworkers³⁵⁹ to afford the expected thiophene aminonitrile **346**. Different solvents and bases were attempted for this reaction. Ethanol as solvent and morpholine as base was found to be the best conditions with 63% yield of the target. Compound **346** was then condensed with guanidine hydrochloride in DMSO to give **347** in 64% yield.³⁶⁰

Compounds **285-294** were synthesized from **347** with a slightly modified oxidative thiolation procedure initially reported by Gangjee *et al.*³⁶¹ The original procedure required protection of the 2,4-diamino groups, which significantly lowered the overall yield (25% on average). In addition, the original procedure required 16 h of reaction time to afford both thiolation and deprotection.

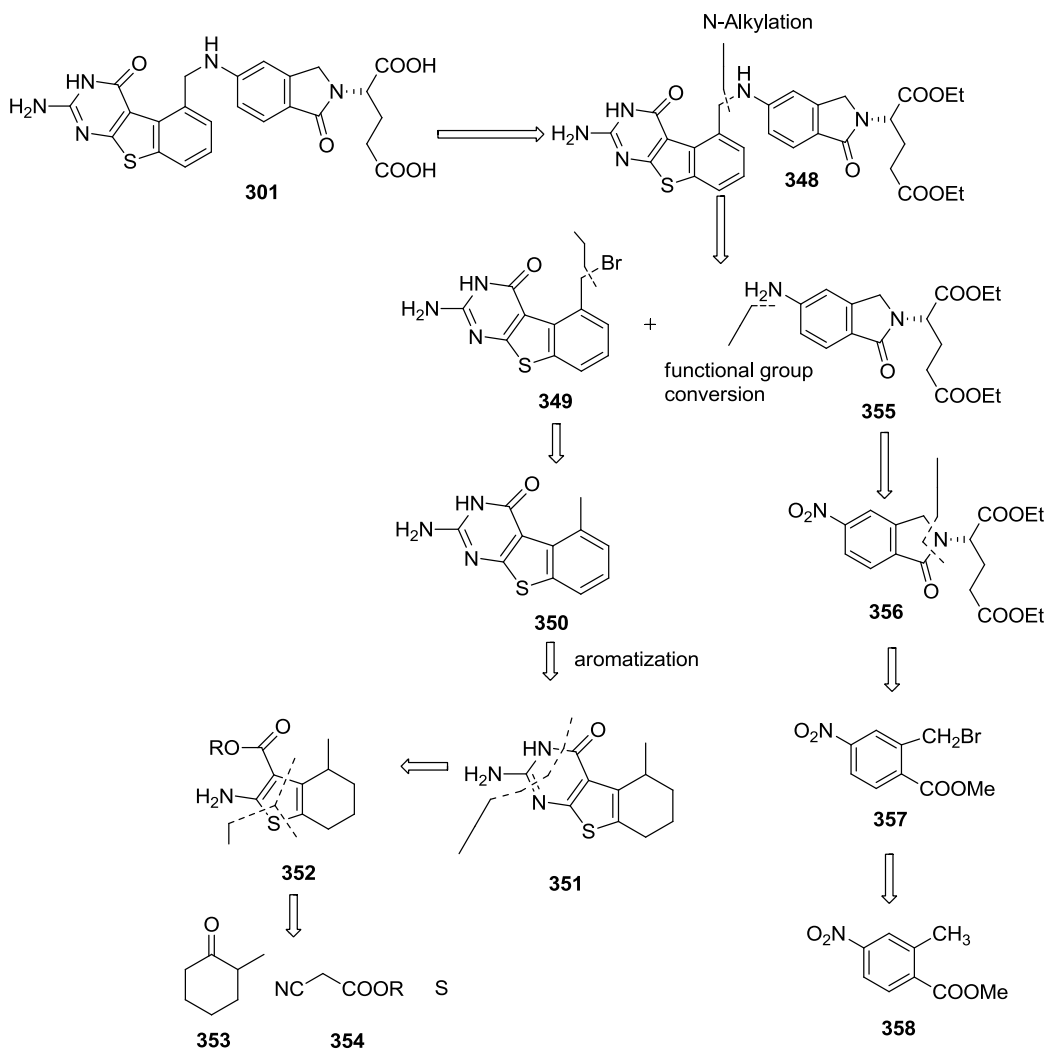
After several attempts of varying the reaction time, temperature and the amount of the iodine in bench-top reactions and microwave irradiation, it was discovered that the best procedure for the reaction was to suspend one equivalent of **347**, two equivalents of the appropriately substituted thiophenols and one equivalent of iodine in ethanol-water (2:1) in a microwave reaction vial and irradiated at 180 °C for 10-20 min. After the reaction mixture was cooled to ambient temperature, the mixture was washed with saturated sodium thiosulfate solution and then concentrated under reduced pressure. The residue was loaded on a silica gel column and eluted with 5% MeOH in CHCl₃. It was determined that the byproduct in this reaction was the disulfide, obtained on oxidation from the thiophenol. Compounds **285-294** were obtained in yields ranging from 40% to 78%. This modified synthetic procedure afforded the target compounds **285-294** with an improvement in the overall yield to 50% on average.

The structures of **285-294** were established by ¹H NMR where the disappearance of C6 proton at 6.49 ppm (compound **347**) and the presence of the requisite protons of the 6-substituted thiols at 6.30-7.30 ppm. The 2,4-diamino protons were deshielded, due to the deshielding zone created by the substitutions at 6-position. Compounds **285-294** were also characterized by elemental analysis or high resolution MS (HRMS).

2. 6,5,6-Tricyclic Benzo[4,5]thieno[2,3-*d*]pyrimidines as Dual Thymidylate Synthase and Dihydrofolate Reductase Inhibitors

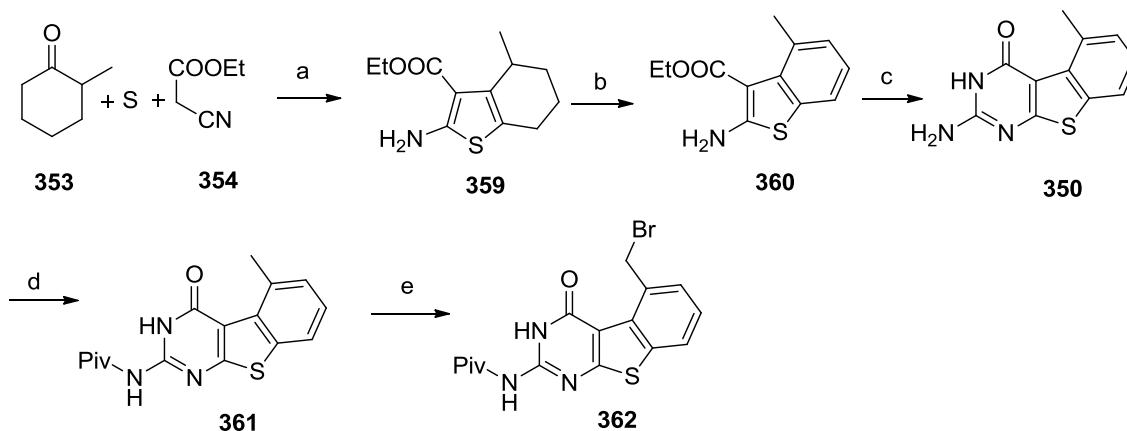
Based on retro-synthetic analysis, it was anticipated that target compound **301** could be divided into two parts: the central tricyclic scaffold **349** and the isoindolinone side chain **355**. *N*-alkylation reaction of **349** with **355** followed by saponification would afford **301**.

Scheme 49. Retro synthetic analysis to classical analogue (2*S*)-2-(5-[(2-amino-4-oxo-3,4-dihydro[1]benzothieno[2,3-*d*]pyrimidin-5-yl)methyl]amino}-1-oxo-1,3-dihydro-2*H*-isoindol-2-yl)pentanedioic acid **301**



The side chain **355** could be obtained from **358** through esterification, bromination, cyclization and reduction (Scheme 49). The central tricyclic **349** could be derived from **350**, which in turn could be synthesized from commercially available 2-methylcyclohexanone through the Gewald reaction, cyclization, aromatization and bromination.

Scheme 50. Synthesis of tricyclic thieno[2,3-*d*]pyrimidine **362**



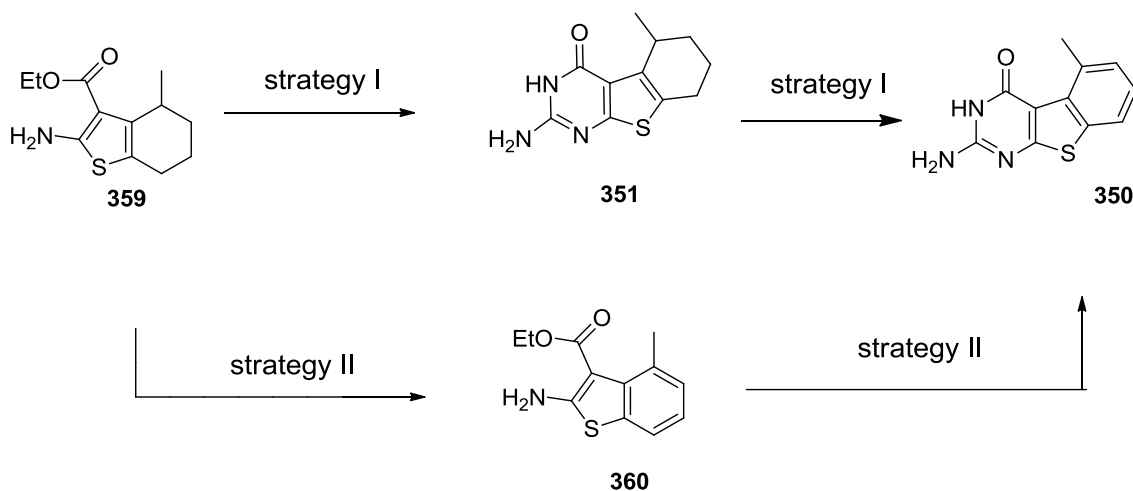
Reagents and conditions:

- (a) ethylcyanoacetate, morpholine, sulfur, ethanol, 45 °C to rt, 12 h; (b) Pd/C, toluene, reflux;
(c) chloroformamidine hydrochloride, DMSO₂, 150 °C; (d) (Piv)₂O, reflux, 3 h; (e) NBS, Bz₂O₂

The synthesis of tricyclic intermediate **362** is presented in Scheme 50. Aromatic intermediate **360** was obtained from **359**. Numerous attempts were made and detailed discussion is provided below (Table 4). The ¹H NMR of compound **360** showed the disappearance of alicyclic protons at 1.54 - 3.17 ppm and appearance of three phenyl protons at 6.98-7.43 ppm. Tricyclic thieno[2,3-*d*]pyrimidine **350** was obtained directly from **360** under similar condensation condition discussed in Scheme 48. Compound **350** showed poor solubility in most organic solvents without 2-amino group protection. It could not be brominated at the 5-methyl group. Hence, the 2-amino group of **350** was protected with pivaloyl anhydride at reflux (71% yield). The pivaloyl protected compound **361** showed good solubility in 1,2-dichloromethane and radical bromination with NBS and a catalytic amount of benzoyl peroxide³⁶² afforded the key intermediate **362** in 42% yield. The ¹H NMR of **362** showed the appearance of a singlet peak at 5.71

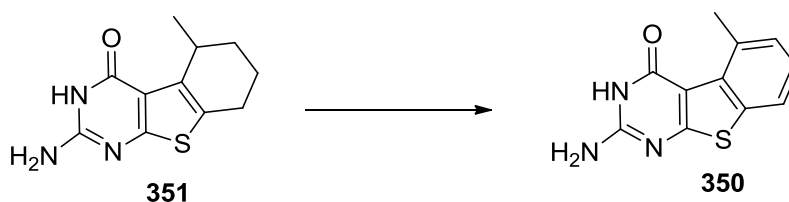
ppm, which corresponded to the benzylic protons, and disappearance of the peak at 3.05 ppm, which corresponded to the 5-CH₃ protons

Scheme 51. Attempted synthesis of key intermediate **350**



The key intermediate in the synthesis of **349** was the aromatic tricyclic thieno[2,3-*d*]pyrimidine **350**, which could be brominated to **349**. Theoretically, there were two strategies to obtain target compound **350**. Strategy I was to synthesize tricyclic thieno[2,3-*d*]pyrimidine **351** first, which can be aromatized to **350**. Strategy II was to aromatize bicyclic intermediate **360** first followed by condensation to give **350**. Since **351** was a versatile intermediate with general applicability, strategy I was attempted first. The conditions that are attempted was summarized in Table 4.

Table 4. Strategy I: Aromatization of tricyclic thieno[2,3-*d*]pyrimidine **351**



Entry	Oxidant	Solvent	Temperature	Time	Yield
1	SeO ₂	HOAc	Reflux	24 h	No reaction
2	MnO ₂	Dioxane	Reflux	12 h, 24 h	No reaction
3	DDQ	Dioxane	Reflux	12 h, 24 h	No reaction
4	DDQ	Toluene	Reflux	12 h	No reaction
5	DDQ	DMSO	Reflux	4 h	trace amount
6	DDQ	DMSO	120 °C (microwave)	30 min	trace amount
7	DDQ	DMF	130 °C (microwave)	10 min	No reaction
8	DDQ	DMF	150 °C (microwave)	20 min	No reaction
9	DDQ	Dioxane	120 °C (microwave)	20 min	No reaction
		/DMSO			
10	DDQ	Toluene	120 °C (microwave)	20 min	No reaction
		/DMSO			

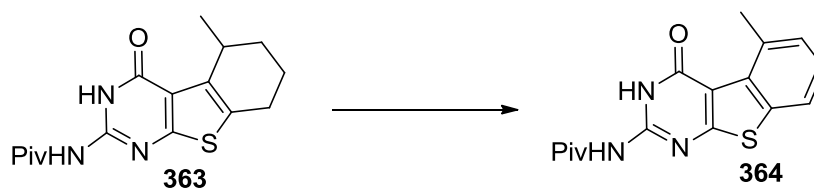
Rosowsky *et. al.*³⁶³ previously reported the synthesis of aromatic tetracyclic thieno[2,3-*d*]pyrimidine *via* SeO₂ in HOAc at reflux. SeO₂ oxidation was attempted first (entry 1 in Table 4). However, there was no new spot on TLC. Gangjee *et. al.*³⁶⁴ reported the oxidation of dihydropyrrolo[2,3-*d*]pyrimidine to aromatic analogues *via* MnO₂. MnO₂ and **351** in dioxane at reflux for 12 h and 24 h (entry 2) were attempted. No new spot was observed on TLC. DDQ had been reported¹⁴ as a dehydrogenation agent. Compound **351** treated with DDQ in dioxane for 12 h at reflux afforded no new spot on TLC. Extending the reaction time to 24 h or using DDQ in toluene did not afford any products (entry 3). High boiling point solvents like DMSO were also tried. Compound **351** and DDQ in

DMSO at reflux for 4 h afforded a light new spot on TLC and some decomposed starting material **351** (entry 5). This sparked our interest in DDQ as aromatization agent.

Microwave irradiation was also evaluated for this reaction. DDQ and **351** in DMSO under microwave irradiation at 120 °C for 30 min (entry 6) gave a trace amount of a new spot on TLC. However, it was difficult to purify this new spot due to its close R_f value with starting material **351** and small quantity of the product. DMF as solvent was also attempted. DDQ and **351** in DMF under microwave irradiation at 130 °C for 10 min (entry 7) and 150 °C for 20 min (entry 8) afforded no new spot on TLC. Mixed solvent system such as DDQ and **351** in dioxane / DMSO (1:1) under microwave irradiation at 120 °C for 20 min (entry 9) and toluene / DMSO (1:1) at 120 °C for 20 min (entry 10) did not afford any new spot on TLC.

The poor solubility of **351** in organic solvent was perhaps responsible for the failure of aromatization. The 2-amino group of **351** was protected with a pivaloyl group and the resulting compound **363** showed good solubility in most organic solvents.

Table 5. Strategy I: Aromatization of tricyclic thieno[2,3-*d*]pyrimidine **363**

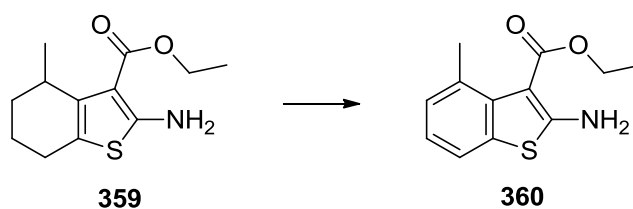


Entry	Oxidant	Solvent	Temperature	Time	Yield
1	DDQ	Dioxane	Reflux	4 h, 8 h, 12 h	No reaction
2	DDQ	Toluene	Reflux	12 h	No reaction
3	DDQ	Benzene	Reflux	12 h	No reaction
4	DDQ	Dioxane /Toluene	Reflux	12 h	No reaction

5	DDQ	DMSO	Reflux	8 h	No reaction
6	DDQ	DMSO	100 °C (microwave)	30 min	No reaction
7	DDQ	DMSO	180 °C (microwave)	30 min	No reaction
8	DDQ	Toluene	100 °C (microwave)	60 min	unisolatable
9	DDQ	Toluene	120 °C (microwave)	30 min	unisolatable

Protected tricyclic thieno[2,3-*d*]pyrimidine **363** and DDQ in dioxane, toluene, benzene, DMSO, dioxane/toluene (1:1) (entries 1-5 in Table 5) at reflux for 4-12 h afforded no new spot on TLC. DDQ and **363** was also attempted under microwave irradiation in DMSO at 100 °C for 30 min (entry 6) and 180 °C for 30 min (entry 7). Neither of them afforded any product. Similarly, DDQ and **363** under microwave irradiation in toluene at 100 °C for 60 min (entry 8) and at 120 °C for 30 min (entry 9) afforded no new spot on TLC.

Table 6. Strategy II: Aromatization of bicyclic intermediate **359**

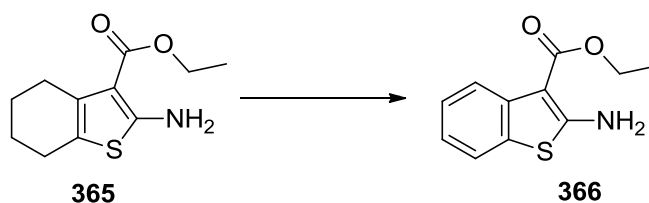


Entry	Oxidant	Solvent	Temperature	Time	Yield
1	MnO ₂	Toluene	Reflux	24 h	No reaction
2	SeO ₂	Toluene	Reflux	24 h	No reaction
3	DDQ	Toluene	Reflux	5 h	No reaction
4	DDQ	Dioxane	140 °C (microwave)	20 min	No reaction

Failure of Strategy I led to the alternate Strategy II, where the bicyclic scaffold was aromatized first. Bicyclic intermediate **359** showed good solubility in most organic solvents. Toluene was chosen as the solvent and MnO₂, SeO₂ and DDQ were chosen as oxidants. Under bench-top condition and microwave irradiation (entries 1-4 in Table 6), none of them gave the target aromatic compound **360**.

After a literature survey, a Pd-C dehydrogenation reaction was found.^{365, 366} Bicyclic intermediate **365**, 10% Pd-C, methylcinnamate and piperidine in refluxing toluene³⁶⁶ did not afford any new spot on TLC, following the reported procedure (entry 1 in Table 7). Since **365** showed good solubility in most organic solvent, CH₂Cl₂ was selected as the solvent (entry 2). After treating **365** with 10% Pd-C in CH₂Cl₂ at reflux for 12 h, a new spot was observed on TLC. When the reaction time was extended to 24 h, the starting material **365** could be still be detected as reacted. In order to characterize the structure of the new spot, the reaction was stopped and the aromatic intermediate **366** was obtained in 30% yield after column chromatography.

Table 7. Strategy II: Aromatization of bicyclic intermediate **365**



Entry	Oxidant	Solvent	Temperature	Time	Yield
1	Pd/C	Toluene, piperidine methylcinnamate	Reflux	24 h	No reaction
2	Pd/C	CH ₂ Cl ₂	Reflux	24 h	30.1 %
3	Pd/C	Toluene	Reflux	24 h	51.6%

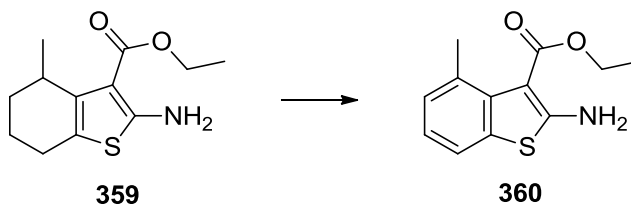
4	Pd/C	Toluene	Reflux	36 h	88%
5	DDQ	Toluene	Reflux	5 h	trace amount
6	DDQ	Toluene	150 °C (microwave)	30 min	trace amount

The spectroscopic data (^1H NMR) and elemental analysis were consistent with the structure of **366**. The ^1H NMR of **366** showed the disappearance of peaks at 1.65-2.61 ppm and the appearance of four phenyl protons at 7.05-7.97 ppm.

In order to increase the conversion rate of this reaction, a higher boiling solvent toluene, was tried (entry 3). However, after 24 h reaction in toluene at reflux, starting material **365** could be still detected on TLC and **366** was obtained in 51.6% yield by column chromatography. These two reaction conditions indicated that a higher reaction temperature may be beneficial (comparing the boiling points of CH_2Cl_2 and toluene). Next the reaction time was extended to 36 h (entry 4) and the TLC showed the formation of one major spot identified as **366** and small amount of by-product. Compound **366** was obtained in 88% yield after column chromatography.

It was important to know whether the 4- CH_3 moiety hampered oxidation, since DDQ did not afford the oxidation of the 4- CH_3 substituted bicyclic intermediate **359**. Intermediate **365** was also treated with DDQ in toluene at reflux and under microwave irradiation (entries 5-6). Both conditions afforded trace amounts of target compound **366**, which suggested that DDQ was probably incapable of aromatizing bicyclic analogues **359** or **365**.

Table 8. Strategy II: Aromatization of bicyclic intermediate **359**



Entry	Oxidant	Solvent	Temperature	Time	Yield
1	Pd/C	Toluene	Reflux	24 h	25.1%
2	Pd/C	Toluene	Reflux	36 h	30.2%
3	Pd/C	Mesitylene	Reflux	48 h	52.1%

The success in the aromatization of **365** generated encouragement for the synthesis of the aromatic intermediate **360**. Compound **359** and 10% Pd-C in toluene at reflux for 4 h afforded a new spot on TLC. When the reaction time was extended to 24 h, some by-products were observed on TLC. Compound **360** was obtained in 25% yield by column chromatography (entry 1 in Table 8).

The ¹H NMR of compound **360** showed the disappearance of allicyclic methylene peaks at 1.54-3.17 ppm and the appearance of three phenyl protons at 6.98-7.43 ppm. To increase the yield of this reaction, the reaction time was extended to 36 h (entry 2). However, the reaction was found to be incomplete even after 36 h and longer reaction times resulted in the decomposition of **359** (TLC) and further complicated the purification. Compound **360** was obtained in 30.2% yield by column chromatography. Since a higher reaction temperature could be beneficial to this reaction, high boiling

solvent like mesitylene were also tried (entry 3). Compound **359** and 10% Pd-C in mesitylene at reflux for 48 h afforded **360** in 52% yield after column chromatography. The reaction, however, was still found to be incomplete (TLC). The low yield of this reaction might also be due to the steric hindrance of the 4-CH₃ group.

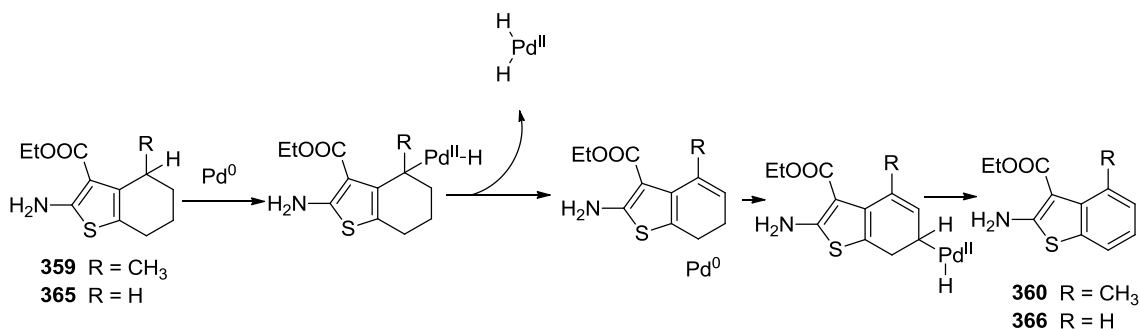
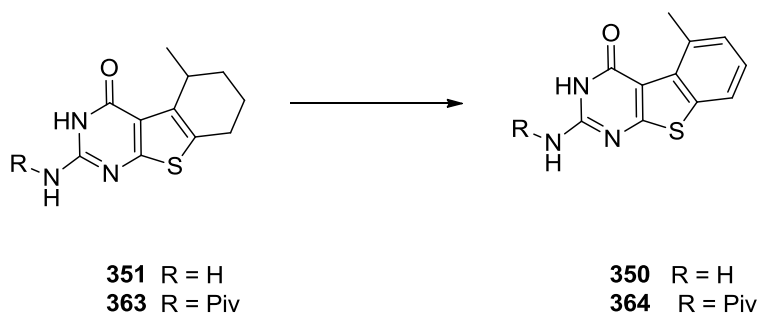


Figure 63. Proposed mechanism of aromatization of **359** and **365**

Grossman *et al*³⁶⁷ discussed the mechanism of Pd-C as a dehydrogenation agent. The mechanism of aromatization of **359** and **365** was proposed as shown in Figure 63. Through an oxidative insertion process, Pd⁰ (Pd-C) is inserted between carbon and hydrogen to form a Pd^{II} species, which then undergoes a β -hydride elimination to cleave the Pd^{II} species with the formation of a double bond. The same process is repeated for a second round to give the aromatized target compounds **360** and **366**. In this reaction, stoichiometric amount of Pd-C is necessary, since Pd⁰ can not be regenerated from the Pd^{II} species. The steric hindrance of the 4- methyl group in **359** might hamper the initial step of Pd⁰ insertion.

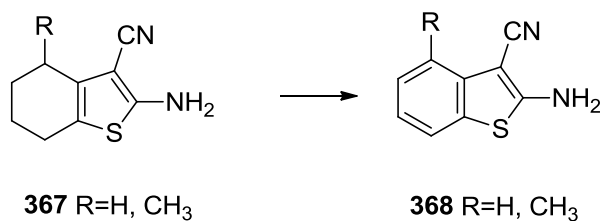
Table 9. Application of Pd-C in aromatization of tricyclic thieno[2,3-*d*]pyrimidines **351** and **363**



Entry	Oxidant	Solvent	Temperature	Time	Yield
1	Pd/C	Toluene	reflux	48 h	No reaction
2	Pd/C	Mesitylene	reflux	48 h	No reaction

Pd-C as a dehydrogenation agent was applied to the aromatization of **351** and **363** in toluene and mesitylene (Table 6) at reflux. After 24 h, there was no new spot observed on TLC, which indicated that this method was not applicable to the tricyclic thieno[2,3-*d*]pyrimidine scaffold.

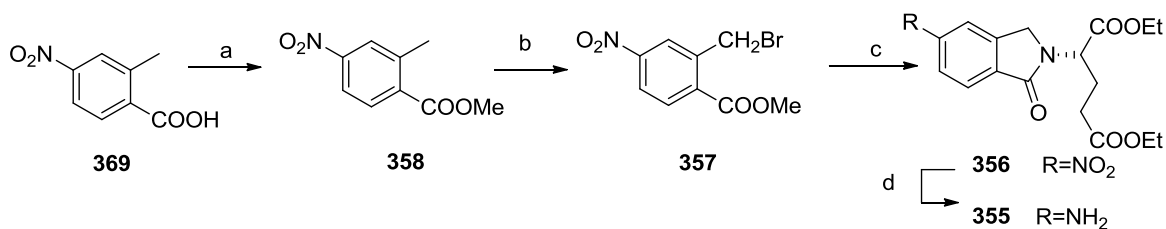
Table 10. Application of Pd-C condition in aromatization of bicyclic thieno[2,3-*d*]pyrimidines **364** and **365**



Entry	Oxidant	Solvent	Temperature	Time	Yield
1	Pd/C	Toluene	reflux	24 h	No reaction
2	Pd/C	Mesitylene	reflux	24 h	No reaction

Pd-C as a dehydrogenation agent was also applied to the bicyclic intermediates **367**. Surprisingly, after reaction in toluene and mesitylene at reflux for 24 h, neither gave the target compound (Table 10). Comparing **359** and **365** with **367**, the only difference was the 3-substitution. When the substitution was an ester group, Pd-C worked. However, the reaction did not work when the substitution was a nitrile group. The reason behind this is still not clear.

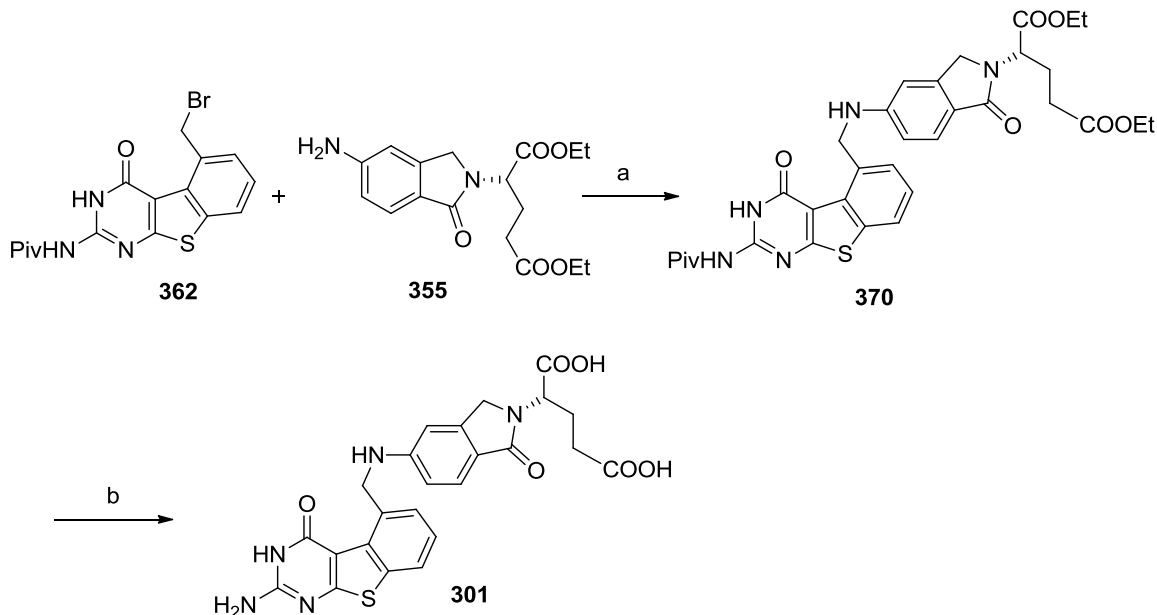
Scheme 52. Synthesis of side-chain of **355**



Reagents and conditions: (a) SOCl_2 , MeOH; (b) NBS, Bz_2O_2 ; (c) diethyl glutamate, K_2CO_3 ; (d) H_2 , Pd/C.

Following a literature procedure,³⁶⁸ amine **355** was synthesized as shown in Scheme 52. Esterification of **369** with $\text{SOCl}_2/\text{MeOH}$ afforded **358** in 91% yield and radical bromination with *N*-bromosuccinimide and a catalytic amount of benzoyl peroxide afforded **357** in 48% yield (Scheme 52). The ^1H NMR of **357** showed the disappearance of protons at 2.69 ppm (CH_3) and appearance of protons at 4.86 ppm (CH_2Br). Treatment with excess diethyl L-glutamate hydrochloride and K_2CO_3 in DMF at room temperature afforded isoindoline **356** as orange oil in 56% yield. The ^1H NMR of **356** showed the appearance of protons at 4.51–4.83 ppm (isoindoline CH_2) and 5.09–5.14 ppm ($\text{Glu}\alpha\text{-CH}$). Reduction of the nitro group in **356** afforded the amine **355** in 92% yield.

Scheme 53. Synthesis of classical analogue **301**

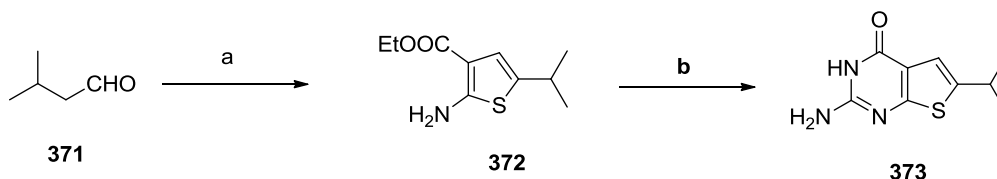


Reagents and conditions: (a) DMF, reflux; (b) 1 N NaOH, 60 °C.

With central tricyclic building block **362** and side chain **355** in hand, a *N*-alkylation reaction³⁶⁹ was carried out to give intermediate **370** in 38% yield. Hydrolysis of the ethyl ester and removal of pivaloyl protecting group of **370** with 1 N NaOH followed by acid workup gave target compound **301** in 34% yield (Scheme 53). The ¹H NMR of **301** showed six aromatic protons at 6.64-7.72 ppm and two benzylic protons at 5.13-5.14 ppm as doublet. The expected NH at 6.74 ppm exchanged with D₂O indicated the success of the condensation reaction. The presence of the requisite protons of the side chain also confirmed the structure of **301**. The structure of **301** was further confirmed by HRMS.

3. *N*-{4-[(2-amino-6-isopropyl-4-oxo-3,4-dihydrothieno[2,3-*d*]pyrimidin-5-yl)sulfanyl]benzoyl}benzoyl-L-glutamic acid **4** and nonclassical analogues **304-313**

Scheme 54. Synthesis of thieno[2,3-*d*]pyrimidine **373**

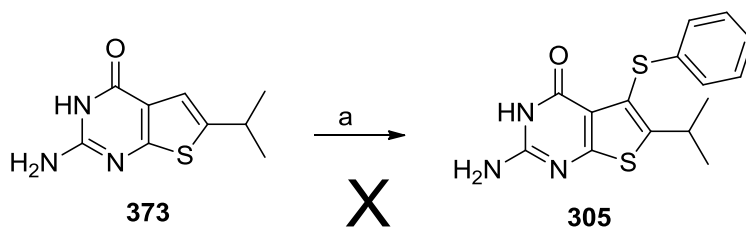


Reagents and conditions:

(a) Ethylcyanoacetate, morpholine, sulfur, ethanol, 45 °C to rt, 12 h; (b) chloroformamide hydrochloride, DMSO, 125 °C, 120 min

Commercially available isovaleraldehyde **371** reacted with sulfur, ethyl cyanoacetate and morpholine in EtOH for 24 h at room temperature under Gewalt reaction conditions to afford **372** in 78% yield. Cyclization of **372** with chloroformamide hydrochloride afforded the thieno[2,3-*d*]pyrimidine **373** in 87% yield (Scheme 54).

Scheme 55. Synthesis of thieno[2,3-*d*]pyrimidine **305**

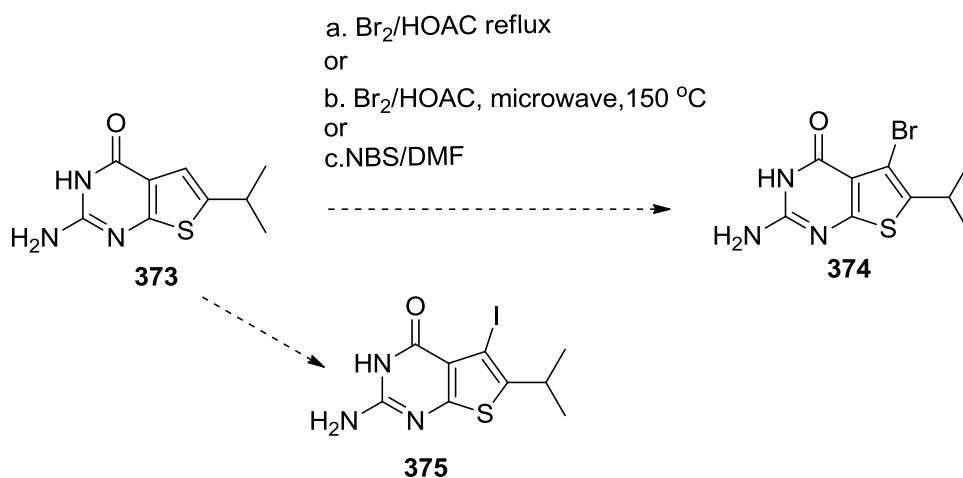


Reagents and conditions: (a) I₂/EtOH/H₂O, microwave (180 °C, 30 min)

With the intermediate **373** in hand, oxidative thiolation at C5-position was attempted to afford target compound **305**. However, following previously reported procedure, the reaction of **373** with benzenethiol and I₂ in a mixture of ethanol/water (2:1) under microwave irradiation at 180 °C for 30 min did not afford **305** (Scheme 55). One possible reason of this reaction might be the steric hindrance of the 6-isopropyl group,

which hampers the addition of the thiol to the 5- position. Due to the failure of the one-step oxidative thiolation, it became necessary to explore an alternative strategy to afford the target compounds.

Scheme 56. Attempted synthesis of key intermediates **374** or **375**

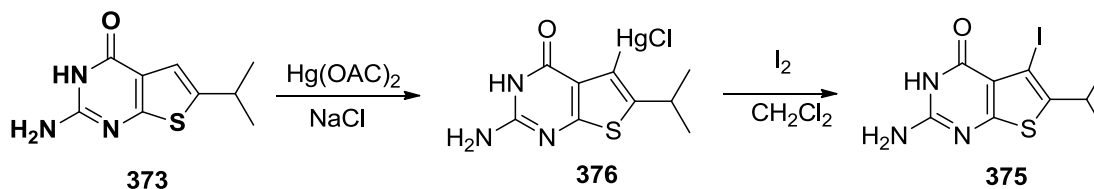


A two-step reaction to introduce thiols to the C5-position was attempted. The 5-halogen substituted thieno[2,3-*d*]pyrimidines **374** or **375** could undergo coupling reactions to afford the 5-thiol substituted thieno[2,3-*d*]pyrimidines. Thus compound **374** or **375** were the key intermediates for the transformation. The first approach for the synthesis of **374** was to utilize NBS in DMF at room temperature and at reflux for 24 h (Scheme 56). All these attempts failed. Halogenation at 5-position using NIS did not afford the desired intermediate either. Recently, Gangjee *et al.*³⁷⁰ reported a convenient C5-bromination reaction of 2-amino-4-oxo-6-methylthieno[2,3-*d*]pyrimidin with bromine under microwave irradiation. So bromine in acetic acid at reflux and microwave irradiation at 150 °C for 30 min were also attempted (Scheme 56) but was unsuccessful.

To our surprise, all efforts to introduce the halogen into the 5-position were unsuccessful. The possible reason might be the steric hindrance of the 6- isopropyl group,

which hampered the addition of the halogen to the 5- position. Thus, an alternative halogenation method had to be considered.

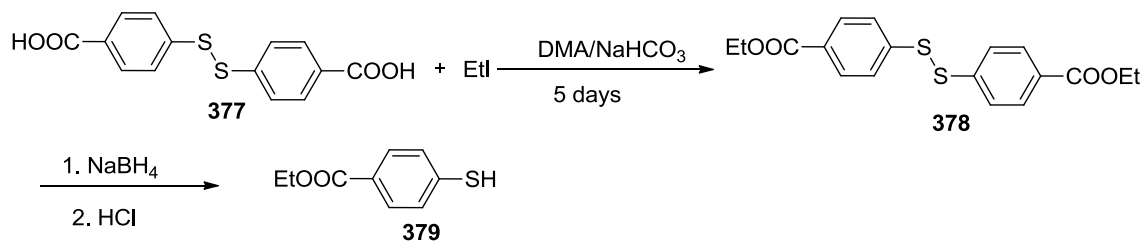
Scheme 57. Synthesis of key intermediate **375**



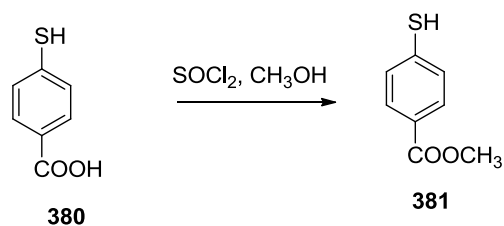
After a literature survey, a two-step reaction for iodine introduction at the 5- or 6- position was found.³⁷¹ Compound **373** (Scheme 57) was reacted with mercuric acetate at 150 °C and then treated with brine. The resulting solid **376** was collected through filtration and was used for the iodination reaction without further purification. Iodine was added to a solution of **376** in CH_2Cl_2 and **375** was obtained in 68% yield (two-step reaction). The ^1H NMR of **375** showed the disappearance of the C5-proton at 6.78 ppm. Compound **375** was also characterized by elemental analysis.

Scheme 58. The synthesis of thio ester **381**

Method I

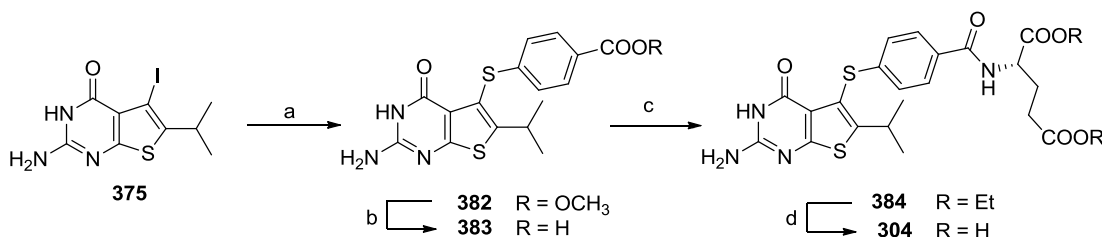


Method II



The synthesis of the classical analogue **304** required the thio ester **379** or **381**, which were not commercially available. As previously reported,³⁷⁰ compound **379** was synthesized from the commercially available disulfide **377**, which was esterified to **378** *via* ethyl iodide. Reduction of **378** to the corresponding sodium salt of ethyl 4-mercaptobenzoate **379** was achieved using sodium borohydride in ethanol (Method I in Scheme 58). Another method was developed and is also described in Scheme 58 (Method II). Thionyl chloride was added dropwise to a stirred solution of commercially available 4-mercaptobenzoic acid in MeOH. When the addition was complete the mixture was left to stand at room temperature for 12 h to obtain a yellow solid. The filtrate was concentrated under reduced pressure to afford a yellow solid **381** in 94% yield. This method had the advantage over the previously reported Method I of having a shortened sequence and higher yield. The ¹H NMR spectrum showed the presence of a singlet at 3.6 ppm which exchanged on addition of D₂O indicating the presence of SH group.

Scheme 59. Synthesis of classical analogue **304** *via* Buchward coupling



Reagents and conditions:

- (a) ethyl 4-mercaptobenzoate, Pd₂dba₃, Xantphos, i-Pr₂NEt, DMF, microwave 190 °C, 60 min;
- (b) 1 N NaOH, EtOH, rt, 18 h;
- (c) L-glutamic acid diethyl ester hydrochloride, 2-chloro-4,6-dimethoxy-1,3,5-triazine, N-methylmorpholine, DMF, rt, 5 h;
- (d) 1 N NaOH, EtOH, rt, 24 h.

With intermediate **375** in hand, two different coupling conditions were attempted, including the Buchward coupling of **375** with methyl 4-mercaptobenzoate in the presence

of *i*-Pr₂NEt, Pd₂dba₃, Xantphos³⁷² under microwave irradiation at 190 °C, which afforded **382** in 64% yield (Scheme 59), and the Ullmann coupling³⁷³ of **375** and appropriate arylthiols in the presence of CuI and K₂CO₃ in DMF under microwave irradiation at 100 °C for 60-120 min, which afforded **305-313** in 75-91% yield (Scheme 60).

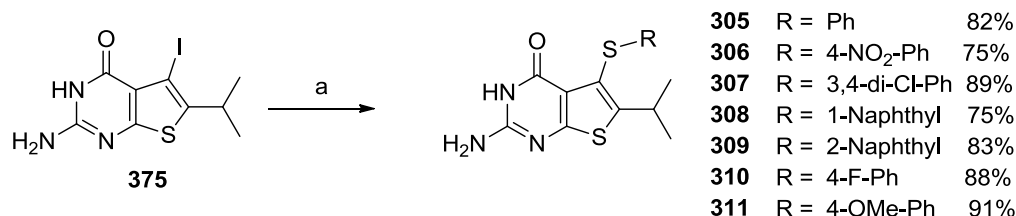
For the synthesis of the classical compound **304**, the required intermediate **382** was prepared through the Buchward coupling in 64 % yield (Scheme 59). The ¹H NMR spectrum of **382** showed the presence of two doublets at 7.06 ppm and 7.78 ppm, which confirmed the structure of **382**. Hydrolysis of the ethyl ester of **382** with 1 N NaOH in ethanol followed by acid workup gave the corresponding acid **383** in 98% yield. With 2-Cl-4,6-dimethoxy-1,3,5-triazine and 4-methylmorpholine as the coupling reagents, acid **383** were coupled with diethyl-L-glutamate hydrochloride to afford compound **384** in 95% yield.

The ¹H NMR spectrum of **384** revealed the expected peptide NH doublet at 8.60 ppm and 8.62 ppm, which exchanged with D₂O. The splitting pattern of Gluα-CH was simplified to a singlet on the addition of D₂O since the exchange of the NH proton prevented the coupling. Hydrolysis of **384** in 1 N NaOH followed by acid workup gave target compound **304** in 83% yield. Compound **304** was also characterized by ¹H NMR and elemental analysis.

Comparing these two coupling reactions, the Ullmann coupling had the advantage over Buchward coupling of both higher yield and easier handling since the later required evacuation and backfilling with nitrogen (3 cycles). Compounds **305-311** were synthesized *via* Ullmann coupling (Scheme 60) in good yields. The structures of **305-**

311 were established by ^1H NMR (the presence of the protons of the aryl side chain at 6.76-8.22 ppm) and elemental analysis or HRMS.

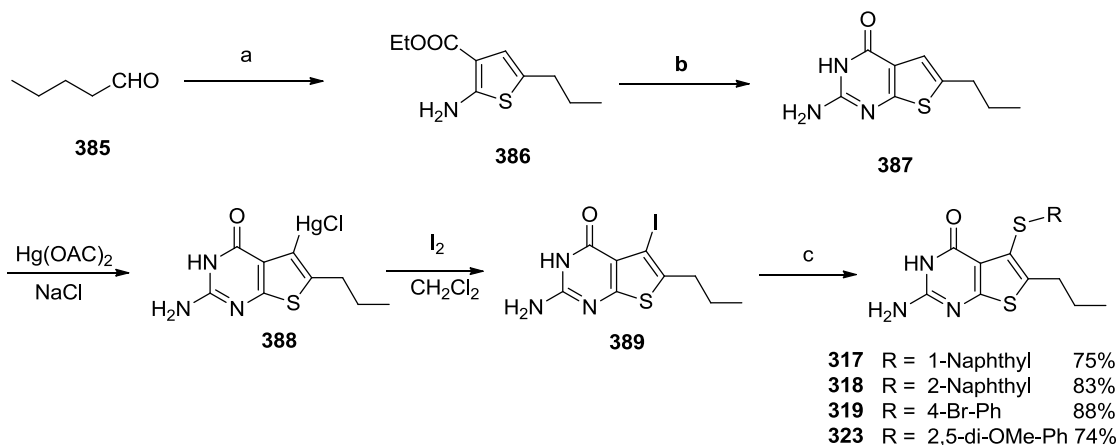
Scheme 60. Synthesis of nonclassical analogues **305-311** *via* Ullmann coupling



Reagents and conditions: (a) arylthiols, CuI, K₂CO₃, DMF, microwave 100 °C, 60-120 min.

4. Synthesis of nonclassical analogues 2-amino-6-propyl-5- substituted arylthio-thieno[2,3-*d*]pyrimidin-4(3*H*)-one **317-319 and **323**.**

Scheme 61. Synthesis of nonclassical analogues **317-319** and **323**



Reagents and conditions:

(a) Ethylcyanoacetate, morpholine, sulfur, ethanol, 45 °C to rt, 12h; (b) chloroformamidine hydrochloride, DMSO₂, 120 °C, 120 min; (c) arylthiols, CuI, K₂CO₃, DMF, microwave 100 °C, 60-120 min

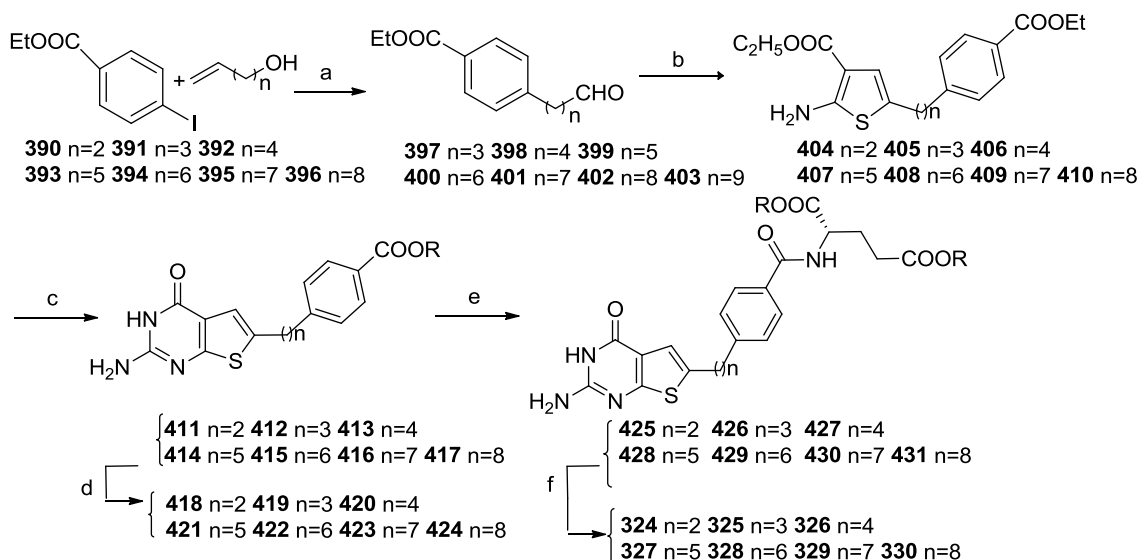
Commercially available valeraldehyde **385** was reacted with sulfur, ethyl cyanoacetate and morpholine in EtOH for 24 h at room temperature under Gewald reaction conditions to afford **386** (Scheme 61) in 78% yield. Cyclization of **386** with

chloroformamidine hydrochloride afforded the thieno[2,3-*d*]pyrimidine **387** in 80% yield. Compound **387** was reacted with mercuric acetate at 150 °C and then treated with brine. The resulting solid **388** was collected by filtration and was used for the iodination reaction without further purification. Iodine was added to a solution of **388** in CH₂Cl₂ and **389** was obtained in 68% yield (two-step reaction).

Compounds **317-319** and **323** were obtained using Ullmann coupling reported previously, which entailed the treatment of **389** with substituted thiophenols in the presence of CuI and K₂CO₃ in DMF under microwave irradiation at 100 °C for 60-120 min. The structures of **317-319** and **323** were established by ¹H NMR (the presence of the protons of the aryl side chain at 6.77-8.22 ppm) and HRMS.

7. Synthesis of 2-amino-4-oxo-6-substituted thieno[2,3-*d*]pyrimidines with 2 to 8 carbon bridge length analogues **324-330**.

Scheme 62. Synthesis of thieno[2,3-*d*]pyrimidines **324-330**



Reagents and conditions:

(a) 10% Pd(AcO)₂, Bu₄NCl, LiCl, LiOAc, DMF, 80 °C, 12 h; (b) S, CN-CH₂-COOEt, morpholine rt 24 h; (c) chloroformamidine hydrochloride, DMSO₂, 140 °C, 4 h; (d) 1 N NaOH, EtOH, rt, 12h; (e) 4-methylmorpholine, 2-Cl-4,6-dimethoxy-1,3,5-triazine, DMF, diethyl L- glutamate hydrochloride, 10 h; (f) 1 N NaOH, EtOH, rt, 24 h.

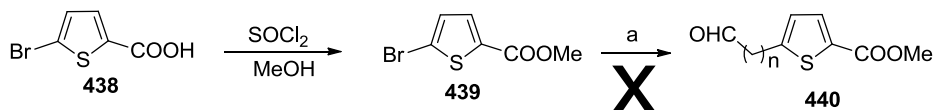
Target compounds **324-330** were synthesized as shown in Scheme 62. The appropriate allyl alcohols **390-396** were treated with palladium diacetate, ethyl 4-iodobenzoate, LiCl, LiOAc and Bu₄NCl in DMF to afford the aldehydes **397-403** (80-85% yield).³⁷⁴ A modified reaction temperature of 80 °C from that reported in the literature improved the yield. Aldehydes **397-403** were then reacted with sulfur, ethyl cyanoacetate and morpholine in EtOH for 24 h at room temperature under Gewald reaction conditions to afford **404-410**. Cyclization of **404-410** with chloroformamidinium hydrochloride afforded the thieno[2,3-*d*]pyrimidines **411-417** in 55-80% yield. Hydrolysis of the ethyl esters of **411-417** with 1 N NaOH in ethanol followed by acid workup gave the corresponding acids **418-424**. With 2-Cl-4,6-dimethoxy-1,3,5-triazine and 4-methylmorpholine as the coupling reagents, acids **418-424** were coupled with diethyl-L-glutamate hydrochloride to afford compounds **425-431** (69-77%). Hydrolysis of **425-431** in 1 N NaOH, followed by acid workup gave target compounds **324-330** in 96-98% yield (Scheme 62). The ¹H NMR spectrum of **324-330** revealed the expected peptide NH doublet at 8.50- 8.60 ppm, which exchanged on addition of D₂O. The splitting pattern of Gluα-CH was reduced to a singlet on addition of D₂O following the exchange of NH proton. Compounds **324-330** were also confirmed by elemental analysis.

12. Synthesis of *N*-({5-[4-(2-amino-4-oxo-3,4-dihydrothieno[2,3-*d*]pyrimidin-6-yl)but-1-yn-1-yl]thiophen-2-yl}carbonyl)-L-glutamic acid **333.**

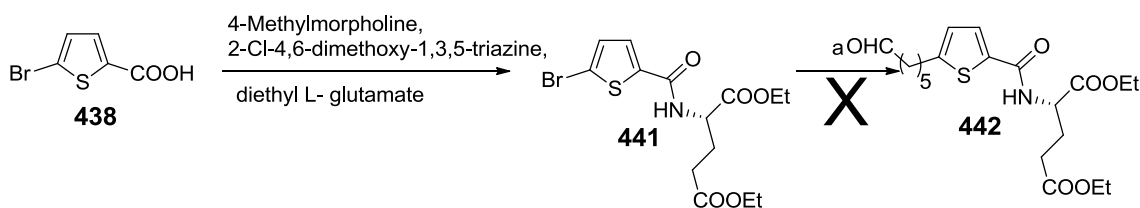
The one-step palladium-catalyzed coupling of allylic alcohols with aryl halides (I, Br) with the previously reported reaction condition (Scheme 62) could afford the aldehydes in high yield. However, when starting material **439**, obtained *via* esterification

from **438**, was attempted under these conditions, the desired aldehyde **440** was not obtained (Scheme 63).

Scheme 63. Attempted synthesis of key intermediate **44**



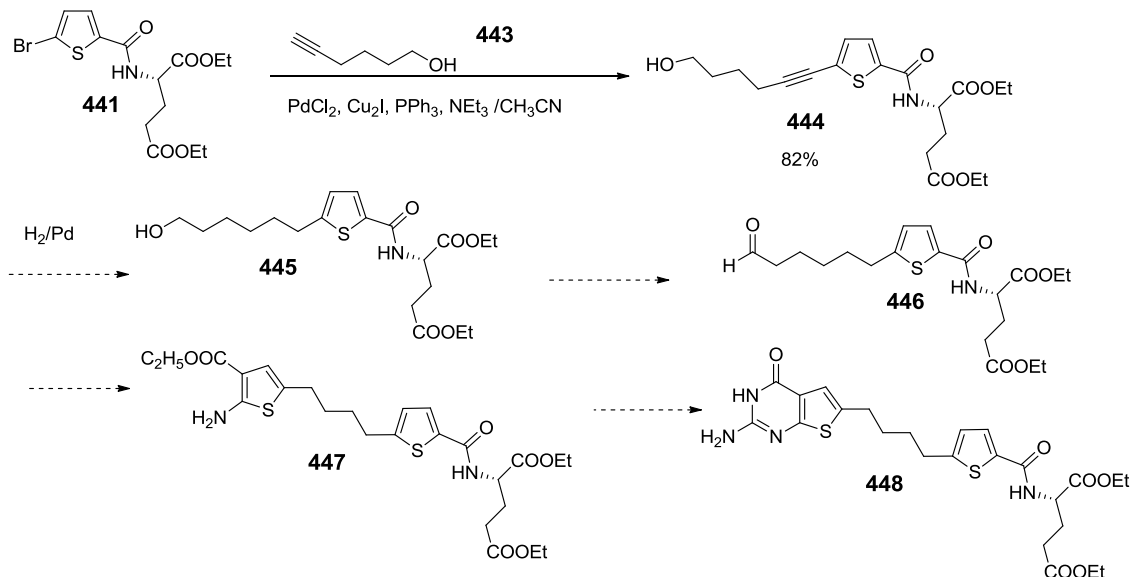
Reagents and conditions: (a) 10% Pd(AcO)₂, Bu₄NCl, LiCl, LiOAc, DMF 80 °C 12 h.



Reagents and conditions: (a) 10% Pd(AcO)₂, Bu₄NCl, LiCl, LiOAc, DMF 80 °C 12 h.

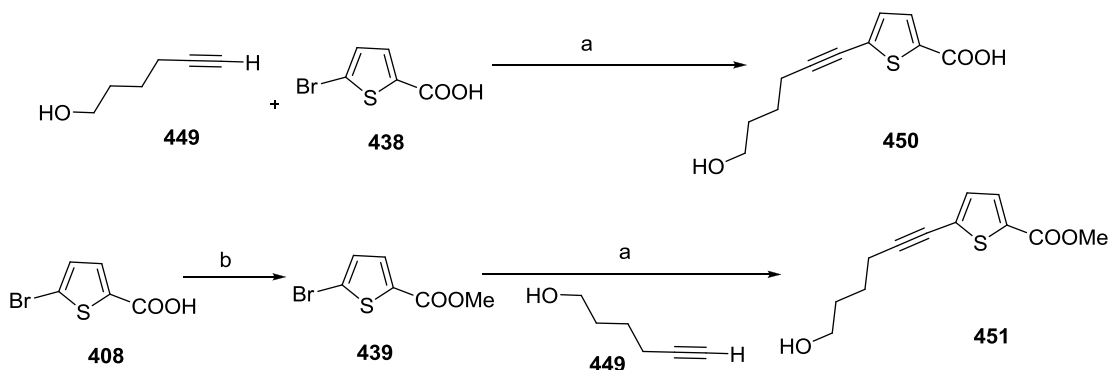
Intermediate **441** was synthesized using previously reported procedures. Coupling of **438** with diethyl-L-glutamate hydrochloride afforded **441** in 83% yield. Compound **441** was then reacted with allylic alcohol in the presence of palladium catalyst, however no desired aldehyde **442** was obtained.

Scheme 64. Proposed synthesis of key intermediate **448**



Compound **444** (Scheme 64) was synthesized by microwave assisted Sonogashira coupling of **441** with hex-5-yn-1-ol in 71% yield. The reaction was attempted using CH₃CN as solvent, triethylamine as base, PdCl₂ as catalyst and Cu₂I as an additive under microwave irradiation at 100 °C for 10 min. Based on the retro-synthetic analysis, it was predicted that target compound **448** could be obtained, after several functional group conversion steps from **444**. With **444** in hand, the reduction of the triple bond, followed by a Swern oxidation could afford aldehyde **446**, a key intermediate for target **448**. However, the subsequent harsh reaction conditions, including reflux and high temperature could racemize the chiral center on the glutamate side-chain. Thus, an alternate synthetic strategy for the target compound **448** was explored.

Scheme 65. Synthesis of intermediate 451

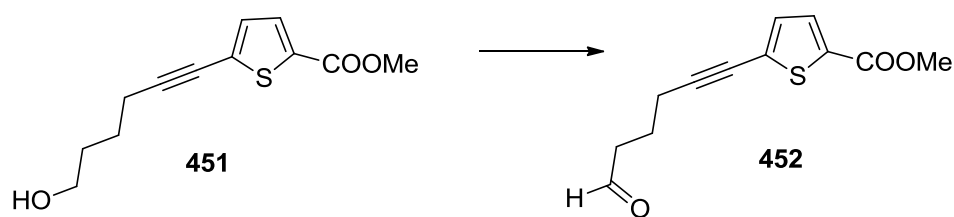


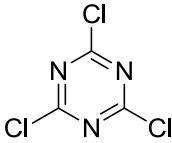
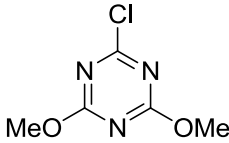
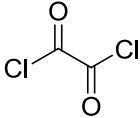
Reagents and conditions:

(a) PdCl₂, Cu₂I, PPh₃, NEt₃, CH₃CN, microwave 110 °C 10 min; (b) SOCl₂, MeOH, 0 °C to rt, 2 days.

Reaction of alcohol **449** (Scheme 65) and **438** was carried out in CH₃CN at 100 °C for 10 min under microwave irradiation following previously reported Sonogashira coupling conditions with low yield of 27% (Scheme 65).³⁷⁵ The reaction was found to be incomplete (TLC). Protection of the carboxylic acid **438** as methyl ester **439** increased the yield to 85% (Scheme 65). The ¹H NMR of **451** showed eight protons at 1.54-3.43 ppm revealing the success of the Sonogashira coupling/

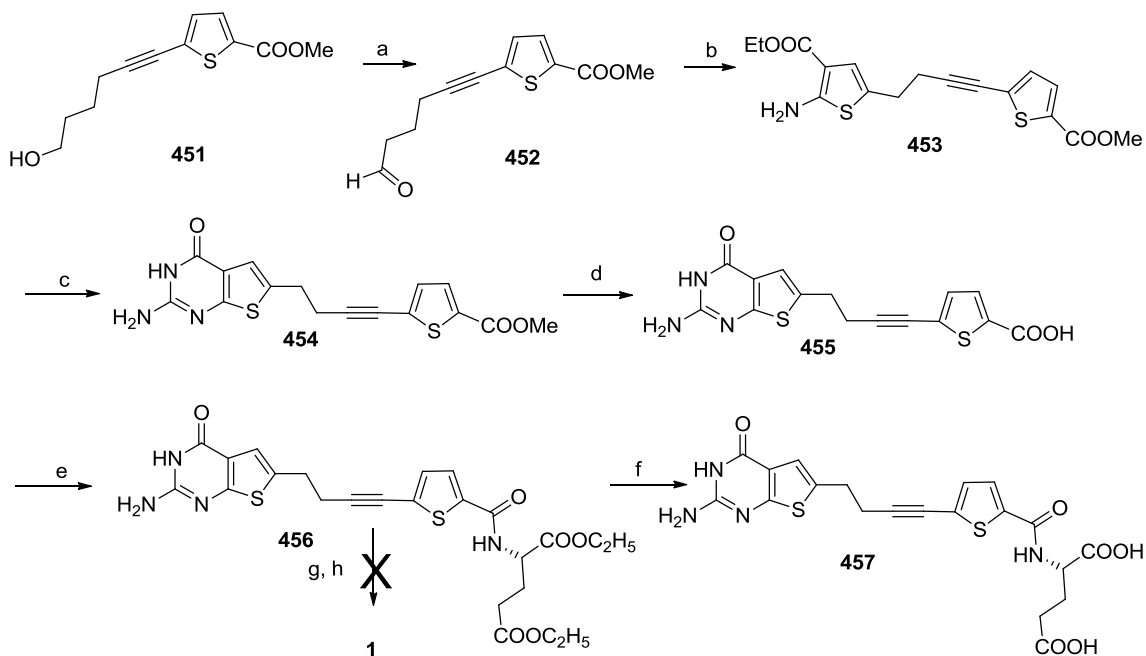
Table 11. Attempted synthesis of aldehyde **452**



Conditions	Temperature	Reagent 1	Reagent 2	Reagent 3	Yield
1	0 °C--r. t.		DMSO	NEt ₃	No reaction
2	0 °C--r. t.		DMSO	NEt ₃	No reaction
3	-78 °C--r. t.		DMSO	NEt ₃	87%

The aldehyde **452** was obtained by oxidation of **451** (Table 11). Three different Swern oxidation conditions were attempted, including modified conditions (entries 1-2 in Table 11) and normal condition (entry 3). Neither of modified conditions worked for **451** while a normal Swern oxidation afforded **452** in 87% yield.

Scheme 66. Synthesis of thieno[2,3-*d*]pyrimidine **457**



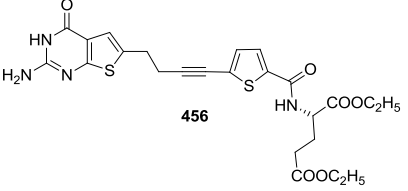
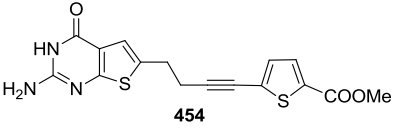
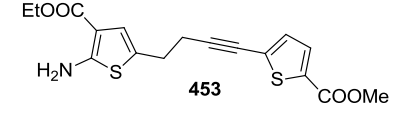
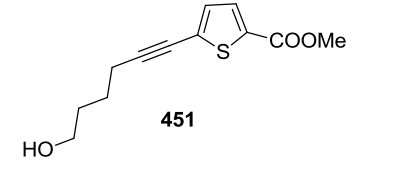
Reagents and conditions:

(a) DMSO, Et₃N, -78 °C to rt; (b) ethylcyanoacetate, morpholine, sulfur, ethanol, 45 °C to rt, 12h; (c) chloroformamide hydrochloride, DMSO₂, 125 °C, 120 min; (d) 1 N NaOH, EtOH, rt, 18 h; (e) L-glutamic acid diethyl ester hydrochloride, 2-chloro-4,6-dimethoxy-1,3,5-triazine, *N*-methylmorpholine, DMF, rt, 5 h; (f) 1 N NaOH, EtOH, rt, 24 h; (g) H₂, Pd/C, 55 psi; (h) 1 N NaOH, EtOH, rt, 24 h.

Aldehyde **452** (Scheme 66) reacted with sulfur, ethyl cyanoacetate and morpholine in EtOH for 24 h at room temperature under Gewald reaction conditions to afford **453** in 40% yield. Cyclization of **453** with chloroformamide hydrochloride afforded the thieno[2,3-*d*]pyrimidine **454** in 52% yield. Hydrolysis of the ethyl ester **454** with 1 N NaOH in ethanol followed by acid workup gave the acid **455** in 94% yield. Compound **456** was synthesized using the procedure previously reported. Coupling of **455** with diethyl-L-glutamate hydrochloride afforded **456** in 78% yield. Hydrolysis of **456** in 1 N NaOH, followed by acid workup gave target compound **457** in 92% yield (Scheme 66).

The ^1H NMR spectrum of **457** revealed the expected peptide NH doublet at 8.62 ppm and 8.71 ppm, which exchanged on the addition of D_2O . The splitting pattern of Glu-CH was simplified on the addition of D_2O . Compound **457** was also confirmed by HRMS.

Table 12. Comparison of hydrogenation with different intermediates*

Substrate	Reaction time	Description	Yield
 <p>456</p>	8 h	TLC: only one spot NMR: no reduction	No reaction
 <p>454</p>	8h, 16h, 24h, 48h	TLC: two spots but difficult to separate	70% reduction (NMR)
 <p>453</p>	24 h, 48h	TLC: Only one spot	30% reduction (NMR)
 <p>451</p>	24 h	TLC : a complete reduction confirmed by NMR	Quantitative

*10% Pd/C as the catalyst and H_2 pressure is 55psi.

Different hydrogenation conditions and substrates are compared for the synthesis of **448**. Initial attempts to reduce the triple bond derived from the Sonogashira reaction was hydrogenation with 10% Pd-C in a mixture of methanol and 5 drops of acetic acid.

Intermediate **456** was attempted first and no desired product spot was detected on TLC after 8 h of reaction. Since the reduced compound may have the same R_f value on TLC as **456**, ^1H NMR was carried out to characterize the spot obtained after its isolation. It was found that there was no reduced product.

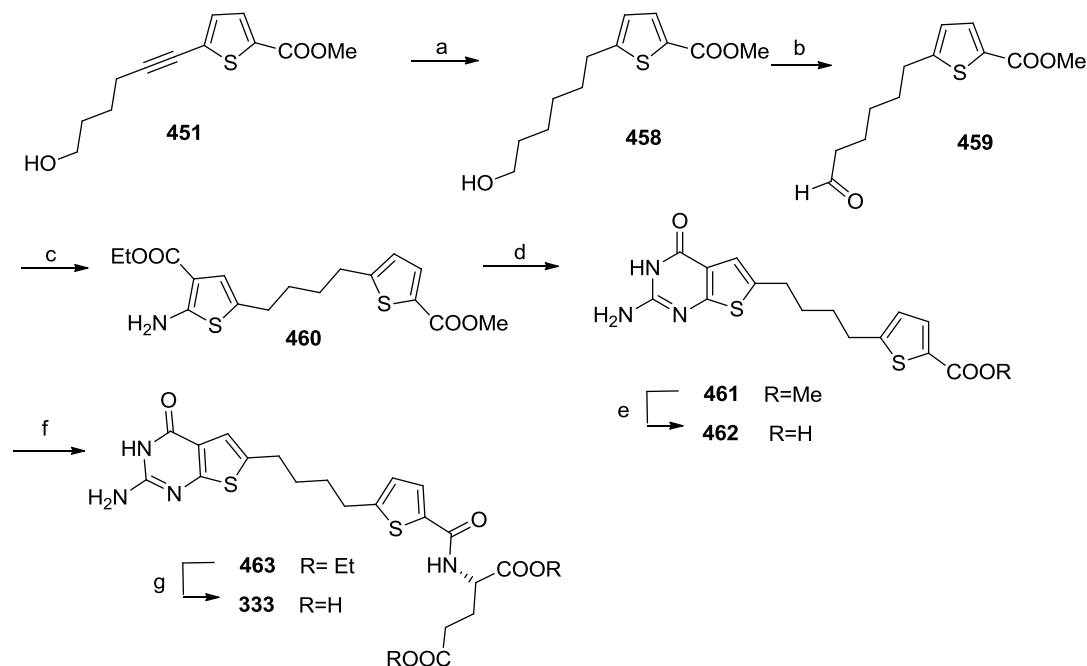
Intermediate **454** was also attempted and a new spot was visible on TLC after 8 h of reaction (Table 12). However, the two spots on TLC had very close R_f values and were not separable *via* column chromatography. The reaction time was increased to 16 h and **454** could be detected on TLC. The reaction was found to be incomplete (TLC) even after 48 h. The ^1H NMR of the mixture showed that about 70% of **454** had been reduced.

Intermediate **453** was also attempted and no new spot was found on TLC after 24 h and 48 h. The ^1H NMR of crude product suggested 30% of **453** was reduced.

To our surprise, it was difficult to reduce these triple bond intermediates using catalytic hydrogenation. The possible reason might be that trace amount of sulfur from the Gewald reaction could poison Pd-C catalyst. Although sulfur was removed by filtration after reaction, there might be trace amount of residual sulfur even after several column chromatography purification. To overcome the possible poisoning effect of sulfur, intermediate **451**, the intermediate prior to Gewald reaction, was used for the catalytic reduction. The reaction was complete (TLC) after 24 h reaction with quantitative yield (Table 12). The ^1H NMR of the reduced compound **458** (Scheme 66) showed the appearance of a triplet that integrated for two protons at 2.79-2.83 ppm and multiple

peaks integrated for two protons at 1.38-1.67 ppm corresponding to two methylene groups. Thus it was decided to carry out the reduction prior to the Gewald reaction.

Scheme 67. Synthesis of thieno[2,3-*d*]pyrimidine 333



Reagents and conditions:

(a) 10% Pd-C, H₂; (b) DMSO, Et₃N, -78 °C to rt; (c) ethylcyanoacetate, morpholine, sulfur, 45 °C to rt; (d) chloroformamide hydrochloride, DMSO, 125 °C, 120 min; (e) 1 N NaOH, EtOH, rt, 18 h; (f) L-glutamic acid diethyl ester hydrochloride, 2-chloro-4,6-dimethoxy-1,3,5-triazine, N-methylmorpholine, rt, 5 h; (g) 1 N NaOH, EtOH, rt, 24 h.

Compound **458** (Scheme 67) was synthesized by catalytic hydrogenation of **451** in 92% yield and the key intermediate aldehyde **459** was obtained by oxidation of **458** via Swern Oxidation in 83% yield (Scheme 67). With key aldehyde **459** in hand, thiophene intermediate **460** was obtained in 63% yield following the previously reported procedures for the Gewald reaction. Cyclization of **460** with chloroformamide hydrochloride afforded the thieno[2,3-*d*]pyrimidine **461** in 85% yield. Hydrolysis of **461** with 1 N NaOH in ethanol followed by acid workup gave acid **462**. Compound **463** was synthesized using procedure previously reported. Coupling of **462** with diethyl-L-

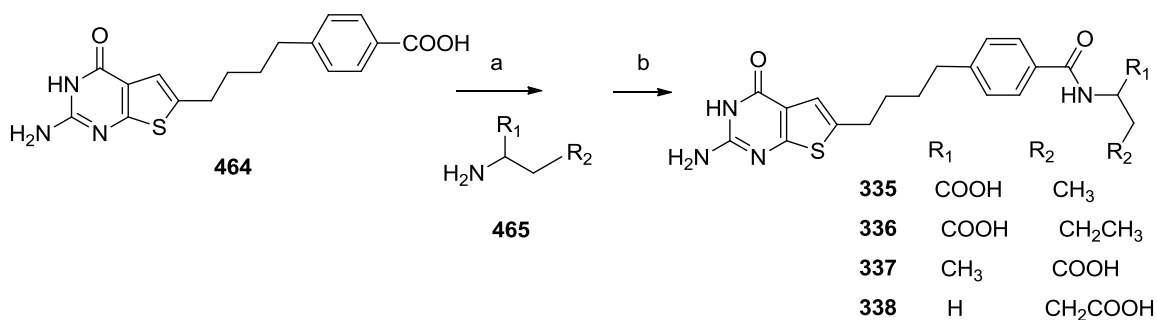
glutamate hydrochloride afforded **463** in 75% yield. Hydrolysis of **463** in 1 N NaOH, followed by acid workup gave target compound **333** in 94% yield (Scheme 67).

The ^1H NMR spectrum of **333** revealed the expected peptide NH doublet at 8.47 ppm and 8.49 ppm, which exchanged on the addition of D_2O . The splitting pattern of $\text{Glu}\alpha\text{-CH}$ was simplified on addition of D_2O since the exchange of NH proton destroyed the coupling. Compound **333** was also confirmed by elemental analysis.

9. Synthesis of classical thieno[2,3-*d*]pyrimidines **335-338** with different amino acid in place of the glutamate.

Acid **464** (Scheme 68) was synthesized using procedures previously reported. Following a previously reported procedure, coupling of **464** with appropriate commercially available amines afforded the desired compounds **335-338**.

Scheme 68. Synthesis of thieno[2,3-*d*]pyrimidines **335-338**



Reagents and conditions:

(a) 4-methylmorpholine, 2-Cl-4,6-dimethoxy-1,3,5-triazine, DMF ; (f) 1 N NaOH, EtOH, rt, 12 h.

The ^1H NMR spectrum of **335** revealed the expected peptide NH doublet at 8.46 ppm and 8.48 ppm, which exchanged on addition of D_2O . Additionally, the presence of multiple peaks at 4.25-4.31 ppm ($\alpha\text{-CH}$) and the presence of a triplet at 0.93-0.97 ppm ($\gamma\text{-CH}_3$) integrating for three protons confirmed the structure of **335**.

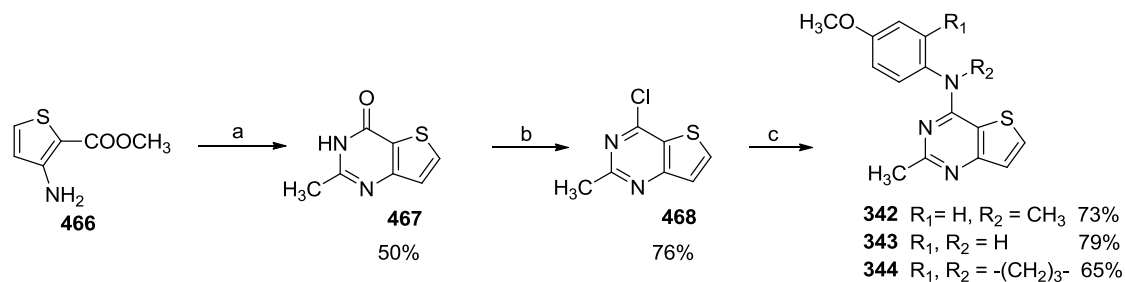
The ^1H NMR spectrum of **336** revealed the expected peptide NH doublet at 8.47 ppm and 8.49 ppm, which exchanged on addition of D_2O , and the presence of the requisite protons of the amino acid side chain confirmed the structure of **336**.

The ^1H NMR spectrum of **337** revealed the expected peptide NH doublet at 8.20 ppm and 8.22 ppm, which exchanged on addition of D_2O . Additionally, the presence of multiple peaks at 4.29-4.36 ppm ($\alpha\text{-CH}$) and the presence of doublet peaks at 1.16-1.18 ppm ($\alpha\text{-CH}_3$) confirmed the structure of **337**.

The ^1H NMR spectrum of **338** revealed the expected peptide NH doublet at 8.38 ppm and 8.41 ppm, which exchanged on addition of D_2O , and the presence of the requisite protons of the amino acid side chain confirmed the structure of **338**. Compounds **335-338** were also confirmed by elemental analysis.

15. Synthesis of N^4 -aryl-2-methyl-thieno[3,2-*d*]pyrimidines **342-344**.

Scheme 69. Synthesis of thieno[3,2-*d*]pyrimidines **342-344**



Reagents and conditions: (a) $\text{HCl}(\text{g})$, CH_3CN ; (b) POCl_3 , reflux ;(c) BuOH , reflux

The conversion of ethyl 2-amino-thiophene-3-carboxylate to 2-methyl thieno[2,3-*d*]pyrimidin-4(3H)-one is reported in the literature. Using a similar method, commercially available **466** (Scheme 69) was dissolved in CH_3CN and HCl gas was bubbled through the solution to afford **467** as a white solid in 50% yield. Chlorination at the 4-position reacted on treatment with POCl_3 at reflux to afford the key intermediate **468** in 76%

yield. The displacement of the 4-chloro moiety of **468** with appropriate anilines and tetrahydroquinolines afforded the target compounds **342-344** in yields that ranged from 65% to 79%.

The ^1H NMR of the **342** showed the appearance of two new peaks at 3.49-3.84 ppm, which corresponded to OCH_3 and N-CH_3 , supporting the structure of **342**. Moreover, the ^1H NMR of **342** showed the appearance of two new doublets at 7.04-7.39 ppm, which corresponded to the 4-substituted aromatic aniline.

The ^1H NMR of **343** showed the appearance of a new singlet peak at 3.78 ppm, which corresponded to OCH_3 . Similarly, it showed the appearance of two new doublets at 6.95-7.62 ppm, which corresponded to the 4-substituted aromatic aniline. The appearance of a new singlet at 9.52 ppm, which exchanged with D_2O and corresponded to the 4-NH, also supported the structure of **343**.

The ^1H NMR of **344** showed appearance of a new singlet at 3.78 ppm, which corresponded to the OCH_3 . It also showed the appearance of peaks at 1.89-4.02 ppm with integration value of six protons, which corresponded to the three methylene groups of the tetrahydroquinoline, supporting the structure of **344**. Compounds **342-344** were also confirmed by elemental analysis.

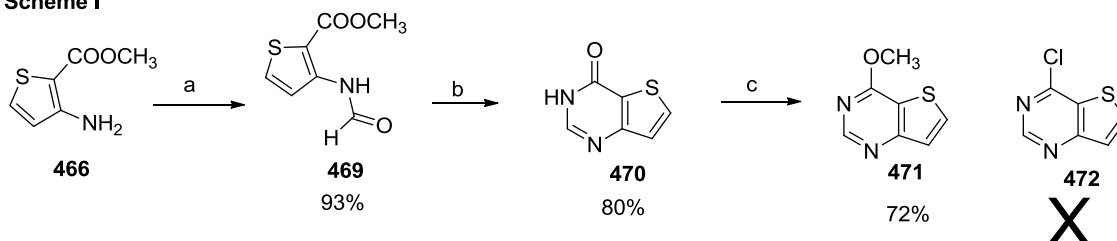
16. Synthesis of *N*-(4-methoxyphenyl)-*N*-methylthieno[3,2-*d*]pyrimidin-4-amine **474**.

Compound **470** (Scheme 70) was synthesized according to literature procedures.³⁷⁶ Commercially available **466** was reacted with acetic anhydride to give **469** in 93% yield, which was used for the next step without further purification. Cyclization of **469** with ammonium formate in formamide provided thieno[3,2-*d*]pyrimidin-4(3*H*)-one

470 in 80% yield. Although it was a 2-step reaction, the overall yield (74%) was acceptable.

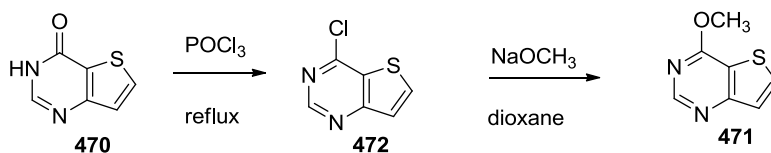
Scheme 70. Synthesis of thieno[3,2-*d*]pyrimidine **471**

Scheme I



Reagents and conditions: (a) Ac_2O , HCOOH ; (b) NH_4COOH , HCONH_2 ; (c) POCl_3 , reflux

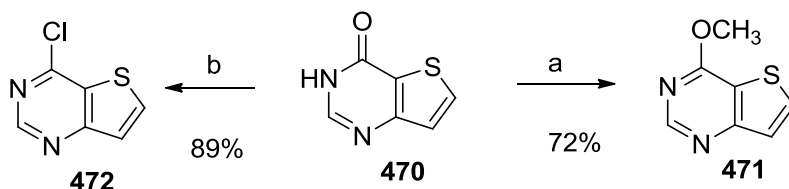
Scheme II



Interestingly, following previously reported procedures, chlorination at the 4-position with POCl_3 at reflux afforded **471** instead of **472**. The ^1H NMR of the **471** showed appearance of a singlet at 4.13 ppm with an integration of three protons, which corresponded to OCH_3 . Moreover, the 3-NH peak at 12.48 ppm for **470** disappeared. The structure of compound **471** was also confirmed by elemental analysis.

This reaction was repeated for three times and each time **471** was obtained instead of **472**. It is of interest to determine where the methoxy group come from. A search of the literature²⁰ revealed that **471** had been synthesized from **472** with sodium methoxide (Scheme II in Scheme 70). However, sodium methoxide was never used in the present work. The possible resource of this methoxy group might be methanol that was used for preparing the silica gel plug for column chromatography.

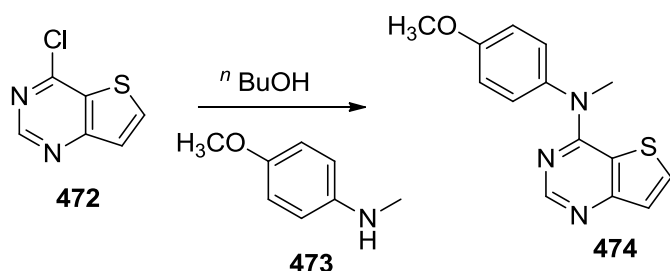
Scheme 71. Synthesis of thieno[3,2-*d*]pyrimidine **472**



Reagents and conditions: (a) POCl₃, reflux, (b) POCl₃, reflux, avoid methanol

Following previously reported chlorination procedure and avoiding the use of methanol, thieno[3,2-*d*]pyrimidine **470** was reacted with POCl₃ to afford **472** in 89% yield (Scheme 71), which verified that the methanol was the source of 4-methoxyl group in the previously isolated **471** (Scheme 70).

Scheme 72. Synthesis of thieno[3,2-*d*]pyrimidine **474**



The displacement of the 4-chloro moiety of **472** with 4-methoxy-*N*-methylaniline afforded target compound **474** (Scheme 72). The ¹H NMR of the **474** showed the appearance of two new peaks at 3.49 ppm and 3.84 ppm, which corresponded to the OCH₃ and *N*-CH₃ respectively, supporting the structure of **474**. The ¹H NMR of the **474** also showed the appearance of two new doublets at 7.05-7.41 ppm, which corresponded to the 4-substituted aniline. Compound **474** was also confirmed by elemental analysis.

V. SUMMARY

A total of one hundred and nineteen compounds were synthesized. Among them thirty-nine new final target compounds were designed, synthesized characterized and evaluated from these projects. These compounds are as follows

1. **5-Methyl-6-(phenylsulfanyl)thieno[2,3-*d*]pyrimidine-2,4-diamine (285).**
2. **6-[(4-Methoxyphenyl)sulfanyl]-5-methylthieno[2,3-*d*]pyrimidine-2,4-diamine (286).**
3. **6-[(2,6-Dimethylphenyl)sulfanyl]-5-methylthieno[2,3-*d*]pyrimidine-2,4-diamine (287).**
4. **6-[(3,4-Dimethylphenyl)sulfanyl]-5-methylthieno[2,3-*d*]pyrimidine-2,4-diamine (288).**
5. **6-[(2,5-Dimethoxyphenyl)sulfanyl]-5-methylthieno[2,3-*d*]pyrimidine-2,4-diamine (289).**
6. **6-[(3,4-Dimethoxyphenyl)sulfanyl]-5-methylthieno[2,3-*d*]pyrimidine-2,4-diamine (290).**
7. **5-Methyl-6-[(3,4,5-trimethoxyphenyl)sulfanyl]thieno[2,3-*d*]pyrimidine-2,4-diamine (291).**
8. **5-Methyl-6-[(4-nitrophenyl)sulfanyl]thieno[2,3-*d*]pyrimidine-2,4-diamine (292).**
9. **6-[(3,4-Dichlorophenyl)sulfanyl]-5-methylthieno[2,3-*d*]pyrimidine-2,4-diamine (293).**
10. **5-Methyl-6-(1-naphthylsulfanyl)thieno[2,3-*d*]pyrimidine-2,4-diamine (294).**

11. (2S)-2-(5-{{(2-amino-4-oxo-3,4-dihydro[1]benzothieno[2,3-*d*]pyrimidin-5-yl)methyl}amino}-1-oxo-1,3-dihydro-2H-isoindol-2-yl)pentanedioic acid (301).
12. 2-Amino-4-oxo-6-isopropyl-5-phenylsulfanylthieno[2,3-*d*]pyrimidine (305).
13. 2-Amino-6-isopropyl-5-[(4-nitrophenyl)sulfanyl]thieno[2,3-*d*]pyrimidin-4(3*H*)-one (306).
14. 2-Amino-5-[(3,4-dichlorophenyl)sulfanyl]-6-isopropylthieno[2,3-*d*]pyrimidin-4(3*H*)-one (307). Using the general procedure above compound 307
15. 2-Amino-6-isopropyl-5-(1-naphthylsulfanyl)thieno[2,3-*d*]pyrimidin-4(3*H*)-one (308).
16. 2-Amino-6-isopropyl-5-(2-naphthylsulfanyl)thieno[2,3-*d*]pyrimidin-4(3*H*)-one (309).
17. 2-Amino-5-[(4-fluorophenyl)sulfanyl]-6-isopropylthieno[2,3-*d*]pyrimidin-4(3*H*)-one (310).
18. 2-Amino-5-[(4-methoxyphenyl)sulfanyl]-6-isopropylthieno[2,3-*d*]pyrimidin-4(3*H*)-one (311).
19. *N*-{4-[(2-amino-6-isopropyl-4-oxo-3,4-dihydrothieno[2,3-*d*]pyrimidin-5-yl)sulfanyl]benzoyl}-L-glutamic acid (304).
20. 2-Amino-6-propyl-5-(1-naphthylsulfanyl)thieno[2,3-*d*]pyrimidin-4(3*H*)-one (317).
21. 2-Amino-6-propyl-5-(2-naphthylsulfanyl)thieno[2,3-*d*]pyrimidin-4(3*H*)-one (318).

22. 2-Amino-6-propyl-5-(4-bromophenyl sulfanyl)thieno[2,3-*d*]pyrimidin-4(3*H*)-one (319).
23. 2-Amino-6-propyl-5-[(2,5-dimethoxyphenyl)sulfanyl]-thieno[2,3-*d*]pyrimidin-4(3*H*)-one (323).
24. *N*-{4-[2- (2-Amino-4-oxo-3,4-dihydrothieno[2,3-*d*]pyrimidin-6-yl)ethyl]benzoyl}-L-glutamic acid (324).
25. *N*-{4-[3- (2-Amino-4-oxo-3,4-dihydrothieno[2,3-*d*]pyrimidin-6-yl)propyl]benzoyl}-L-glutamic acid (325).
26. *N*-{4-[4- (2-Amino-4-oxo-3,4-dihydrothieno[2,3-*d*]pyrimidin-6-yl)butyl]benzoyl}-L-glutamic acid (326).
27. *N*-{4-[5- (2-Amino-4-oxo-3,4-dihydrothieno[2,3-*d*]pyrimidin-6-yl)pentyl]benzoyl}-L-glutamic acid (327).
28. *N*-{4-[6- (2-Amino-4-oxo-3,4-dihydrothieno[2,3-*d*]pyrimidin-6-yl)hexyl]benzoyl}-L-glutamic acid (328).
29. *N*-{4-[7- (2-Amino-4-oxo-3,4-dihydrothieno[2,3-*d*]pyrimidin-6-yl)heptyl]benzoyl}-L-glutamic acid (329).
30. *N*-{4-[8- (2-Amino-4-oxo-3,4-dihydrothieno[2,3-*d*]pyrimidin-6-yl)octyl]benzoyl}-L-glutamic acid (330).
31. *N*-({5-[4-(2-amino-4-oxo-3,4-dihydrothieno[2,3-*d*]pyrimidin-6-yl)butyl]thiophen-2-yl}carbonyl)-L-glutamic acid (333).
32. (2*S*)-2-({4-[4-(2-Amino-4-oxo-3,4-dihydrothieno[2,3-*d*]pyrimidin-6-yl)butyl]benzoyl}amino)butanoic acid (335).

33. *N*-{4-[4-(2-Amino-4-oxo-3,4-dihydrothieno[2,3-*d*]pyrimidin-6-yl)butyl]benzoyl}norvaline (336).
34. 3-({4-[4-(2-Amino-4-oxo-3,4-dihydrothieno[2,3-*d*]pyrimidin-6-yl)butyl]benzoyl}amino)butanoic acid (337).
35. 4-({4-[4-(2-Amino-4-oxo-3,4-dihydrothieno[2,3-*d*]pyrimidin-6-yl)butyl]benzoyl}amino)butanoic acid (338).
36. *N*-(4-Methoxyphenyl)-*N*,2-dimethylthieno[3,2-*d*]pyrimidin-4-amine (342)
37. *N*-(4-Methoxyphenyl)-2-methylthieno[3,2-*d*]pyrimidin-4-amine (343)
38. 6-Methoxy-1-(2-methylthieno[3,2-*d*]pyrimidin-4-yl)-1,2,3,4-tetrahydroquinoline (344)
39. *N*-(4-Methoxyphenyl)-*N*-methylthieno[3,2-*d*]pyrimidin-4-amine (474).

Among them twenty one thieno[2,3-*d*]pyrimidines were designed and synthesized as dual TS and DHFR inhibitors. One benzo[4,5]thieno[2,3-*d*]pyrimidines was designed and synthesized as dual TS and DHFR inhibitor. Thirteen thieno[2,3-*d*]pyrimidines were designed and synthesized as GARFTase inhibitors with folate receptor (FR) specificity and antitumor activity. Four thieno[3,2-*d*]pyrimidines were designed and synthesized as RTK inhibitors with antimitotic antitumor activity.

Compound **285-294** were designed as sulfur isosteres of lead pyrrolo[2,3-*d*]pyrimidines and showed potent and selective dual TS and DHFR inhibitory activity.

Compound **301** with a tricyclic benzo[4,5]thieno[2,3-*d*]pyrimidine scaffold and a flexible and rigid benzoylglutamate were synthesized as dual thymidylate synthase (TS) and dihydrofolate reductase (DHFR) inhibitors. Compared to the 2-methyl analog, compounds with a 2-NH₂ group increases hTS inhibition by more than 10-fold and also

afford excellent hDHFR inhibition ($IC_{50} = 0.09-0.1 \mu\text{M}$). The X-ray crystal structures of **301** with hDHFR reveal, for the first time, the binding mode of tricyclics benzo[4,5]thieno[2,3-*d*]pyrimidine with human DHFR.

Classical analogues **304** and nine nonclassical analogues **305-311** were synthesized as potential dual thymidylate synthase (TS) and dihydrofolate reductase (DHFR) inhibitors. The classical compound **304** showed potent human TS ($IC_{50} = 80 \text{ nM}$) inhibition. Compared to the 6-methyl and 6-ethyl analogs, the 6-isopropyl compound was 47-fold less potent as human DHFR inhibitor, which indicated that the bulk of the 6-substitution pattern determines the binding of 2-amino-4-oxo-6-substituted lthieno[2,3-*d*]pyrimidine with human DHFR.

To further explore the substitution effects at 6-position, a series of nonclassical 2-amino-6-propyl-4-oxo-3,4-dihydrothieno[2,3-*d*]pyrimidines **317-319** and **323** were designed and synthesized. These series of compounds restored DHFR inhibitory activities and showed remarkable selectivities among DHFRs from different species. Compound **317** in this series showed an remarkable 1000-fold selectivity against *T. gondii* DHFR over human DHFR, which is better than any compound known in the literature.

A series of seven 2-amino-4-oxo-6-substituted thieno[2,3-*d*]pyrimidines **324-330** ($n = 2-8$) were synthesized as selective folate receptor (FR) α and β substrates and as antitumor agents. This series of compounds revealed for the first time that transport of classical compounds by FRs can be independent from RFC or PCFT. To further investigate the structural requirements of antifolates with respect to FR substrate activity and antitumor activity, **335-338** with variations in the glutamate moiety and **333** with

variations in side chain aryl group in thieno[2,3-*d*]pyrimidine antifolates were designed and synthesized.

In addition, bicyclic substituted thieno[2,3-*d*]- and theino[3,2-*d*]pyrimidines **342-344** and **474** were synthesized as antimitotic agents. These compounds showed potent inhibition of tumor cells in culture and extended the structure-activity relationship for the bicyclic scaffolds in the antimitotic area.

VI. EXPERIMENTAL SECTION

General Methods for Synthesis:

All evaporations were carried out *in vacuo* with a rotary evaporator. Analytical samples were dried *in vacuo* (0.2 mm Hg) in an Abderhalden drying apparatus over P₂O₅. Thin-layer chromatography (TLC) was performed on silica gel plates with fluorescent indicator. Spots were visualized by UV light (254 and 365 nm). All analytical samples were homogeneous on TLC in at least two different solvent systems. Purification by column and flash chromatography was carried out using Merck silica gel 60 (200-400 mesh). The amount (weight) of silica gel for column chromatography was in the range of 50-100 times the amount (weight) of the crude compounds being separated. Columns were dry packed unless specified otherwise. Solvent systems are reported as volume percent mixture. Melting points were determined on a Mel-Temp II melting point apparatus and are uncorrected. Proton nuclear magnetic resonance (¹H NMR) spectra were recorded on a Bruker WH-300 (300MHz) spectrometer. The chemical shift (δ) values are reported as parts per million (ppm) relative to tetramethylsilane as internal standard; s = singlet, d = doublet, t = triplet, q = quartet, m = multiplet, br s = broad singlet, exch = protons exchangeable by addition of D₂O. Elemental analyses were performed by Atlantic Microlab, Inc., Norcross, GA. Elemental compositions were within $\pm 0.4\%$ of the calculated values. Fractional moles of water or organic solvents frequently found in some analytic samples could not be removed despite 24 h of drying *in vacuo* and were confirmed, where possible, by their presence in the ¹H NMR spectrum. All solvents and chemicals were purchased from Aldrich Chemical Co. or Fisher

Scientific and were used as received except anhydrous solvents which were freshly dried in the laboratory.

2-Amino-4-methylthiophene-3-carbonitrile (346). A mixture of sulfur (3.2 g, 0.1 mol), acetone (5.8 g, 0.1 mol), malononitrile (6.6 g, 0.1 mol) and EtOH (100 mL) were placed in a round bottom flask and warmed to 45 °C and treated dropwise with morpholine (8.7 g, 0.1 mol) over 15 min. The mixture was stirred for 4 h at 45 °C and 24 h at room temperature. Unreacted sulfur was removed by filtration, and the filtrate was concentrated under reduced pressure to afford a brown oil. The residue was loaded on a silica gel column packed with silica gel and eluted with 10% ethyl acetate in hexane to afford **346** (8.6 g, 63%) as a brown solid; R_f 0.52 (hexane/EtOAc 3:1); $^1\text{H NMR}$ (CDCl_3) δ 2.19 (s, 3 H, 4- CH_3), 4.79 (s, 2 H, NH_2 exch), 5.97 (s, 1 H, 5-CH).

5-Methylthieno[2,3-*d*]pyrimidine-2,4-diamine (347). A mixture of **346** (0.55 g, 4 mmol) and guanidine (1.8 g, 20 mmol) in DMSO (7 mL) was heated at 190 °C for 2 h. The reaction solution was evaporated in vacuo to dryness, and the residue was purified by column chromatography on silica gel with 5% MeOH in CHCl_3 as the eluent to afford **346** (0.46 g, 64%) as a brown solid; mp 205.2-205.6 °C, (lit.¹⁰ mp 210-212 °C); R_f 0.49 (MeOH/ CHCl_3 , 1:6); $^1\text{H NMR}$ ($\text{DMSO-}d_6$) δ 2.41 (s, 3 H, 5- CH_3), 5.99 (s, 2 H, NH_2 exch), 6.39 (s, 2 H, NH_2 exch), 6.49 (s, 1 H, 6-CH). This compound was used directly for next step of reaction without further characterization.

General Procedure for the Synthesis of Compounds 285-294.

Compounds **285-294** were synthesized from **347**, appropriately substituted thiophenols and iodine. To a microwave reaction vial was added **347** (0.09 g, 0.5 mmol), benzenethiol (0.11 g, 1 mmol) and iodine (0.127 g, 0.5 mmol), and a mixture of ethanol/water (2:1, 5

mL). The reaction mixture was irradiated in a microwave apparatus at 180 °C for 20 min. After the reaction mixture was cooled to ambient temperature, the mixture was washed with saturated sodium thiosulfate solution (15 mL) and the mixture was concentrated under reduced pressure. The residue was loaded on a silica gel column packed with silica gel and eluted with 5% MeOH in CHCl₃. The fractions containing the desired product (TLC) were pooled and evaporated to afford the product.

5-Methyl-6-(phenylsulfanyl)thieno[2,3-*d*]pyrimidine-2,4-diamine (285). Compound **285** (0.093 g, 64.9%) was obtained from **347** (0.09 g, 0.5 mmol), benzenethiol (0.11 g, 1 mmol) and iodine (0.127 g, 0.5 mmol) as yellow solid; mp 238.6-239.1 °C; *R_f* 0.45 (CHCl₃/MeOH, 6: 1); ¹H NMR (DMSO-*d*₆) δ 2.51 (s, 3 H, 5-CH₃), 6.25 (s, 2 H, NH₂ exch), 6.65 (s, 2 H, NH₂ exch), 7.11-7.17 (d, 2 H, C₆H₅), 7.18, 7.19 (d, 1 H, C₆H₅), 7.27-7.30 (d, 2 H, C₆H₅); Anal. calcd. for (C₁₃H₁₂N₄S₂): C, 54.14; H, 4.19; N, 19.43; S, 22.24; found: C, 53.93; H, 4.41; N, 19.09; S, 21.85.

6-[(4-Methoxyphenyl)sulfanyl]-5-methylthieno[2,3-*d*]pyrimidine-2,4-diamine (286). Compound **286** (0.122 g, 77%) was obtained from **347** (0.09 g, 0.5 mmol), 4-methoxybenzenethiol (0.14 g, 1 mmol) and iodine (0.127 g, 0.5 mmol) as yellow solid; mp 208.2-208.5 °C, *R_f* 0.51 (CHCl₃/MeOH, 6: 1); ¹H NMR (DMSO-*d*₆) δ 2.51 (s, 3 H, 5-CH₃), 3.68 (s, 3 H, OCH₃), 6.19 (s, 2 H, NH₂ exch), 6.59 (s, 2 H, NH₂ exch), 6.87-6.89 (d, 2 H, C₆H₄), 7.12-7.14 (d, 2 H, C₆H₄); Anal. calcd. for (C₁₄H₁₄N₄OS₂ · 0.7 CH₃OH): C, 51.79; H, 4.97; N, 16.44; S, 18.81; found: C, 52.0293; H, 4.62; N, 16.34; S, 18.49.

6-[(2,6-Dimethylphenyl)sulfanyl]-5-methylthieno[2,3-*d*]pyrimidine-2,4-diamine (287).

Compound **287** (0.063 g, 40%) was obtained from **347** (0.09 g, 0.5 mmol), 2,6-dimethyl-

benzenethiol (0.138 g, 1 mmol) and iodine (0.127 g, 0.5 mmol) as yellow solid; mp 213.5-214.4 °C; R_f 0.48 (CHCl₃/MeOH, 6: 1); ¹H NMR (DMSO-*d*₆) δ 2.43 (s, 6 H, 2 CH₃), 2.54 (s, 3 H, CH₃), 6.19 (s, 2 H, NH₂ exch), 6.63 (s, 2 H, NH₂ exch), 7.17 (br s, 3 H, C₆H₃); Anal. calcd. for (C₁₅H₁₆N₄S₂ · 0.5 CH₃OH): C, 55.99; H, 5.46; N, 16.85; S, 19.29; found: C, 56.09; H, 5.25; N, 17.05; S, 19.19.

6-[(3,4-Dimethylphenyl)sulfanyl]-5-methylthieno[2,3-*d*]pyrimidine-2,4-diamine (288).

Compound **288** (0.093 g, 59%) was obtained from **347** (0.09 g, 0.5 mmol), 3,4-dimethylbenzenethiol (0.138 g, 1 mmol) and iodine (0.127 g, 0.5 mmol) as yellow solid; mp 223.8-224.6 °C; R_f 0.48 (CHCl₃/MeOH, 6: 1); ¹H NMR (DMSO-*d*₆) δ 2.11 (s, 9 H, 3 CH₃), 6.19 (s, 2 H, NH₂ exch), 6.58 (s, 2 H, NH₂ exch), 6.57, 6.59 (d, 1 H, C₆H₃), 6.78 (s, 1 H, C₆H₃), 7.03, 7.05 (d, 1 H, C₆H₃); Anal. calcd. for (C₁₅H₁₆N₄S₂ · 0.4 CH₃OH): C, 56.17; H, 5.39; N, 17.01; S, 19.48; found: C, 56.48; H, 5.20; N, 16.82; S, 19.32.

6-[(2,5-Dimethoxyphenyl)sulfanyl]-5-methylthieno[2,3-*d*]pyrimidine-2,4-diamine (289).

Compound **289** (0.085 g, 49.1%) was obtained from **347** (0.09 g, 0.5 mmol), 2,5-dimethoxybenzenethiol (0.17 g, 1 mmol) and iodine (0.127 g, 0.5 mmol) as yellow solid; mp 213.8-214.0 °C; R_f 0.51 (CHCl₃/MeOH, 6: 1); ¹H NMR (DMSO-*d*₆) δ 2.45 (s, 3 H, 5-CH₃), 3.57 (s, 3 H, OCH₃), 3.80 (s, 3 H, OCH₃), 6.10 (s, 1 H, C₆H₃), 6.26 (s, 2 H, NH₂ exch), 6.66 (s, 2 H, NH₂ exch), 6.70-6.72 (d, 1 H, C₆H₃), 6.93-6.94 (d, 1 H, C₆H₃); HRMS (EI) calcd for C₁₅H₁₆N₄O₂S₂ 348.0756, found 348.0754.

6-[(3,4-Dimethoxyphenyl)sulfanyl]-5-methylthieno[2,3-*d*]pyrimidine-2,4-diamine (290).

Compound **290** (0.101 g, 58 %) was obtained from **347** (0.09 g, 0.5 mmol), 3,4-dimethoxy-benzenethiol (0.17 g, 1 mmol) and iodine (0.127 g, 0.5 mmol) as yellow solid; mp 182.8-183.6 °C; R_f 0.48 (CHCl₃/MeOH, 6: 1); ¹H NMR (DMSO-*d*₆) δ 2.45 (s, 3 H, 5-CH₃), 3.68 (s, 6 H, 2 CH₃), 6.19 (s, 2 H, NH₂ exch), 6.62 (s, 2 H, NH₂ exch), 6.66, 6.68 (d, 1 H, C₆H₃), 6.80 (s, 1 H, C₆H₃), 6.89, 6.91 (d, 1 H, C₆H₃); Anal. calcd. for (C₁₅H₁₆N₄O₂S₂ · 0.5 CH₃OH): C, 51.08; H, 4.98; N, 15.37; S, 17.59; found: C, 51.18; H, 4.75; N, 15.44; S, 17.45.

5-Methyl-6-[(3,4,5-trimethoxyphenyl)sulfanyl]thieno[2,3-*d*]pyrimidine-2,4-diamine (291). Compound **291** (0.184 g, 69.3 %) was obtained from **347** (0.126 g, 0.7 mmol), 3,4,5-trimethoxybenzenethiol (0.28 g, 1.4 mmol) and iodine (0.177 g, 0.7 mmol) as white solid; mp 245.8-246.5 °C; R_f 0.53 (CHCl₃/MeOH, 6: 1); ¹H NMR (DMSO-*d*₆) δ 2.47 (s, 3 H, 5-CH₃), 3.58 (s, 3 H, OCH₃), 3.70 (s, 6 H, 2 OCH₃), 6.19 (s, 2 H, NH₂ exch), 6.38 (s, 2 H, C₆H₂), 6.61 (s, 2 H, NH₂ exch); Anal. calcd. for (C₁₆H₁₈N₄O₃S₂): C, 50.78; H, 4.79; N, 14.80; S, 16.94; found: C, 50.69; H, 4.95; N, 14.59; S, 16.75.

5-Methyl-6-[(4-nitrophenyl)sulfanyl]thieno[2,3-*d*]pyrimidine-2,4-diamine (292). Compound **292** (0.087 g, 57.3%) was obtained from **347** (0.1 g, 0.55 mmol), 4-nitrobenzenethiol (0.17 g, 1.1 mmol) and iodine (0.14 g, 0.55 mmol) as yellow solid; mp 292-293 °C; R_f 0.50 (CHCl₃/MeOH, 6: 1); ¹H NMR (DMSO-*d*₆) δ 2.45 (s, 3 H, 5-CH₃), 6.36 (s, 2 H, NH₂ exch), 6.74 (s, 2 H, NH₂ exch), 7.32, 7.34 (d, 2 H, C₆H₄), 8.17, 8.19 (d, 2 H, C₆H₄); Anal. calcd. for (C₁₃H₁₁N₅O₂S₂ · 0.2 CH₃OH): C, 46.66; H, 3.50; N, 20.61; S, 18.87; found: C, 46.49; H, 3.54; N, 20.55; S, 18.70.

6-[(3,4-Dichlorophenyl)sulfanyl]-5-methylthieno[2,3-*d*]pyrimidine-2,4-diamine (293). Compound **293** (0.196 g, 78.5 %) was obtained from **347** (0.126 g, 0.7 mmol),

3,4-dichlorobenzenethiol (0.25 g, 1.4 mmol) and iodine (0.177 g, 0.7 mmol) as yellow solid; mp 238.6-238.9 °C; R_f 0.51 (CHCl₃/MeOH, 6: 1); ¹H NMR (DMSO-*d*₆) δ 2.41 (s, 3 H, 5-CH₃), 6.21 (s, 2 H, NH₂ exch), 6.61 (s, 2 H, NH₂ exch), 6.93 (s, 1 H C₆H₃), 7.24 (s, 1 H, C₆H₃), 7.43 (s, 1 H, C₆H₃); Anal. calcd. for (C₁₃H₁₀Cl₂N₄S₂): C, 43.70; H, 2.82; N, 15.68; S, 17.95; Cl, 19.84; found: C, 43.64; H, 2.93; N, 15.48; S, 17.68; Cl, 20.01.

5-Methyl-6-(1-naphthylsulfanyl)thieno[2,3-*d*]pyrimidine-2,4-diamine (294).

Compound **294** (0.055 g, 74 %) was obtained from **347** (0.04 g, 0.22 mmol), naphthalene-1-thiol (0.07 g, 0.44 mmol) and iodine (0.056 g, 0.22 mmol) as yellow solid; mp 233.8-234.4 °C; R_f 0.54 (CHCl₃/MeOH, 5: 1); ¹H NMR (DMSO-*d*₆) δ 2.54 (s, 3 H, 5-CH₃), 6.26 (s, 2 H, NH₂ exch), 6.67 (s, 2 H, NH₂ exch), 7.05, 7.07 (d, 1 H, C₁₀H₇), 7.41-7.45 (t, 1 H, C₁₀H₇), 7.59-7.67 (m, 2 H, C₁₀H₇), 7.78, 7.80 (d, 1 H, C₁₀H₇), 7.96, 7.99 (d, 1 H, C₁₀H₇), 8.23, 8.26 (d, 1 H, C₁₀H₇); HRMS (EI) calcd for C₁₇H₁₄N₄S₂ 338.0659, found 338.0658.

General Procedure for the Synthesis of Compounds 359, 365.

A mixture of sulfur (1 mmol), the appropriate ketone (1 mmol), ethyl cyanoacetate (1 mmol) and EtOH (5 mL) were placed in a round bottom flask and warmed to 45 °C and treated dropwise with morpholine (1 mmol) over 15 min. The mixture was stirred for 5 h at 45 °C and 24 h at room temperature. Unreacted sulfur was removed by filtration, and the filtrate was concentrated under reduced pressure to afford an orange oil. The residue was loaded on a silica gel column packed with silica gel and eluted with 10% ethyl acetate in hexane. The fractions containing the desired product (TLC) were pooled and evaporated to afford the products.

Ethyl 2-amino-4,5,6,7-tetrahydro-1-benzothiophene-3-carboxylate (365). Compound **365** (10.12 g, 89.8 %) was obtained as an yellow solid by reacting cyclohexanone (5.6 g, 50 mmol) with sulfur (1.6 g, 50 mmol) and ethyl cyanoacetate (5.65 g, 50 mmol) as described in the General Procedure above; mp 111.6-111.9 °C; R_f 0.43 (hexane/EtOAc 3:1); $^1\text{H NMR}$ (DMSO- d_6): δ 1.23-1.26 (t, 3 H, $\text{COOCH}_2\text{CH}_3$), 1.67-1.71 (m, 4 H), 2.41-2.43 (t, 2 H), 2.58-2.61 (t, 2 H), 4.12-4.17 (q, 2 H, $\text{COOCH}_2\text{CH}_3$), 7.20 (s, 2 H, NH_2 exch). This compound was used directly for next step of reaction without further characterization.

Ethyl 2-amino-4-methyl-4,5,6,7-tetrahydro-1-benzothiophene-3-carboxylate (359). Compound **359** (6.97 g, 80.9 %) was obtained as an orange solid by reacting 2-methylcyclohexanone (4.04 g, 36 mmol) with sulfur (1.1 g, 36 mmol) and ethyl cyanoacetate (4.07 g, 36 mmol) as described in the General Procedure above; mp 69.9-71 °C; R_f 0.44 (hexane/EtOAc 3:1); $^1\text{H NMR}$ (DMSO- d_6): δ 1.08-1.10 (d, 3 H, 2- CH_3), 1.25-1.28 (t, 3 H, $\text{COOCH}_2\text{CH}_3$), 1.57-1.78 (m, 4 H), 2.39-2.43 (m, 2 H), 3.15-3.17 (m, 1 H), 4.10-4.24 (q, 2 H, $\text{COOCH}_2\text{CH}_3$), 7.23 (s, 2 H, NH_2 exch).

General Procedure for the Synthesis of Compounds 360 and 366.

A mixture of **359** or **365** (1 g), 10 % Pd-C (1 g) and toluene (30 mL) were placed in a round bottom flask and refluxed for 1-2 days. The mixture was cooled to room temperature and Pd-C was removed by filtration, and the filtrate was concentrated under reduced pressure to afford a brown oil. The residue was loaded on a silica gel column packed with silica gel and eluted with 10% ethyl acetate in hexane. The fractions containing the desired product (TLC) were pooled and evaporated to afford the products.

Ethyl 2-amino-1-benzothiophene-3-carboxylate (366). Compound **366** (1.84 g, 82.3 %) was obtained as an light yellow solid by reacting **365** (2.25 g, 9.98 mmol) with 10 % Pd-C (2.25 g) as described in the General Procedure above; mp 107.5-108.2 °C; R_f 0.37 (hexane/EtOAc 3:1); $^1\text{H NMR}$ (DMSO- d_6): δ 1.34-1.37 (t, 3 H, $\text{COOCH}_2\text{CH}_3$), 4.29-4.33 (q, 2 H, $\text{COOCH}_2\text{CH}_3$), 7.05- 7.08 (m, 1 H, C_6H_4), 7.24- 7.27 (m, 1 H, C_6H_4), 7.60, 7.62 (d, 1 H, C_6H_4), 7.97, 7.98 (d, 1 H, C_6H_4), 7.97 (s, 2 H, NH_2 exch); Anal. calcd. for ($\text{C}_{11}\text{H}_{11}\text{NO}_2\text{S}$): C, 59.71; H, 5.01; N, 6.33; S, 14.49; found: C, 59.60; H, 5.01; N, 6.25; S, 14.40

Ethyl 2-amino-4-methyl-1-benzothiophene-3-carboxylate (360). Compound **360** (0.123 g, 52.1%) was obtained as an orange semi solid by reacting **359** (0.239 g, 1 mmol) with 10 % Pd-C (0.239 g) as described in the General Procedure above (use mesitylene as solvent); R_f 0.38 (hexane/EtOAc 3:1); $^1\text{H NMR}$ (DMSO- d_6): δ 1.29-1.32 (t, 3 H, $\text{COOCH}_2\text{CH}_3$), 2.38 (s, 3 H, CH_3), 4.25-4.30 (q, 2 H, $\text{COOCH}_2\text{CH}_3$), 6.98-7.04 (m, 2 H, C_6H_3), 7.44, 7.45 (d, 1 H, C_6H_3), 7.43 (s, 2 H, NH_2 exch).

General Procedure for the Synthesis of Compounds 351 and 350.

A mixture of appropriate thiophene and chloroformamidine hydrochloride (1:4) in DMSO₂ was heated at 140° C for 4 h. The mixture was cooled to room temperature and water (15 mL) was added and ammonium hydroxide was used to neutralize the suspension. The brown solid, obtained by filtration, was washed with water and dried over P₂O₅ vacuum. The solid was dissolved in methanol and silica gel was added. A dry silica gel plug was obtained after evaporation of the solvent. The plug was loaded on to a silica gel column and eluted with 5% methanol in chloroform. The fractions containing the desired product (TLC) were pooled and evaporated to afford the products.

2-Amino-5-methyl-5,6,7,8-tetrahydro[1]benzothieno[2,3-*d*]pyrimidin-4(3H)-one

(351). Compound **351** (0.46 g, 59.7%) was obtained as a light yellow solid by reacting **359** (0.74 g, 3.28 mmol) with chloroformamidine hydrochloride (1.51 g, 13.12 mmol) in DMSO₂ (4 g) as described in the General Procedure above. mp > 299.3-300 °C; *R_f* 0.5 (MeOH/CHCl₃, 1:6); ¹H NMR (DMSO-*d*₆) δ 1.18-1.20 (d, 3 H, CH₃), 1.59-1.61 (m, 1 H), 1.71-1.83 (m, 3 H), 2.54-2.64 (m, 2 H), 3.15-3.18 (m, 1 H), 6.39 (s, 2 H, 2-NH₂ exch), 10.73 (s, 1 H, 3-NH exch); Anal. calcd. for (C₁₁H₁₃N₃SO · 0.2 H₂O): C, 55.30; H, 5.65; N, 17.59; S, 13.42; found: C, 55.19; H, 5.65; N, 17.33; S, 13.17.

2-Amino-5-methyl[1]benzothieno[2,3-*d*]pyrimidin-4(3H)-one (350). Compound **350** (0.29 g, 60.7 %) was obtained as a yellow solid by reacting **360** (0.49 g, 2.07 mmol) with chloroformamidine hydrochloride (1.19 g, 10.37 mmol) in DMSO₂ (2 g) as described in the General Procedure above. mp > 300 °C; *R_f* 0.41 (MeOH/CHCl₃, 1:6); ¹H NMR (DMSO-*d*₆) δ 2.87 (s, 3 H, CH₃), 6.82 (s, 2 H, 2-NH₂ exch), 7.13- 7.17 (m, 2 H, C₆H₃), 7.57, 7.59 (d, 1 H, C₆H₃), 10.92 (s, 1 H, 3-NH exch).

2,2-Dimethyl-*N*-(5-methyl-4-oxo-3,4-dihydro[1]benzothieno[2,3-*d*]pyrimidin-2-yl)propanamide (364). To a 100 mL round-bottomed flask was added **350** (1.34 g, 5.8 mmol) and excess Piv₂O (4 eq). The mixture was refluxed for 2 h. The silica gel plug obtained was loaded onto a silica gel column and eluted with 1:8 ethyl acetate/*n*-hexane to afford **364** (1.299 g, 70.9 %) as a white solid, mp 178.3-179.5 °C; *R_f* 0.35 (hexane/EtOAc 3:1); ¹H NMR (CDCl₃) δ 1.35 (s, 9 H, 3 CH₃ of Piv), 3.05 (s, 3 H, 5-CH₃), 7.28 (m, 2 H, C₆H₃), 7.56, 7.59 (d, 1 H, C₆H₃), 8.14 (s, 1 H, NH exch), 11.86 (s, 1 H, NH exch).

2,2-Dimethyl-N-(5-methyl-4-oxo-3,4-dihydro[1]benzothieno[2,3-*d*]pyrimidin-2-yl)propanamide (362) A solution of **364** (1.1 g, 3.49 mmol) in 1,2-dichloroethane (50 mL) was treated with *N*-bromosuccinimide (0.62 g, 3.49 mmol) and benzoyl peroxide (50 mg), and the mixture was refluxed for 1 day. The mixture was cooled to room temperature and washed with water, and evaporated to an orange solid. The solid was dissolved in methanol and silica gel was added. A dry silica gel plug was obtained after evaporation of the solvent. The plug was loaded on to a silica gel column and eluted with 6 % ethyl acetate in hexane to afford **362** (0.577 g, 41.9 %) as a orange solid; mp 217.8-219.1 °C; R_f 0.3 (hexane/EtOAc 3:1); $^1\text{H NMR}$ (CDCl_3) δ 1.27 (s, 9 H, 3 CH_3 of Piv), 5.71 (s, 2 H, CH_2Br), 7.30, 7.33 (d, 1 H, C_6H_3), 7.43, 7.46 (d, 1 H, C_6H_3), 7.64, 7.66 (d, 1 H, C_6H_3), 8.07 (s, 1 H, NH exch), 11.99 (s, 1 H, NH exch). This compound was used directly for next step of reaction without further characterization.

Methyl 2-methyl-4-nitrobenzoate (358). Thionyl chloride (4.3 g, 36.45 mmol) was added dropwise to a stirred solution of **369** (3 g, 16.57 mmol) in MeOH (25 mL) while maintaining the internal temperature below 12 °C. When addition was complete the mixture was left to stand at room temperature for 12h to obtain white solid. And the filtrate was concentrated under reduced pressure to afford white solid. The solid was washed with hexane and ethyl ether to afford **358** (2.95 g, 91.3 %); mp 153.7-154.4 °C (lit.³⁹ mp 153-154 °C); R_f 0.43 (hexane/EtOAc 3:1); $^1\text{H NMR}$ (CDCl_3) δ 2.69 (s, 3 H, CH_3), 3.95 (s, 3 H, COOCH_3), 8.02-8.11 (m, 3 H, C_6H_3).

Methyl 2-(bromomethyl)-4-nitrobenzoate (357). A solution of **358** (2.57 g, 13.19 mmol) in 1,2-dichloroethane (100 mL) was treated with *N*-bromosuccinimide (2.3 g, 13.19 mmol) and benzoyl peroxide (0.26 g), and the mixture was refluxed for 2 days,

then cooled, washed with water, and evaporated to an yellow oil (3.52 g). The oil was dissolved in acetone and silica gel was added. A dry silica gel plug was obtained after evaporation of the solvent. The plug was loaded on to a silica gel column and eluted with 10 % ethyl acetate in hexane to afford **357** (1.73 g, 48.2 %) as a yellow oil; R_f 0.53 (hexane/EtOAc 3:1); $^1\text{H NMR}$ (CDCl_3) δ 3.89 (s, 3 H, COOCH_3), 4.86 (s, 2 H, CH_2Br), 7.98-8.23 (m, 3 H, C_6H_3). This compound was used directly for next step of reaction without further characterization.

Diethyl (2S)-2-(5-nitro-1-oxo-1,3-dihydro-2H-isoindol-2-yl)pentanedioate (356). The oil **357** (0.85 g, 3.1 mmol) was stirred for 16 h with diethyl glutamate hydrochloride (1.54 g, 6.4 mmol) and powdered K_2CO_3 (1.7 g, 12 mmol) in DMA (3 mL) under argon. The reaction mixture was diluted with water (20 mL) and extracted with EtOAc (3 X 20 mL). The combined EtOAc solutions were washed twice with brine, dried, and evaporated to an orange oil. The oil was dissolved in methanol and silica gel was added. A dry silica gel plug was obtained after evaporation of the solvent. The plug was loaded on to a silica gel column and eluted with 25 % ethyl acetate in hexane to afford to afford **356** (0.63 g, 55.7 %) as a orange oil; R_f 0.44 (hexane/EtOAc 1:1); $^1\text{H NMR}$ (CDCl_3) δ 1.17-1.22 (t, 3 H, $\text{COOCH}_2\text{CH}_3$), 1.26-1.31 (t, 3 H, $\text{COOCH}_2\text{CH}_3$), 2.19-2.49 (m, 4 H, $\text{CHCH}_2\text{CH}_2\text{COOEt}$), 4.02-4.23 (2q, 4 H, $\text{COOCH}_2\text{CH}_3$), 4.51-4.83 (dd, 2 H, $-\text{CH}_2-$), 5.09-5.14 (m, 1 H, $\text{CHCH}_2\text{CH}_2\text{COOEt}$), 8.00-8.03 (d, 1 H, C_6H_3), 8.36 (br s, 2 H, C_6H_3). This compound was used directly for next step of reaction without further characterization.

Diethyl (2S)-2-(5-amino-1-oxo-1,3-dihydro-2H-isoindol-2-yl)pentanedioate (355). To a Parr hydrogenation bottle was added **356** (0.55 g, 1.51 mmol), 10% Pd/C (0.09 g) and

EtOAc (30 mL). Hydrogenation was carried out at 55 psi for 12 h. After filtration, the organic phase was evaporated at vacuum to afford **355** (0.467 g, 92.5 %) as a orange oil; R_f 0.19 (hexane/EtOAc 1:1); $^1\text{H NMR}$ (CDCl_3) δ 1.17-1.19 (t, 3 H, $\text{COOCH}_2\text{CH}_3$), 1.20-1.25 (t, 3 H, $\text{COOCH}_2\text{CH}_3$), 2.20-2.51 (m, 4 H, $\text{CHCH}_2\text{CH}_2\text{COOEt}$), 4.02-4.28 (m, 6 H, 2 $\text{COOCH}_2\text{CH}_3$, NH_2 exch), 4.22-4.51 (dd, 2 H, $-\text{CH}_2-$), 5.03-5.07 (m, 1 H, $\text{CHCH}_2\text{CH}_2\text{COOEt}$), 6.69-6.73 (m, 2 H, C_6H_3), 7.60, 7.63 (d, 1 H, C_6H_3). This compound was used directly for next step of reaction without further characterization.

Diethyl (2S)-2-{{5-[(2-(2,2-dimethylpropanoyl)amino]-4-oxo-3,4-dihydro[1]benzothieno[2,3-*d*]pyrimidin-5-yl)methyl]amino}-1-oxo-1,3-dihydro-2H-isoindol-2-yl}pentanedioate (370). A stirred solution of **362** (0.18 g, 0.46 mmol) in dry DMF (5 mL) was treated with **355** (0.31 g, 0.91 mmol) and K_2CO_3 (0.095 g, 0.69 mmol) was stirred for 1 h at 80 °C under argon. The cooled reaction mixture was filtered and the filtrate was evaporated to obtain orange solid. The solid was dissolved in methanol and silica gel was added. A dry silica gel plug was obtained after evaporation of the solvent. The plug was loaded on to a silica gel column and eluted with ethyl acetate: hexane (1: 1) to afford **370** (0.112 g, 37.7 %) as a yellow solid; R_f 0.19 (hexane/EtOAc 1:1). It was used directly in the next step.

(2S)-2-(5-{{(2-amino-4-oxo-3,4-dihydro[1]benzothieno[2,3-*d*]pyrimidin-5-yl)methyl}amino}-1-oxo-1,3-dihydro-2H-isoindol-2-yl)pentanedioic acid (301). To a 50 mL round flask was added s **370** (0.112 g, 0.173 mmol), aqueous 1 N NaOH (3 mL) and methanol (12 mL). The mixture was refluxed for 12 h. The methanol was evaporated under reduced pressure and the residue was dissolved in water (5 mL). The solution was cooled to 0 °C and carefully acidified to pH 3 with drop wise addition of 1 N HCl. The

resulting suspension was left at 0 °C for 2 h and the residue was collected by filtration. Washed with water (5 mL) and dried over P₂O₅/vacuum at 50 °C to afford **301** (0.03 g, 34 %) as a orange solid; *R_f* 0.33 (MeOH/CHCl₃, 1:6 + 1 drop of gl. HOAc); ¹H NMR (DMSO-*d*₆): δ 1.97-2.20 (m, 4 H, Gluβ-CH₂, Gluγ-CH₂), 4.21-4.25 (m, 2 H, isoindolinyl CH₂), 4.68-4.71 (m, 1 H, Gluα-CH), 5.13, 5.14 (d, 2 H, Benzylic CH₂), 6.64 (br s, 2 H, C₆H₃), 6.74 (s, 1 H, NH exch), 6.89 (s, 2 H, 2-NH₂ exch), 7.20-7.26 (t, 1 H, C₆H₃), 7.30-7.33 (d, 1 H, C₆H₃), 7.39-7.42 (dd, 1 H, C₆H₃), 7.69-7.72 (d, 1 H, C₆H₃), 11.11 (s, 1 H, 3-NH exch), 12.78 (s, 2 H, 2COOH exch). HRMS (ESI, pos mode) *m/z* [M + H]⁺ calcd for C₂₄H₂₁N₅O₆S, 508.1285; found, 508.1321.

Ethyl 2-amino-5-isopropylthiophene-3-carboxylate (372). A mixture of sulfur (1.92 g, 60 mmol), isovaleraldehyde (5.17 g, 60 mmol), ethyl cyanoacetate (6.78 g, 60 mmol) and EtOH (100 mL) were placed in a round bottom flask and warmed to 45 °C and treated dropwise with morpholine (5.23 g, 60 mmol) over 15 min. The mixture was stirred for 4 h at 45 °C and 24 h at room temperature. Unreacted sulfur was removed by filtration, and the filtrate was concentrated under reduced pressure to afford an orange oil. The residue was loaded on a silica gel column packed with silica gel and eluted with 10 % ethyl acetate in hexane to afford **372** (9.97 g, 78%) as a orange solid; *R_f* 0.66 (hexane/EtOAc 3:1); ¹H NMR (CDCl₃) δ 1.24-1.25 (d, 6 H, CH (CH₃)₂), 1.32-1.35 (t, 3 H, COOCH₂CH₃), 2.86-2.97 (m, 1 H, CH (CH₃)₂), 4.23-4.28 (q, 2 H, COOCH₂CH₃), 5.78 (s, 2 H, NH₂ exch), 6.63 (s, 1 H, 4-H); HRMS (EI) calcd for C₁₀H₁₅NO₂S *m/z* = 213.0823, found *m/z* = 213.0828.

2-Amino-6-isopropylthieno[2,3-*d*]pyrimidin-4(3*H*)-one (373). A mixture of **372** (2.2 g, 10.3 mmol) and chloroformamidinium hydrochloride (4.7 g, 41 mmol) in DMSO₂ (15 g,

153 mmol) was heated at 150 °C for 2 h. The mixture was cooled to room temperature and water (30 mL) was added and ammonium hydroxide was used to neutralize the suspension. The brown solid, obtained by filtration, was washed with water and dried over P₂O₅ vacuum. The solid was dissolved in methanol and silica gel was added. The plug was loaded on to a silica gel column and eluted with 5% methanol in chloroform to afford **373** (1.88 g, 87%) as a yellow solid; mp > 300 °C; *R_f* 0.25 (MeOH/CHCl₃, 1:6); ¹H NMR (DMSO-*d*₆) δ 1.23-1.25 (d, 6 H, CH (CH₃)₂), 2.99-3.06 (m, 1 H, CH (CH₃)₂), 6.46 (s, 2 H, 2-NH₂ exch), 6.78 (s, 1 H, 5-H), 10.81 (s, 1 H, 3-NH exch); Anal. (C₉H₁₁N₃SO) C, H, N, S

Methyl 4-sulfanylbenzoate (381). Thionyl chloride (2.64 g, 22 mmol) was added dropwise to a stirred solution of 4-mercaptobenzoic acid (1.54 g, 10 mmol) in MeOH (20 mL) while maintaining the internal temperature below 12 °C. When addition was complete the mixture was left to stand at room temperature for 12 h to obtain yellow solid. And the filtrate was concentrated under reduced pressure to afford yellow solid. The solid was washed with hexane and ethyl ether to afford **381** (1.577 g, 93.7%) as light yellow solid; mp 99.7-101.5 °C; *R_f* 0.58 (hexane/EtOAc 3:1); ¹H NMR (CDCl₃) δ 3.60 (s, 1 H, SH, exch), 3.89 (s, 3 H, COOCH₃), 7.27, 7.30 (d, 2 H, C₆H₄), 7.87, 7.90 (d, 2 H, C₆H₄).

2-Amino-5-iodo-6-isopropylthieno[2,3-*d*]pyrimidin-4(3*H*)-one (375). To a mixture of **373** (2.5 g, 11.9 mmol) in glacial acetic acid (60 mL) was added mercuric acetate (5.69 g, 17.93 mmol) at room temperature. The mixture was heated at 100 °C for 3 h. Then the mixture was poured into a brine solution (60 mL) and stirred for 30 min. The yellow solid **376** (4.2 g, 78.9%) obtained by filtration was washed with water and hexane and dried

over P₂O₅ vacuum; mp 252.7 °C. Compound **376** (3.5 g, 7.8 mmol) was dissolved in CH₂Cl₂ (100 mL) and I₂ (3.85 g, 15.2 mmol) was added. The resulting mixture stirred for 5 h at room temperature. The mixture was washed with 2 N NaS₂O₃ and dried via MgSO₄. The plug was loaded on to a silica gel column and eluted with 3% methanol in chloroform to afford **375** (2.25g, 86%) as a yellow solid; mp 252.7 °C; *R_f* 0.26 (MeOH/CHCl₃, 1:10); ¹H NMR (DMSO-*d*₆) δ 1.20-1.22 (d, 6 H, CH (CH₃)₂), 3.23-3.30 (m, 1 H, CH (CH₃)₂), 6.57 (s, 2 H, 2-NH₂ exch), 10.90 (s, 1 H, 3-NH exch); Anal. calcd. for (C₉H₁₀IN₃SO): C, 32.25; H, 3.01; N, 12.54; S, 9.57; I, 37.86; found: C, 32.35; H, 2.97; N, 12.37; S, 9.48; I, 37.69.

General procedure for the synthesis of compounds **305-311** and **382**.

A mixture of appropriate arylthiols (1.5 eq), K₂CO₃ (1.5 eq), CuI (1.3 eq) and **375** (1 eq) in dry DMF (5 mL) was irradiated in a microwave at 100 °C for 60-120 min. After the reaction mixture was cooled to room temperature, the mixture was filtered; the filtrate was concentrated under reduced pressure. The solid was dissolved in methanol and silica gel was added. A dry silica gel plug was obtained after evaporation of the solvent. The plug was loaded on to a silica gel column and eluted with 2 % methanol in chloroform.

2-Amino-4-oxo-6-isopropyl-5-phenylsulfanylthieno[2,3-*d*]pyrimidine (305). Using the general procedure above compound **305** (0.13 g, 82.3 %) was obtained as a brown solid by reacting **375** (0.167 g, 0.5 mmol), benzenethiol (0.083 g, 0.75 mmol), K₂CO₃ (0.103 g, 0.75 mmol) and CuI (0.12 g, 0.65 mmol) in DMF (5 mL) was irradiated in a microwave at 100 °C for 60 min. *R_f* 0.38 (MeOH/CHCl₃, 1:6); mp 269.8-270.2 °C; ¹H NMR (DMSO-*d*₆) δ 1.17-1.19 (d, 6 H, CH (CH₃)₂), 3.57-3.65 (m, 1 H, CH (CH₃)₂), 6.59 (s, 2

H, 2-NH₂ exch), 6.98-7.24 (m, 5 H, C₆H₅), 10.74 (s, 1 H, 3-NH exch); HRMS (EI) calcd for C₁₅H₁₅N₃O₃S₂ m/z [M + H]⁺ = 318.0735, found m/z = 318.0739.

2-Amino-6-isopropyl-5-[(4-nitrophenyl)sulfanyl]thieno[2,3-*d*]pyrimidin-4(3*H*)-one (306). Using the general procedure above compound **306** (0.108 g, 75.4 %) was obtained as a yellow solid by reacting **375** (0.134 g, 0.4 mmol), 4-nitrobenzenethiol (0.093 g, 0.6 mmol), K₂CO₃ (0.083 g, 0.6 mmol) and CuI (0.099 g, 0.52 mmol) in DMF (5 mL) was irradiated in a microwave at 100 °C for 120 min. *R_f* 0.41 (MeOH/CHCl₃, 1:6); mp 148.8-149.3 °C; ¹H NMR (DMSO-*d*₆) δ 1.20-1.22 (d, 6 H, CH (CH₃)₂), 3.52-3.58 (m, 1 H, CH (CH₃)₂), 6.65 (s, 2 H, 2-NH₂ exch), 7.17-7.19 (d, 2 H, C₆H₄), 8.07-8.09 (d, 2 H, C₆H₄), 10.80 (s, 1 H, 3-NH exch); HRMS (EI) calcd for C₁₅H₁₄N₄O₃S₂ m/z = 362.0507, found m/z = 362.0516.

2-Amino-5-[(3,4-dichlorophenyl)sulfanyl]-6-isopropylthieno[2,3-*d*]pyrimidin-4(3*H*)-one (307). Using the general procedure above compound **307** (0.172 g, 89.1 %) was obtained as a yellow solid by reacting **375** (0.167 g, 0.5 mmol), 3,4-dichlorobenzenethiol (0.134 g, 0.75 mmol), K₂CO₃ (0.103 g, 0.75 mmol) and CuI (0.124 g, 0.65 mmol) in DMF (5 mL) was irradiated in a microwave at 100 °C for 60 min. *R_f* 0.41 (MeOH/CHCl₃, 1:6); mp 205 °C; ¹H NMR (DMSO-*d*₆) δ 1.19-1.21 (d, 6 H, CH (CH₃)₂), 3.54-3.61 (m, 1 H, CH (CH₃)₂), 6.65 (s, 2 H, 2-NH₂ exch), 6.90, 6.92 (dd, 1 H, C₆H₃), 7.24 (s, 1 H, C₆H₃), 7.46, 7.48 (d, 1 H, C₆H₃), 10.79 (s, 1 H, 3-NH exch); Anal. calcd. for (C₁₅H₁₃Cl₂N₃S₂O · 0.3 CH₃OH): C, 46.41; H, 3.61; N, 10.61; S, 16.20; Cl, 17.91; found: C, 46.02; H, 3.43; N, 10.30; S, 16.41; Cl, 17.99.

2-Amino-6-isopropyl-5-(1-naphthylsulfanyl)thieno[2,3-*d*]pyrimidin-4(3*H*)-one (308). Using the general procedure above compound **308** (0.137 g, 74.9 %) was obtained as a

brown solid by reacting **375** (0.167 g, 0.5 mmol), naphthalene-1-thiol (0.12 g, 0.75 mmol), K₂CO₃ (0.103 g, 0.75 mmol) and CuI (0.124 g, 0.65 mmol) in DMF (5 mL) was irradiated in a microwave at 100 °C for 90 min. *R_f* 0.34 (MeOH/CHCl₃, 1:10); mp 243.7-244 °C; ¹H NMR (DMSO-*d*₆) δ 1.17-1.19 (d, 6 H, CH (CH₃)₂), 3.59-3.62 (m, 1 H, CH (CH₃)₂), 6.61 (s, 2 H, 2-NH₂ exch), 6.76, 6.78 (d, 1 H, C₁₀H₇), 7.29-7.33 (t, 1 H, C₁₀H₇), 7.57-7.67 (m, 3 H, C₁₀H₇), 7.92, 7.94 (d, 1 H, C₁₀H₇), 8.20, 8.22 (d, 1 H, C₁₀H₇), 10.73 (s, 1 H, 3-NH exch); HRMS (EI) calcd for C₁₉H₁₇N₃OS₂ m/z = 367.0812, found m/z = 367.0813.

2-Amino-6-isopropyl-5-(2-naphthylsulfanyl)thieno[2,3-*d*]pyrimidin-4(3*H*)-one (309).

Using the general procedure above compound **309** (0.152 g, 83.1 %) was obtained as a brown solid by reacting **375** (0.167 g, 0.5 mmol), naphthalene-2-thiol (0.12 g, 0.75 mmol), K₂CO₃ (0.103 g, 0.75 mmol) and CuI (0.124 g, 0.65 mmol) in DMF (5 mL) was irradiated in a microwave at 100 °C for 90 min. *R_f* 0.38 (MeOH/CHCl₃, 1:10); mp 180-180.6 °C; ¹H NMR (DMSO-*d*₆) δ 1.19-1.21 (d, 6 H, CH (CH₃)₂), 3.62-3.69 (m, 1 H, CH (CH₃)₂), 6.61 (s, 2 H, 2-NH₂ exch), 7.15, 7.17 (d, 1 H, C₁₀H₇), 7.42-7.45 (m, 3 H, C₁₀H₇), 7.72-7.82 (m, 3 H, C₁₀H₇), 10.73 (s, 1 H, 3-NH exch); HRMS (EI) calcd for C₁₉H₁₇N₃OS₂ m/z = 367.0813, found m/z = 367.0813.

2-Amino-5-[(4-fluorophenyl)sulfanyl]-6-isopropylthieno[2,3-*d*]pyrimidin-4(3*H*)-one (310).

Using the general procedure above compound **310** (0.147 g, 88 %) was obtained as a yellow solid by reacting **375** (0.167 g, 0.5 mmol), 4-fluorobenzenethiol (0.096 g, 0.75 mmol), K₂CO₃ (0.103 g, 0.75 mmol) and CuI (0.124 g, 0.65 mmol) in DMF (5 mL) was irradiated in a microwave at 100 °C for 90 min. *R_f* 0.31 (MeOH/CHCl₃, 1:10); mp 282.2-282.4 °C; ¹H NMR (DMSO-*d*₆) δ 1.18-1.20 (d, 6 H, CH (CH₃)₂), 3.61-3.69 (m, 1 H, CH

(CH₃)₂), 6.60 (s, 2 H, 2-NH₂ exch), 7.11-7.14 (m, 4 H, C₆H₄), 10.75 (s, 1 H, 3-NH exch); HRMS (EI) calcd for C₁₅H₁₄N₃OS₂F m/z = 355.0562, found m/z = 355.0559.

2-Amino-5-[(4-methoxyphenyl)sulfanyl]-6-isopropylthieno[2,3-*d*]pyrimidin-4(3*H*)-one (311). Using the general procedure above compound **311** (0.159 g, 91.4 %) was obtained as a light yellow solid by reacting **375** (0.167 g, 0.5 mmol), 4-methoxy benzenethiol (0.105 g, 0.75 mmol), K₂CO₃ (0.103 g, 0.75 mmol) and CuI (0.124 g, 0.65 mmol) in DMF (5 mL) was irradiated in a microwave at 100 °C for 90 min. *R_f* 0.29 (MeOH/CHCl₃, 1:10); mp 241.6-242 °C; ¹H NMR (DMSO-*d*₆) δ 1.19 (m, 6 H, CH (CH₃)₂), 3.68 (br s, 4 H, OCH₃ and CH (CH₃)₂), 6.58 (s, 2 H, 2-NH₂ exch), 6.83 (br s, 2 H, C₆H₄), 7.06 (br s, 2 H, C₆H₄), 10.75 (s, 1 H, 3-NH exch); Anal. calcd. for (C₁₆H₁₇N₃S₂O₂ · 0.4 H₂O): C, 54.18; H, 5.06; N, 11.85; S, 18.08; found: C, 54.25; H, 4.81; N, 11.55; S, 17.85.

4-(2-Amino-6-isopropyl-4-oxo-3,4-dihydro-thieno[2,3-*d*]pyrimidine-5-ylsulfanyl)-benzoic acid methyl ester (382). To a suspension of **375** (0.24 g, 0.72 mmol), *i*-Pr₂Net (0.18 g, 1.44 mmol) and DMF (5 mL) was added catalyst Pd₂dba₃ (0.016 g, 0.017 mmol), Xantphos (0.024 g, 0.034 mmol) and methyl 4-mercaptobenzoate (0.24 g, 1.44 mmol). The mixture was degassed twice and backfilled with nitrogen. The reaction mixture was irradiated in a microwave at 190 °C for 1 h. After the reaction mixture was cooled to room temperature, the mixture was filtered. The filtrate was concentrated under reduced pressure. The solid was dissolved in methanol and silica gel was added. A dry silica gel plug was obtained after evaporation of the solvent. The plug was loaded on to a silica gel column and eluted with 2 % methanol in chloroform and **382** (0.17 g, 64 %) was obtained

as a white solid. R_f 0.34 (MeOH/CHCl₃, 1:6); mp 220.4-220.8 °C; ¹H NMR (DMSO-*d*₆) δ 1.18-1.20 (d, 6 H, CH (CH₃)₂), 3.52-3.59 (m, 1 H, CH (CH₃)₂), 3.80 (s, 3 H, COOCH₃), 6.62 (s, 2 H, 2-NH₂ exch), 7.06, 7.08 (d, 2 H, C₆H₄), 7.78, 7.80 (d, 2 H, C₆H₄), 10.77 (s, 1 H, 3-NH exch); HRMS (EI) calcd for C₁₇H₁₇N₃O₃S₂ m/z [M + Na]⁺ = 398.0609, found m/z = 398.0591.

4-[(2-Amino-6-isopropyl-4-oxo-3,4-dihydrothieno[2,3-*d*]pyrimidin-5-yl)sulfanyl]benzoic acid (383). To a solution of **382** (0.08 g, 0.21 mmol) in ethanol (20 mL) was added aqueous 1 N NaOH (10 mL) and the reaction mixture stirred at room temperature for 12 h. The ethanol was evaporated under reduced pressure and the residue was dissolved in water (5 mL). The solution was carefully acidified to pH 3 with the drop wise addition of 1 N HCl. The resulting suspension was left at 0 °C for an hour and then the residue was collected by filtration, washed with water (5 mL) and dried over P₂O₅ under vacuum at 50 °C to afford **383** (0.075 g, 97.7 %) as a white solid. R_f 0.43 (MeOH/CHCl₃, 1: 6+ 1 drop of gl. HOAc); mp >350 °C; ¹H NMR (DMSO-*d*₆) δ 1.18-1.20 (d, 6 H, CH (CH₃)₂), 3.53-3.60 (m, 1 H, CH (CH₃)₂), 6.64 (s, 2 H, 2-NH₂ exch), 7.03, 7.05 (d, 2 H, C₆H₄), 7.76, 7.78 (d, 2 H, C₆H₄), 10.78 (s, 1 H, 3-NH exch), 12.74 (s, 1 H, COOH exch).

Diethyl N-(4-{[2-amino-4-oxo-6-(propan-2-yl)-3,4-dihydrothieno[2,3-*d*]pyrimidin-5-yl)sulfanyl}benzoyl)-L-glutamate (384). To a solution of **383** (0.05 g, 0.14 mmol) in anhydrous DMF (10 mL) was added N-methylmorpholine (0.017 g, 0.17 mmol) and 2-chloro-4,6-dimethoxy-1,3,5-triazine (0.03 g, 0.17 mmol). The resulting mixture was stirred at room temperature for 2 h. N-methylmorpholine (0.017 g, 0.17 mmol) and diethyl-L- glutamate hydrochloride (0.034 g, 0.14 mmol) were added to the mixture. The

reaction mixture was stirred for an additional 3 h at room temperature and silica gel was added to this solution and the suspension evaporated under reduced pressure. The plug obtained was loaded on a silica gel column and eluted with 2% methanol in chloroform and **384** (0.072 g, 94.7 %) was obtained as a yellow solid. R_f 0.33 (MeOH/CHCl₃, 1:6); mp > 300 °C; ¹H NMR (DMSO-*d*₆) δ 1.13-1.17 (t, 6 H, 2 COOCH₂CH₃), 1.18-1.20 (d, 6 H, CH (CH₃)₂), 1.95-2.22 (m, 2 H Gluβ-CH₂), 2.40-2.43 (t, 2 H, Gluγ-CH₂), 3.53-3.60 (m, 1 H, CH (CH₃)₂), 4.37-4.41 (m, 4 H, 2 COOCH₂CH₃), 4.45-4.52 (1 H, m, Gluα-CH), 6.61 (s, 2 H, 2-NH₂ exch), 7.02, 7.04 (d, 2 H, C₆H₄), 7.70, 7.72 (d, 2 H, C₆H₄), 8.60, 8.62 (d, 1 H, CONH exch), 10.74 (s, 1 H, 3-NH exch); HRMS (EI) calcd for C₂₅H₃₀N₄O₆S₂ m/z [M + Na]⁺ = 569.1504, found m/z = 569.1511.

***N*-{4-[(2-amino-6-isopropyl-4-oxo-3,4-dihydrothieno[2,3-*d*]pyrimidin-5-yl)sulfanyl]benzoyl}-L-glutamic acid (304).** To a solution of **384** (0.072 g, 0.132 mmol) in ethanol (6 mL) was added aqueous 1 N NaOH (3 mL) and the reaction mixture stirred at room temperature for 3 h. The ethanol was evaporated under reduced pressure and the residue was dissolved in water (5 mL). The solution was cooled to 0 °C and carefully acidified to pH 3 with drop wise addition of 1 N HCl. The resulting suspension was left at 0 °C for 2 h and the residue was collected by filtration. Washed with water (5 mL) and dried over P₂O₅/vacuum at 50 °C to afford **304** (0.053 g, 83%) as white solid. R_f 0.41 (MeOH/CHCl₃, 1:6+ 1 drop of gl. HOAc); mp 192.4-192.8 °C; ¹H NMR (DMSO-*d*₆) δ 1.19-1.21 (d, 6 H, CH (CH₃)₂), 1.96-2.23 (m, 2 H Gluβ-CH₂), 2.31-2.35 (t, 2 H, Gluγ-CH₂), 3.54-3.61 (m, 1 H, CH (CH₃)₂), 4.31-4.39 (1 H, m, Gluα-CH), 6.61 (s, 2 H, 2-NH₂ exch), 7.02, 7.04 (d, 2 H, C₆H₄), 7.70, 7.72 (d, 2 H, C₆H₄), 8.47, 8.49 (d, 1 H, CONH exch), 10.75 (s, 1 H, 3-NH exch), 12.40 (s, 2H, COOH exch); Anal. calcd. for

(C₂₁H₂₂N₄S₆O₂ · 1.5 H₂O): C, 48.73; H, 4.87; N, 10.82; S, 12.39; found: C, 48.59; H, 5.01; N, 10.65; S, 12.08.

Ethyl 2-amino-5-propylthiophene-3-carboxylate (386). A mixture of sulfur (1.92 g, 60 mmol), isovaleraldehyde (5.17 g, 60 mmol), ethyl cyanoacetate (6.78 g, 60 mmol) and EtOH (100 mL) were placed in a round bottom flask and warmed to 45 °C and treated dropwise with morpholine (5.23 g, 60 mmol) over 15 min. The mixture was stirred for 4 h at 45 °C and 24 h at room temperature. Unreacted sulfur was removed by filtration, and the filtrate was concentrated under reduced pressure to afford an orange oil. The residue was loaded on a silica gel column packed with silica gel and eluted with 10% ethyl acetate in hexane to afford **386** (9.97 g, 78%) as a orange liquid; *R_f* 0.66 (hexane/EtOAc 3:1); ¹H NMR (CDCl₃) δ 0.93-0.97 (t, 3 H, CH₂CH₂CH₃), 1.31-1.35 (t, 3 H, COOCH₂CH₃), 1.55-1.64 (m, 2 H, CH₂CH₂CH₃), 2.53-2.57 (t, 2 H, CH₂CH₂CH₃), 4.22-4.28 (q, 2 H, COOCH₂CH₃), 5.78 (s, 2 H, NH₂ exch), 6.63 (s, 1 H, 4-H). HRMS (EI) calcd for C₁₀H₁₅NO₂S *m/z* = 213.0823, found *m/z* = 213.0828.

2-Amino-6-propylthieno[2,3-*d*]pyrimidin-4(3*H*)-one (387). A mixture of **386** (2.1 g, 9.8 mmol) and chloroformamidine hydrochloride (2.3 g, 29 mmol) in DMSO₂ (7.5 g, 7.5 mmol) was heated at 150 °C for 2 h. The mixture was cooled to room temperature and water (30 mL) was added and ammonium hydroxide was used to neutralize the suspension. The brown solid, obtained by filtration, was washed with water and dried over P₂O₅ vacuum. The solid was dissolved in methanol and silica gel was added. The plug was loaded on to a silica gel column and eluted with 5% methanol in chloroform to afford **387** (1.63 g, 80%) as a yellow solid; mp > 300 °C; *R_f* 0.32 (MeOH/CHCl₃, 1:6); ¹H NMR (DMSO-*d*₆) δ 0.89-0.93 (t, 3 H, CH₂CH₂CH₃), 1.55-1.64 (m, 2 H,

CH₂CH₂CH₃), 2.64-2.68 (t, 2 H, CH₂CH₂CH₃). 6.45 (s, 2 H, 2-NH₂ exch), 6.79 (s, 1 H, 5-H), 10.82 (s, 1 H, 3-NH exch); Anal. calcd. for (C₉H₁₁N₃SO · 0.2 CH₃OH): C, 51.23; H, 5.51; N, 19.48; S, 14.87; found: C, 51.26; H, 5.31; N, 19.34; S, 14.84.

2-Amino-5-iodo-6-propylthieno[2,3-*d*]pyrimidin-4(3*H*)-one (388). To a mixture of **387** (2.5 g, 11.9 mmol) in glacial acetic acid (60 mL) was added mercuric acetate (5.69 g, 17.93 mmol) at room temperature. The mixture was heated at 100 °C for 3 h. Then the mixture was poured into a brine solution (60 mL) and stirred for 30 min. The yellow solid **388** (4.2 g, 78.9%) was obtained by filtration was washed with water and hexane and dried over P₂O₅ vacuum; mp 252.7 °C. Compound **388** (3.5 g, 7.8 mmol) was dissolved in CH₂Cl₂ (100 mL) and I₂ (3.85 g, 15.2 mmol) was added. The resulting mixture attired for 5 h at room temperature. The mixture was washed with 2 N NaS₂O₃ and dried via MgSO₄. The plug was loaded on to a silica gel column and eluted with 3% methanol in chloroform to afford **389** (2.25 g, 86%) as a yellow solid; mp 241 °C; *R_f* 0.26 (MeOH/CHCl₃, 1:10); ¹H NMR (DMSO-*d*₆) δ 0.91-0.95 (t, 3 H, CH₂CH₂CH₃), 1.53-1.63 (m, 2 H, CH₂CH₂CH₃), 2.65-2.68 (t, 2 H, CH₂CH₂CH₃), 6.56 (s, 2 H, 2-NH₂ exch), 10.91 (s, 1 H, 3-NH exch). HRMS (EI) calcd for C₉H₁₀IN₃SO *m/z* = 335.9668, found *m/z* = 335.9641.

General procedure for the synthesis of compounds **317-319** and **323**.

A mixture of appropriate arylthiols (1.5 eq), K₂CO₃ (1.5 eq), CuI (1.3 eq) and **389** (1 eq) in dry DMF (5 mL) was irradiated in a microwave at 100 °C for 60-120 min. After the reaction mixture was cooled to room temperature, the mixture was filtered; the filtrate was concentrated under reduced pressure. The solid was dissolved in methanol and silica

gel was added. A dry silica gel plug was obtained after evaporation of the solvent. The plug was loaded on to a silica gel column and eluted with 2 % methanol in chloroform.

2-Amino-6-propyl-5-(1-naphthylsulfanyl)thieno[2,3-*d*]pyrimidin-4(3*H*)-one (317).

Using the general procedure above compound **317** (0.137 g, 74.9 %) was obtained as a yellow solid by reacting **389** (0.167 g, 0.5 mmol), naphthalene-1-thiol (0.12 g, 0.75 mmol), K₂CO₃ (0.103 g, 0.75 mmol) and CuI (0.124 g, 0.65 mmol) in DMF (5 mL) was irradiated in a microwave at 100 °C for 90 min. *R*_f 0.39 (MeOH/CHCl₃, 1:10); mp > 300 °C; ¹H NMR (DMSO-*d*₆) δ 0.80-0.83 (t, 3 H, CH₂CH₂CH₃), 1.49-1.56 (m, 2 H, CH₂CH₂CH₃), 2.8-2.83 (t, 2 H, CH₂CH₂CH₃), 6.59 (s, 2 H, 2-NH₂ exch), 6.77, 6.79 (d, 1 H, C₁₀H₇), 7.28-7.32 (t, 1 H, C₁₀H₇), 7.55-7.66 (m, 3 H, C₁₀H₇), 7.91, 7.93 (d, 1 H, C₁₀H₇), 8.20, 8.22 (d, 1 H, C₁₀H₇), 10.73 (s, 1 H, 3-NH exch); HRMS (ESI, pos mode) *m/z* [M + H]⁺ calcd for C₁₉H₁₇N₃OS₂, 368.0886; found, 368.0891.

2-Amino-6-propyl-5-(2-naphthylsulfanyl)thieno[2,3-*d*]pyrimidin-4(3*H*)-one (318).

Using the general procedure above compound **318** (0.152 g, 83.1 %) was obtained as a light brown solid by reacting **389** (0.167 g, 0.5 mmol), naphthalene-2-thiol (0.12 g, 0.75 mmol), K₂CO₃ (0.103 g, 0.75 mmol) and CuI (0.124 g, 0.65 mmol) in DMF (5 mL) was irradiated in a microwave at 100 °C for 90 min. *R*_f 0.50 (MeOH/CHCl₃, 1:10); mp 257.3-257.6 °C; ¹H NMR (DMSO-*d*₆) δ 0.82-0.86 (t, 3 H, CH₂CH₂CH₃), 1.50-1.60 (m, 2 H, CH₂CH₂CH₃), 2.84-2.88 (t, 2 H, CH₂CH₂CH₃), 6.57 (s, 2 H, 2-NH₂ exch), 7.14, 7.17 (d, 1 H, C₁₀H₇), 7.43-7.45 (m, 3 H, C₁₀H₇), 7.70-7.81 (m, 3 H, C₁₀H₇), 10.71 (s, 1 H, 3-NH exch); HRMS (ESI, pos mode) *m/z* [M + H]⁺ calcd for C₁₉H₁₇N₃OS₂, 368.0886; found, 368.0886.

2-Amino-6-propyl-5-(4-bromophenyl sulfanyl)thieno[2,3-*d*]pyrimidin-4(3*H*)-one

(319). Using the general procedure above compound **319** (0.147 g, 88 %) was obtained as a light brown solid by reacting **389** (0.167 g, 0.5 mmol), 4-chlorobenzenethiol (0.096 g, 0.75 mmol), K₂CO₃ (0.103 g, 0.75 mmol) and CuI (0.124 g, 0.65 mmol) in DMF (5 mL) was irradiated in a microwave at 100 °C for 90 min. *R_f* 0.41 (MeOH/CHCl₃, 1:10); mp 288.4-289.0 °C; ¹H NMR (DMSO-*d*₆) δ 0.83-0.86 (t, 3 H, CH₂CH₂CH₃), 1.48-1.58 (m, 2 H, CH₂CH₂CH₃), 2.80-2.84 (t, 2 H, CH₂CH₂CH₃), 6.58 (s, 2 H, 2-NH₂ exch), 6.91, 6.93 (d, 2 H, C₆H₄), 7.37, 7.40 (d, 2 H, C₆H₄), 10.74 (s, 1 H, 3-NH exch); HRMS (ESI, pos mode) *m/z* [M + H]⁺ calcd for C₁₅H₁₄BrN₃OS₂, 396.9824; found, 396.9815.

2-Amino-6-propyl-5-[(2,5-dimethoxyphenyl)sulfanyl]-thieno[2,3-*d*]pyrimidin-4(3*H*)-one (323).

Using the general procedure above compound **323** (0.224 g, 74 %) was obtained as a light brown solid by reacting **389** (0.268 g, 0.8 mmol), 2,5-dimethoxybenzenethiol (0.204 g, 1.2 mmol), K₂CO₃ (0.165 g, 1.2 mmol) and CuI (0.247 g, 1.04 mmol) in DMF (10 mL) was irradiated in a microwave at 100 °C for 60 min. *R_f* 0.41 (MeOH/CHCl₃, 1:10); mp > 300 °C; ¹H NMR (DMSO-*d*₆) δ 0.83-0.87 (t, 3 H, CH₂CH₂CH₃), 1.48-1.53 (m, 2 H, CH₂CH₂CH₃), 2.77-2.81 (t, 2 H, CH₂CH₂CH₃), 3.53 (s, 3 H, OCH₃), 3.80 (s, 3 H, OCH₃), 5.94, 5.95 (d, 1 H, C₆H₃), 6.59-6.62 (d, 3 H, 2-NH₂ exch overlapped with 1 H in C₆H₃), 6.86, 6.88 (d, 1 H, C₆H₃), 10.77 (s, 1 H, 3-NH exch); HRMS (ESI, pos mode) *m/z* [M + H]⁺ calcd for C₁₅H₁₄BrN₃OS₂, 396.9824; found, 396.9815.

General Procedure for the Synthesis of Compounds 397-403.

To a 250 mL round bottom flask, fitted with a magnetic stir bar, were placed palladium diacetate (0.269 g, 1.2 mmol), the appropriate allyl alcohol (20 mmol), ethyl 4-

iodobenzoate (5.52 g, 20 mmol), LiCl (0.848 g, 20 mmol), LiOAc (3.3 g, 50 mmol) and Bu₄NCl (11.12 g, 40 mmol) and DMF (40 mL). The mixture was stirred vigorously at 70 °C for 24 h. The reaction mixture was cooled to room temperature and water (80 mL), ethyl acetate (100 mL) was added. The ethyl acetate layer was separated, washed with brine (30 mL x 3), dried over anhydrous sodium sulfate, and concentrated under reduced pressure to afford a brown oil. The residue was loaded on a silica gel column packed with silica gel and eluted with 5% ethyl acetate in hexane. The fractions containing the desired product (TLC) were pooled and evaporated to afford the product.

Ethyl 4- (4-oxobutyl)benzoate (397). Using the general procedure **397** was obtained as a colorless liquid (4.11 g, 87.2 %); *R_f* 0.70 (hexane/EtOAc 3:1); ¹H NMR (CDCl₃): δ 1.37-1.41 (t, 3 H, COOCH₂CH₃), 1.96-2.01 (m, 2 H, CH₂CH₂CH₂CHO), 2.36-2.49 (q, 2 H, CH₂CH₂CH₂CHO), 2.69-2.76 (t, 2 H, CH₂CH₂CH₂CHO), 4.36-4.38 (q, 2 H, COOCH₂CH₃), 7.23, 7.25 (d, 2 H, C₆H₄), 7.96, 7.99 (d, 2 H, C₆H₄), 9.77 (s, 1 H, CHO). This compound was unstable and could not be analyzed by HRMS and was used directly for the next step.

Ethyl 4- (5-oxopentyl)benzoate (398). Using the general procedure **398** was obtained as a colorless liquid (4.36 g, 87.9 %); *R_f* 0.71 (hexane/EtOAc 3:1); ¹H NMR (CDCl₃): δ 1.33-1.36 (t, 3 H, COOCH₂CH₃), 1.62-1.64 (m, 4 H, CH₂CH₂CH₂CH₂CHO), 2.38-2.42 (m, 2 H, CH₂CH₂CH₂CH₂CHO), 2.66-2.71 (m, 2 H, CH₂CH₂CH₂CH₂CHO), 4.32-4.37 (q, 2 H, COOCH₂CH₃), 7.22, 7.24 (d, 2 H, C₆H₄), 7.94, 7.96 (d, 2 H, C₆H₄), 9.79 (s, 1 H, CHO). HRMS (ESI, pos mode) *m/z* [M + Na]⁺ calcd for C₁₄H₁₈O₃, 257.1154; found, 257.1144.

Ethyl 4- (6-oxohexyl)benzoate (399). Using the general procedure **399** was obtained as a colorless liquid (3.25 g, 65.5 %); R_f 0.73 (hexane/EtOAc 3:1); $^1\text{H NMR}$ (CDCl_3): δ 1.22-1.27 (t, 5 H, $\text{COOCH}_2\text{CH}_3$ and $\text{CH}_2\text{CH}_2\text{CH}_2\text{CH}_2\text{CH}_2\text{CHO}$), 1.47-1.57 (m, 4 H, $\text{CH}_2\text{CH}_2\text{CH}_2\text{CH}_2\text{CH}_2\text{CHO}$), 2.26-2.31 (m, 2 H, $\text{CH}_2\text{CH}_2\text{CH}_2\text{CH}_2\text{CH}_2\text{CHO}$), 2.51-2.56 (m, 2 H, $\text{CH}_2\text{CH}_2\text{CH}_2\text{CH}_2\text{CH}_2\text{CHO}$), 4.19-4.26 (q, 2 H, $\text{COOCH}_2\text{CH}_3$), 7.09, 7.11 (d, 2 H, C_6H_4), 7.81, 7.84 (d, 2 H, C_6H_4), 9.62 (s, 1 H, CHO). This compound was unstable and could not be analyzed by HRMS and was used directly for the next step.

Ethyl 4- (7-oxoheptyl)benzoate (400). Using the general procedure **400** was obtained as a colorless liquid (4.3 g, 82.06 %); R_f 0.74 (hexane/EtOAc 3:1); $^1\text{H NMR}$ (CDCl_3): δ 1.17-1.27 (m, 7 H, $\text{COOCH}_2\text{CH}_3$ and $\text{CH}_2\text{CH}_2\text{CH}_2\text{CH}_2\text{CH}_2\text{CH}_2\text{CHO}$), 1.44-1.55 (m, 4 H, $\text{CH}_2\text{CH}_2\text{CH}_2\text{CH}_2\text{CH}_2\text{CH}_2\text{CHO}$), 2.25-2.31 (m, 2 H, $\text{CH}_2\text{CH}_2\text{CH}_2\text{CH}_2\text{CH}_2\text{CH}_2\text{CHO}$), 2.49-2.54 (t, 2 H, $\text{CH}_2\text{CH}_2\text{CH}_2\text{CH}_2\text{CH}_2\text{CH}_2\text{CHO}$), 4.19-4.26 (q, 2 H, $\text{COOCH}_2\text{CH}_3$), 7.09, 7.11 (d, 2 H, C_6H_4), 7.82, 7.85 (d, 2 H, C_6H_4), 9.61 (s, 1 H, CHO). This compound was unstable and could not be analyzed by HRMS and was used directly for the next step.

Ethyl 4- (8-oxooctyl)benzoate (401). Using the general procedure **401** was obtained as a colorless liquid (4.63 g, 88.3 %); R_f 0.76 (hexane/EtOAc 3:1); $^1\text{H NMR}$ (CDCl_3): δ 1.32-1.42 (m, 9 H, $\text{COOCH}_2\text{CH}_3$ and $\text{CH}_2\text{CH}_2\text{CH}_2\text{CH}_2\text{CH}_2\text{CH}_2\text{CH}_2\text{CHO}$), 1.50-1.68 (m, 4 H, $\text{CH}_2\text{CH}_2\text{CH}_2\text{CH}_2\text{CH}_2\text{CH}_2\text{CH}_2\text{CHO}$), 2.13-2.45 (m, 2 H, $\text{CH}_2\text{CH}_2\text{CH}_2\text{CH}_2\text{CH}_2\text{CH}_2\text{CH}_2\text{CHO}$), 2.59-2.68 (m, 2 H, $\text{CH}_2\text{CH}_2\text{CH}_2\text{CH}_2\text{CH}_2\text{CH}_2\text{CH}_2\text{CHO}$), 4.34-4.41 (q, 2H, $\text{COOCH}_2\text{CH}_3$), 7.22, 7.24 (d, 2 H,

C₆H₄), 7.94, 7.97 (d, 2 H, C₆H₄), 9.36 (s, 1 H, CHO). This compound was unstable and could not be analyzed by HRMS and was used directly for the next step.

Ethyl 4- (9-oxononyl)benzoate (402). Using the general procedure **402** was obtained as a colorless liquid (4.53 g, 78.1 %); *R_f* 0.76 (hexane/EtOAc 3:1); ¹H NMR (CDCl₃): δ 1.34-1.53 (m, 11 H, COOCH₂CH₃ and CH₂CH₂CH₂CH₂CH₂CH₂CH₂CH₂CH₂CHO), 1.60-1.63 (m, 4 H, CH₂CH₂CH₂CH₂CH₂CH₂CH₂CH₂CHO), 2.33-2.41 (m, 2 H, CH₂CH₂CH₂CH₂CH₂CH₂CH₂CH₂CHO), 2.62-2.65 (t, 2 H, CH₂CH₂CH₂CH₂CH₂CH₂CH₂CH₂CHO), 4.33-4.37 (q, 2 H, COOCH₂CH₃), 7.22, 7.23 (d, 2 H, C₆H₄), 7.94, 7.96 (d, 2 H, C₆H₄), 9.35 (s, 1 H, CHO). HRMS (ESI, pos mode) *m/z* [M + K]⁺ calcd for C₁₈H₂₆O₃, 329.1519; found, 329.1498.

Ethyl 4- (10-oxodecyl)benzoate (403). Using the general procedure **403** was obtained as a colorless liquid (5.05 g, 83.5 %); *R_f* 0.77 (hexane/EtOAc 3:1); ¹H NMR (CDCl₃): δ 1.29-1.38 (m, 13 H, COOCH₂CH₃ and CH₂CH₂CH₂CH₂CH₂CH₂CH₂CH₂CH₂CHO), 1.52-1.56 (m, 4 H, CH₂CH₂CH₂CH₂CH₂CH₂CH₂CH₂CH₂CHO), 2.23-2.30 (m, 2 H, CH₂CH₂CH₂CH₂CH₂CH₂CH₂CH₂CH₂CHO), 2.52-2.55 (t, 2 H, CH₂CH₂CH₂CH₂CH₂CH₂CH₂CH₂CHO), 4.23-4.27 (q, 2 H, COOCH₂CH₃), 7.22, 7.24 (d, 2 H, C₆H₄), 7.94, 7.96 (d, 2 H, C₆H₄), 9.56 (s, 1 H, CHO). HRMS (ESI, pos mode) *m/z* [M + Na]⁺ calcd for C₁₉H₂₈O₃, 327.1936; found, 327.1950.

General Procedure for the Synthesis of Compounds 404-410.

A mixture of sulfur (1 mmol), the appropriate aldehyde (1 mmol), ethyl cyanoacetate (1 mmol) and EtOH (5 mL) were placed in a round bottom flask and warmed to 45 °C and treated dropwise with morpholine (1 mmol) over 15 min. The mixture was stirred for 5 h at 45 °C and 24 h at room temperature. Unreacted sulfur was removed by filtration, and

the filtrate was concentrated under reduced pressure to afford an orange oil. The residue was loaded on a silica gel column packed with silica gel and eluted with 10% ethyl acetate in hexane. The fractions containing the desired product (TLC) were pooled and evaporated to afford the products.

Ethyl 2-amino-5-{2-[4- (ethoxycarbonyl)phenyl]ethyl}thiophene-3-carboxylate (404).

Compound **404** (3.68 g, 67.65 %) was obtained as an orange liquid by reacting **397** (3.7 g, 15.67 mmol) with sulfur (0.5 g, 15.67 mmol) and ethyl cyanoacetate (1.78 g, 15.67 mmol) as described in the General Procedure above; R_f 0.68 (hexane/EtOAc 3:1); ^1H NMR (CDCl_3): δ 1.30-1.34 (t, 3 H, $\text{COOCH}_2\text{CH}_3$), 1.36-1.41 (t, 3 H, $\text{COOCH}_2\text{CH}_3$), 2.88-2.97 (m, 4 H, $\text{C}_6\text{H}_4\text{-CH}_2\text{CH}_2$), 4.21-4.27 (q, 2 H, $\text{COOCH}_2\text{CH}_3$), 4.33-4.40 (q, 2 H, $\text{COOCH}_2\text{CH}_3$), 5.79 (s, 2 H, NH_2exch), 6.63 (s, 1 H, 4-H), 7.23, 7.26 (d, 2 H, C_6H_4), 7.95, 7.98 (d, 2 H, C_6H_4). HRMS (ESI, pos mode) m/z $[\text{M} + \text{Na}]^+$ calcd for $\text{C}_{18}\text{H}_{21}\text{NO}_4\text{S}$, 370.1089; found, 370.1112.

Ethyl 2-amino-5-{3-[4- (ethoxycarbonyl) phenyl]propyl}thiophene-3-carboxylate

(405). Compound **405** (1.49 g, 65.32 %) was obtained as an orange liquid by reacting **398** (1.58 g, 6.31 mmol), sulfur (0.20 g, 6.31 mmol) and ethyl cyanoacetate (0.71 g, 6.31 mmol) as described in the General Procedure above; R_f 0.69 (hexane/EtOAc 3:1); ^1H NMR (CDCl_3): δ 1.32-1.36 (t, 3 H, $\text{COOCH}_2\text{CH}_3$), 1.37-1.42 (t, 3 H, $\text{COOCH}_2\text{CH}_3$) 1.88-1.98 (p, 2 H, $\text{C}_6\text{H}_4\text{-CH}_2\text{CH}_2\text{CH}_2$), 2.59-2.64 (t, 2 H, $\text{C}_6\text{H}_4\text{-CH}_2\text{CH}_2\text{CH}_2$), 2.69-2.74 (t, 2 H, $\text{C}_6\text{H}_4\text{-CH}_2\text{CH}_2\text{CH}_2$), 4.23-4.30 (q, 2 H, $\text{COOCH}_2\text{CH}_3$), 4.34-4.41 (q, 2 H, $\text{COOCH}_2\text{CH}_3$), 5.80 (s, 2 H, NH_2 exch), 6.65 (s, 1 H, 4-H), 7.23, 7.26 (d, 2 H, C_6H_4), 8.00, 8.03 (d, 2 H, C_6H_4). HRMS (ESI, pos mode) m/z $[\text{M} + \text{Na}]^+$ calcd for $\text{C}_{19}\text{H}_{23}\text{NO}_4\text{S}$, 384.1245; found, 384.1281.

Ethyl 2-amino-5-{4-[4- (ethoxycarbonyl)phenyl]butyl}thiophene-3-carboxylate (406).

Compound **406** (2.99 g, 66.73 %) was obtained as an orange liquid by reacting **399** (2.96 g, 11.92 mmol), sulfur (0.38 g, 11.92 mmol) and ethyl cyanoacetate (1.35 g, 11.92 mmol) as described in the General Procedure above; R_f 0.71 (hexane/EtOAc 3:1); ^1H NMR (CDCl_3): δ 1.27-1.32 (t, 3 H, $\text{COOCH}_2\text{CH}_3$), 1.33-1.37 (t, 3 H, $\text{COOCH}_2\text{CH}_3$), 1.57-1.69 (m, 4 H, $\text{C}_6\text{H}_4\text{-CH}_2\text{CH}_2\text{CH}_2\text{CH}_2$), 2.54-2.59 (t, 2 H, $\text{C}_6\text{H}_4\text{-CH}_2\text{CH}_2\text{CH}_2\text{CH}_2$), 2.62-2.67 (t, 2 H, $\text{C}_6\text{H}_4\text{-CH}_2\text{CH}_2\text{CH}_2\text{CH}_2$), 4.18-4.25 (q, 2 H, $\text{COOCH}_2\text{CH}_3$), 4.29-4.36 (q, 2 H, $\text{COOCH}_2\text{CH}_3$), 5.73 (s, 2 H, NH_2 exch), 6.58 (s, 1 H, 4-H), 7.18, 7.21 (d, 2 H, C_6H_4), 7.90, 7.93 (d, 2 H, C_6H_4). HRMS (ESI, pos mode) m/z $[\text{M} + \text{Na}]^+$ calcd for $\text{C}_{20}\text{H}_{25}\text{NO}_4\text{S}$, 398.1402; found, 398.1392.

Ethyl 2-amino-5-{5-[4- (ethoxycarbonyl) phenyl]pentyl}thiophene-3-carboxylate (407).

Compound **407** (2.62 g, 63.17 %) was obtained as an orange liquid by reacting **400** (2.8 g, 10.67 mmol), sulfur (0.34 g, 10.67 mmol) and ethyl cyanoacetate (1.20 g, 10.67 mmol) as described in the General Procedure above; R_f 0.71 (hexane/EtOAc 3:1); ^1H NMR (CDCl_3): δ 1.37-1.47 (m, 8 H, $2\text{COOCH}_2\text{CH}_3$ and $\text{C}_6\text{H}_4\text{-CH}_2\text{CH}_2\text{CH}_2\text{CH}_2\text{CH}_2$), 1.62-1.76 (m, 4 H, $\text{C}_6\text{H}_4\text{-CH}_2\text{CH}_2\text{CH}_2\text{CH}_2\text{CH}_2$), 2.60-2.65 (t, 2 H, $\text{C}_6\text{H}_4\text{-CH}_2\text{CH}_2\text{CH}_2\text{CH}_2\text{CH}_2$), 2.69-2.74 (t, 2 H, $\text{C}_6\text{H}_4\text{-CH}_2\text{CH}_2\text{CH}_2\text{CH}_2\text{CH}_2$), 4.28-4.35 (q, 2 H, $\text{COOCH}_2\text{CH}_3$), 4.39-4.46 (q, 2 H, $\text{COOCH}_2\text{CH}_3$), 5.85 (s, 2 H, NH_2 exch), 6.66 (s, 1 H, 4-H), 7.28, 7.30 (d, 2 H, C_6H_4), 8.00, 8.03 (d, 2 H, C_6H_4). HRMS (ESI, pos mode) m/z $[\text{M} + \text{Na}]^+$ calcd for $\text{C}_{21}\text{H}_{27}\text{NO}_4\text{S}$, 412.1559; found, 412.1537.

Ethyl 2-amino-5-{6-[4- (ethoxycarbonyl)phenyl]hexyl}thiophene-3-carboxylate (408).

Compound **408** (3.62 g, 68.86 %) was obtained as an orange liquid by reacting **401**

(3.6 g, 13.03 mmol), sulfur (0.42 g, 13.03 mmol) and ethyl cyanoacetate (1.47 g, 13.03 mmol) as described in the General Procedure above; R_f 0.73 (hexane/EtOAc 3:1); ^1H NMR (CDCl_3): δ 1.31-1.41 (m, 10 H, $2\text{COOCH}_2\text{CH}_3$ and $\text{C}_6\text{H}_4\text{-CH}_2\text{CH}_2\text{CH}_2\text{CH}_2$ CH_2CH_2), 1.46-1.66 (m, 4 H, $\text{C}_6\text{H}_4\text{-CH}_2\text{CH}_2\text{CH}_2\text{CH}_2\text{CH}_2\text{CH}_2$), 2.53-2.58 (t, 2 H, $\text{C}_6\text{H}_4\text{-CH}_2\text{CH}_2\text{CH}_2\text{CH}_2\text{CH}_2\text{CH}_2$), 2.62-2.69 (t, 2 H, $\text{C}_6\text{H}_4\text{-CH}_2\text{CH}_2\text{CH}_2\text{CH}_2\text{CH}_2\text{CH}_2$), 4.22-4.29 (q, 2 H, $\text{COOCH}_2\text{CH}_3$), 4.33-4.40 (q, 2 H, $\text{COOCH}_2\text{CH}_3$), 5.77 (s, 2 H, NH_2 exch), 6.62 (s, 1 H, 4-H), 7.22, 7.26 (d, 2 H, C_6H_4), 7.94, 7.97 (d, 2 H, C_6H_4). HRMS (ESI, pos mode) m/z $[\text{M} + \text{Na}]^+$ calcd for $\text{C}_{22}\text{H}_{29}\text{NO}_4\text{S}$, 426.1715; found, 426.1688.

Ethyl 2-amino-5-{7-[4-(ethoxycarbonyl)phenyl]heptyl}thiophene-3-carboxylate

(409). Compound **409** (1.94 g, 63.5 %) was obtained as an orange liquid by reacting **402** (2.1 g, 7.2 mmol), sulfur (0.23 g, 7.2 mmol) and ethyl cyanoacetate (0.81 g, 7.2 mmol) as described in the General Procedure above; R_f 0.72 (hexane/EtOAc 3:1); ^1H NMR (CDCl_3): δ 1.29-1.41 (m, 12 H, $2\text{COOCH}_2\text{CH}_3$ and $\text{C}_6\text{H}_4\text{-CH}_2\text{CH}_2\text{CH}_2\text{CH}_2\text{CH}_2$ CH_2CH_2), 1.46-1.66 (m, 4 H, $\text{C}_6\text{H}_4\text{-CH}_2\text{CH}_2\text{CH}_2\text{CH}_2\text{CH}_2\text{CH}_2\text{CH}_2$), 2.51-2.58 (t, 2 H, $\text{C}_6\text{H}_4\text{-CH}_2\text{CH}_2\text{CH}_2\text{CH}_2\text{CH}_2\text{CH}_2\text{CH}_2$), 2.60-2.71 (t, 2 H, $\text{C}_6\text{H}_4\text{-CH}_2\text{CH}_2\text{CH}_2\text{CH}_2\text{CH}_2\text{CH}_2\text{CH}_2$), 4.20-4.27 (q, 2 H, $\text{COOCH}_2\text{CH}_3$), 4.31-4.38 (q, 2 H, $\text{COOCH}_2\text{CH}_3$), 5.86 (s, 2 H, NH_2 exch), 6.60 (s, 1 H, 4-H), 7.20, 7.23 (d, 2 H, C_6H_4), 7.94, 7.96 (d, 2 H, C_6H_4). HRMS (ESI, pos mode) m/z $[\text{M} + \text{Na}]^+$ calcd for $\text{C}_{23}\text{H}_{31}\text{NO}_4\text{S}$, 440.1872; found, 440.1837.

Ethyl 2-amino-5-{8-[4-(ethoxycarbonyl)phenyl]octyl}thiophene-3-carboxylate

(410).

Compound **410** (4.77 g, 62.4 %) was obtained as an orange liquid by reacting **403** (5.4 g, 17.7 mmol), sulfur (0.57 g, 17.7 mmol) and ethyl cyanoacetate (2.0 g, 17.7 mmol) as

described in the General Procedure above; R_f 0.74 (hexane/EtOAc 3:1); $^1\text{H NMR}$ (CDCl_3): δ 1.30-1.43 (m, 14 H, $2\text{COOCH}_2\text{CH}_3$ and $\text{C}_6\text{H}_4\text{-CH}_2\text{CH}_2\text{CH}_2\text{CH}_2\text{CH}_2\text{CH}_2$ CH_2CH_2), 1.47-1.66 (m, 4 H, $\text{C}_6\text{H}_4\text{-CH}_2\text{CH}_2\text{CH}_2\text{CH}_2\text{CH}_2\text{CH}_2\text{CH}_2\text{CH}_2$), 2.53-2.58 (t, 2H, $\text{C}_6\text{H}_4\text{-CH}_2\text{CH}_2\text{CH}_2\text{CH}_2\text{CH}_2\text{CH}_2\text{CH}_2\text{CH}_2$), 2.62-2.67 (t, 2 H, $\text{C}_6\text{H}_4\text{-CH}_2\text{CH}_2\text{CH}_2\text{CH}_2\text{CH}_2\text{CH}_2\text{CH}_2\text{CH}_2$), 4.21-4.28 (q, 2 H, $\text{COOCH}_2\text{CH}_3$), 4.32-4.39 (q, 2 H, $\text{COOCH}_2\text{CH}_3$), 5.77 (s, 2 H, NH_2 exch), 6.61 (s, 1 H, 4-H), 7.21, 7.24 (d, 2 H, C_6H_4), 7.94, 7.97 (d, 2 H, C_6H_4). HRMS (ESI, pos mode) m/z $[\text{M} + \text{Na}]^+$ calcd for $\text{C}_{24}\text{H}_{33}\text{NO}_4\text{S}$, 454.2028; found, 454.2016.

General Procedure for the Synthesis of Compounds 411-417.

A mixture of appropriate thiophene and chloroformamidine hydrochloride (1:4) in DMSO_2 was heated at 140°C for 4 h. The mixture was cooled to room temperature and water (15 mL) was added. Ammonium hydroxide was used to neutralize the suspension. The brown solid, obtained by filtration, was washed with water and dried over P_2O_5 vacuum. The solid was dissolved in methanol and silica gel was added. A dry silica gel plug was obtained after evaporation of the solvent. The plug was loaded on to a silica gel column and eluted with 5% methanol in chloroform. The fractions containing the desired product (TLC) were pooled and evaporated to afford the products.

Ethyl 4-[2-(2-amino-4-oxo-3,4-dihydrothieno[2,3-*d*]pyrimidin-6-yl)ethyl]benzoate (411). Using the General Procedure above compound **411** (0.73 g, 71.51 %) was obtained as a yellow solid by reacting **404** (0.7 g, 2.96 mmol) and chloroformamidine hydrochloride (1.30 g, 11.85 mmol); mp $274.6\text{-}275.9^\circ\text{C}$; R_f 0.53 (MeOH/ CHCl_3 , 1:6); $^1\text{H NMR}$ ($\text{DMSO-}d_6$): δ 1.28-1.33 (t, 3 H, $\text{COOCH}_2\text{CH}_3$), 2.98-3.04 (m, 4 H, $\text{C}_6\text{H}_4\text{-}$

CH₂CH₂), 4.25-4.32 (q, 2 H, COOCH₂CH₃), 6.46 (s, 2 H, 2-NH₂ exch), 6.77 (s, 1 H, 5-H), 7.37, 7.40 (d, 2 H, C₆H₄), 7.85, 7.88 (d, 2 H, C₆H₄), 10.81 (s, 1 H, 3-NH exch). Anal. calcd. for (C₁₇H₁₇N₃O₃S₂): C, 59.46; H, 4.99; N, 12.24; S, 9.34; found: C, 59.44; H, 5.06; N, 12.08; S, 9.23.

Ethyl 4-[3-(2-amino-4-oxo-3,4-dihydrothieno[2,3-*d*]pyrimidin-6-yl)propyl]benzoate (412). Using the General Procedure above compound **412** (0.43 g, 81.13 %) was obtained as a yellow solid by reacting **405** (0.54 g, 1.49 mmol) and chloroformamidine hydrochloride (0.68 g, 5.9 mmol); mp 224.4-225.3 °C; *R_f* 0.53 (MeOH/CHCl₃, 1:6); ¹H NMR (DMSO-*d*₆): δ 1.28-1.33 (t, 3 H, COOCH₂CH₃), 1.86-1.96 (p, 2 H, C₆H₄-CH₂CH₂CH₂), 2.68-2.74 (m, 4 H, C₆H₄-CH₂CH₂CH₂), 4.26-4.33 (q, 2 H, COOCH₂CH₃), 6.46 (s, 2 H, 2-NH₂ exch), 6.82 (s, 1 H, 5-H), 7.35, 7.37 (d, 2 H, C₆H₄), 7.87, 7.89 (d, 2 H, C₆H₄), 10.81 (s, 1 H, 3-NH exch). Anal. calcd. for (C₁₈H₁₉N₃O₃S · 0.4 CH₃OH): C, 59.69; H, 5.61; N, 11.35; S, 8.66; found: C, 59.73; H, 5.21; N, 11.55; S, 8.60.

Ethyl 4-[4-(2-amino-4-oxo-3,4-dihydrothieno[2,3-*d*]pyrimidin-6-yl)butyl]benzoate (413). Using the General Procedure above compound **413** (1.05 g, 76.51 %) was obtained as a yellow solid by reacting **406** (1.40 g, 3.71 mmol) and chloroformamidine hydrochloride (1.70 g, 14.84 mmol); mp 273.5-275 °C; *R_f* 0.54 (MeOH/CHCl₃, 1:6); ¹H NMR (DMSO-*d*₆): δ 1.27-1.32 (t, 3 H, COOCH₂CH₃), 2.47-2.52 (m, 4 H, C₆H₄-CH₂CH₂CH₂CH₂), 2.65-2.73 (m, 4 H, C₆H₄-CH₂CH₂CH₂CH₂), 4.24-4.32 (q, 2 H, COOCH₂CH₃), 6.44 (s, 2 H, 2-NH₂ exch), 6.78 (1 H, s, 5-H), 7.31, 7.34 (d, 2 H, C₆H₄), 7.84, 7.87 (d, 2 H, C₆H₄), 10.84 (s, 1 H, 3-NH exch). Anal. calcd. for (C₁₉H₂₁N₃O₃S · 0.2 H₂O): C, 60.84; H, 5.75; N, 11.20; S, 8.55; found: C, 60.86; H, 5.64; N, 11.56; S, 8.62.

Ethyl 4-[5- (2-amino-4-oxo-3,4-dihydrothieno[2,3-*d*]pyrimidin-6-yl)pentyl]benzoate (414). Using the General Procedure above compound **414** (0.56 g, 54.37 %) was obtained as a yellow solid by reacting **407** (1.08 g, 2.76 mmol) and chloroformamidinium hydrochloride (1.58 g, 13.8 mmol); mp 219.3-220.1 °C; R_f 0.55 (MeOH/CHCl₃, 1:6); ¹H NMR (DMSO-*d*₆): δ 1.27-1.31 (t, 5 H, COOCH₂CH₃ and C₆H₄-CH₂CH₂CH₂CH₂CH₂), 1.54-1.64 (m, 4 H, C₆H₄-CH₂CH₂CH₂CH₂CH₂), 2.59-2.69 (m, 4 H, C₆H₄-CH₂CH₂CH₂CH₂CH₂), 4.24-4.31 (q, 2 H, COOCH₂CH₃), 6.45 (s, 2 H, 2-NH₂ exch), 6.78 (s, 1 H, 5-H), 7.31, 7.34 (d, 2 H, C₆H₄), 7.83, 7.86 (d, 2 H, C₆H₄), 10.86 (1 H, s, 3-NH exch). Anal. calcd. for (C₂₀H₂₃N₃O₃S): C, 62.32; H, 6.01; N, 10.90; S, 8.32; found: C, 62.48; H, 6.08; N, 10.79; S, 8.31.

Ethyl 4-[6- (2-amino-4-oxo-3,4-dihydrothieno[2,3-*d*]pyrimidin-6-yl)hexyl]benzoate (415). Using the General Procedure above compound **415** (0.78 g, 67.24 %) was obtained as a yellow solid by reacting **408** (1.18 g, 2.91 mmol) and chloroformamidinium hydrochloride (1.30 g, 11.64 mmol); mp 196.8-197.4 °C; R_f 0.53 (MeOH/CHCl₃, 1:6); ¹H NMR (DMSO-*d*₆): δ 1.27-1.32 (m, 7 H, COOCH₂CH₃ and C₆H₄-CH₂CH₂CH₂CH₂CH₂CH₂), 1.50-1.61 (m, 4 H, C₆H₄-CH₂CH₂CH₂CH₂CH₂CH₂), 2.50-2.71 (m, 4 H, C₆H₄-CH₂CH₂CH₂CH₂CH₂CH₂), 4.25-4.32 (q, 2 H, COOCH₂CH₃), 6.53 (s, 2 H, 2-NH₂ exch), 6.85 (s, 1 H, 5-H), 7.36, 7.39 (d, 2 H, C₆H₄), 7.91, 7.94 (d, 2 H, C₆H₄), 10.82 (1 H, s, 3-NH exch). Anal. calcd. for (C₂₁H₂₅N₃O₃S · 0.2 H₂O): C, 62.02; H, 6.39; N, 10.33; S, 7.88; found: C, 62.42; H, 6.48; N, 11.06; S, 7.74.

Ethyl 4-[7- (2-amino-4-oxo-3,4-dihydrothieno[2,3-*d*]pyrimidin-6-yl)heptyl]benzoate (416). Using the General Procedure above compound **416** (0.67 g, 67.7 %) was obtained as a yellow solid by reacting **409** (1 g, 2.4 mmol) and chloroformamidinium hydrochloride

(1.4 g, 12 mmol); mp 190.2-192.1 °C; R_f 0.55 (MeOH/CHCl₃, 1:6); ¹H NMR (DMSO-*d*₆): δ 1.16-1.33 (m, 9 H, COOCH₂CH₃ and C₆H₄-CH₂CH₂CH₂CH₂CH₂CH₂CH₂CH₂), 1.56 (m, 4 H, C₆H₄-CH₂CH₂CH₂CH₂CH₂CH₂CH₂CH₂), 2.50-2.69 (m, 4 H, C₆H₄-CH₂CH₂CH₂CH₂CH₂CH₂CH₂CH₂CH₂), 4.25-4.32 (q, 2 H, COOCH₂CH₃), 6.46 (s, 2 H, 2-NH₂ exch), 6.76 (s, 1 H, 5-H), 7.30, 7.33 (d, 2 H, C₆H₄), 7.85, 7.87 (d, 2 H, C₆H₄), 10.83 (s, 1 H, 3-NH exch). HRMS (ESI, pos mode) m/z [M + Na]⁺ calcd for C₂₂H₂₇N₃O₃S, 436.5266; found, 436.5239.

Ethyl 4-[8-(2-amino-4-oxo-3,4-dihydrothieno[2,3-*d*]pyrimidin-6-yl)octyl]benzoate (417). Using the General Procedure above compound **417** (1.52 g, 70.3 %) was obtained as a yellow solid by reacting **410** (2.18 g, 5.05 mmol) and chloroformamidine hydrochloride (2.3 g, 20.2 mmol); 274.5-276.2 °C; R_f 0.54 (MeOH/CHCl₃, 1:6); ¹H NMR (DMSO-*d*₆): δ 1.13-1.33 (m, 11H, COOCH₂CH₃ and C₆H₄-CH₂CH₂CH₂CH₂CH₂CH₂CH₂CH₂CH₂), 1.55 (m, 4 H, C₆H₄-CH₂CH₂CH₂CH₂CH₂CH₂CH₂CH₂CH₂CH₂), 2.50-2.72 (m, 4 H, C₆H₄-CH₂CH₂CH₂CH₂CH₂CH₂CH₂CH₂CH₂CH₂), 4.25-4.32 (q, 2 H, COOCH₂CH₃), 6.46 (s, 2 H, 2-NH₂ exch), 6.78 (s, 1 H, 5-H), 7.31, 7.33 (d, 2 H, C₆H₄), 7.85, 7.87 (d, 2 H, C₆H₄), 10.84 (1 H, s, 3-NH exch). HRMS (ESI, pos mode) m/z [M + Na]⁺ calcd for C₂₃H₂₉N₃O₃S, 450.1827; found, 450.1790.

General Procedure for the Synthesis of Compounds 418-424.

To a solution of **411-417** in ethanol (10-50 mL) was added aqueous 1 N NaOH and the reaction mixture stirred at room temperature for 12 h. The ethanol was evaporated under reduced pressure and the residue was dissolved in water (5-10 mL). The solution was carefully acidified to pH 3 with the drop wise addition of 1 N HCl. The resulting

suspension was left at 0 °C for an hour and then the residue was collected by filtration, washed with water (5 mL) and dried over P₂O₅/vacuum at 50 °C to afford the free acids **418-424**.

4-[2- (2-Amino-4-oxo-3,4-dihydrothieno[2,3-*d*]pyrimidin-6-yl)ethyl]benzoic acid

(418). Using the General Procedure described above compound **418** (0.529 g, 95.0 %) was obtained as a white solid from **411** (0.61 g, 1.77 mmol) by hydrolysis in ethanol (50 mL) and 1 N NaOH (25 mL); mp >300 °C; *R_f* 0.55 (MeOH/CHCl₃, 1:6 + 1 drop of gl. HOAc); ¹H NMR (DMSO-*d*₆): δ 2.97-2.99 (t, 2 H, C₆H₄-CH₂CH₂), 3.02-3.41 (t, 2 H, C₆H₄-CH₂CH₂), 6.50 (s, 2 H, 2-NH₂ exch), 6.78 (s, 1 H, 5-H), 7.35, 7.38 (d, 2 H, C₆H₄), 7.83, 7.86 (d, 2 H, C₆H₄), 10.85 (1 H, s, 3-NH exch), 12.76 (1 H, s, COOH exch). Anal. calcd. for (C₁₅H₁₃N₃O₃S · 0.6 HCl): C, 53.42; H, 4.06; N, 12.46; S, 9.51; Cl, 1.85; found: C, 53.59; H, 3.93; N, 12.41; S, 9.34; Cl, 1.88.

4-[3- (2-Amino-4-oxo-3,4-dihydrothieno[2,3-*d*]pyrimidin-6-yl)propyl]benzoic acid

(419). Using the General Procedure described above compound **419** (0.18 g, 92.6 %) was obtained as a white solid from **412** (0.22 g, 0.60 mmol) under hydrolysis in ethanol (20 mL) and 1 N NaOH (10 mL); mp 292.7-293.4 °C; *R_f* 0.52 (MeOH/CHCl₃, 1:6 + 1 drop of gl. HOAc); ¹H NMR (DMSO-*d*₆): δ 1.85-1.95 (m, 2 H, C₆H₄-CH₂CH₂CH₂), 2.66-2.73 (m, 4 H, C₆H₄-CH₂CH₂CH₂), 6.58 (s, 2 H, 2-NH₂ exch), 6.82 (s, 1 H, 5-H), 7.35, 7.39 (d, 2 H, C₆H₄), 7.85, 7.88 (d, 2 H, C₆H₄), 10.94 (s, 1 H, 3-NH exch), 12.79 (s, 1 H, COOH exch). Anal. calcd. for (C₁₆H₁₅N₃O₃S · 0.7 CH₃OH): C, 57.01; H, 5.10; N, 11.94; S, 9.11; found: C, 56.79; H, 4.75; N, 11.92; S, 9.20.

4-[4- (2-Amino-4-oxo-3,4-dihydrothieno[2,3-*d*]pyrimidin-6-yl)butyl]benzoic acid

(420). Using the General Procedure described above compound **420** (0.138 g, 93.6 %)

was obtained as a yellow solid **413** (0.16 g, 0.43 mmol) under hydrolysis in ethanol (15 mL) and 1 N NaOH (7 mL); mp >300°C; R_f 0.52 (MeOH/CHCl₃, 1:6 + 1 drop of gl. HOAc); ¹H NMR (DMSO-*d*₆): δ 1.59-1.62 (m, 4 H, C₆H₄-CH₂CH₂CH₂CH₂), 2.65-2.75 (m, 4 H, C₆H₄-CH₂CH₂CH₂CH₂), 6.46 (s, 2 H, 2-NH₂ exch), 6.79 (s, 1 H, 5-H), 7.29, 7.32 (d, 2 H, C₆H₄), 7.83, 7.86 (d, 2 H, C₆H₄), 10.83 (s, 1 H, 3-NH exch), 12.77 (s, 1 H, COOH exch). Anal. calcd. for (C₁₇H₁₇N₃O₃S · 0.5 H₂O): C, 57.94; H, 5.15; N, 11.92; S, 9.10; found: C, 58.15; H, 5.02; N, 11.92; S, 9.05.

4-[5- (2-Amino-4-oxo-3,4-dihydrothieno[2,3-*d*]pyrimidin-6-yl)pentyl]benzoic acid (421). Using the General Procedure described above compound **421** (0.199 g, 93.3 %) was obtained as a white solid from **414** (0.23 g, 0.60 mmol) under hydrolysis in ethanol (20 mL) and 1 N NaOH (10 mL); mp 259.4-260 °C; R_f 0.52 (MeOH/CHCl₃, 1:6 + 1 drop of HOAc); ¹H NMR (DMSO-*d*₆): δ 1.28-1.38 (m, 2 H, C₆H₄-CH₂CH₂CH₂CH₂CH₂), 1.56-1.66 (m, 4 H, C₆H₄-CH₂CH₂CH₂CH₂CH₂), 2.61-2.71 (p, 4 H, C₆H₄-CH₂CH₂CH₂CH₂CH₂), 6.45 (s, 2 H, 2-NH₂ exch), 6.79 (s, 1 H, 5-H), 7.29, 7.32 (d, 2 H, C₆H₄), 7.83, 7.85 (d, 2 H, C₆H₄), 10.82 (s, 1 H, 3-NH exch), 12.77 (s, 1 H, COOH exch). Anal. calcd. for (C₁₈H₁₉N₃O₃S · 0.4 H₂O): C, 59.29; H, 5.47; N, 11.52; S, 8.79; found: C, 59.48; H, 5.38; N, 11.43; S, 9.15.

4-[6- (2-Amino-4-oxo-3,4-dihydrothieno[2,3-*d*]pyrimidin-6-yl)hexyl]benzoic acid (422). Using the General Procedure described above compound **422** (0.141 g, 95.2 %) was obtained as a yellow solid from **415** (0.16 g, 0.40 mmol) and ethanol (15 mL) and 1 N NaOH (7 mL); mp 282-283.8 °C; R_f 0.52 (MeOH/CHCl₃, 1:6 + 1 drop of HOAc); ¹H NMR (DMSO-*d*₆): δ 1.31-1.32 (m, 4 H, C₆H₄-CH₂CH₂CH₂CH₂CH₂CH₂), 1.51-1.60 (m, 4

H, C₆H₄-CH₂CH₂CH₂CH₂CH₂CH₂), 2.59-2.69 (p, 4 H, C₆H₄-CH₂CH₂CH₂CH₂CH₂CH₂), 6.45 (s, 2 H, 2-NH₂ exch), 6.78 (s, 1 H, 5-H), 7.28, 7.31 (d, 2 H, C₆H₄), 7.83, 7.85 (d, 2 H, C₆H₄), 10.82 (s, 1 H, 3-NH exch), 12.76 (s, 1 H, COOH exch). Anal. calcd. for (C₁₉H₂₁N₃O₃S): C, 61.44; H, 5.70; N, 11.31; S, 8.63; found: C, 61.18; H, 5.73; N, 11.05; S, 8.46.

4-[7- (2-Amino-4-oxo-3,4-dihydrothieno[2,3-*d*]pyrimidin-6-yl)heptyl]benzoic acid

(423). Using the General Procedure described above compound **423** (0.22 g, 94.9 %) was obtained as a white solid from **416** (0.25 g, 0.60 mmol) and ethanol (20 mL) and 1 N NaOH (10 mL); mp 233.8-235 °C; *R_f* 0.51 (MeOH/CHCl₃, 1:6 + 1 drop of gl. HOAc); ¹H NMR (DMSO-*d*₆): δ 1.29 (m, 6 H, C₆H₄-CH₂CH₂CH₂CH₂CH₂CH₂CH₂), 1.53-1.58 (m, 4 H, C₆H₄-CH₂CH₂CH₂CH₂CH₂CH₂CH₂), 2.60-2.69 (m, 4 H, C₆H₄-CH₂CH₂CH₂CH₂CH₂CH₂CH₂), 6.46 (s, 2 H, 2-NH₂ exch), 6.78 (s, 1 H, 5-H), 7.29, 7.31 (d, 2 H, C₆H₄), 7.83, 7.85 (d, 2 H, C₆H₄), 10.83 (s, 1 H, 3-NH exch), 12.74 (s, 1 H, COOH exch). HRMS (ESI, pos mode) *m/z* [M + Na]⁺ calcd for C₂₀H₂₃N₃O₃S, 408.1358; found, 408.1380.

4-[8- (2-Amino-4-oxo-3,4-dihydrothieno[2,3-*d*]pyrimidin-6-yl)octyl]benzoic acid

(424). Using the General Procedure described above compound **424** (0.22 g, 92.8 %) was obtained as a yellow solid from **417** (0.26 g, 0.60 mmol) and ethanol (20 mL) and 1 N NaOH (9 mL). It is yellow solid; *R_f* 0.53 (MeOH/CHCl₃, 1:6 + 1 drop of gl. HOAc); ¹H NMR (DMSO-*d*₆): δ 1.29 (m, 8 H, C₆H₄-CH₂CH₂CH₂CH₂CH₂CH₂CH₂CH₂CH₂), 1.56 (m, 4 H, C₆H₄-CH₂CH₂CH₂CH₂CH₂CH₂CH₂CH₂CH₂), 2.60-2.69 (m, 4 H, C₆H₄-CH₂CH₂CH₂CH₂CH₂CH₂CH₂CH₂CH₂CH₂CH₂CH₂), 6.46 (s, 2 H, 2-NH₂ exch), 6.78 (s, 1 H, 5-H), 7.29, 7.31 (d, 2 H, C₆H₄), 7.83, 7.85 (d, 2 H, C₆H₄), 10.83 (s, 1 H, 3-NH exch), 12.75 (s, 1 H, COOH exch).

HRMS (ESI, pos mode) m/z $[M + Na]^+$ calcd for $C_{21}H_{25}N_3O_3S$, 422.1514; found, 422.1553.

General Procedure for the Synthesis of Compound 425-431.

To a solution of **418-424** (0.1 mmol) in anhydrous DMF (5-10 mL) was added N-methylmorpholine (0.12 mmol) and 2-chloro-4,6-dimethoxy-1,3,5-triazine (0.12 mmol). The resulting mixture was stirred at room temperature for 2 h. N-methylmorpholine (0.12 mmol) and diethyl-L- glutamate hydrochloride (0.1 mmol) were added to the mixture. The reaction mixture was stirred for an additional 3 h at room temperature and silica gel was added to this solution and the suspension evaporated under reduced pressure. The plug obtained was loaded on a silica gel column and eluted with 2% methanol in chloroform. The fractions containing the desired product (TLC) were pooled and evaporated to afford the products.

Diethyl N-{4-[2- (2-amino-4-oxo-3,4-dihydrothieno[2,3-*d*]pyrimidin-6-yl)ethyl]benzoyl}-L-glutamate (425). Using the General Procedure described above compound **425** (0.114 g, 71.5 %) was obtained as a white solid from **418** (0.126 g, 0.40 mmol); mp 153.4-154 °C; R_f 0.63 (MeOH/ $CHCl_3$, 1:6); 1H NMR (DMSO- d_6): δ 1.14-1.21 (m, 6 H, $2COOCH_2CH_3$), 1.95-2.23 (m, 2 H, Glu β - CH_2), 2.41-2.46 (t, 2 H, Glu γ - CH_2), 2.97-3.05 (m, 4 H, $C_6H_4-CH_2CH_2$), 4.00-4.06 (q, 2 H, $2COOCH_2CH_3$), 4.08-4.14 (q, 2 H, $COOCH_2CH_3$), 4.38-4.45 (m, 1 H, Glu α -CH), 6.45 (s, 2 H, 2-NH $_2$ exch), 6.79 (s, 1 H, 5-H), 7.33, 7.36 (d, 2 H, C_6H_4), 7.77, 7.80 (d, 2 H, C_6H_4), 8.63-8.66 (d, 1 H, CONH exch), 10.81 (s, 1 H, 3-NH exch). Anal. calcd. for ($C_{24}H_{28}N_4O_6S$): C, 57.59; H, 5.64; N, 11.19; S, 6.41; found: C, 57.42; H, 5.77; N, 11.00; S, 6.36.

Diethyl N-{4-[3-(2-amino-4-oxo-3,4-dihydrothieno[2,3-*d*]pyrimidin-6-yl)propyl]}

benzoyl}-L-glutamate (426). Using the General Procedure described above compound **426** (0.106 g, 73.1 %) was obtained as a yellow solid from **419** (0.10 g, 0.30 mmol); mp 122.5-123.2 °C; R_f 0.63 (MeOH/CHCl₃, 1:6); ¹H NMR (DMSO-*d*₆): δ 1.15-1.21 (m, 6 H, 2COOCH₂CH₃), 1.89-1.93 (m, 2 H, C₆H₄-CH₂CH₂CH₂), 1.99-2.11 (m, 2 H, Gluβ-CH₂), 2.41-2.45 (t, 2 H, Gluγ-CH₂), 2.68-2.71 (m, 4 H, C₆H₄-CH₂CH₂CH₂), 4.00-4.13 (m, 4 H, 2COOCH₂CH₃), 4.41-4.45 (m, 1 H, Gluα-CH), 6.47 (s, 2 H, 2-NH₂ exch), 6.82 (s, 1 H, 5-H), 7.30, 7.33 (d, 2 H, C₆H₄), 7.79, 7.82 (d, 2 H, C₆H₄), 8.64-8.66 (d, 1 H, CONH exch), 10.86 (1 H, s, 3-NH exch). Anal. calcd. for (C₂₅H₃₀N₄O₆S · 0.2 H₂O): C, 57.94; H, 5.91; N, 10.81; S, 6.19; found: C, 57.81; H, 5.88; N, 10.88; S, 6.06.

Diethyl N-{4-[4- (2-amino-4-oxo-3,4-dihydrothieno[2,3-*d*]pyrimidin-6-yl)butyl]

benzoyl}-L-glutamate (427). Using the General Procedure described above compound **427** (0.134 g, 67.0 %) was obtained as a white solid from **420** (0.13 g, 0.38 mmol); mp 166.8-167.3 °C; R_f 0.64 (MeOH/CHCl₃, 1:6); ¹H NMR (DMSO-*d*₆): δ 1.13-1.20 (m, 6 H, 2COOCH₂CH₃), 1.57-1.62 (m, 4 H, C₆H₄-CH₂CH₂CH₂CH₂), 1.95-2.12 (m, 2 H, Gluβ-CH₂), 2.40-2.45 (t, 2 H, Gluγ-CH₂), 2.65-2.75 (m, 4 H, C₆H₄-CH₂CH₂CH₂CH₂), 4.00-4.13 (m, 4 H, 2COOCH₂CH₃), 4.38-4.45 (m, 1 H, Gluα-CH), 6.46 (s, 2 H, 2-NH₂ exch), 6.79 (s, 1 H, 5-H), 7.35, 7.38 (d, 2 H, C₆H₄), 7.84, 7.87 (d, 2 H, C₆H₄), 8.63-8.65 (d, 1 H, CONH exch), 10.85 (s, 1 H, 3-NH exch). Anal. calcd. for (C₂₆H₃₂N₄O₆S): C, 59.07; H, 6.10; N, 10.60; S, 6.07; found: C, 59.07; H, 6.18; N, 10.47; S, 5.97.

Diethyl N-{4-[5- (2-amino-4-oxo-3,4-dihydrothieno[2,3-*d*]pyrimidin-6-yl)pentyl]

benzoyl}-L-glutamate (428). Using the General Procedure described above compound **428** (0.108 g, 68.7 %) was obtained as a white solid from **421** (0.10 g, 0.29 mmol); mp 144.2-144.8 °C; R_f 0.64 (MeOH/CHCl₃, 1:6); ¹H NMR (DMSO-*d*₆): δ 1.14-1.21 (m, 8 H,

2COOCH₂CH₃ and C₆H₄-CH₂CH₂CH₂CH₂CH₂), 1.57-1.66 (p, 4 H, C₆H₄-CH₂CH₂CH₂CH₂CH₂), 1.93-2.17 (m, 2 H, Gluβ-CH₂), 2.41-2.46 (t, 2 H, Gluγ-CH₂), 2.61-2.72 (p, 4 H, C₆H₄-CH₂CH₂CH₂CH₂CH₂), 4.01-4.14 (m, 4 H, 2COOCH₂CH₃), 4.38-4.46 (m, 1 H, Gluα-CH), 6.46 (s, 2 H, 2-NH₂ exch), 6.79 (s, 1 H, 5-H), 7.29, 7.31 (d, 2 H, C₆H₄), 7.78, 7.80 (d, 2 H, C₆H₄), 8.63, 8.66 (d, 1 H, CONH exch), 10.83 (s, 1 H, 3-NH exch). HRMS (ESI, pos mode) m/z [M + Na]⁺ calcd for C₂₇H₃₄NO₄S, 565.2097; found, 565.2134.

Diethyl N-{4-[6- (2-amino-4-oxo-3,4-dihydrothieno[2,3-*d*]pyrimidin-6-yl)hexyl]benzoyl}-L-glutamate (429). Using the General Procedure described above compound **429** (0.170 g, 80.57 %) was obtained as a white solid from **422** (0.14 g, 0.38 mmol); mp 153.7-154.4 °C; *R_f* 0.64 (MeOH/CHCl₃, 1:6); ¹H NMR (DMSO-*d*₆): δ 1.12-1.19 (m, 6 H, 2COOCH₂CH₃), 1.30-1.32 (m, 4 H, C₆H₄-CH₂CH₂CH₂CH₂CH₂CH₂), 1.54-1.58 (m, 4 H, C₆H₄-CH₂CH₂CH₂CH₂CH₂CH₂), 1.94-2.14 (m, 2 H, Gluβ-CH₂), 2.39-2.44 (t, 2 H, Gluγ-CH₂), 2.58-2.69 (m, 4 H, C₆H₄-CH₂CH₂CH₂CH₂CH₂CH₂), 3.99-4.12 (m, 4 H, 2COOCH₂CH₃), 4.36-4.45 (m, 1 H, Gluα-CH), 6.45 (s, 2 H, 2-NH₂ exch), 6.78 (s, 1 H, 5-H), 7.27, 7.30 (d, 2 H, C₆H₄), 7.77, 7.80 (d, 2 H, C₆H₄), 8.63, 8.65 (d, 1 H, CONH exch), 10.86 (s, 1 H, 3-NH exch). Anal. calcd. for (C₂₈H₃₆N₄O₆S): C, 60.41; H, 6.52; N, 10.06; S, 5.76; found: C, 60.42; H, 6.59; N, 10.07; S, 5.61.

Diethyl N-{4-[7- (2-amino-4-oxo-3,4-dihydrothieno[2,3-*d*]pyrimidin-6-yl)heptyl]benzoyl}-L-glutamate (430). Using the General Procedure described above compound **430** (0.183 g, 66.8 %) was obtained as a semisolid from **423** (0.19 g, 0.48 mmol); *R_f* 0.65 (MeOH/CHCl₃, 1:6); It was used directly in the next step without further characterization.

Diethyl N-{4-[8- (2-amino-4-oxo-3,4-dihydrothieno[2,3-*d*]pyrimidin-6-yl)octyl]

benzoyl}-L-glutamate (431). Using the General Procedure described above compound **431** (0.170 g, 68.20 %) was obtained as a yellow solid from **424** (0.16 g, 0.40 mmol); R_f 0.64 (MeOH/CHCl₃, 1:6); ¹H NMR (DMSO-*d*₆): δ 1.12-1.19 (m, 6 H, 2COOCH₂CH₃), 1.32-1.56 (m, 8 H, C₆H₄-CH₂CH₂CH₂CH₂CH₂CH₂CH₂CH₂), 1.58-1.62 (m, 4 H, C₆H₄-CH₂CH₂CH₂CH₂CH₂CH₂CH₂CH₂), 1.98-2.24 (m, 2 H, Gluβ-CH₂), 2.41-2.45 (t, 2 H, Gluγ-CH₂), 2.59-2.69 (m, 4 H, C₆H₄-CH₂CH₂CH₂CH₂CH₂CH₂CH₂CH₂), 4.01- 4.12 (4 H, m, 2COOCH₂CH₃), 4.38-4.47 (m, 1 H, Gluα-CH), 6.46 (s, 2 H, 2-NH₂ exch), 6.78 (s, 1 H, 5-H), 7.27, 7.29 (d, 2 H, C₆H₄), 7.78, 7.80 (d, 2 H, C₆H₄), 8.63, 8.65 (d, 1 H, CONH exch), 10.83 (s, 1 H, 3-NH exch). HRMS (ESI, pos mode) m/z [M + Na]⁺ calcd for C₃₀H₄₀N₄O₆S, 607.7212; found, 607.7233.

General Procedure for the Synthesis of Compounds 324-330.

To a solution of **425-431** in ethanol (5-10 mL) was added aqueous 1 N NaOH and the reaction mixture stirred at room temperature for 3 h. The ethanol was evaporated under reduced pressure and the residue was dissolved in water (5-10 mL). The solution was cooled to 0 °C and carefully acidified to pH 3 with drop wise addition of 1 N HCl. The resulting suspension was left at 0 °C for 12 h and the residue was collected by filtration. Washed with water (5 mL) and dried over P₂O₅/vacuum at 50 °C to afford the free acids **324-330**.

***N*-{4-[2- (2-Amino-4-oxo-3,4-dihydrothieno[2,3-*d*]pyrimidin-6-yl)ethyl]benzoyl}-L-glutamic acid (324).** Using the General Procedure described above compound **324** (0.064 g, 97.7 %) was obtained from **425** (0.075 g, 0.15 mmol) as a white solid; mp 167.7-168.4 °C; R_f 0.62 (MeOH/CHCl₃, 1:6 + 1 drop of gl. HOAc); ¹H NMR (DMSO-*d*₆): δ 1.89-2.12 (m, 2 H, Gluβ-CH₂), 2.32-2.37 (t, 2 H, Gluγ-CH₂), 2.97-3.04 (m, 4 H,

C₆H₄-CH₂CH₂), 4.34-4.44 (m, 1 H, Glu α -CH), 6.45 (s, 2 H, 2-NH₂ exch), 6.79 (s, 1 H, 5-H), 7.32, 7.36 (d, 2 H, C₆H₄), 7.78, 7.81 (d, 2 H, C₆H₄), 8.51-8.53 (d, 1 H, CONH exch), 10.81 (s, 1 H, 3-NH exch), 12.40 (s, 2 H, 2COOH exch). Anal. calcd. for (C₂₀H₂₀N₄O₆S · 0.5 H₂O): C, 52.97; H, 4.67; N, 12.36; S, 7.07; found: C, 52.92; H, 4.75; N, 12.11; S, 6.82.

***N*-{4-[3- (2-Amino-4-oxo-3,4-dihydrothieno[2,3-*d*]pyrimidin-6-yl)propyl]benzoyl}-L-glutamic acid (325).** Using the General Procedure described above compound **325** (0.071 g, 96.5 %) was obtained from **426** (0.083 g, 0.16 mmol) as a white solid; mp 155.5-156.1 °C; *R_f* 0.62 (MeOH/CHCl₃, 1:6 + 1 drop of HOAc); ¹H NMR (DMSO-*d*₆): δ 1.91-2.10 (m, 4 H, Glu β -CH₂ and C₆H₄-CH₂CH₂CH₂), 2.32-2.36 (t, 2 H, Glu γ -CH₂), 2.66-2.73 (q, 4 H, C₆H₄-CH₂CH₂CH₂), 4.37-4.38 (m, 1 H, Glu α -CH), 6.47 (s, 2 H, 2-NH₂ exch), 6.81 (s, 1 H, 5-H), 7.30, 7.32 (d, 2 H, C₆H₄), 7.79, 7.82 (d, 2 H, C₆H₄), 8.50, 8.53 (d, 1 H, CONH exch), 10.83 (s, 1 H, 3-NH exch), 12.51 (s, 2 H, 2COOH exch). Anal. calcd. for (C₂₁H₂₂N₄O₆S · 0.5 CH₃OH): C, 54.42; H, 5.10; N, 11.81; S, 6.76; found: C, 54.32; H, 5.20; N, 11.0652; S, 6.38.

***N*-{4-[4- (2-Amino-4-oxo-3,4-dihydrothieno[2,3-*d*]pyrimidin-6-yl)butyl]benzoyl}-L-glutamic acid (326).** Using the General Procedure described above compound **326** (0.086 g, 95.8 %) was obtained from **427** (0.10 g, 0.19 mmol) as a yellow solid; mp 154.5-154.9° C; *R_f* 0.64 (MeOH/CHCl₃, 1:6 + 1 drop of HOAc); ¹H NMR (DMSO-*d*₆): δ 1.61-1.62 (m, 4 H, C₆H₄-CH₂CH₂CH₂CH₂), 1.91-2.10 (m, 2 H, Glu β -CH₂), 2.32-2.37 (t, 2 H, Glu γ -CH₂), 2.66-2.73 (q, 4 H, C₆H₄-CH₂CH₂CH₂CH₂), 4.36-4.41 (m, 1 H, Glu α -CH), 6.46 (s, 2 H, 2-NH₂ exch), 6.79 (s, 1 H, 5-H), 7.28, 7.30 (d, 2 H, C₆H₄), 7.78, 7.81

(d, 2 H, C₆H₄), 8.51, 8.54 (d, 1 H, CONH exch), 10.83 (s, 1 H, 3-NH exch), 12.41 (s, 2 H, 2COOH exch). Anal. calcd. for (C₂₂H₂₄N₄O₆S · 0.5 H₂O): C, 54.88; H, 5.23; N, 11.64; S, 6.66; found: C, 55.11; H, 5.10; N, 11.35; S, 6.48.

***N*-{4-[5- (2-Amino-4-oxo-3,4-dihydrothieno[2,3-*d*]pyrimidin-6-yl)pentyl]benzoyl}-L-glutamic acid (327).** Using the General Procedure described above compound **327**

(0.071 g, 97.9 %) was obtained from **428** (0.080 g, 0.15 mmol) as a white solid; mp 132.6-133 °C; *R_f* 0.64 (MeOH/CHCl₃, 1:6 + 1 drop of gl. HOAc); ¹H NMR (DMSO-*d*₆): δ 1.16-1.23 (m, 2 H, C₆H₄-CH₂CH₂CH₂CH₂CH₂), 1.59-1.63 (m, 4 H, C₆H₄-CH₂CH₂CH₂CH₂CH₂), 1.89-2.12 (m, 2 H, Gluβ-CH₂), 2.32-2.37 (t, 2 H, Gluγ-CH₂), 2.59-2.71 (m, 4 H, C₆H₄-CH₂CH₂CH₂CH₂CH₂), 4.37-4.39 (m, 1 H, Gluα-CH), 6.47 (s, 2 H, 2-NH₂ exch), 6.79 (s, 1 H, 5-H), 7.35, 7.37 (d, 2 H, C₆H₄), 7.85, 7.88 (d, 2 H, C₆H₄), 8.56, 8.59 (d, 1 H, CONH exch), 10.83 (s, 1 H, 3-NH exch), 12.47 (s, 2 H, 2COOH exch). Anal. calcd. for (C₂₃H₂₆N₄O₆S · 0.5 C₂H₅OH): C, 56.57; H, 5.74; N, 10.99; S, 6.29; found: C, 56.65; H, 5.57; N, 10.67; S, 6.42.

***N*-{4-[6- (2-Amino-4-oxo-3,4-dihydrothieno[2,3-*d*]pyrimidin-6-yl)hexyl]benzoyl}-L-glutamic acid (328).** Using the General Procedure described above compound **328**

(0.086 g, 98.6 %) was obtained from **429** (0.098 g, 0.17 mmol) as a solid; mp 139.7-141.1 °C; *R_f* 0.64 (MeOH/CHCl₃, 1:6 + 1 drop of gl. HOAc); ¹H NMR (DMSO-*d*₆): δ 1.32 (s, 4 H, C₆H₄-CH₂CH₂CH₂CH₂CH₂CH₂), 1.57 (s, 4 H, C₆H₄-CH₂CH₂CH₂CH₂CH₂CH₂), 1.93-2.09 (m, 2 H, Gluβ-CH₂), 2.33-2.35 (m, 2 H, Gluγ-CH₂), 2.62-2.68 (m, 4 H, C₆H₄-CH₂CH₂CH₂CH₂CH₂CH₂), 4.38-4.39 (m, 1 H, Gluα-CH), 6.47 (s, 2 H, 2-NH₂ exch), 6.78 (s, 1 H, 5-H), 7.35, 7.37 (d, 2 H, C₆H₄), 7.85, 7.87 (d, 2

H, C₆H₄), 8.57, 8.60 (d, 1 H, CONH exch), 10.85 (s, 1 H, 3-NH exch), 12.40 (s, 2 H, 2COOH exch). Anal. calcd. for (C₂₄H₂₈N₄O₆S · 0.4 H₂O): C, 56.77; H, 5.72; N, 11.03; S, 6.32; found: C, 57.03; H, 5.63; N, 10.71; S, 6.15.

***N*-{4-[7- (2-Amino-4-oxo-3,4-dihydrothieno[2,3-*d*]pyrimidin-6-yl)heptyl]benzoyl}-L-glutamic acid (329).** Using the General Procedure described above compound **329**

(0.287 g, 97.9 %) was obtained from **430** (0.326 g, 0.57 mmol) as a yellow solid; mp 134.9-135.5 °C; *R_f* 0.64 (MeOH/CHCl₃, 1:6 + 1 drop of gl. HOAc); ¹H NMR (DMSO-*d*₆): δ 1.35 (m, 6 H, C₆H₄-CH₂ CH₂CH₂CH₂CH₂CH₂CH₂), 1.59 (s, 4 H, C₆H₄-CH₂CH₂CH₂CH₂CH₂CH₂CH₂CH₂), 1.90-2.08 (m, 2 H, Gluβ-CH₂), 2.32-2.35 (m, 2 H, Gluγ-CH₂), 2.59-2.68 (m, 4 H, C₆H₄-CH₂CH₂CH₂CH₂CH₂CH₂CH₂), 4.36-4.40 (m, 1 H, Gluα-CH), 6.44 (s, 2 H, 2-NH₂ exch), 6.77 (s, 1 H, 5-H), 7.26, 7.28 (d, 2 H, C₆H₄), 7.77, 7.79 (d, 2 H, C₆H₄), 8.50, 8.51 (d, 1 H, CONH exch), 10.82 (s, 1 H, 3-NH exch), 12.38 (s, 2 H, 2COOH exch). Anal. calcd. for (C₂₅H₃₀N₄O₆S · 0.5 H₂O): C, 57.35; H, 5.97; N, 10.70; S, 6.12; found: C, 56.97; H, 6.07; N, 10.57; S, 6.03.

***N*-{4-[8- (2-Amino-4-oxo-3,4-dihydrothieno[2,3-*d*]pyrimidin-6-yl)octyl]benzoyl}-L-glutamic acid (330).** Using the General Procedure described above compound **330**

(0.087 g, 97.6 %) was obtained from **431** (0.1 g, 0.17 mmol) as a brown solid; mp 122.2-123 °C; *R_f* 0.66 (MeOH/CHCl₃, 1:6 + 1 drop of gl. HOAc); ¹H NMR (DMSO-*d*₆): δ 1.38 (m, 8 H, C₆H₄-CH₂CH₂CH₂CH₂CH₂CH₂CH₂CH₂CH₂), 1.57 (s, 4 H, C₆H₄-CH₂CH₂CH₂CH₂CH₂CH₂CH₂CH₂), 1.92-2.11 (m, 2 H, Gluβ-CH₂), 2.32-2.35 (m, 2 H, Gluγ-CH₂), 2.59-2.68 (m, 4 H, C₆H₄-CH₂CH₂CH₂CH₂CH₂CH₂CH₂CH₂), 4.35-4.39 (m, 1 H, Gluα-CH), 6.44 (s, 2 H, 2-NH₂ exch), 6.77 (s, 1 H, 5-H), 7.26, 7.28 (d, 2 H, C₆H₄),

7.77, 7.79 (d, 2 H, C₆H₄), 8.50-8.51 (d, 1 H, CONH exch), 10.81 (s, 1 H, 3-NH exch), 12.80 (s, 2 H, 2COOH exch). Anal. calcd. for (C₂₆H₃₂N₄O₆S · 0.6 H₂O): C, 57.89; H, 6.20; N, 10.38; S, 5.94; found: C, 57.64; H, 6.15; N, 10.35; S, 6.14.

Methyl 5-bromothiophene-2-carboxylate (439). Thionyl chloride (2.64 g, 1.6 mL, 22 mmol) was added dropwise to a stirred solution of **408** (2.07 g, 10 mmol) in MeOH (20 mL) while maintaining the internal temperature below 12 °C. When addition was complete the mixture was left to stand at room temperature for 12h to obtain white solid. And the filtrate was concentrated under reduced pressure to afford white solid. The solid was washed with hexane and ethyl ether to afford **13** (2.05 g, 93%) as white solid; mp 59.5-61.0 °C; *R_f* 0.55 (hexane/EtOAc 3:1); ¹H NMR (DMSO-*d*₆) δ 3.80 (s, 3 H), 7.36, 7.37 (d, 1 H), 7.63, 7.64 (d, 1 H).

Methyl 5-(6-hydroxyhex-1-yn-1-yl)thiophene-2-carboxylate (451). A mixture of **439** (0.66 g, 3 mmol), hex-5-yn-1-ol (0.323 g, 3.3 mmol), PdCl₂ (0.033 g), PPh₃ (0.132 g), CuI (0.033 g), NEt₃ (15 mL) and CH₃CN (2.5 mL) was irradiated to 100 °C for 10 min under microwave. The reaction mixture was then made in to plug and loaded on a silica gel column and eluted with hexane/EtOAc 3:1 to afford **451** (1.19 g, 83%) as a colorless liquid: *R_f* 0.21 (hexane/EtOAc 2:1); ¹H NMR (DMSO-*d*₆) δ 1.54 (m, 4 H), 2.48 (m, 2 H), 3.39-3.42 (t, 2 H), 3.80 (s, 3 H), 7.25, 7.26 (d, 1 H), 7.69, 7.70 (d, 1 H).

Methyl 5-(6-oxohex-1-yn-1-yl)thiophene-2-carboxylate (452). A solution of CH₂Cl₂ (8 mL) and oxalyl chloride (0.31 g, 3.3 mmol) was placed in a 50 mL 3-neck round bottom flask with an ballon and two dropping funnels containing DMSO (0.51 mL) dissolved in CH₂Cl₂ (2 mL) and **451**(0.716 g, 3 mmol) in CH₂Cl₂ (4 mL). The DMSO was added to the stirred oxalyl chloride solution at -60°C. The reaction mixture was stirred for 2 min

and **451** was added within 5 min. Stirring was continued for an additional 15 min. NEt_3 (2.3 mL) was added and the reaction mixture was stirred for 5 min and then allowed to warm to room temperature. CH_2Cl_2 (10 mL) was added to the reaction mixture and then washed with H_2O (3 mL) for 3 times. The organic layer was then dried over anhydrous Na_2SO_4 to give **452** (0.62 g, 87%) as a colorless liquid; R_f 0.16 (hexane/EtOAc 3:1); ^1H NMR ($\text{DMSO}-d_6$) δ 1.79-1.84 (p, 2 H), 2.51-2.55 (t, 2 H), 2.57-2.60 (t, 2 H), 3.82 (s, 3 H), 7.28, 7.29 (d, 1 H), 7.71, 7.72 (d, 1 H), 9.70-9.71 (t, 1 H, CHO). This compound was used directly for next step of reaction without further characterization.

Methyl 5-{4-[5-amino-4-(ethoxycarbonyl)thiophen-2-yl]but-1-yn-1-yl}thiophene-2-carboxylate (453). A mixture of **452** (0.78 g, 3.3 mmol), sulfur (0.11 g, 3.3 mmol), ethyl cyanoacetate (0.37 g, 3.3 mmol) and EtOH (20 mL) were placed in a round bottom flask and warmed to 45 °C and treated dropwise with morpholine (0.29 g, 3.3 mmol) over 15 min. The mixture was stirred for 4 h at 45 °C and 24 h at room temperature. Unreacted sulfur was removed by filtration, and the filtrate was concentrated under reduced pressure to afford an orange oil. The residue was loaded on a silica gel column packed with silica gel and eluted with 10% ethyl acetate in hexane to afford **453** (0.48 g, 40%) of as a orange liquid; R_f 0.38 (hexane/EtOAc 3:1); ^1H NMR ($\text{DMSO}-d_6$) δ 1.21-1.24 (t, 3 H), 2.68-2.72 (t, 2 H), 2.79-2.82 (t, 2 H), 3.81 (s, 3 H, COOCH_3), 4.11-4.17 (q, 2 H), 6.64 (s, 1 H), 7.16 (s, 2 H, 2- NH_2 exch), 7.25, 7.26 (d, 1 H), 7.70, 7.71 (d, 1 H).

Methyl 5-[4-(2-amino-4-oxo-3,4-dihydrothieno[2,3-*d*]pyrimidin-6-yl)but-1-yn-1-yl]thiophene-2-carboxylate (454). A mixture of **453** (0.4 g, 1.1 mmol) and chloroformamide hydrochloride (0.5 g, 4.4 mmol) in DMSO_2 (2 g, 2.04 mmol) was heated at 150 °C for 2 h. The mixture was cooled to room temperature and water (10 mL)

was added. Then ammonium hydroxide was used to neutralize the suspension. The brown solid, obtained by filtration, was washed with water and dried over P₂O₅ vacuum. The solid was dissolved in methanol and silica gel was added. The plug was loaded on to a silica gel column and eluted with 5% methanol in chloroform to afford **454** (0.2g, 52%) as a brown solid; mp > 300 °C; *R_f* 0.32 (MeOH/CHCl₃ 1:6); ¹H NMR (DMSO-*d*₆) δ 2.66-2.72 (m, 2 H), 2.79-2.82 (m, 2 H), 3.81 (s, 3 H), 6.46 (s, 2 H, 2-NH₂ exch), 7.20, 7.21 (d, 1 H), 7.62, 7.63 (d, 1 H), 7.7 (s, 1 H), 10.83 (s, 1 H, 3-NH exch). This compound was used directly for next step of reaction without further characterization.

5-[4-(2-Amino-4-oxo-3,4-dihydrothieno[2,3-*d*]pyrimidin-6-yl)but-1-yn-1-yl]thiophene-2-carboxylic acid (455). To a solution of **454** (0.16 g, 0.44 mmol) in ethanol (16 mL) was added aqueous 1 N NaOH (8 mL) and the reaction mixture stirred at room temperature for 12 h. The ethanol was evaporated under reduced pressure and the residue was dissolved in water (5 mL). The solution was carefully acidified to pH 3 with the drop wise addition of 1 N HCl. The resulting suspension was left at 0 °C for an hour and then the residue was collected by filtration, washed with water (5 mL) and dried over P₂O₅/vacuum at 50 °C to afford **455** (0.142 g, 94 %) as a brown solid; mp >300 °C; *R_f* 0.43 (MeOH/CHCl₃, 1:6+ 1 drop of HOAc); ¹H NMR (DMSO-*d*₆) δ 2.68-2.75 (m, 2 H), 2.80-2.82 (m, 2 H), 6.47 (s, 2 H, 2-NH₂ exch), 7.20, 7.21 (d, 1 H), 7.62, 7.63 (d, 1 H), 7.7 (s, 1 H), 10.85 (s, 1 H, 3-NH exch), 13.19 (s, 1 H, COOH exch). This compound was used directly for next step of reaction without further characterization.

Diethyl *N*-({5-[4-(2-amino-4-oxo-3,4-dihydrothieno[2,3-*d*]pyrimidin-6-yl)but-1-yn-1-yl]thiophen-2-yl}carbonyl)-*L*-glutamate (456). To a solution of **455** (0.13 g, 0.38 mmol) in anhydrous DMF (15 mL) was added *N*-methylmorpholine (0.045 g, 0.45 mmol)

and 2-chloro-4,6-dimethoxy-1,3,5-triazine (0.079 g, 0.45 mmol). The resulting mixture was stirred at room temperature for 2 h. N-methylmorpholine (0.045 g, 0.45 mmol) and diethyl-L- glutamate hydrochloride (0.09 g, 0.376 mmol) were added to the mixture. The reaction mixture was stirred for an additional 3 h at room temperature and silica gel was added to this solution and the suspension evaporated under reduced pressure. The plug obtained was loaded on a silica gel column and eluted with 2% methanol in chloroform and **456** (0.155 g, 78 %) was obtained as a brown solid; mp 187.6-188.8 °C; R_f 0.31 (MeOH/CHCl₃, 1:6); ¹H NMR (DMSO-*d*₆) δ 1.13-1.19 (t, 6 H), 1.95-2.23 (m, 2 H Gluβ-CH₂), 2.40-2.44 (t, 2 H, Gluγ-CH₂), 2.65-2.72 (m, 2 H), 3.02-3.05 (m, 2 H), 4.01--4.13 (m, 4 H), 4.41 (m, 1 H, Gluα-CH), 6.48 (s, 2 H, 2-NH₂ exch), 6.86, 6.88 (d, 1 H), 7.38, 7.40 (d, 1 H), 7.78, 7.79(d, 1 H), 8. 63, 8.71 (d, 1 H, CONH exch), 10.89 (s, 1 H, 3-NH exch).

***N*-({5-[4-(2-amino-4-oxo-3,4-dihydrothieno[2,3-*d*]pyrimidin-6-yl)but-1-yn-1-yl]thiophen-2-yl}carbonyl)-L-glutamic acid (**457**)**. To a solution of **456** in ethanol (8 mL) was added aqueous 1 N NaOH (4 mL) and the reaction mixture stirred at room temperature for 3 h. The ethanol was evaporated under reduced pressure and the residue was dissolved in water (5 mL). The solution was cooled to 0 °C and carefully acidified to pH 3 with drop wise addition of 1 N HCl. The resulting suspension was left at 0 °C for 2 h and the residue was collected by filtration. Washed with water (5 mL) and dried over P₂O₅/vacuum at 50 °C to afford **457** (0.083 g, 92%) as light yellow solid; mp 158.9-161.1 °C; R_f 0.29 (MeOH/CHCl₃, 1:6+ 1 drop of gl. HOAc); ¹H NMR (DMSO-*d*₆) δ 1.89-2.13 (m, 2 H Gluβ-CH₂), 2.31-2.35 (t, 2 H, Gluγ-CH₂), 2.62-2.72 (m, 2 H), 3.02-3.05 (m, 2 H), 4.34 (1 H, m, Gluα-CH), 6.46 (s, 2 H, 2-NH₂ exch), 6.86-6.88(d, 1 H), 7.24, 7.25 (d, 1 H),

7.78, 7.79 (d, 1 H), 8.62, 8.71 (d, 1 H, CONH exch), 10.83 (s, 1 H, 3-NH exch), 12.52 (s, 2H, COOH exch); HRMS (ESI, pos mode) m/z $[M + H]^+$ calcd for $C_{20}H_{18}N_4O_6S_2$, 475.0668; found, 475.0757.

Methyl 5-(6-hydroxyhexyl)thiophene-2-carboxylate (458). To a Parr hydrogenation bottle was added **451** (0.714 g, 3 mmol), 10% Pd/C (0.07 g) and MeOH (30 mL).

Hydrogenation was carried out at 55 psi for 24 h. After filtration, the organic phase was evaporated at vacuum to afford **458** (0.662 g, 92%) as a colorless liquid; R_f 0.11

(hexane/EtOAc 3:1); 1H NMR (DMSO- d_6) δ 1.27-1.31 (m, 4 H), 1.38 (m, 2 H), 1.61 (m, 2 H), 2.79-2.83 (t, 2 H), 3.34-3.37 (t, 3 H), 3.77 (s, 3 H), 6.93, 6.95 (d, 1 H), 7.62, 7.63 (d, 1 H). This compound was used directly for next step of reaction without further characterization.

Methyl 5-(6-oxohexyl)thiophene-2-carboxylate(459). A solution of CH_2Cl_2 (8 mL) and oxalyl chloride (0.31 g, 3.3 mmol) was placed in a 50 mL 3-neck round bottom flask with an ballon and two dropping funnels containing DMSO (0.51 mL) dissolved in CH_2Cl_2 (2 mL) and **458** (0.728 g, 3 mmol) in CH_2Cl_2 (4 mL). The DMSO was added to the stirred oxalyl chloride solution at $-60^\circ C$. The reaction mixture was stirred for 2 min and **458** was added within 5 min. Stirring was continued for an additional 15 min. NEt_3 (2.3 mL) was added and the reaction mixture was stirred for 5 min and the allowed to warm to room temperature. CH_2Cl_2 (10 mL) was added to the reaction mixture and then washed with H_2O (3 mL) for 3 times. The organic layer was then dried over anhydrous Na_2SO_4 to give **459** (0.605 g, 83%) as a colorless liquid; R_f 0.2 (hexane/EtOAc 3:1); 1H NMR (DMSO- d_6) δ 1.27-1.32 (m, 2 H), 1.49-1.53 (t, 2 H), 1.59-1.65 (t, 2 H), 2.39-2.43 (t, 2 H), 2.79-2.83 (t, 2 H), 3.77 (s, 3 H), 6.94, 6.95 (d, 1 H), 7.62, 7.63 (d, 1 H), 9.63 (t, 1 H, CHO).

This compound was used directly for next step of reaction without further characterization.

Methyl 5-{4-[5-amino-4-(ethoxycarbonyl)-2-thienyl]butyl}thiophene-2-carboxylate (460). A mixture of **459** (0.8g, 3.3 mmol), sulfur (0.11 g, 3.3 mmol), ethyl cyanoacetate (0.38 g, 3.3 mmol) and EtOH (20 mL) were placed in a round bottom flask and warmed to 45 °C and treated dropwise with morpholine (0.29 g, 3.3 mmol) over 15 min. The mixture was stirred for 4 h at 45 °C and 24 h at room temperature. Unreacted sulfur was removed by filtration, and the filtrate was concentrated under reduced pressure to afford an orange oil. The residue was loaded on a silica gel column packed with silica gel and eluted with 10% ethyl acetate in hexane to afford **460** (0.77 g, 63%) as a orange liquid; R_f 0.35 (hexane/EtOAc 3:1); $^1\text{H NMR}$ (DMSO- d_6) δ 1.20-1.24 (t, 3 H), 1.49-1.56 (m, 2 H), 1.60-1.67 (m, 2 H), 2.52-2.56 (t, 2 H), 2.83-2.86 (t, 2 H), 3.77 (s, 3 H), 4.10-4.15 (q, 2 H), 6.49 (s, 1 H), 6.94, 6.95 (d, 1 H), 7.10 (s, 2 H, 2-NH₂ exch), 7.62, 7.63 (d, 1 H). This compound was used directly for next step of reaction without further characterization.

Methyl 5-[4-(2-amino-4-oxo-3,4-dihydrothieno[2,3-*d*]pyrimidin-6-yl)butyl]thiophene-2-carboxylate (461). A mixture of **460** (0.69 g, 1.87 mmol) and chloroformamide hydrochloride (0.86 g, 7.49 mmol) in DMSO₂ (4 g, 4.08 mmol) was heated at 150 °C for 2 h. The mixture was cooled to room temperature and water (10 mL) was added. Then ammonium hydroxide was used to neutralize the suspension. The brown solid, obtained by filtration, was washed with water and dried over P₂O₅ vacuum. The solid was dissolved in methanol and silica gel was added. The plug was loaded on to a silica gel column and eluted with 5% methanol in chloroform to afford **461** (0.58 g ,

85%) as a yellow solid; mp > 300 °C; R_f 0.30 (MeOH/CHCl₃, 1:6); ¹H NMR (DMSO-*d*₆) δ 1.59-1.68 (m, 4 H), 2.70-2.74 (t, 2 H), 2.85-2.88 (t, 2 H), 3.77 (s, 3 H), 6.45 (s, 2 H, 2-NH₂ exch), 6.79 (s, 1 H), 6.95, 6.96 (d, 1 H), 7.62, 7.63 (d, 1 H), 10.82 (s, 1 H, 3-NH exch). This compound was used directly for next step of reaction without further characterization.

5-[4-(2-Amino-4-oxo-3,4-dihydrothieno[2,3-*d*]pyrimidin-6-yl)butyl]thiophene-2-carboxylic acid (462). To a solution of **461** (0.41 g, 1.13 mmol) in ethanol (40 mL) was added aqueous 1 N NaOH (20 mL) and the reaction mixture stirred at room temperature for 12 h. The ethanol was evaporated under reduced pressure and the residue was dissolved in water (15 mL). The solution was carefully acidified to pH 3 with the drop wise addition of 1 N HCl. The resulting suspension was left at 0 °C for an hour and then the residue was collected by filtration, washed with water (15 mL) and dried over P₂O₅/vacuum at 50 °C to afford **462** (0.38 g, 97 %) as a yellow solid; mp >300 °C; R_f 0.35 (MeOH/CHCl₃, 1:6+ 1 drop of gl. HOAc); ¹H NMR (DMSO-*d*₆) δ 1.64 (m, 4 H), 2.71-2.74 (t, 2 H), 2.83-2.86 (t, 2 H), 6.45 (s, 2 H, 2-NH₂ exch), 6.79 (s, 1 H), 6.90, 6.91 (d, 1 H), 7.53, 7.54 (d, 1 H), 10.83 (s, 1 H, 3-NH exch), 12.84 (s, 1 H, COOH exch). This compound was used directly for next step of reaction without further characterization.

Diethyl N-({5-[4-(2-amino-4-oxo-3,4-dihydrothieno[2,3-*d*]pyrimidin-6-yl)butyl]thiophen-2-yl}carbonyl)-L-glutamate (463). To a solution of **462** (0.34 g, 0.97 mmol) in anhydrous DMF (20 mL) was added N-methylmorpholine (0.12 g, 1.16 mmol) and 2-chloro-4,6-dimethoxy-1,3,5-triazine (0.20 g, 1.16 mmol). The resulting mixture was stirred at room temperature for 2 h. N-methylmorpholine (0.045 g, 0.45 mmol) and diethyl-L- glutamate hydrochloride (0.23 g, 0.97mmol) were added to the mixture. The

reaction mixture was stirred for an additional 3 h at room temperature and silica gel was added to this solution and the suspension evaporated under reduced pressure. The plug obtained was loaded on a silica gel column and eluted with 2% methanol in chloroform and **463** (0.388 g, 75 %) was obtained as a light yellow solid; mp 155.7-156.6 °C; R_f 0.33 (MeOH/CHCl₃, 1:6); ¹H NMR (DMSO-*d*₆) δ 1.13-1.19 (t, 6 H), 1.64 (m, 4 H), 1.93-2.13 (m, 2 H Gluβ-CH₂), 2.38-2.42 (t, 2 H, Gluγ-CH₂), 2.71-2.74 (t, 2 H), 2.81-2.84 (t, 2 H), 4.01--4.13 (m, 4 H), 4.33-4.39 (m, 1 H, Gluα-CH), 6.44 (s, 2 H, 2-NH₂ exch), 6.79(s, 1 H), 6.87, 6.88 (d, 1 H), 7.66, 7.67 (d, 1 H), 8.59, 8.61 (d, 1H, CONH exch), 10.81 (s, 1 H, 3-NH exch). This compound was used directly for next step of reaction without further characterization.

***N*-({5-[4-(2-amino-4-oxo-3,4-dihydrothieno[2,3-*d*]pyrimidin-6-yl)butyl]thiophen-2-yl}carbonyl)-L-glutamic acid (333)**. To a solution of **463** (0.52 g, 0.97 mmol) in ethanol (40 mL) was added aqueous 1 N NaOH (20 mL) and the reaction mixture stirred at room temperature for 3 h. The ethanol was evaporated under reduced pressure and the residue was dissolved in water (15 mL). The solution was cooled to 0 °C and carefully acidified to pH 3 with drop wise addition of 1 N HCl. The resulting suspension was left at 0 °C for 2 h and the residue was collected by filtration. Washed with water (15 mL) and dried over P₂O₅/vacuum at 50 °C to afford **333** (0.43 g, 94%) as white solid; mp 116.4-117.8 °C; R_f 0.25 (MeOH/CHCl₃, 1:6+ 1 drop of gl. HOAc); ¹H NMR (DMSO-*d*₆) δ 1.64 (m, 4 H), 1.85-2.07 (m, 2 H Gluβ-CH₂), 2.30-2.34 (t, 2 H, Gluγ-CH₂), 2.71-2.74 (t, 2 H), 2.81-2.84 (t, 2 H), 4.31 (1 H, m, Gluα-CH), 6.41 (s, 2 H, 2-NH₂ exch), 6.79 (s, 1 H), 6.87, 6.88 (d, 1 H), 7.66, 7.67 (d, 1 H), 8.47, 8.49 (d, 1 H, CONH exch), 10.82 (s, 1 H, 3-NH

exch), 12.44 (s, 2H, COOH exch); Anal. calcd. for (C₂₀H₂₂N₄S₂O₆ · 1.2 H₂O): C, 48.03; H, 4.92; N, 11.20; S, 12.82; found: C, 47.76; H, 4.92; N, 11.20; S, 12.82.

General Procedure for the Synthesis of Compounds 335-338.

To a solution of **464** (0.1 mmol) in anhydrous DMF (5-10 mL) was added N-methylmorpholine (0.12 mmol) and 2-chloro-4,6-dimethoxy-1,3,5-triazine (0.12 mmol). The resulting mixture was stirred at room temperature for 2 h. N-methylmorpholine (0.12 mmol) and amines (0.1 mmol) were added to the mixture. The reaction mixture was stirred for an additional 3 h at room temperature and silica gel was added to this solution and the suspension evaporated under reduced pressure. The plug obtained was loaded on a silica gel column and eluted with 2% methanol in chloroform. The fractions containing the desired product (TLC) were pooled and evaporated to afford the appropriate esters. To a solution of esters in ethanol (5-10 mL) was added aqueous 1 N NaOH and the reaction mixture stirred at room temperature for 3 h. The ethanol was evaporated under reduced pressure and the residue was dissolved in water (5-10 mL). The solution was cooled to 0 °C and carefully acidified to pH 3 with drop wise addition of 1 N HCl. The resulting suspension was left at 0 °C for 12 h and the residue was collected by filtration. Washed with water (5 mL) and dried over P₂O₅/vacuum at 50 °C to afford the free acids **335-338**.

(2S)-2-({4-[4-(2-Amino-4-oxo-3,4-dihydrothieno[2,3-*d*]pyrimidin-6-yl)butyl]benzoyl}amino)butanoic acid (335). Using the General Procedure described above compound **335** (0.04 g, 67.9 %) was obtained as a light yellow solid; mp 164.4-165.3 °C; *R_f* 0.39 (MeOH/CHCl₃, 1:6 + 1 drop of gl. HOAc); ¹H NMR (DMSO-*d*₆): δ 0.93-0.97 (t, 3 H, γ-CH₃), 1.61-1.63 (m, 4 H, C₆H₄-CH₂CH₂CH₂CH₂), 1.73-1.93 (m, 2 H, β-CH₂), 2.66-2.76

(m, 4 H, C₆H₄-CH₂CH₂CH₂CH₂), 4.25-4.31 (m, 1 H, α-CH), 6.46 (s, 2 H, 2-NH₂ exch), 6.80 (s, 1 H, 5-H), 7.29, 7.31 (d, 2 H, C₆H₄), 7.80, 7.82 (d, 2 H, C₆H₄), 8.46, 8.48 (d, 1 H, CONH exch), 10.83 (s, 1 H, 3-NH exch), 12.53 (s, 1 H, COOH exch). Anal. calcd. for (C₂₁H₂₄N₄O₄S · 0.5 H₂O): C, 57.65; H, 5.76; N, 12.81; S, 7.33; found: C, 57.72; H, 5.70; N, 12.54; S, 7.13.

***N*-{4-[4-(2-Amino-4-oxo-3,4-dihydrothieno[2,3-*d*]pyrimidin-6-yl)butyl]benzoyl}**

norvaline (336). Using the General Procedure described above compound **336** (0.072 g, 63.3 %) was obtained as a light yellow solid; mp 139.7-141.5 °C; *R_f* 0.40 (MeOH/CHCl₃, 1:6 + 1 drop of gl. HOAc); ¹H NMR (DMSO-*d*₆): δ 0.88-0.92 (t, 3 H, δ-CH₃), 1.35-1.44 (m, 2 H, γ-CH₂), 1.61-1.65 (m, 4 H, C₆H₄-CH₂CH₂CH₂CH₂), 1.74-1.80 (q, 2 H, β-CH₂), 2.66-2.69 (t, 2 H, C₆H₄-CH₂CH₂CH₂CH₂), 2.72-2.75 (t, 2 H, C₆H₄-CH₂CH₂CH₂CH₂), 4.34-4.39 (m, 1 H, α-CH), 6.47 (s, 2 H, 2-NH₂ exch), 6.80 (s, 1 H, 5-H), 7.28, 7.30 (d, 2 H, C₆H₄), 7.80, 7.82 (d, 2 H, C₆H₄), 8.47, 8.49 (d, 1 H, CONH exch), 10.84 (s, 1 H, 3-NH exch), 12.55 (s, 1 H, COOH exch). Anal. calcd. for (C₂₂H₂₆N₄O₄S · 0.5 H₂O): C, 58.52; H, 6.03; N, 12.41; S, 7.10; found: C, 58.12; H, 5.87; N, 12.25; S, 6.95.

3-({4-[4-(2-Amino-4-oxo-3,4-dihydrothieno[2,3-*d*]pyrimidin-6-yl)butyl]benzoyl}

amino)butanoic acid (337). Using the General Procedure described above compound **337** (0.062 g, 65.5 %) was obtained as a yellow solid; mp 180.1-181.8 °C; *R_f* 0.40 (MeOH/CHCl₃, 1:6 + 1 drop of gl. HOAc); ¹H NMR (DMSO-*d*₆): δ 1.16-1.18 (d, 3 H, α-CH₃), 1.60-1.62 (m, 4 H, C₆H₄-CH₂CH₂CH₂CH₂), 2.36-2.42 (q, 1 H, β-CH), 2.54-2.60 (q, 1 H, β-CH), 2.64-2.67 (t, 2 H, C₆H₄-CH₂CH₂CH₂CH₂), 2.71-2.74 (t, 2 H, C₆H₄-CH₂CH₂CH₂CH₂), 4.29-4.36 (m, 1 H, α-CH), 6.47 (s, 2 H, 2-NH₂ exch), 6.79 (s, 1 H, 5-H), 7.26, 7.28 (d, 2 H, C₆H₄), 7.73, 7.75 (d, 2 H, C₆H₄), 8.20, 8.22 (d, 1 H, CONH exch),

10.84 (s, 1 H, 3-NH exch), 12.16 (s, 1 H, COOH exch). Anal. calcd. for (C₂₁H₂₄N₄O₄S · 0.4 H₂O): C, 57.89; H, 5.74; N, 12.86; S, 7.36; found: C, 57.89; H, 5.56; N, 12.64; S, 7.20.

4-({4-[4-(2-Amino-4-oxo-3,4-dihydrothieno[2,3-*d*]pyrimidin-6-yl)butyl]benzoyl}amino)butanoic acid (338). Using the General Procedure described above compound **338** (0.063 g, 66.7 %) was obtained as a yellow solid; mp 250.4-251.6 °C; *R_f* 0.31 (MeOH/CHCl₃, 1:6 + 1 drop of gl. HOAc); ¹H NMR (DMSO-*d*₆): δ 1.60-1.62 (m, 4 H, C₆H₄-CH₂CH₂CH₂CH₂), 1.71-1.78 (p, 2 H, β-CH₂), 2.25-2.29 (t, 1 H, γ-CH₂), 2.64-2.67 (t, 2 H, C₆H₄-CH₂CH₂CH₂CH₂), 2.72-2.75 (t, 2 H, C₆H₄-CH₂CH₂CH₂CH₂), 3.23-3.28 (q, 2 H, α-CH₂), 6.47 (s, 2 H, 2-NH₂ exch), 6.80 (s, 1 H, 5-H), 7.26, 7.28 (d, 2 H, C₆H₄), 7.74, 7.76 (d, 2 H, C₆H₄), 8.38-8.41 (t, 1 H, CONH exch), 10.84 (s, 1 H, 3-NH exch), 12.05 (s, 1 H, COOH exch). Anal. calcd. for (C₂₁H₂₄N₄O₄S · 0.8 C₂H₅OH): C, 58.33; H, 6.24; N, 12.04; S, 6.89; found: C, 58.49; H, 5.98; N, 11.83; S, 6.68.

2-Methylthieno[3,2-*d*]pyrimidin-4(3H)-one (467). To a stirred solution of **466** (1.57 g, 10 mmol) in CH₃CN (20 mL), HCl gas was bulbed and the mixture was allowed to stir at room temperature for 2h. Some white solid was precipitated and was collected by filtration, and the filtrate was concentrated under reduced pressure to afford white solid. White solid was recrystallized in methanol and **467** (0.8 g, 50%) was obtained; mp 236.4-236.7 °C; *R_f* 0.33 (MeOH/CHCl₃, 1:10); ¹H NMR (DMSO-*d*₆) δ 2.37 (s, 3 H, 2-CH₃), 7.30, 7.31(d, 1 H), 8.12, 8.14 (d, 1 H), 12.38 (s, 1 H, 3-NH exch).

4-Chloro-2-methylthieno[3,2-*d*]pyrimidine (468) A stirred mixture of **467** (0.6 g, 3.6 mmol) and POCl₃ (10 mL) was refluxed for 2 h. Then solvent was removed under reduced pressure to afford brown residue. The residue was loaded on a silica gel column

packed with silica gel and eluted with 25% ethyl acetate in hexane to afford **468** (0.5 g, 76%) as white powder; mp 81-81.4 °C; R_f 0.56 (hexane/EtOAc 1:1); $^1\text{H NMR}$ (DMSO- d_6) δ 2.37 (s, 3 H, 2-CH₃), 7.30, 7.31 (d, 1 H), 8.13, 8.14 (d, 1 H). This compound was used directly for next step of reaction without further characterization.

***N*-(4-Methoxyphenyl)-*N*,2-dimethylthieno[3,2-*d*]pyrimidin-4-amine (342)** A mixture of **468** (0.184 g, 1 mmol), 4-methoxy-*N*-methylaniline (0.15 g, 1.1 mmol) and *n*-BuOH (7 mL) was refluxed. After completion of the reaction, as indicated by TLC, the reaction solvent was removed under reduced pressure. The residue was loaded on a silica gel column packed with silica gel and eluted with 25% ethyl acetate in hexane to afford **342** (0.23 g, 81%) as light brown powder; mp 137.5-137.9 °C; R_f 0.56 (hexane/EtOAc 1:1); $^1\text{H NMR}$ (DMSO- d_6) δ 2.54 (s, 3 H, 2-CH₃), 3.49 (s, 3 H, OCH₃), 3.84 (s, 3 H, N-CH₃), 7.04, 7.06 (d, 2 H, C₆H₄), 7.18, 7.19 (d, 1 H), 7.37, 7.39 (d, 2 H, C₆H₄), 7.85, 7.86 (d, 1 H). Anal. calcd. for (C₁₅H₁₅N₃SO•0.2 H₂O): C, 62.35; H, 5.37; N, 14.54; S, 11.10; found: C, 62.48; H, 5.37; N, 14.47; S, 11.25.

***N*-(4-Methoxyphenyl)-2-methylthieno[3,2-*d*]pyrimidin-4-amine (343)** A mixture of **468** (0.184 g, 1 mmol), 4-methoxyaniline (0.12 g, 1.1 mmol) and *n*-BuOH (7 mL) was refluxed. After completion of the reaction, as indicated by TLC, the reaction solvent was removed under reduced pressure. The residue was loaded on a silica gel column packed with silica gel and eluted with 25% ethyl acetate in hexane to afford **343** (0.22 g, 82%) as light brown powder; mp 117.8-118.2 °C; R_f 0.50 (hexane/EtOAc 1:1); $^1\text{H NMR}$ (DMSO- d_6) δ 2.49 (s, 3 H, 2-CH₃), 3.78 (s, 3 H, OCH₃), 6.95, 6.97 (d, 2 H, C₆H₄), 7.32, 7.33 (d, 1 H), 7.60, 7.62 (d, 2 H, C₆H₄), 8.10, 8.12 (d, 1 H), 9.52 (s, 1 H, NH exch). Anal. calcd. for

(C₁₄H₁₃N₃SO•0.2 C₆H₁₄): C, 63.26; H, 5.52; N, 14.56; S, 11.11; found: C, 63.05; H, 5.27; N, 14.69; S, 11.17.

6-Methoxy-1-(2-methylthieno[3,2-*d*]pyrimidin-4-yl)-1,2,3,4-tetrahydroquinoline

(344) A mixture of **468** (0.4 g, 2.17 mmol), 6-methoxy-1,2,3,4-tetrahydroquinoline (0.177g, 1.08 mmol) and nBuOH (10 mL) was refluxed. After completion of the reaction, as indicated by TLC, the reaction solvent was removed under reduced pressure. The residue was loaded on a silica gel column packed with silica gel and eluted with 20% ethyl acetate in hexane to afford **344** (0.218 g, 65%) of as white powder; mp 127.5-128 °C; *R_f* 0.21 (hexane/EtOAc 1:1); ¹H NMR (DMSO-*d*₆) δ 1.89-1.96 (m, 2 H), 2.56 (s, 3 H, 2-CH₃), 2.69-2.72 (t, 2 H), 3.78(s, 3 H, OCH₃), 3.99-4.02 (t, 2 H), 6.75-6.78 (dd, 1 H, C₆H₃), 6.89 (s, 1 H, C₆H₃), 7.00, 7.02 (d, 1 H, C₆H₃), 7.25, 7.27 (d, 1 H), 7.93, 7.94 (d, 1 H). Anal. calcd. for (C₁₇H₁₇N₃SO): C, 65.57; H, 5.50; N, 13.49; S, 10.30; found: C, 65.67; H, 5.46; N, 13.49; S, 10.30.

Methyl 3-(formylamino)thiophene-2-carboxylate (469). Fomic acid (12 mL) was added to acetic anhydride (18 mL) while cooling in an ice bath. Compound **466** (3.09 g, 19.8 mmol) was added to the cold solution in a small portions. The cooling bath was removed and the resulting suspension was stirred at room temperature for 4h. The mixture was diluted with water (30 mL) and white needle solid **469** (3.36 g, 93%) was collected by filtration; mp 90.5 °C; *R_f* 0.58 (hexane/EtOAc 1:1); ¹H NMR (DMSO-*d*₆) δ 3.85 (s, 3 H, COOCH₃), 7.90, 7.91(d, 1 H), 7.99, 8.01(d, 1 H), 8.42 (s, 1 H), 10.38 (s, 1 H, exch). This compound was used directly for next step of reaction without further characterization.

Thieno[3,2-*d*]pyrimidin-4(3*H*)-one (470). To a solution of ammonium formate (3.4 g, 54 mmol) in formamide (5 mL) at 150 °C was added **469** (1.85 g, 10 mmol) as a solid in small portions. The resulting solution was heated at 150 °C for 4 h and then allowed to stand at room temperature for 12 h. The precipitate that formed was collected by filtration to give **470** (1.21 g, 80%) as white needles; mp 215.8-216.4 °C; R_f 0.23 (MeOH/CHCl₃, 1:10); ¹H NMR (DMSO-*d*₆) δ 7.40, 7.41(d, 1 H), 8.16 (s, 1 H, 2-H), 8.18, 8.19 (d, 1 H), 12.48 (s, 1 H, 3-NH exch). This compound was used directly for next step of reaction without further characterization.

4-Methoxythieno[3,2-*d*]pyrimidine (471). A stirred mixture of **470** (0.7 g, 4.6 mmol) and POCl₃ (12 mL) was refluxed for 2 h. Then solvent was removed under reduced pressure to afford brown residue. The residue was loaded on a silica gel column packed with silica gel and eluted with 2% methanol in CHCl₃ to afford **471** (0.55 g, 72%) as white powder; mp 100.5 °C; R_f 0.43 (hexane/EtOAc 1:1); ¹H NMR (DMSO-*d*₆) δ 4.13 (s, 3 H, OCH₃), 7.60, 7.61 (d, 1 H), 8.35, 8.36 (d, 1 H), 8.78 (s, 1 H, 2-H). Anal. calcd. for (C₇H₆N₂SO): C, 50.59; H, 3.64; N, 16.86; S, 19.29; found: C, 50.60; H, 3.61; N, 16.79; S, 19.22.

4-Chlorothieno[3,2-*d*]pyrimidine (472). A stirred mixture of **470** (0.15 g, 1 mmol) and POCl₃ (6 mL) was refluxed for 2 h. Then solvent was removed under reduced pressure to afford brown residue. The residue was loaded on a silica gel column packed with silica gel and eluted with 25% ethyl acetate in hexane to afford **472** (0.15 g, 89%) as white powder. The whole process should avoid using of methanol; mp 62.8-63.2 °C; R_f 0.34 (hexane/EtOAc 3:1); ¹H NMR (DMSO-*d*₆) δ 7.77, 7.78 (d, 1 H), 8.61, 8.62 (d, 1 H), 9.06 (s, 1 H, 2-H).

***N*-(4-Methoxyphenyl)-*N*-methylthieno[3,2-*d*]pyrimidin-4-amine (474).** A mixture of **472** (0.141 g, 0.83 mmol), 4-methoxy-*N*-methylaniline (0.114 g, 0.83 mmol) and *n*-BuOH (7 mL) was refluxed. After completion of the reaction, as indicated by TLC, the reaction solvent was removed under reduced pressure. The residue was loaded on a silica gel column packed with silica gel and eluted with 25% ethyl acetate in hexane to afford **474** (0.175 g, 78%) as light brown powder; mp 132.6-133.0 °C; *R_f* 0.49 (hexane/EtOAc 1:1); ¹H NMR (DMSO-*d*₆) δ 3.49 (s, 3 H, OCH₃), 3.84 (s, 3 H, N-CH₃), 7.05, 7.07 (d, 2 H, C₆H₄), 7.27, 7.29 (d, 1 H), 7.38, 7.41 (d, 2 H, C₆H₄), 7.90, 7.91 (d, 1 H), 8.58 (s, 1 H, 2-H). Anal. calcd. for (C₁₄H₁₃N₃SO): C, 61.97; H, 4.83; N, 15.49; S, 11.82; found: C, 61.95; H, 4.76; N, 15.38; S, 11.70.

VII. BIBLIOGRAPHY

1. Kisliuk, R. L. Folate Biochemistry in Relation to Antifolate Selectivity. In *Antifolate Drugs in Cancer Therapy*. Jackman, A., Ed.; Humann Press: Totowa, **1999**, pp 13-36.
2. Kisliuk, R. L.; Gaumont, Y.; Powers, J. F.; Thorndike, J.; Nair, M. G.; Piper, J. R. Synergistic Growth Inhibition by Combination of Antifolates. In *Evaluation of Folate Metabolism in Health and Disease*. Picciano, M. F.; Stokstad, E. L. R.; Gregory, J. F.; Alan R.; Ed.; Liss: New York, **1990**, pp 79-89.
3. Hitchings, G. A. Folate Antagonists as Antibacterial and Antiprotozoal Agents. *Ann. N. Y. Acad. Sci.* **1971**, *186*, 444-451.
4. Gangjee, A.; Elzein, E.; Kothare, M.; Vasudevan, A. Classical and Nonclassical Antifolates as Potential Antitumor, Antipneumocystis and Antitoxoplasma Agents. *Curr. Pharm. Des.* **1996**, *2*, 263-280.
5. Calvert, H. An Overview of Folate Metabolism: Features Relevant to the Action and Toxicities of Antifolate Anticancer Agents. *Semin. Oncol.* **1999**, *26*, 3-10.
6. Kisliuk, R. L.; Gaumont, Y.; Powers, J. F.; Thorndike, J.; Nair, M. G.; Piper, J. R. Synergistic Growth Inhibition by Combination of Antifolates. In *Folic Acid Metabolism in Health and Disease*; Picciano, M. F., Stokstad, E. L. R., Gregory, J. F. III, Eds.; Wiley-Liss: New York, 1990; pp 79-89.
7. Douglas, K. T. The Thymidylate Synthesis Cycle and Anticancer Drugs. *Med. Res. Rev.* **1987**, *7*, 441-445.
8. Hitchings, G. H.; Smiths, S. L. Dihydrofolate Reductases as Targets. In *Adv. Enzyme Regulation*. Weber; Ed., Pergamon Press: **1979**, Vol 18, pp 349-371.

9. Blakley, R. L. *The Biochemistry of Folic Acid and Related Pteridines*; Neuberger, A., Tatum, E. L., Eds.; North Holland Publishing Co.: Amsterdam, 1969; pp 92-94.
10. MacKenzie, R. E. Biogenesis and Interconversion of Substituted Tetrahydrofolates. In *Folates and Pterins Chemistry and Biochemistry*; Blakley, R. L., Benkovic, S. J., Eds.; Wiley: New York, 1984; Vol. I, pp 255-306.
11. Petero, G. J.; Kohne, C. H. Fluoropyrimidines as Antifolate Drugs. *Antifolate Drugs Cancer Ther.* **1999**, 101-145.
12. Bolin, J. T.; Filman, D.J.; Matthews, D. A.; Hamlin, R. C.; Kraut, J. Crystal Structures of Escherichia coli and Lactobacillus casei Dihydrofolate Reductase Refined at 1.7 Å Resolution. I. General Features and Binding of Methotrexate. *J. Biol. Chem.* **1982**, 257, 13650-13662.
13. Brown, K. A.; Howell, E. E.; Kraut, J. Long-Range Structural Effects in a Second-Site Revertant of a Mutant Dihydrofolate Reductase. *Proc. Natl. Acad. Sci. USA*, **1993**, 90, 11753-11756.
14. Bystroff, C.; Kraut, J. Crystal Structure of Unliganded Escherichia coli Dihydrofolate Reductase. Ligand-induced Conformational Changes and Cooperativity in Binding. *Biochemistry* **1991**, 30, 2227-2239.
15. Gargaro, A. R.; Soteriou, A.; Frenkiel, T. A.; Bauer, C. J.; Birdsall, B.; Polshakov, V.I.; Barsukov, I.L.; Roberts, G.C.; Feeney, J. The Solution Structure of the Complex of Lactobacillus casei Dihydrofolate Reductase with Methotrexate. *J. Mol. Biol.* **1998**, 227, 119-134.
16. Polshakov, V. I.; Birdsall, B.; Frenkiel, T. A.; Gargaro, A. R.; Feeney, J. Structure and Dynamics in Solution of the Complex of Lactobacillus casei

- Dihydrofolate Reductase with the New Lipophilic Antifolate Drug Trimetrexate. *Protein Sci.*, **1999**, 8, 467-481.
17. Cody, V.; Galitsky, N.; Rak, D.; Luft, J. R.; Pangboarn, W.; Queener, S. F. Ligand-Induced Conformational Changes in the Crystal Structures of *Pneumocystis carinii* Dihydrofolate Reductase Complexes with Folate and NADP⁺. *Biochemistry* **1999**, 38, 4303-4312.
18. Cody, V.; Galitsky, N.; Rak, D.; Luft, J. R.; Pangboarn, W.; Gangjee, A.; Devraj, R.; Queener, S. F. Comparison of Ternary Complexes of *Pneumocystis carinii* and Wild-type Human Dihydrofolate Reductase with Coenzyme NADPH and a Novel Classical Antitumor Furo[2,3-*d*]pyrimidine Antifolate. *Acta Crystallogr. Sect. D*, **1997**, 53, 638-649.
19. Roth, B. Design of Dihydrofolate Reductase Inhibitors from X-Ray Crystal Structures. *Fed. Proc.* **1986**, 45, 2765-2772.
20. Costi, M. P.; Ferrari, S. Update on Antifolate Drugs Targets. *Curr. Drug Targets.* **2001**, 2, 135-166.
21. Carreras, C. W.; Santi, D. V. The Catalytic Mechanism and Structure of Thymidylate Synthase. *Ann. Rev. Biochem.* **1995**, 64, 721-762.
22. Rosowsky, A. Chemistry and Biological Activity of Antifolates. In *Progress in Medicinal Chemistry*; Ellis, G. P., West, G. B. Eds.; Elsevier Science Publishers: Amsterdam, 1989; pp 1-252.
23. Jackman, A. L. Antifolate Drugs: Past and Future Perspectives. In *Antifolate Drugs in Cancer Therapy*; Jackman, A. L. Ed.; Humana Press: Totowa, NJ, 1999; pp 1-12.
24. Shane, B. Folylpolyglutamate Synthesis and Role in the Regulation of one-carbon

- Metabolism. *Vitam Horm* **1989**, *45*, 263-335.
25. Gangjee, A.; Dubash, N. P.; Zeng, Y.; McGuire, J. J. Recent Advances in the Chemistry and Biology of Poly- γ -glutamate Synthetase Substrates and Inhibitors. *Curr. Med. Chem.: Anti-Cancer Agents* **2002**, *2*, 331-335.
26. Kisliuk, R. L.; Gaumont, Y.; Baugh, C. M.; Galivan, J.; Maley, G. F.; Maley, F. In *Chemistry and Biology of Pteridines*. Kisliuk, R. L.; Brown, G. M., Eds.; Elsevier North-Holland: New York, 1979, pp 261.
27. Allegra, C. J.; Chabner, B. A.; Tuazon, C. U.; Ogata Arakaki, D.; Baird, B.; Drake, J. C.; Masur, H. Treatment of *Pneumocystis carinii* Pneumonia with Trimetrexate in Acquired Immunodeficiency Syndrome (AIDS). *Semin. Oncol.* **1988**, *15*, 46-49.
28. Gangjee, A.; Elzein, E.; Kothare, M.; Vasudevan, A. Classical and Nonclassical Antifolates as Potential Antitumor, Antipneumocystis and Antitoxoplasma Agents. *Curr. Pharm. Des.* **1996**, *2*, 263-280.
29. Jackman, A. L. Antifolate Drugs: Past and Future Perspectives. In *Antifolate Drugs in Cancer Therapy*; Jackman, A. L. Ed.; Humana Press: Totowa, NJ, 1999; pp 1-12.
30. Jackman, A. L.; Kelland, L. R.; Kimbell, R.; Brown, M.; Gibson, W.; Aherne, G. W.; Hardcastle, A.; Boyle, F. T. Mechanisms of Acquired Resistance to the Quinazoline Thymidylate Synthase Inhibitor ZD1694 (Tomudex) in One Mouse and Three Human Cell Lines. *Br. J. Cancer* **1995**, *71*, 914-924.
31. Zhao, R. B.; Qiu, A. D.; Tsai, E.; Jansen, M.; Akabas, M. H.; Goldman, I. D. The Proton-coupled Folate Transporter: Impact on Pemetrexed Transport and on Antifolates Activities Compared with the Reduced Folate Carrier. *Mol Pharmacol.* **2008**, *74*, 854-862.

32. Matherly, L. H.; Goldman, D. I. Membrane Transport of Folates. *Vitam. Horm.* **2003**, *66*, 403-456.
33. Salazar, M. D.; Ratnam, M. The Folate Receptor: What does it Promise in Tissue-Targeted Therapeutics? *Cancer Metastasis Rev.* **2007**, *26*, 141-152.
34. Qiu, A.; Jansen, M.; Sakaris, A.; Min, S. H.; Chattopadhyay, S.; Tsai, E.; Sandoval, C.; Zhao, R.; Akabas, M. H.; Goldman, I. D. Identification of an Intestinal Folate Transporter and the Molecular Basis for Hereditary Folate Malabsorption. *Cell* **2006**, *127*, 917-928.
35. Zhao, R.; Goldman, I. D. The Molecular Identity and Characterization of a Proton-Coupled Folate Transporter--PCFT; Biological Ramifications and Impact on the Activity of Pemetrexed. *Cancer Metastasis Rev* **2007**, *26*, 129-139.
36. Deng, Y.; Wang, Y.; Cherian, C.; Hou, Z.; Buck, S. A.; Matherly, L. H.; Gangjee, A. Synthesis and Discovery of High Affinity Folate Receptor-specific Glycinamide Ribonucleotide Formyltransferase Inhibitors with Antitumor Activity. *J. Med. Chem.* **2008**, *51*, 5052-5063.
37. Goldman, I. D.; Lichtenstein, N. S.; Oliverio, V. T. Carrier-mediated Transport of the Folic Acid Analogue, Methotrexate, in the L1210 leukemia cell. *J. Biol. Chem.* **1968**, *243*, 5007-5017.
38. Matherly, L. H.; Hou, Z.; Deng, Y. Human Reduced Folate Carrier: Translation of Basic Biology to Cancer Etiology and Therapy. *Cancer Metastasis Rev.* **2007**, *26*, 111-128.
39. Zhao, R.; Goldman, I. D. Resistance to Antifolates. *Oncogene* **2003**, *22*, 7431-7457.
40. Ragoussis, J.; Senger, G.; Trowsdale, J.; Campbell, I. G. Genomic Organization of

- the Human Folate Receptor Genes on Chromosome 11q13. *Genomics* **1992**, *14*, 423-430.
41. Campbell, I. G.; Jones, T. A.; Foulkes, W. D.; Trowsdale, J. Folate-binding Protein is a Marker for Ovarian Cancer. *Cancer Res.* **1991**, *51*, 5329-5338.
42. Ross, J. F.; Chaudhuri, P. K.; Ratnam, M. Differential Regulation of Folate Receptor Isoforms in Normal and Malignant Tissues *in vivo* and in Established Cell Lines Physiologic and Clinical Implications. *Cancer* **1994**, *73*, 2432-2443.
43. Weitman, S. D.; Lark, R. H.; Coney, L. R.; Fort, D. W.; Frasca, V.; Zurawski, V. R., Jr.; Kamen, B. A. Distribution of the Folate Receptor GP38 in Normal and Malignant Cell Lines and Tissues. *Cancer Res.* **1992**, *52*, 3396-3401.
44. Jansen, G. Receptor- and Carrier-mediated Transport Systems for Folates and Antifolates, In *Antifolate Drugs in Cancer Therapy*; Jackman, A. L. Ed.; Humana Press: Totowa, NJ, 1999; pp 293-321.
45. Antony, A. C. Folate Receptors. *Annu. Rev. Nutr.* **1996**, *16*, 501-521.
46. Jackman, A. L.; Theti, D. S.; Gibbs, D. D. Antifolates Targeted Specifically to the Folate Receptor. *Adv. Drug. Deliv. Rev.* **2004**, *56*, 1111-1125.
47. Swietach, P.; Vaughan-Jones, R. D.; Harris, A. L. Regulation of Tumor pH and the Role of Carbonic Anhydrase 9. *Cancer Metastasis Rev.* **2007**, *26*, 299-310.
48. Cisneros, R. J.; Silks, L. A.; Dunlap, R. B. *Drugs Fut.* **1988**, *13*, 859.
49. Pogolotti, A. L., Jr.; Santi, D. V. The Catalytic Activity of Thymidylate Synthase. In *Bioorganic Chemistry*; van Tamelen, E. E., Ed.; Academic Press: Orlando, FL, 1977; Vol. 1, pp 277-311.
50. Benkovic, S. J. On the Mechanism of Folate Cofactors. *Acc. Chem. Res.* **1978**, *11*,

314-320.

51. Sliker, L. J.; Benkovic, S. J. Synthesis of (6R,11S)- and (6R,11R)-5,10-Methylene [11-1H,2H]Tetrahydrofolate. Stereochemical Paths of Serine Hydroxy Methyl Transferase, 5,10-Methylene Tetrahydrofolate Dehydrogenase and Thymidylate Synthase Catalyses. *J. Am. Chem. Soc.* **1984**, *106*, 1833-1838.
52. Santi, D.V.; Danenberg, P.V. Folates in Pyrimidine Nucleotide Biosynthesis. In *Folates and Pterins*. Blakeley, R.L., Benkovic, S.J. Eds. Wiley, New York, **1984**, Vol 1, pp 345-398.
53. Benkovic, S. J. On the Mechanism of Action of Folate and Biopterin Requiring Enzymes. *Ann. Rev. Biochem.* **1980**, *49*, 227-251.
54. Humphreys, G. K.; Greenberg, D. M. Studies on the Conversion of Deoxyuridic Acid to Thymidylic Acid by a Soluble Extract from Rat Thymus. *Arch. Biochem. Biophys.* **1958**, *78*, 275-287.
55. Perry, K. M.; Fauman, E.; Finer-Moore, J. S.; Montfort, W. R.; Maley, C. F.; Maley, F.; Stroud, R. M. Plastic Adaptation toward Mutations in Proteins: Structural Comparison of Thymidylate Synthases. *Proteins* **1990**, *8*, 315-313.
56. Ercikan, E.; Banerjee, D.; Waltham, M.; Schnieders, B.; Scotto, K. W., Bertino, J. R. Translational Regulation of the Synthesis of Dihydrofolate Reductase. *Adv. Exp. Med. Biol.* **1993**, *338*, 537-540.
57. Ercikan-Abali, E. A.; Banerjee, D.; Waltham, M. C.; Skacel, N.; Scotto, K. W.; Bertino, J. R. Dihydrofolate Reductase Protein Inhibits Its Own Translation by Binding to Dihydrofolate Reductase mRNA Sequences within the Coding Region. *Biochemistry* **1997**, *36*, 12317-12322.

58. Sotelo-Mundo, R. R.; Ciesla, J.; Dzik, J. M.; Rode, W.; Maley, F.; Maley, G. F.; Hardy, L. W.; Montfort, W. R. Crystal Structure of Rat Thymidylate Synthase Inhibited by Tomudex, a Potent Anticancer Drug. *Biochemistry* **1999**, *38*, 1087-1094.
59. Hardy, L. W.; Finer-Moore, J. S.; Montfort, W. R.; Jones, M. O.; Santi, D. V.; Stroud, R. M. Atomic Structure of Thymidylate Synthase: Target for Rational Drug Design. *Science* **1987**, *235*, 448-455.
60. Finer-Moore, J.; Fauman, E. B.; Foster, P. G.; Perry, K. M.; Santi, D. V.; Stroud, R. M. Refined Structures of Substrate-Bound and Phosphate-Bound Thymidylate Synthase from *Lactobacillus casei*. *J. Mol. Biol.* **1993**, *232*, 1101-1116.
61. Knighton, D. R.; Kan, C. C.; Howland, E.; Janson, C. A.; Hostomska, Z.; Welsh, K. M.; Matthews, D. A. Structure of and Kinetic Channeling in Bifunctional Dihydrofolate Reductase-Thymidylate Synthase. *Nat. Struct. Biol.* **1994**, *1*, 186-194.
62. Anderson, A. C.; Perry, K. M.; Freymann, D. M.; Stroud, R. M. The Crystal Structure of Thymidylate Synthase from *Pneumocystis carinii* Reveals a Fungal Insert Important for Drug Design. *J. Mol. Biol.* **2000**, *297*, 645-657.
63. Kamb, A.; Finer-Moore, J. S.; Stroud, R. M. Structural Basis for Recognition of Polyglutamyl Folates by Thymidylate Synthase. *Biochemistry* **1992**, *31*, 9883-9890.
64. Kamb, A.; Finer-Moore, J. S.; Stroud, R. M. Cofactor Triggers the Conformational Change in Thymidylate Synthase: Implications for an Ordered Binding Mechanism. *Biochemistry* **1992**, *31*, 12876-12884.
65. Matthews, D. A.; Appelt, K.; Oatley, J. S.; Xuong, N. H. Crystal Structure of *Escherichia coli* Thymidylate Synthase Containing Bound 5-Fluoro-2'-deoxyuridylate and 10-Propargyl-5,8-dideazafolate. *J. Mol. Biol.*, **1990**, *214*, 923-936.

66. Matthews, D. A.; Villafranca, J. E.; Janson, C. A.; Smith, W. W.; Welsh, K.; Freer, S. Stereochemical Mechanism of Action for Thymidylate Synthase Based on the X-ray Structure of the Covalent Inhibitory Ternary Complex with 5-Fluoro-2'-deoxyuridylate and 5,10-Methylenetetrahydrofolate. *J. Mol. Biol.* **1990**, *214*, 937-948.
67. Montfort, W. R.; Perry, K. M.; Fauman, E. B.; Finer-Moore, J. S.; Maley, G. F.; Maley, F.; Stroud, R. M. Pairwise Specificity and Sequential Binding in Enzyme Catalysis: Thymidylate Synthase. *Biochemistry*, **1990**, *29*, 6977-6986.
68. Montfort, W. R.; Perry, K. M.; Fauman, E. B.; Finer-Moore, J. S.; Maley, G. F.; Hardy, L.; Maley, F.; Stroud, R. M., Structure, Multiple Site Binding, and Segmental Accommodation in Thymidylate Synthase on Binding dUMP and an Anti-folate. *Biochemistry* **1990**, *29*, 6964-6977.
69. Fauman, E. B.; Rutenber, E. E.; Maley, G. F.; Maley, F.; Stroud, R. M., Water-mediated Substrate/product Discrimination: the Product Complex of Thymidylate Synthase at 1.83 Å. *Biochemistry* **1994**, *33*, 1502-1511.
70. Phan, J.; Koli, S.; Minor, W.; Dunlap, R. B.; Berger, S. H.; Lebioda, L. Human Thymidylate Synthase is in the Closed Conformation when Complexed with dUMP and Raltitrexed, An Antifolate Drug. *Biochemistry* **2001**, *40*, 1897-1902.
71. Sayre, P. H.; Finer-Moore, J. S.; Fritz, T. A.; Biermann, D.; Gates, S. B.; MacKellar, W. C.; Patel, V. F.; Stroud, R. M. Multi-Targeted Antifolates Aimed at Avoiding Drug Resistance Form Covalent Closed Inhibitory Complexes with Human and *Escherichia coli* Thymidylate Synthases. *J. Mol. Biol.* **2001**, *313*, 813-829.
72. Costi, M. P., Thymidylate Synthase Inhibition: a Structure-based Rationale for Drug Design. *Med Res Rev* **1998**, *18*, 21-42.

73. Heidelberger, C. On the Rational Development of a New Drug: the Example of the Fluorinated Pyrimidines. *Cancer Treat Rep.* 1981, **65**, 3-9.
74. Heidelberger, C.; Chaudhuri, N. K.; Danenberg, P.; Duchinsky, R., Schnitzer, R. J.; Plevin, E.; Schener, J. Fluorinated Pyrimidines: a New Class of Tumorinhibitory Compounds. *Nature* **1957**, *179*, 663-666.
75. Pinedo, H. M.; Peters, G. F. Fluorouracil: Biochemistry and Pharmacology. *J. Clin. Oncol.* **1988**, *6*, 1653-1664.
76. Papamichael, D. The Use of Thymidylate Synthase Inhibitors in the Treatment of Advanced Colorectal Cancer: Current Status. *Oncologist* **1999**, *4*, 478-487.
77. Sotos, G. A.; Grogan, L.; Allegra, C. J. Preclinical and Clinical Aspects of Biomodulation of 5-Fluorouracil. *Cancer Treat. Rev.* **1994**, *20*, 11-49.
78. Aschele, C.; Sobrero, A.; Faderan, M. A.; Bertino, J. R. Novel Mechanism(s) of Resistance to 5-Fluorouracil in Human Colon Cancer (HCT-8) Sublines Following Exposure to Two Different Clinically Relevant Dose Schedules. *Cancer Res.* **1992**, *52*, 1855-1864.
79. Calvert, A. H.; Alison, D. L.; Harland, S. J.; Robinson, B. A.; Jackman, A. L.; Jones, T. R.; Newell, D. R.; Siddik, Z. H.; Wiltshaw, E.; McElwain, T. J. A Phase I Evaluation of the Quinazoline Antifolate Thymidylate Synthase Inhibitor, N10-propargyl-5,8-dideazafolic Acid, CB3717. *J. Clin. Oncol.* **1986**, *4*, 1245-1252.
80. Jackman, A. L.; Calvert, A. H. Folate-based Thymidylate Synthase Inhibitors as Anticancer Drugs. *Ann. Oncol.* **1995**, *6*, 871-881.
81. Jones, T. R.; Smithers, M. J.; Betteridge, R. F.; Taylor, M. A.; Jackman, A. L.; Calvert, A. H.; Davies, L. C.; Harrap, K. R. Quinazoline Antifolates Inhibiting TS:

- Variations in the Amino Acid. *J. Med. Chem.* **1986**, *29*, 1112-1118.
82. Jones, t. R.; Thornton, T. J.; Flinn, A.; Jackman, A. L.; Newell, D. R.; Calvert, H. Quinazoline Antifolate Inhibiting TS: 2-Desamino Derivatives with Enhanced Solubility and Potency. *J. Med. Chem.* **1989**, *32*, 847-852.
83. Jackman, A. L.; Taylor, G. A.; Gibson, W.; Kimbell, R.; Brown, M.; Calvert, A. H.; Judson, I. R.; Hughes, L. R. ICI D1694, A Quinazoline Antifolate Thymidylate Synthase Inhibitor That is a Potent Inhibitor of L1210 Tumour Cell Growth In Vitro and In Vivo: A New Agent for Clinical Study. *Cancer Res.* **1991**, *51*, 5579-5586.
84. Comella, P.; De Vita, F.; Mancarella, S.; De Lucia, L.; Biglietto, M.; Casaretti, R.; Farris, A.; Ianniello, G. P.; Lorusso, V.; Avallone, A.; Carteni, G.; Leo, S. S.; Catalano, G.; De Lena, M.; Comella, G. Biweekly Irinotecan or Raltitrexed plus 6S-leucovorin and Bolus 5-Fluorouracil in Advanced Colorectal Carcinoma: a Southern Italy Cooperative Oncology Group Phase II-III Randomized Trial. *Ann. Oncol.* **2000**, *11*, 1323-1333.
85. Lewis, N.; Scher, R.; Weiner, L. M.; Engstrom, P.; Szarka, C.; Gallo, J.; Adams, A.; Litwin, S.; Kilpatrick, D.; Brady, D.; Meropol, N. Phase I and Pharmacokinetic Study of Irinotecan in Combination with Raltitrexed (abstract 757). *Proc. Am. Soc. Clin. Oncol.* **2000**.
86. Scheithauer, W.; Kornek, G. V.; Ulrich-Pur, H.; Penz, M.; Raderer, M.; Salek, T.; Haider, K.; Kwasny, W.; Depisch, D. Oxaliplatin plus Raltitrexed in Patients with Advanced Colorectal Carcinoma: Results of a Phase I-II Trial. *Cancer* **2001**, *91*, 1264-1271.
87. Jackman, A. L.; Kimbell, R.; Aherne, G. W.; Brunton, L.; Jansen, G.; Stephens, T. C.;

- Smith, M. N.; Wardleworth, J. M.; Boyle, F. T. Cellular pharmacology and in vivo Activity of a New Anticancer Agent, ZD9331: a Water-soluble, Nonpolyglutamatable, Quinazoline-based Inhibitor of Thymidylate Synthase. *Clin. Cancer Res.* **1997**, *3*, 911-921.
88. Marsham, P. R.; Wardleworth, J. M.; Boyle, F. T.; Hennequin, L. F.; Kimbell, R.; Brown, M.; Jackman, A. L. Design and Synthesis of Potent Non-polyglutamatable Quinazoline Antifolate Thymidylate Synthase Inhibitors. *J. Med. Chem.* **1999**, *42*, 3809-3820.
89. Goh, B. C.; Ratain, M. J.; Bertucci, D.; Smith, R.; Mani, S.; Vogelzang, N. J.; Schilsky, R. L.; Hutchison, M.; Smith, M.; Averbuch, S.; Douglass, E. Phase I Study of ZD9331 on Short Daily Intravenous Bolus Infusion for 5 Days Every 3 Weeks with Fixed Dosing Recommendations. *J. Clin. Oncol.* **2001**, *19*, 1476-1484.
90. Theodoulou, M.; Llombart, A.; Cruciani, G.; Bloch, R.; Campos, L.; Tung, N.; Borges, V.; Perry, M.; Rowland, K.; Schuster, M.; Kneuper-Hall, R.; Hudis, C. Pemetrexed Disodium (Alimta, LY231514, MTA) in Locally Advanced or Metastatic Breast Cancer (MBC) Patients (Pts) with Prior Anthracycline or Anthracenedione and Taxane Treatment: Phase II Study (abstract 506). *Proc. Am. Soc. Clin. Oncol.* **2000**.
91. Radar, J.; Clarke-Pearson, D.; Moore, M.; Carson, L.; Holloway, R.; Kao, M. S.; Wiznitzer, I.; Douglass, E. Phase II Trial of ZD9331 as Third-line Therapy for Patients with Ovarian Carcinoma. *Ann. Oncol.* **2000**, *11*, 83.
92. Schulz, J.; Douglass, E. ZD9331 as Second- or Third-line Therapy in Patients with Advanced Colorectal Cancer: a Phase II Multicenter Trial. *Ann. Oncol.* **2000**, *11*, 62.
93. Webber, S. E.; Bleckman, T. M.; Attard, J.; Deal, J. G.; Kathardekar, V.; Welsh,

- K. M.; Webber, S.; Janson, C. A.; Matthews, D. A.; Smith, W. W.; Freer, S. T.; Jordan, S. R.; Bacquet, R. J.; Howland, E. F.; Booth, C. L. J.; Ward, R. W.; Hermann, S. M.; White, J.; Morse, C. A.; Hillard, J. A.; Bartlett, C. A. Design and Synthesis of Thymidylate Synthase Inhibitors Using Protein Crystal Structures: The Synthesis and Biological Evaluation of a Novel Class of 5-Substituted Quinazolines. *J. Med. Chem.* **1993**, *36*, 733-746.
94. Taylor, E. C.; Harrington, P. J.; Fletcher, S. R.; Beardsley, G. P.; Moran, R. G., Synthesis of the Antileukemic Agents 5,10-Dideazaaminopterin and 5,10-Dideaza-5,6,7,8-tetrahydroaminopterin. *J. Med. Chem.* **1985**, *28*, 914-921.
95. Moran, R. G.; Taylor, E. C.; Berdsley, G. P. 5,10-Dideaza-5,6,7,8-tetrahydrotetrahydrofolic Acid (DDATHF), A Potent Antifolate Inhibitory to *de novo* Purine Synthesis. *Proc. Am. Assoc. Cancer Res.* **1985**, *26*, 231.
96. Shih, C.; Thornton, D. E. Preclinical Pharmacology Studies and the Clinical Development of a Novel Multitargeted Antifolate, MTA (LY231514). In *Antifolate Drugs in Cancer Therapy*; Jackman, A. L., Ed.; Humana Press: Totowa, NJ, 1999; pp 183-201.
97. Schultz, R. M.; Chen, V. J.; Bewley, J. R.; Roberts, E. F.; Shih, C.; Dempsey, J. A. Biological Activity of the Multitargeted Antifolate, MTA (LY231514), in Human Cell Lines with Different Resistance Mechanisms to Antifolate Drugs. *Semin. Oncol.* **1999**, *26*, 68-73.
98. Taylor, E. C.; Patel, H. H. Synthesis of Pyrrolo[3,4-*d*]pyrimidine Analogues of the Potent Antitumor Agent N-[4-[2-(2-Amino-3,4-dihydro-4-oxo-7*H*-pyrrolo[2,3-*d*]pyrimidin-5-yl)ethyl]-benzoyl]-L-glutamic Acid LY231514) *Tetrahedron* **1992**, *48*,

8089-8100.

99. Taylor, E. C.; Patel, H. H.; Sabitha, G.; Chaudhari, R. Synthesis of Thieno[2,3-*d*]pyrimidine Analogues of the Potent Antitumor Agent, N-{4-[2-(2-Amino-4(3H)-oxo-7H-pyrrolo [2,3-*d*]pyrimidin-5-yl)ethyl]B enzoyl }-LGlutamic Acid. (LY 231514) *Heterocycles*. **1996**, *43*, 349-365.
100. Taylor, E. C. Design and Synthesis of Folate Dependent Enzymes as Antitumor Agents. *Adv. Exp. Med. Biol.* **1993**, *338*, 387-408.
101. Taylor, E. C.; Young, W. B.; Chaudhari, R.; Patel, M. Synthesis of a Regioisomer of N-[4-(2-amino-3,4-dihydro-4-oxo-7H- pyrrolo[2,3-*d*]pyrimidine-5-yl)ethyl]benzoyl]-L-glutamic Acid (LY231514), an Active Thymidylate Synthase Inhibitor and Antitumor Agent. *Heterocycles*. **1993**, *36*, 1897-1908.
102. Gangjee, A.; Devraj, R. D.; McGuire, J. J.; Kisliuk, R. L. 5-ArylthioSubstituted 2-Amino-4-oxo-6-methylpyrrolo[2,3-*d*]pyrimidine Antifolates as Thymidylate Synthase Inhibitors and Antitumor Agents. *J. Med. Chem.* **1995**, *38*, 4495-4501.
103. Temple, C., Jr.; Bennett, L. L., Jr.; Rose, J. D.; Elliott, R. D.; Montgomery, J. A.; Mangum, J. H. Synthesis of Pseudo Cofactor Analogues as Potential Inhibitors of the Folate Enzymes. *J. Med. Chem.* **1982**, *25*, 161-166.
104. Gangjee, A.; Donkor, I. O.; Kisliuk, R. L.; Gaumont, Y.; Thorndike, J., Synthesis and Biological Activity of 5,11-Methylenetetrahydro-5- deazahomofolic acid. *J. Med. Chem.* **1991**, *34*, 611-616.
105. Pendergast, W.; Dickerson, S. H.; Johnson, J. V.; Dev, I. K.; Ferone, R.; Duch, D. S.; Smith, G. K. Benzoquinazoline Inhibitors of Thymidylate Synthase: Enzyme Inhibitory Activity and Cytotoxicity of some Sulfonamidobenzoylglutamate and

- Related Derivatives. *J. Med. Chem.* **1993**, *36*, 3464-3471.
106. Duch, D. S.; Banks, S.; Dev, I. K.; Dickerson, S. H.; Ferone, R.; Heath, L. S.; Humphreys, J.; Knick, V.; Pendergast, W.; Singer, S.; et al., Biochemical and Cellular Pharmacology of 1843U89, a Novel Benzoquinazoline Inhibitor of Thymidylate Synthase. *Cancer. Res.* **1993**, *53*, 810-818.
107. Bavetsias, V.; Marriott, J. H.; Melin, C.; Kimbell, R.; Matusiak, Z. S.; Boyle, F. T.; Jackman, A. L., Design and synthesis of Cyclopenta[g]quinazoline-based antifolates as inhibitors of thymidylate synthase and potential antitumor agents(.). *J Med Chem* **2000**, *43*, 1910-1926.
108. Clendeninn, N. J.; Peterkin, J. J.; Webber, S.; Shetty, B. V.; Koda, R. T.; Leichman, L.; Leichman, C. G.; Jeffers, S.; Muggia, F. M.; O'Dwyer, P. J. AG-331, a "Non-classical" Lipophilic Thymidylate Synthase Inhibitor for the Treatment of Solid Tumors. *Ann. Oncol.* **1994**, *4*, 133.
109. O'Dwyer, P. J.; Laub, P. B.; DeMaria, D.; Qian, M.; Reilly, D.; Giantonio, B.; Johnston, A. L.; Wu, E. Y.; Bauman, L.; Clendeninn, N. J.; Gallo, J. M. Phase I Trial of the Thymidylate Synthase Inhibitor AG331 as a 5-Day Continuous Infusion. *Clin. Cancer Res.* **1996**, *2*, 1685.
110. Belani, C.; Aqarwala, S.; Johnson, J.; Cohn, A.; Bernstein, J.; Langer, C.; Jones, V.; White, C.; Lob, K.; White, D.; Chew, T.; Johnston, A.; Clendeninn, N. A Phase II trial of Thymitaq (AG337) in Patients with Squamous Cell Carcinoma of the Head and Neck (abstract 1381). *Proc. Am. Soc. Clin. Oncol.* **1997**.
111. Webber, S. E.; Bleckman, T. M.; Attard, J.; Deal, J. g.; Kathardekar, V.; Welsh, K. M.; Webber, S.; Janson, C. A.; Matthews, D. A.; Smith, W. W.; Freer, S. T.; Jordan,

- S. R.; Bacquet, R. J.; Howland, E. F.; Booth, C. L. J.; Ward, R. W.; Hermann, S. M.; White, J.; Morse, C. A.; Hillard, J. A.; Bartlett, C. A. Design and Synthesis of Thymidylate Synthase Inhibitors Using Protein Crystal Structures: The Synthesis and Biological Evaluation of a Novel Class of 5-Substituted Quinazolines. *J. Med. Chem.* **1993**, *36*, 733-746.
112. Gangjee, A.; Mavandadi, F.; Kisliuk, R. L.; Queener, S. F. 2-Amino-4-oxo-5-substituted-pyrrolo[2,3-*d*]pyrimidines as Nonclassical Antifolate Inhibitors of Thymidylate Synthase. *J. Med. Chem.* **1996**, *39*, 4563-4568.
113. Polshakov, V. I. Dihydrofolate Reductase: Structural Aspects of Mechanism of Enzyme Catalysis and Inhibition. *Russ. Chem. Bull., Intl. Ed.* **2001**, *50*, 1733-1751.
114. Sawaya, M. R. and Kraut, J. Loop and Subdomain Movements in Mechanism of *Escherichia coli* Dihydrofolate Reductase: Crystallographic Evidence. *Biochemistry*, **1997**, *36*, 586-603.
115. Warren, M. S.; Brown, K. A.; Farnum, M. F.; Howell, E. E. and Kraut, J. Investigation of the Functional Role of tryptophan-22 in *Escherichia coli* Dihydrofolate Reductase by Site-directed Mutagenesis. *Biochemistry*, **1991**, *30*, 11092-11103.
116. Folkman, J. Tumour Angiogenesis: Therapeutic Implications. *New Engl. J. Med.*, **1971**, *285*, 1182-1186.
117. Schnell, J. R.; Dyson, H. J.; Wright, P. E. Structure, Dynamics, and Catalytic Function of Dihydrofolate Reductase. *Annu. Rev. Biophys. Biomol. Struct.* **2004**, *33*, 119-140.
118. Cummins, P. L. and Gready, J. E. Energetically Most Likely Substrate and

- Activity-site Protonation sites and Pathways in the Catalytic Mechanism of Dihydrofolate Reductase. *J. Am. Chem. Soc.*, **2001**, *123*, 3418-3428.
119. Gready, J. E. Theoretical Studies on the Activation of the Pterin Cofactor in the Catalytic Mechanism of Dihydrofolate Reductase. *Biochemistry*, **1985**, *24*, 4761-4766.
120. Falco, E. A.; Hitchings, G. H.; Russell, P. B.; VanderWert, H. Antimalarials as Antagonists of Purines and Pteroylglutamic acid. *Nature* **1949**, *164*, 107.
121. Champness, J. N.; Achari, A.; Ballantine, S. P.; Bryant, P. K.; Delves, C. J.; Stammers, D. K. The Structure of *Pneumocystis carinii* Dihydrofolate Reductase to 1.9 Å Resolution. *Structure* **1994**, *2*, 915-924.
122. Gleckman, R. A. Introduction of Trimethoprim: a Mixed Blessing. *Urology* **1981**, *17*, 460-461.
123. Jordan, G. W.; Krajden, S. F.; Hoepflich, P. D.; Wong, G. A.; Peirce, T. H.; Rausch, D. C. Trimethoprim-sulfamethoxazole in Chronic Bronchitis. *Can. Med. Assoc. J.* **1975**, *112*, 91-95.
124. Kovacs, J. A.; Masur, H. *Pneumocystis carinii* Pneumonia: A Comparison Between Patients with Acquired Immunodeficiency Syndrome and Patients with Other Immunodeficiencies. *Ann. Int. Med.* **1984**, *100*, 663-671.
125. Kovacs, J. A.; Allegra, C. J.; Masur, H. Characterization of DHFR of *Pneumocystis carinii* and *Toxoplasma gondii*. *Experimental Parasitology* **1990**, *71*, 60-68.
126. Allegra, C. J.; Chabner, B. A.; Tuazon, C. U.; Ogata-Arakaki, D.; Baird, B.; Drake, J. C.; Simmons, J. T.; Lack, E. E.; Shelhamer, J. A.; Ballis, F. Trimetrexate for the

- Treatment of *Pneumocystis carinii* Pneumonia in Patients with the Acquired Immunodeficiency Syndrome. *N. Engl. J. Med.* **1987**, *317*, 978-986.
127. Ivanetich, K. M.; Santi, D. V. Thymidylate Synthase-Dihydrofolate Reductase in Protozoa. *Exp. Parasitol.* **1990**, *70*, 367-371.
128. Grumont, R.; Washtein, W. L.; Caput, D.; Santi, D. V. Bifunctional Thymidylate Synthase-Dihydrofolate from *Leishmania tropica*: Sequence Homology with the Corresponding Monofunctional Proteins. *Proc. Natl. Acad. Sci. USA.* **1986**, *83*, 5387-5391.
129. Deroin, F.; Chastang, C. In vitro Effect of Folate Inhibitors on *Toxoplasma gondii*. *Antimicrobial Agents and Chemotherapy.* **1989**, *33*, 1753-1759.
130. Roos, D. S. Primary Structure of the Dihydrofolate Reductase-Thymidylate Synthase Gene from *Toxoplasma gondii*. *J. Biol. Chem.* **1993**, *268*, 6269-6280.
131. Taylor, E. C.; Harrington, P.; Shih, C. A Facile Route to Open Chain Analogues of DDATHF. *Heterocycles* **1989**, *28*, 1167-1172.
132. Shih, C.; Gossett, L. S.; Worzalla, J. F.; Rinzel, S. M.; Grindey, G. B.; Harrington, P. M.; Taylor, E. C., Synthesis and Biological Activity of Acyclic Analogues of 5,10-dideaza-5,6,7,8-tetrahydrofolic acid. *J. Med. Chem.* **1992**, *35*, 1109-1116.
133. Rosowsky, A.; Bader, H.; Wright, J. E.; Moran, R. G. 5-Deaza-7-desmethylene Analogues of 5,10-Methylene-5,6,7,8-tetrahydrofolic Acid and Related Compounds: Synthesis and *In vitro* Biological Activity. *J. heterocycl. Chem.* **1994**, *31*, 1241.
134. Montgomery, J. A.; Elliot, R. D.; Straight, S. L.; Temple, C. Deaza Analogues of

- Amethopterin. *Ann. N. Y. Acad. Sci.*, **1971**, *186*, 227-234.
135. Elliot, R. D.; Temple, C.; Frye, J. L.; Montgomery, J. A. Potential Folic Acid Antagonists. VI. The Synthesis of 1- and 3-Deazamethotrexate. *J. Org. Chem.* **1971**, *36*, 2818-2823.
136. Baker, B. R. In *Design of Active-Site-Directed Irreversible Enzyme Inhibitors*; Wiley: New York, 1967; pp 199.
137. Montgomery, J. A.; Piper, J. R. In *Folate Antagonists as Therapeutic Agents*; Sirotnak, F. M.; Burchall, J. J.; Ensminger, W. B.; Montgomery, J. A., Eds.; Academic Press: Orlando, 1984, pp 219-260.
138. Piper, J. R.; McCaleb, G. S.; Montgomery, J. A.; Kisliuk, R. L.; Gaumont, Y.; Sirotnak, F. M. Syntheses and Antifolate Activity of 5-methyl-5-deaza Analogs of Aminopterin, Methotrexate, Folic Acid, and N10-methylfolic acid *J. Med. Chem.* **1986**, *29*, 1080-1086.
139. Su, T. L.; Huang, J. T.; Burchenal, J. H.; Watanabe, K. A.; Fox, J. J. Synthesis and Biological Activity of 5-Deaza Analogs of Aminopterin and Folic Acid. *J. Med. Chem.* **1986**, *48*, 4852-4857.
140. Piper, J. R.; Ramamurthy, b.; Johnson, C. A.; Maddry, J. A.; Otter, G. M.; Sirotnak, F. M. Further Evaluation of 5-Alkyl-5-Deaza Antifolates. 5-Propyl and 5-Butyl-5-Deaza Analogues of Aminopterin and Methotrexate. *J. Heterocycl. Chem.* **1995**, *32*, 1205-1212.
141. Sirotnak, F. M.; Schmmid, F. A.; Otter, G. M.; Piper, J. R. Montgomery, J. A. Structural Design, Biochemical Properties and Evidence for Improved Therapeutic Activity of 5-Alkyl Derivatives of 5-Deazaminopterin and 5-Deazamethotrexate

- Compared to Methotrexate in Murine Tumor Models. *Cancer Res.* **1988**, *48*, 5686-5691.
142. Sirinivasan, A.; Broom, A. D. Pyridopyrimidines. 12. Synthesis of 8-Deaza Analogs of Aminopterin and Folic Acid. *J. Org. Chem.* **1981**, *46*, 1777-1781.
143. Kuehl, M.; Brixner, D. T.; Broom, A. D.; Avery, T.; Blakeley, R. L. Cytotoxicity, Uptake, Polyglutamate Formation and Antileukemic Effects of 8-Deaza Analogues of Methotrexate and Aminopterin in Mice. *Cancer Res.* **1988**, *48*, 1481-1488.
144. Hynes, J. B.; Harmon, S. J.; Floyd, G. G.; Farrington, M.; Hart, L. D.; Washtein, W. L.; Susten, S. S.; Freisheim, J. H. Chemistry and Antitumor Evaluation of Selected 2,4-Diaminoquinazoline Analogues of Folic Acid. *J. Med. Chem.* **1985**, *28*, 209-215.
145. Calvert, A. H.; Jones, T. R.; Dady, P. J.; Gzelakowska, S. b.; Paine, R. M.; Taylor, G. A.; Harrap, K. P. Quinazoline Antifolates with Dual Biochemical Loci of Action. Biochemical and Biological Studies Directed Towards Overcoming MTX resistance. *Eur. J. Cancer* **1980**, *16*, 713-722.
146. DeGraw, J. L.; Christie, P. H.; Tagawa, H.; Kisliuk, R. L.; Gaumont, Y.; Schmid, F. A.; Sirotnak, F. M. Synthesis and Biological Activity of Resolved C-10 Diastereomers of 10-Methyl and 10-Ethyl-10-Deazaaminopterin. *J. Med. Chem.* **1986**, *29*, 1056-1061.
147. Taylor, E. C.; Hamby, J. M.; Shih, C.; Grindey, G. B.; Rinzel, S. M.; Beardsley, G. P.; Moran, R. G. Synthesis and Antitumor Activity of 5-Deaza-5,6,7,8-tetrahydrofolic acid and its N-10 Substituted Analogues. *J. Med. Chem.* **1989**, *32*, 1517-1522.
148. DeGraw, J. L.; Christie, P. H.; Brown, V. H.; Kelly, L. F.; Kisliuk, R. L.; Gaumont,

- Y.; Sirotnak, F. M. Synthesis and Antifolate Properties of 10-Alkyl-8,10-Dideaza-Aminopterin. *J. Med. Chem.* **1984**, *27*, 376-380.
149. DeGraw, J. L.; Kelly, L. F.; Kisliuk, R. L.; Gaumont, Y.; Sirotnak, F. M. In *Chemistry and Biology of Pterindines*. Blair, J. A.; Ed.; Walter De Gruyter: Berlin. **1983**, pp 457-461.
150. Yan, S. J.; Weinstock, L. T.; Cheng, C. C. N-[2-(2,4-Diamino-6-quinazoliny)ethyl]benzoyl-L-glutamic Acid. *J. Heterocycl. Chem.* **1979**, *16*, 541.
151. Gangjee, A.; Mavandadi, F.; Queener, S. F.; McGuire, J. J. Novel 2,4-Diamino-5-Substituted Pyrrolo[2,3-*d*]pyrimidines as Classical and Nonclassical Antifolates Inhibitors of DHFR. *J. Med. Chem.* **1995**, *38*, 2158-2165.
152. Gangjee, A.; Mavandadi, F.; Queener, S. F. Effect of N-Methylation and Bridge Atom Variation on The Activity of 5-Substituted 2,4-Diamino-pyrrolo[2,3-*d*]pyrimidines Against Dihydrofolate Reductase Form *P. Carinii* and *T. gondii*. *J. Med. Chem.* **1997**, *40*, 1173-1177.
153. Aso, K.; Hitaka, T.; Yukishige, K.; Ootsu, K.; Akimoto, H. Synthesis and Antitumor Activity of Pyrro[2,3-*d*]pyrimidine Antifolates with a Bridge Chain Containing a Nitrogen Atom. *Chem. Pharm. Bull.* **1995**, *43*, 256-161.
154. Shih, C.; Gossett, L. S. The Synthesis of N-4-[(2-Amino-4-Substituted-[(pyrrolo[2,3-*d*]pyrimidin-5-yl)ethyl]benzoyl)-L-glutamic Acids as Antineoplastic Agents. *Heterocycles* **1993**, *35*, 825-841.
155. Shih, C.; Gossett, L. S.; Hu, Y.; Mendelson, L. G.; Habeck, L. L.; Grindey, G. B.; Schultz, R. M.; Andis, S. L.; Moran, R. g.; Freisheim, J. H. The Discovery of 4-Deoxy-5,10-Dideazatetrahydrofolic Acid (4-H DDATHF) and N-{2-Amino-[5,6-

- dihydro-(pyrrolo[2,3-*d*]pyrimidin-5-yl)ethyl}benzoyl}-L-glutamic Acid
Dihydrofolate Reductase Inhibitors. Presented at the Tenth International Symposium,
Chemistry and Biology of Pteridines and Folates. Orange Beach. AL, March 21-26,
1993; Abstr:F14.
156. Miwa, T.; Hitaka, T.; Akirnoto, H. A Novel Synthetic Approach to Pyrrolo[2,3-*d*]
pyrimidine Antifolates. *J. Org. Chem.* **1993**, *58*, 1696-1701.
157. Miwa, T.; Hitaka, T.; Akimoto, H.; Nomura, H. Novel Pyrrolo[2,3-*d*]pyrimidine
Antifolates: Synthesis and Antitumor Activities. *J. Med. Chem.* **1991**, *34*, 555-560.
158. Gangjee, A.; Yu, J.; McGuire, J. J.; Cody, V.; Galitsky, N.; Kisliuk, R. L.; Queener,
S. F. Design, Synthesis, and X-Ray Crystal Structure of a Potent Dual Inhibitor of
Thymidylate Synthase and Dihydrofolate Reductase as an Antitumor Agent. *J. Med.
Chem.* **2000**, *43*, 3837-3851.
159. Gangjee, A.; Devraj, R.; McGuire, J. J.; Kisliuk, R. L.; Queener, S. F.; Barrows, L.
R. Classical and Nonclassical Furo[2,3-*d*]pyrimidines as Novel Antifolates:
Synthesis and Biological Activities. *J. Med. Chem.* **1994**, *37*, 1169-1176.
160. Gangjee, A.; Devraj, R.; McGuire, J. J.; Kisliuk, R. L. Effect of Bridge Variation on
Antifolate and Antitumor Activity of Classical 5-Substituted 2,4-Diaminofuro[2,3-
d]pyrimidines. *J. Med. Chem.* **1995**, *38*, 3798-3805.
161. Kotake, Y.; Lijima, A.; Yoshimatsu, K.; Tamai, N.; Ozawa, Y.; Koyanagi, N.;
Kitoh, K.; Nomura, H. Synthesis and Antitumor Activities of Novel 6-5 Fused Ring
Heterocyclic Antifolates: N-[ω -(2-Amino-4-substituted-6,7-dihydro
cyclopental[*d*]pyrimidin-5-yl)alkyl}benzoyl}-L-glutamic acids. *J. Med. Chem.* **1994**,

- 37, 1616-1624.
162. Kotake, Y.; Okauchi, T.; Lijima, A.; Yoshimatsu, K.; Nomura, H. Novel 6-5 Fused Ring Heterocyclic Antifolates with Potent Antitumor Activity Bridge Modifications and Heterocyclic Benzoyl Isosteres of 2,4-Diamino-6,7-dihydro-5-*H*-cyclopenta[*d*]pyrimidine Antifolates. *Chem. Pharm. Bull.* **1995**, *43*, 829-841.
163. DeGraw, J. I.; Colwell, W. T.; Kisliuk, R. L.; Gaumont, Y.; Sirotnak, F. M., Synthesis and Antifolate Properties of 5,10-methylenetetrahydro-8,10-dideazaminopterin. *J. Med. Chem.* **1986**, *29*, 1786-1789.
164. Su, T. L.; Yang, Y. K.; Huang, J.T.; Ren, W.Y.; Watanabe, K. A.; Chou, T. C. Synthesis of 4-[(1,3-Diaminopyrrolo[3',4':4'5']pyrido[2,3-*d*]pyrimidin-8-yl)benzoyl]-L-glutamic Acid as Potential Antifolates. *J. Heterocycl. Chem.* **1993**, *30*, 1437-1443.
165. DeGraw, J. I.; Christie, P. H.; Colwell, W. T.; Sirotnak, F. M., Synthesis and Antifolate Properties of 5,10-ethano-5,10-dideazaaminopterin. *J. Med. Chem.* **1992**, *35*, 320-324.
166. Falco, E. A.; Goodwin, L. G.; Hitchings, G. H.; Rollo, J. M.; Russell, P. B. 2,4-Diaminopyrimidines. A New Series of Antimalarials. *Br. J. Pharmacol.* **1951**, *6*, 185-200.
167. Falco, E. A.; DuBrewl, S.; Hitchings, G.H. 2,4-Diamino Pyrimidines as Antimalarials. 11. 5-Benzyl Derivatives. *J. Am. Chem. Soc.* **1951**, *73*, 3758-3762.
168. Bushby, S. R. M.; Hitchings, G. H. Trimethoprim, A Sulfonamide Potentiator. *Br. J. Pharmacol. Chemother.* **1968**, *33*, 72-90.

169. Jonak, J. P.; Mead, L. H.; Ho, Y. K.; Zakrzewski, S. F. Effect of the Substituent at C6 on the Biological Activity of 2,4-Diamino-5-(10-adamantyl)pyrimidines. *J. Med. Chem.* **1973**, *16*, 724-729.
170. Zakrzewski, S. F.; Dave, C.; Rosen, F. Comparison of the Antitumor Activities and Toxicity of the 2,4-5(1-adamantyl)-6-methylpyrimidine and 2,4-Diamino-5(1-adamantyl)6-ethyl-pyrimidine. *J. Natl. Cancer Invest.* **1978**, *60*, 1029-1033.
171. Bliss, E. A.; Griffin, R. J.; Stevens, M. F. G. Structural Studies on Bioactive Compounds. Part 5. Synthesis and Properties of 2,4-Diaminopyrimidine DHFR Inhibitors Bearing Lipophilic Azido Groups. *J. Chem. Soc. Perk. Trans. I* **1987**, *1*, 2217- 2228.
172. Baker, B. R.; Laurens, G. T. Irreversible Enzyme Inhibitors. CXXIX. P-(4,6-Diamino-1,2-dihydro-2,2-dimethyl-s-triazin-1-yl) phenyl Propionyl Sulfanyl Fluoride, an Active Site Irreversible Inhibitor of DHFR. V. Effects of Substitution on the Benzene Sulfonyl Fluoride Moiety on Isozyme Specificity. *J. Med. Chem.* **1968**, *11*, 677-682.
173. Bertino, J. R.; Sawicki, W. L.; Moroson, A. R.; Cashmore, A. R.; Elslager, E.F. 2,4-Diamino-5-Methyl-6-[(3,4,5-trimethoxyanilino)methyl]quinazoline(TMQ), a Potent Nonclassical Folate Antagonist Inhibitor. *Biochem. Pharmacol.* **1979**, *28*, 1983-1987.
174. O'Dwyer, P. J.; Shoemaker, D. D.; Plowman, J.; Cradock, J.; Grillo-Lopez, A.; Leyland-Jones, B. Trimetrexate-A New Antifolate Entering Clinical Trials. *Invest.*

- New Drugs*. **1985**, 3, 71-75.
175. Harris, N. V.; Smith, C.; Bowden, K. Antifolate and Antibacterial Activity of 6-Substituted 2,4-Diamino Quinazolines. *Eur. J. Med. Chem.* **1992**, 27, 7-18.
176. Gangjee, A.; Zaveri, N.; Kothare, M.; Kisliuk, R. L.; Queener, S. Nonclassical 2,4-Diamino-6-(aminomethyl)-5,6,7,8-tetrahydroquinazoline Antifolates. *J. Med. Chem.* **1995**, 38, 3660-3668.
177. News. FDA Approves Trimetrexate As A Second line Therapy for *Pneumocystis carinii* Pneumonia *Am. J. Hosp. Pharm.* **1994**, 51, 591-592.
178. Grivsky, E. M.; Lee, S.; Sigel, C. W.; Duch, D. S.; Nichol, C. Synthesis and Antitumor Activity of 2,4-diamino-6-(2,5-dimethoxybenzyl)-5-methylpyrido[2,3-*d*]pyrimidine A. *J. Med. Chem.* **1980**, 23, 327-329.
179. (a). Gangjee, A.; Shi, J.; Queener, S. F.; Barows, L. R.; Kisliuk, R. L. Synthesis of 5-Methyl-5-Deaza Nonclassical Antifolates as Inhibitors of Dihydrofolate Reductase and as Potential Antipneumocystis and Antitoxoplasma and Antitumor Agents. *J. Med. Chem.* **1993**, 36, 3437-3443. (b). Gangjee, A.; Adair, O.; Queener, S. F. *Pneumocystis carinii* and *Toxoplasma gondii* Dihydrofolate Reductase Inhibitors and Antitumor Agents: Synthesis and Biological Activities of 2,4-Diamino-5-methyl-6-((monosubstituted aniline)methyl)pyrido- [2,3-*d*]pyrimidines. *J. Med. Chem.* **1999**, 42, 2447-2455.

180. Rosowsky, A.; Mota, C.; Wright, J. E.; Freisheim, J. H.; Huesner, J. J.; McCormack, J. J.; Queener, S. F. 2,4-Diaminothieno[2,3-*d*]pyrimidines. Analogues of Trimetrexate and Piritrexim as Potential Inhibitors of *Pneumocystis carinii* and *Toxoplasma gondii* Dihydrofolate Reductase. *J. Med. Chem.* **1993**, *36*, 3103-3112.
181. Gangjee, A.; Lin, X.; Queener, S. F. Design, Synthesis, and Biological Evaluation of 2,4-Diamino-5-methyl-6-substituted-pyrrolo[2,3-*d*]pyrimidines as Dihydrofolate Reductase Inhibitors. *J. Med. Chem.* **2004**, *47*, 3689-3692.
182. Gangjee, A.; Guo, X.; Queener, S. F.; Cody, V.; Galitsky, N.; Luft, J. R.; Pangborn, W. Selective *Pneumocystis carinii* Dihydrofolate Reductase Inhibitors: Design, Synthesis, and Biological Evaluation of New 2,4-Diamino-5-substituted furo[2,3-*d*]pyrimidines. *J. Med. Chem.* **1998**, *41*, 1263-1271.
183. Gangjee, A.; Dubash, N. P.; Queener, S. F. The Synthesis of New 2,4-Diaminofuro[2,3-*d*]pyrimidines with 5-Biphenyl, Phenoxyphenyl and Tricyclic Substitutions as Dihydrofolate Reductase Inhibitors. *J. Heterocycl. Chem.* **2000**, *37*, 935-942.
184. Wahid, F.; Monneret, C.; Dauzonne, D. Synthesis and Biological Evaluation of 5-arylfuro[2,3-*d*]pyrimidines as Novel Dihydrofolate Reductase Inhibitors. *Chem. Pharm. Bull.* **1999**, *47*, 156-164.
185. Gangjee, A.; Elzein, E.; Queener, S. F.; McGuire, J. J. Synthesis and Biological Activities of Tricyclic Conformationally Restricted Tetrahydropyrido Annulated Furo[2,3-*d*]pyrimidines as Inhibitors of Dihydrofolate Reductase. *J. Med. Chem.* **1998**, *41*, 1409-1416.
186. Kuyper, L.; Baccanari, D. P.; Jones, M. L.; Hunter, R. N.; Tansik, R. L.; Joyner,

- S. S.; Boytos, C. M.; Rudolph, S. K.; Knick, V.; Wilson, R. H.; Caddell, J. M.; Friedman, H. S.; Comley, J. C.; Stables, J. N. High-Affinity Inhibitors of Dihydrofolate Reductase: Antimicrobial and Anticancer Activities of 7,8-Dialkyl-1,3-Diaminopyrrolo[3,2-*f*]quinazolines with Small Molecular Size. *J. Med. Chem.* **1996**, *39*, 892-903.
187. Gangjee, A.; Shi, J. F.; Queener, S. F., Synthesis and Biological Activities of Conformationally Restricted, Tricyclic Nonclassical Antifolates as Inhibitors of Dihydrofolate Reductases. *J. Med. Chem.* **1997**, *40*, 1930-1936.
188. Moran, R. G., Roles of Folylpoly-gamma-glutamate Synthetase in Therapeutics with Tetrahydrofolate Antimetabolites: an overview. *Semin. Oncol.* **1999**, *26*, 24-32.
189. Hughes, L. R.; Stephens, T. C.; Boyle, F. T.; Jackman, A. L. Raltitrexed (Tomudex), a Highly Polyglutamatable Antifolate Thymidylate Synthase Inhibitor: Design and Preclinical Activity. In *Antifolate Drugs in Cancer Therapy*; Jackman, A. L., Ed.; Humana Press: Totowa, NJ, 1999; pp 147-165.
190. Mendelsohn, L. G.; Shih, C.; Chen, V. J.; Habeck, L. L.; Gates, S. B.; Shackelford, K. A. Enzyme Inhibition, Polyglutamation, and the Effect of LY231514 (MTA) on Purine Biosynthesis, *Sem. Oncol.*, **1999**, *26*, 42-47.
191. Sikora, E.; Jackman, A. L.; Newell, D. R.; Calvert, A. H. Formation and Retention and Biological Activity of N^{10} -Propargyl-5,8-dideazafolic Acid (CB 3717) Polyglutamates in L1210 Cells *In Vitro*. *Biochem. Pharmacol.* **1988**, *37*, 4047-4054.
192. Jackman, A. L.; Newell, D. R.; Gibson, W.; Jodrell, D. I.; Taylor, G. A.; Bishop, J. A.; Hughes, L. R.; Calvert, A. H. The Biochemical Pharmacology of the Thymidylate Synthase Inhibitor 2-Desamino-2-methyl- N^{10} -propargyl-5,8-

- dideazafolic Acid (ICI 198583). *Biochem. Pharmacol.* **1991**, *42*, 1885-1895.
193. Nair, M. G.; Abraham, A.; McGuire, J. J.; Kisliuk, R. L.; Galivan, J. H.; Ferone, R. Polyglutamylation as a Determinant of Cytotoxicity of Classical Folate Analog Inhibitors of Thymidylate Synthase and Glycinamide Ribonucleotide Formyltransferase. *Cell. Pharmacol.* **1994**, *1*, 245-249.
194. Bisset, G. M. F.; Pawelczak, K.; Jackman, A. L.; Calvert, A. H.; Hughes, L. R. Syntheses and Thymidylate Synthase Inhibitory Activity of the Poly- γ -glutamyl Conjugates of *N*-[5-[*N*-(3,4-Dihydro-2-methyl-4-oxoquinazolin-6-ylmethyl)-*N*-methylamino]-2-thienoyl]-L-glutamic Acid (ICI D1694) and Other Quinazoline Antifolates. *J. Med. Chem.* **1992**, *35*, 859-866.
195. McGuire, J. J. Antifolate Polyglutamylation in Preclinical and Clinical Antifolate Resistance. In *Antifolate Drugs in Cancer Therapy*; Jackman, A. L., Ed.; Humana Press: Totowa, NJ, 1999; pp 339-364.
196. Barakat, R. R.; Li, W. W.; Lovelace, C.; Bertino, J. R. Intrinsic Resistance of Cervical Squamous Cell Carcinoma Cell Lines to Methotrexate (MTX) as a Result of Decreased Accumulation of Intracellular Methotrexate Polyglutamates. *Gynecol. Oncol.* **1993**, *51*, 54-60.
197. McCloskey, D. E.; McGuire, J. J.; Russell, C. A.; Rowan, B. G.; Bertino, J. R.; Pizzorno, G.; Mini, E. Decreased Folylpolyglutamate Synthetase Activity as a Mechanism of Methotrexate Resistance in CCRF-CEM Human Leukemia Sublines. *J. Biol. Chem.* **1991**, *266*, 6181-6187.
198. Braakhuis, B. J. M.; Jansen, G.; Noordhuis, P.; Kegel, A.; Peters, G. J. Importance of Pharmacodynamics in the *In Vitro* Antiproliferative Activity of the Antifolates

- Methotrexate and 10-Deazaaminopterin Against Human Head and Neck Squamous Cell Carcinoma. *Biochem. Pharmacol.* **1993**, *46*, 2155-2161.
199. Liani, E.; Rothem, L.; Bunni, M. A.; Smith, C. A.; Jansen, G.; Assaraf, Y. G. Loss of Folylpoly- γ -glutamate Synthetase Activity is a Dominant Mechanism of Resistance to Polyglutamylation-Dependent Novel Antifolates in Multiple Human Leukemia Sublines. *Int. J. Cancer* **2003**, *103*, 587-599.
200. Huennekens, F. M.; Vitols, K. S.; Henderson, G. B. Transport of Folate Compounds in Bacterial and Mammalian Cells. *Advances in Enzymology* **1978**, *47*, 313-346.
201. Pizzorno, G.; Chang, Y. M.; McGuire, J. J.; Bertino, J. R. Inherent Resistance of Squamous Carcinoma Cell Lines to Methotrexate as a Result of Decreased Polyglutamation of This Drug. *Cancer Res.* **1989**, *49*, 5275-5280.
202. Cowan, K. H.; Jolivet, J. A. A Methotrexate Resistant Human Breast Cancer Line with Multiple Defects Including Diminished Formation of Mtx Polyglutamates. *J. Biol. Chem.* **1984**, *259*, 10793-10800.
203. Cichowicz, D. J.; Shane, B. Mammalian Folylpoly- γ glutamate Synthetase 2. Substrate Specificity and Kinetic Properties. *Biochemistry*, **1987**, *26*, 513-521.
204. Sheng, Y.; Sun, X.; Shen, Y.; Bogнар, A. L.; Baker, E. N.; Smith, C. A. Structural and Functional Similarities in the ADP-forming Amide Bond Ligase Superfamily: Implications for a Substrate-Induced Conformational Change in Folylpolyglutamate Synthetase. *J. Mol. Biol.* **2000**, *302*, 427-440.
205. Kalman, T. I. Mechanism Based Approaches to Inhibition of the Synthesis and Degradation of Folate and Antifolate Polyglutamates. *Adv. Exp. Med. Biol.* **1993**,

338, 639-643.

206. Sun, X.; Cross, J. A.; Bogнар, A. L.; Baker, E. N.; Smith, C. A. Folate-binding Triggers the Activation of Folylpolyglutamate Synthetase. *J. Mol. Biol.* **2001**, *310*, 1067-1078.
207. Sheng, Y.; Sun, X.; Shen, Y.; Bogнар, A. L.; Baker, E. N.; Smith, C. A. Structural and Functional Similarities in the ADP-forming Amide Bond Ligase Superfamily: Implications for a Substrate-induced Conformational Change in Folylpolyglutamate Synthetase. *J. Mol. Biol.* **2000**, *302*, 427-440.
208. Shim, J. H.; Benkovic, S. J., Catalytic Mechanism of Escherichia coli Glycinamide Ribonucleotide Transformylase Probed by site-directed Mutagenesis and pH-dependent Studies. *Biochemistry* **1999**, *38*, 10024-10031.
209. Welin, M.; Grossmann, J. G.; Flodin, S.; Nyman, T.; Stenmark, P.; Trésaugues, L.; Kotenyova, T.; Johansson, I.; Nordlund, P.; Lehtiö, L. Structural Studies of Tri-functional Human GART. *Nucleic Acids Res.* **2010**, *38*, 7308–7319.
210. Zhang, Y., Desharnais, J., Greasley, S. E., Beardsley, G. P., Boger, D. L., and Wilson, I. A. Crystal Structures of Human GAR Tfase at Low and High pH and with Substrate β -GAR. *Biochemistry*, **2002**, *41*, 14206-14215.
210. Shim, J. H.; Benkovic, S. J., Catalytic Mechanism of Escherichia coli Glycinamide Ribonucleotide Transformylase Probed by site-directed Mutagenesis and pH-dependent

- Studies. *Biochemistry*, **1999**, 38, 10024-10031.
211. Dahms, T. E. S.; Sainz, G.; Giroux, E. L.; Caperelli, C. A.; Smith, J. L. The Apo and Ternary Complex Structures of a Chemotherapeutic Target: Human Glycinamide Ribonucleotide Transformylase. *Biochemistry*, **2005**, 44, 9841-9850.
212. Varney, M. D.; Palmer, C. L.; Romines, W. H. III.; Boritzki, T.; Margosiak, S. A.; Almassy, R.; Janson, C. A., Bartlett, C.; Howland, E. J.; Ferre, R. Protein structure-based design, synthesis, and biological evaluation of 5-thia-2,6-diamino-4(3H)-oxopyrimidines: potent inhibitors of glycinamide ribonucleotide transformylase with potent cell growth inhibition, *J. Med. Chem.* **1997**, 40, 2502-2524.
213. Mendelsohn, L. G.; Worzalla, F.; Walling, J. M. Preclinical and Clinical Evaluation of Glycinamide-ribonucleotide Formyltransferase Inhibitors Lometrexol and LY309887. In *Antifolate Drugs in Cancer Therapy*. Jackman, A., Ed.; Humann Press: Totowa, **1999**, pp 262-280.
214. Taylor, E. C.; Dowling J. E. Synthesis of a Pyrimido[4,5-b]azepine Analog of 5,10-Dideaza-5,6,7,8-tetrahydrofolic Acid(DDATHF). *Bioorg. Med. Chem. Lett.* **1997**, 7, 453-456.
215. Desharnais, J.; Hwang, I.; Zhang, Y.; Tavassoli, A.; Baboval, J.; Benkovic, S. J.; Wilson, I. A.; Boger, D. L., Design, Synthesis and Biological Evaluation of 10-CF₃CO-DDACTHF Analogues and Derivatives as Inhibitors of GAR Tfase and the *de novo* Purine Biosynthetic Pathway. *Bioorg Med Chem* **2003**, 11, 4511-4521.
216. DeMartino, J. K.; Hwang, I.; Xu, L.; Wilson, I. A.; Boger, D. L., Discovery of a Potent, Nonpolyglutamatable Inhibitor of Glycinamide Ribonucleotide Transformylase. *J. Med. Chem.* **2006**, 49, 2998-3002.

217. Sheng, Y.; Sun, X.; Shen, Y.; Bogнар, A. L.; Baker, E. N.; Smith, C. A., Structural and functional similarities in the ADP-forming amide bond ligase superfamily: implications for a substrate-induced conformational change in folsylpolyglutamate synthetase. *J Mol Biol* **2000**, *302*, 427-440.
218. Gewalt K.; Schinke E.; Böttcher H., Heterocyclen aus CH-aciden nitrilen. VII. 2-Aminothiophene aus oxo-Mercaptanen und Methylenaktiven Nitrilen. *Chem. Ber.* **1966**, *99*, 94-100.
219. Rosowsky, A.; Chaykovsky, M.; chen, K. K. N.; Lin, M.; Modest, E. J. 2,4-Diaminothieno[2,3-*d*]Pyrimidines as Antifolates and Antimalarials. 1. Synthesis of 2,4-Diamino-5,6,7,8-Tetrahydrothianaphtheno[2,3-*d*]pyrimidines and Related Compounds. *J. Med. Chem.* **1973**, *16*, 185-188.
220. Zhang, M.; Harper, R. W. A Concise Synthetic Entry to Substituted 2-Aminothieno[2,3-*d*]pyrimidines via a Gewalt Precursor. *Bioorg. Med. Chem. Lett.* **1997**, *7*, 1629-1634.
221. Ishikawa, F.; Yamaguchi, H. Cyclic Guanidines. Xiii. Synthesis of 2-Amino-4-Phenyl-3,4-Dihydrothieno[2,3-*d*]Pyrimidine Derivatives. *Chemical & Pharmaceutical Bulletin* **1980**, *28*, 3172-3177.
222. Dave, K. G.; Shishoo, C. J.; Devani, M. B.; Kalyanaraman, R.; Ananthan, S. et al. Reaction of Nitriles under Acidic Conditions. Part I. A general Method of Synthesis of Condensed Pyrimidines. *J. Heterocyclic Chem.* **1980**, *17*, 1497-1500.
223. Cruceyra, A.; Gomez Parra, V.; Madronero, R. Thiophene Bioisosteres. Iii. 4-Oxo-1,2,3,4-Tetrahydrothieno[2,3-*d*]Pyrimidines. *Anales de Quimica* **1975**, *71*, 103-106.

224. Corral, C.; Madronero, R.; Ulecia, N. Bischler and Friedlaender Reactions with 2-Amino-3-Aroylthiophenes. *Afinidad* **1978**, *35*, 129-133.
225. Konno, S.; Tsunoda, M.; Watanabe, R.; Yamanaka, H.; Fujita, F. et al. Synthesis of Thieno[2,3-*d*]pyrimidine Derivatives and Their Antifungal Activities. *Yakugaku Zasshi* **1989**, *109*, 464-473.
226. Hesse, S.; Perspicace, E.; Kirsch, G., Microwave-assisted Synthesis of 2-Amino Thiophene-3-carboxylic Acid Derivatives, 3H-thieno[2,3-*d*]pyrimidin-4-one and 4-chlorothieno[2,3-*d*]pyrimidine. *Tetrahedron. Lett.* **2007**, *48*, 5261-5264.
227. Horiuchi, T.; Nagata, M.; Kitagawa, M.; Akahane, K.; Uoto, K., Discovery of Novel Thieno[2,3-*d*]pyrimidin-4-yl Hydrazone-based Inhibitors of Cyclin D1-CDK4: Synthesis, Biological Evaluation and Structure-activity Relationships. Part 2. *Bioorgan. Med. Chem.* **2009**, *17*, 7850-7860.
228. Briel, D. Synthesis of Thieno-Heterocycles from Substituted 5(Methylthio) Thiophene-4-Carbonitriles. *Pharmazie* **1998**, *53*, 227-231.
229. Taylor, E. C.; Patel, H. H.; Sabitha, G.; Chaudhari, R. Synthesis of Thieno [2,3 - *d*]pyrimidine Analogues of the Potent Antitumor Agent, N-{4-[2-(2- Amino-4(3H)-oxo-7-H-pyrrolo [2,3-*d*]pyrimidin-5-yl)ethyl]Benzoyl }-LGlutamicAcid. (LY 231514) *Heterocycles*. **1996**, *43*, 349-365.
230. Sakamoto, T.; Kondo, Y.; Watanabe, R.; Yamanaka, H. Condensed Heteroaromatic Ring Systems. Vii. Synthesis of Thienopyridines, Thienopyrimidines, and Furopyridines from O-Substituted NHeteroarylacetylenes. *Chemical & Pharmaceutical Bulletin* **1986**, *34*, 2719-2724.
231. Briel, D.; Wagner, G.; Lohmann, D.; Laban, G. Preparation of 2,4-Diaryl-5-

- Hydroxythieno[2,3-*d*]Pyrimidines as Drugs and Drug Intermediates.: Ger. (East),
1988.
232. El-Dean, A. K. Synthesis of Some Pyrimidothienopyrimidine Derivatives.
Monatshefte fuer chemie **1998**, 129, 523-533.
233. Briel, D.; Wagner, G.; Lohmann, D.; Laban, G. Preparation of 2,4-Diaryl-5-Hydroxythieno[2,3-*d*]Pyrimidines as Drugs and Drug Intermediates.: Ger. (East),**1988.**
234. Ried, W.; Beller, G. Synthesis of Thieno[2,3-*d*]Pyrimidines and Pyrrolo[2,3-*d*]Pyrimidines. *Liebigs Annalen der Chemie* **1988**, 7, 633-642.
235. van Straten, N. C.; Schoonus-Gerritsma, G. G.; van Someren, R. G.; Draaijer, J.; Adang, A. E.; Timmers, C. M.; Hanssen, R. G.; van Boeckel, C. A., The First Orally Active Low Molecular Weight Agonists for the LH Receptor: Thienopyr(im)idines with Therapeutic Potential for Ovulation Induction. *Chembiochem.* **2002**, 3, 1023-1026.
236. Migianu, E.; Kirsch, G., Synthesis of New Thieno[b]azepinediones From alpha-Methylene Ketones. *Synthesis* **2002**, 1096-1100.
237. Thomae, D.; Kirsch, G.; Seck, P., Synthesis of Thiophene Analogues of the Tacrine Series. *Synthesis* **2007**, 1027-1032.
238. Morris, P. E.; Elliott, A. J.; Montgomery, J. A., New Syntheses of 7-Substituted-2-aminothieno- and Furo[3,2-*d*]pyrimidines. *J. Heterocycl. Chem.* **1999**, 36, 423-427.
239. Ren, W.; Rao, K. V.; Klein, R. S., Convenient Synthesis of Substituted 3-Aminothiophene-2-carbonitriles for α -Acetylenic Nitriles and their Conversion to Thieno[2,3-*d*]pyrimidines[1]. *J. Heterocycl. Chem.* **1986**, 23, 1757-1763.

240. Peng, J.; Lin, W.; Jiang, D.; Yuan, S.; Chen, Y., Preparation of a 7 Arylthieno[3,2-d] pyrimidin-4-Amine Library. *J. Comb. Chem.* **2007**, *9*, 431-436.
241. Klemm, L. H.; Wang, J.; Hawkins, L., Synthesis of 3-Amino-2-Carbamoylthiophene and Its Reaction with Cycloalkanones to Form Imines. *J. Heterocycl. Chem.* **1995**, *32*, 1039-1041.
242. Artyomov, V. A.; Rodinovskaya, L. A.; Shestopalov, A. M.; Litvinov, V. P., *N*-Cyanochloroacetamide - A Convenient Reagent for the Regioselective Synthesis of Fused Diaminopyrimidines. *Tetrahedron.* **1996**, *52*, 1011-1026.
243. Sonogashira, K.; Tohda, Y.; Hagihara, N. Convenient Synthesis of Acetylenes. Catalytic Substitutions of Acetylenic Hydrogen with Bromo Alkenes, Iodo Arenes, and Bromopyridines. *Tetrahedron Lett.* **1975**, *16*, 4467-4470.
244. Smith, M.; March, J., *March's Advanced Organic Chemistry*. Wiley-Interscience, **2001**.
245. Wu, P.; Fokin, V. V., Catalytic Azide-alkyne Cycloaddition: Reactivity and Applications. *Aldrichim Acta* **2007**, *40*, 7-17.
246. Corey, E. J.; Fuchs, P. L., A Synthetic Method for Formyl→Ethyne Conversion (RCHO→RC≡CH or RC≡CR'). *Tetrahedron Lett.* **1972**, *36*, 3769-3772.
247. Seyferth, D.; Marmor, R. S.; Hilbert, P., Reactions of Dimethylphosphono substituted Diazoalkanes. (MeO)₂P(O)CR Transfer to Olefins and 1,3-Dipolar Additions of (MeO)₂P(O)C(N₂)R. *J. Org. Chem.* **1971**, *36*, 1379-1386.
248. Gilbert, J. C.; Weerasooriya, U., Diazoethenes: Their Attempted Synthesis from Aldehydes and Aromatic Ketones by Way of the Horner-Emmons Modification of

- the Wittig Reaction. A Facile Synthesis of Alkynes. *J. Org. Chem.* **1982**, *47*, 1837-1845.
249. Muller, S.; Liepold, B.; Roth, G. J.; Bestmann, H. J., An Improved One-pot Procedure for the Synthesis of Alkynes from Aldehydes. *Synlett.* **1996**, 521-522.
250. Ohira, S., Methanolysis of Dimethyl (1-Diazo-2-oxopropyl) Phosphonate: Generation of Dimethyl (Diazomethyl) Phosphonate and Reaction with Carbonyl Compounds. *Synth. Commun.* **1989**, *19*, 561-564.
251. Brown, D. G.; Velthuisen, E. J.; Commerford, J. R.; Brisbois, R. G.; Hoye, T. R., A Convenient Synthesis of Dimethyl (diazomethyl)phosphonate (Seyferth Gilbert reagent). *J. Org. Chem.* **1996**, *61*, 2540-2541.
252. Callant, P.; D'Haenens, L.; Vandewalle, M., Photoinduced Wolff Rearrangement of α -Diazo- β -Ketophosphonates: A Novel Entry into Substituted Phosphonoacetates. *Synth. Commun.* **1984**, *14*, 163-167.
253. Ye, T.; Mckerverey, A. M., Organic Synthesis with α -Diazocarbonyl Compounds. *Chem. Rev.* **1994**, *94*, 1091-1160.
254. Baum, J. S.; Shook, D. A.; Davies, H. M. L.; Smith, H. D., Diazotransfer Reactions with p-Acetamidobenzenesulfonyl Azide. *Synth. Commun.* **1987**, *17*, 1709-1716.
255. Roth, G. J.; Liepold, B.; Muller, S. G.; Bestmann, H. J., Further Improvements of the Synthesis of Alkynes from Aldehydes. *Synthesis* **2004**, 59-62.
256. Meffre, P.; Hermann, S.; Durand, P.; Reginato, G.; Riu, A., Practical One-step Synthesis of Ethynylglycine Synthons From Garner's Aldehyde. *Tetrahedron* **2002**, *58*, 5159-5162.

257. Buchwald, S. L. "Cross Coupling." *Acc. Chem. Res.* **2008**, *41*, 1439-1439.
258. Chinchilla, R.; Najera, C., The Sonogashira Reaction: A Booming Methodology in Synthetic Organic Chemistry. *Chem. Rev.* **2007**, *107*, 874-922.
259. Prim, D.; Campagne, J. M.; Joseph, D.; Andrioletti, B., Palladium-catalysed Reactions of Aryl Halides with Soft, Non-organometallic Nucleophiles. *Tetrahedron* **2002**, *58*, 2041-2075.
260. Ley, S. V.; Thomas, A. W., Modern Synthetic Methods for Copper-mediated C(aryl)-O, C(aryl)-N, and C(aryl)-S Bond Formation. *Angew. Chem. Int. Edit.* **2003**, *42*, 5400-5449.
261. Wu, Y. J.; He, H., Copper-catalyzed Cross-coupling of Aryl Halides and Thiols Using Microwave Heating. *Synlett.* **2003**, 1789-1790.
262. Miljanic, O. S.; Vollhardt, K. P. C.; Whitener, G. D., An Alkyne Metathesis-based Route to Ortho-dehydrobenzannulenes. *Synlett.* **2003**, 29-34.
263. Sperotto, E.; van Klink, G. P. M.; de Vries, J. G.; van Koten, G., Ligand-free Copper-Catalyzed C-S Coupling of Aryl Iodides and Thiols. *J. Org. Chem.* **2008**, *73*, 5625- 5628.
264. Cherng, Y. H., Efficient Nucleophilic Substitution Reactions of Pyrimidyl and Pyrazyl Halides with Nucleophiles, under Focused Microwave Irradiation. *Tetrahedron* **2002**, *58*, 887-890.
265. Sonogashira, K. Tohda, Y.; Hagihara, N. Convenient Synthesis of Acetylenes. Catalytic Substitutions of Acetylenic Hydrogen with Bromo Alkenes, Iodo Arenes, and Bromopyridines. *Tetrahedron Lett.* **1975**, *16*, 4467-4470.

266. Negishi, E. I.; Anastasia, L. Palladium-Catalyzed Alkylation. *Chem. Rev.* **2003**, *103*, 1979-2017.
267. Gangjee, A.; Yu, J.; Kisliuk, R. L.; Haile, . H.; Sobrero, G. and McGuire, J. J.. Design, Synthesis, and Biological Activities of Classical *N*-{4-[2-(2-Amino-4-ethylpyrrolo[2,3-*d*]pyrimidin-5-yl)ethyl]benzoyl}-l-glutamic Acid and Its 6-Methyl Derivative as Potential Dual Inhibitors of Thymidylate Synthase and Dihydrofolate Reductase and as Potential Antitumor Agents, *J. Med. Chem.*, **2003**, *46*, 591–600.
268. Gangjee, A.; Yu, J.; Copper, J. E. and Smith, C. D.. Discovery of Novel Antitumor Antimitotic Agents that Also Reverse Tumor Resistance. *J. Med. Chem.*, **2007**, *50*, 3290–3301.
269. Erdelyi, M.; Langer, V.; Karlen, A.; Gogoll, A., Insight Into β -hairpin Stability: A Structural and Thermodynamic Study of Diastereomeric β -hairpin Mimetics. *New J. Chem.* **2002**, *26*, 834-843.
270. Gangjee, A.; Lin, X.; Kisliuk, R. L.; McGuire, J. J. Synthesis of *N*-{4-[(2,4-Diamino-5-methyl-4,7-dihydro-3H- pyrrolo[2,3-*d*]pyrimidin-6-yl)thio]benzoyl}-L-glutamic Acid and *N*-{4-[(2-Amino-4-oxo-5-methyl-4,7-dihydro-3H-pyrrolo[2,3-*d*]pyrimidin- 6-yl)thio]benzoyl}-L-glutamic Acid as Dual Inhibitors of Dihydrofolate Reductase and Thymidylate Synthase and as Potential Antitumor Agents *J. Med. Chem.* **2005**, *48*, 7215-7222.
271. Gangjee, A.; Lin, X.; Queener, S. F. Design, Synthesis, and Biological Evaluation of New 2,4-Diamino-5-methyl-6-substituted-pyrrolo [2, 3-*d*]pyrimidines as Dihydrofolate Reductase Inhibitors. *J. Med. Chem.* **2004**, *47*, 3689-3692.

272. Masur, H. Problems in the Management of Opportunistic Infections in Patients Infected with Human Immunodeficiency Virus. *J. Infect. Dis.* **1990**, *161*, 858–864.
273. Kovace, J. A.; Hiemenz, J. W.; Macher, A. M.; Stover, D.; Murray, H. W.; Shelhamer, J.; Lane, H. C.; Urmacher, U.; Honig, C.; Longo, D. L.; Parker, M. M.; Nataneon, J. E.; Parrillo, J. E.; Fauci, A. S.; Pizzo, P. A.; Maeur, H. *Pneumocystis carinii* Pneumonia: A Comparison between Patients with the Acquired Immunodeficiency Syndrome and Patients with Other Immunodeficiencies. *Ann. Intern. Med.* **1984**, *100*, 68–71.
274. Seage, G. R.; Losina, E.; Goldie, S. J.; Paltiel, A. D.; Kimmel, A. D.; Freedberg, K. A. The Relationship of Preventable Opportunistic Infections, HIV-1 RNA, and CD4 Cell Counts to Chronic Mortality. *JAIDS, J. Acquired Immune Defic. Syndr.* **2002**, *30*, 421-428.
275. Walzer P D; Foy J; Steele P; White M Synergistic combinations of Ro 11-8958 and other dihydrofolate reductase inhibitors with sulfamethoxazole and dapsone for therapy of experimental pneumocystosis. *Antimicrobial agents and chemotherapy* 1993, *37*, 1436-43.
276. Champness, J. N.; Achari, A.; Ballantine, S. P.; Bryant, P. K.; Delves, C J.; Stammers, D. K. The structure of *Pneumocystis carinii* Dihydrofolate Reductase to 1.9 Å Resolution. *Structure* **1994**, *2*, 915-924.
277. Cody, V.; Wojtczak, A.; Kalman, T. I.; Friesheim, J. H.; Blakley, R. L. Conformational Analysis of Human Dihydrofolate Reductase Inhibitor Complexes: Crystal Structure Determination of Wild Type and F31 Mutant Binary and Ternary Inhibitor Complexes. *Adv. Exp. Med. Biol.* **1993**, *338*, 481-486.

278. Roos, D. S. Primary Structure of the Dihydrofolate Reductase-Thymidylate Synthase Gene from *Toxoplasma gondii*. *J. Biol. Chem.* **1993**, *268*, 6269-6280.
279. Rosowsky, A.; Chaykovsky, M.; Chen, K. K. N.; Lin, M.; Modest, E. J. 2,4-Diaminothieno[2,3-*d*]pyrimidines as Antifolates and Antimalarials. 1. Synthesis of 2,4-Diamino-5,6,7,8-tetrahydrothianaphtheno[2,3-*d*]pyrimidines and Related Compounds. *J. Med. Chem.* **1973**, *16*, 185-188.
280. Rosowsky, A.; Chen, K. K. N.; Lin, M. 2,4-Diaminothieno[2,3-*d*]pyrimidines as Antifolates and Antimalarials. 3. Synthesis of 5,6-Disubstituted Derivatives and Related Tricyclic Analogs. *J. Med. Chem.* **1973**, *16*, 191-194.
281. Elslager, E. F.; Jacob, P.; Werbel, L. M. Folate Antagonists. 6. Synthesis and Antimalarial Effect of Fused 2,4-diaminothieno[2,3-*d*]pyrimidines. *J. Heterocycl. Chem.* **1972**, *9*, 775-782.
282. Rosowsky, A.; Mota, C. E.; Wright, J. E.; Freisheim, J. H.; Heusner, J. J.; McCormack, J. J.; Queener, S. F. 2,4-Diaminothieno[2,3-*d*]pyrimidine Analogues of Trimetrexate and Piritrexim as Potential Inhibitors of *Pneumocystis carinii* and *Toxoplasma gondii* Dihydrofolate Reductase. *J. Med. Chem.* **1993**, *36*, 3103-3112.
283. Gangjee, A.; Qiu, Y.; Kisliuk, R. L. Synthesis Classical and Nonclassical 2-Amino-4-oxo-6-benzyl-thieno[2,3-*d*]pyrimidines as Potential Thymidylate Synthase Inhibitors. *J. Heterocycl. Chem.* **2004**, *41*, 941-946.
284. Hitchings, G. H. Functions of Tetrahydrofolate and the Role of Dihydrofolate Reductase. In *Cellular Metabolism in Inhibition of Folate Metabolism in Chemotherapy*; Hitchings, G. H., Ed.; Springer Verlag: New York. **1983**, 11-23.

285. Jackman, A. L.; Taylor, G. A.; Gibson, W.; Kimbell, R.; Brown, M.; Calvert, A. H.; Judson, I. R.; Hughes, L. R. ICI D1694, a Quinazoline Antifolate Thymidylate Synthase Inhibitor That Is a Potent Inhibitor of L1210 Tumour Cell Growth in Vitro and in Vivo: A New Agent for Clinical Study. *Cancer Res.* **1991**, *51*, 5579-5586.
286. Taylor, E. C.; Kuhnt, D.; Shih, C.; Rinzel, S. M.; Grindey, G. B.; Barredo, J.; Jannatipour, M.; Moran, R. A Dideazatetrahydrofolate Analogue Lacking a Chiral Center at C-6, N-[4-[2-(2-Amino-3,4-dihydro-4-oxo-7H-pyrrolo[2,3-d]pyrimidin-5-yl)ethylbenzoyl]-L-glutamic Acid, Is an Inhibitor of Thymidylate Synthase. *J. Med. Chem.* **1992**, *35*, 4450-4454.
287. Bertino, J. R.; Kamen, B.; Romanini, A. Folate Antagonists. In *Cancer Medicine*; Holland, J. F., Frei, E., Bast, R. C., Kufe, D. W., Morton, D. L., Weichselbaum, R. R., Eds.; Williams and Wilkins: Baltimore, MD, 1997; Vol. 1, pp 907-921.
288. Gibson, W.; Bisset, G. M. F.; Marsham, P. R.; Kelland, L. R.; Judson, I. R.; Jackman, A. L. The Measurement of Polyglutamate Metabolites of the Thymidylate Synthase Inhibitor, ICI D1694, in Mouse and Human Cultured Cells. *Biochem. Pharmacol.* **1993**, *45*, 863-869.
289. Jackman, A. L.; Newell, D. R.; Gibson, W.; Jodrell, D. I.; Taylor, G. A.; Bishop, J. A.; Hughes, L. R.; Calvert, A. H. The Biochemical Pharmacology of the Thymidylate Synthase Inhibitor 2-Desamino-2-methyl- N^{10} -propargyl-5,8-dideazafolic Acid (ICI198583). *Biochem. Pharmacol.* **1991**, *42*, 1885-1895.
290. Nair, M. G.; Abraham, A.; McGuire, J. J.; Kisliuk, R. L.; Galivan, J. H.; Ferone, R. Polyglutamylation as a Determinant of Cytotoxicity of Classical Folate Analog

Inhibitors of Thymidylate Synthase and Glycinamide Ribonucleotide

Formyltransferase. *Cell. Pharmacol.* **1994**, *1*, 245-249.

291. Bisset, G. M. F.; Pawelczak, K.; Jackman, A. L.; Calvert, A. H.; Hughes, L. R. Syntheses and Thymidylate Synthase Inhibitory Activity of the Poly- γ -glutamyl Conjugates of *N*-[5-[*N*-(3,4-Dihydro-2-methyl-4-oxoquinazolin-6-ylmethyl)-*N*-methylamino]-2-thienoyl]-L-glutamic Acid (ICI D1694) and Other Quinazoline Antifolates. *J. Med. Chem.* **1992**, *35*, 859-866.
292. Jackman, A. L.; Taylor, G. A.; Gibson, W.; Kimbell, R.; Brown, M.; Calvert, A. H.; Judson, I. R.; Hughes, L. R. ICI D1694, a Quinazoline Antifolate Thymidylate Synthase Inhibitor That Is a Potent Inhibitor of L1210 Tumour Cell Growth in Vitro and in Vivo: A New Agent for Clinical Study. *Cancer Res.* **1991**, *51*, 5579-5586.
293. Taylor, E. C.; Kuhnt, D.; Shih, C.; Rinzel, S. M.; Grindey, G. B.; Barredo, J.; Jannatipour, M.; Moran, R. A Dideazatetrahydrofolate Analogue Lacking a Chiral Center at C-6, *N*-[4-[2-(2-Amino-3,4-dihydro-4-oxo-7H-pyrrolo[2,3-d]pyrimidin-5-yl)ethylbenzoyl]-L-glutamic Acid, Is an Inhibitor of Thymidylate Synthase. *J. Med. Chem.* **1992**, *35*, 4450-4454.
294. Barakat, R. R.; Li, W. W.; Lovelace, C.; Bertino, J. R. Intrinsic Resistance of Cervical Squamous Cell Carcinoma Cell Lines to Methotrexate (MTX) as a Result of Decreased Accumulation of Intracellular Methotrexate Polyglutamates. *Gynecol. Oncol.* **1993**, *51*, 54-60.
295. Braakhuis, B. J. M.; Jansen, G.; Noordhuis, P.; Kegel, A.; Peters, G. J. Importance of Pharmacodynamics in the *In Vitro* Antiproliferative Activity of the Antifolates

- Methotrexate and 10-Deazaaminopterin Against Human Head and Neck Squamous Cell Carcinoma. *Biochem. Pharmacol.* **1993**, *46*, 2155-2161.
296. Liani, E.; Rothem, L.; Bunni, M. A.; Smith, C. A.; Jansen, G.; Assaraf, Y. G. Loss of Folylpoly- γ -glutamate Synthetase Activity is a Dominant Mechanism of Resistance to Polyglutamylated Novel Antifolates in Multiple Human Leukemia Sublines. *Int. J. Cancer* **2000**, *87*, 2583-2588.
- Sheng, Y.; Sun, X.; Shen, Y.; Bogner, A. L.; Baker, E. N.; Smith, C. A. Structural and Functional Similarities in the ADP-forming Amide Bond Ligase Superfamily: Implications for a Substrate-Induced Conformational Change in Folylpolyglutamate Synthetase. *J. Mol. Biol.* **2000**, *302*, 427-440.
297. Kalman, T. I. Mechanism Based Approaches to Inhibition of the Synthesis and Degradation of Folate and Antifolate Polyglutamates. *Adv. Exp. Med. Biol.* **1993**, *338*, 639-643.
298. Gangjee, A.; Devraj, R.; McGuire, J. J.; Kisliuk, R. L. 5-Arylthio Substituted 2-Amino-4-oxo-6-methylpyrrolo[2,3-*d*]pyrimidine Antifolates as Thymidylate Synthase Inhibitors and Antitumor Agents. *J. Med. Chem.* **1995**, *38*, 4495-4502.
299. Marsham, P. R.; Jackman, A. L.; Barker, A. J.; Boyle, F. T.; Pegg, S. J.; Wardleworth, J. M.; Kimbell, R.; O'Connor, B. M.; Calvert, A. H.; Hughes, L. R. Quinazoline Antifolate Thymidylate Synthase Inhibitors: Replacement of Glutamic Acid in the C2-Methyl Series. *J. Med. Chem.* **1995**, *38*, 994-1004.
300. Tripos Inc., 1699 South Hanley Road, St. Louis, MO 63144.
301. Dev, I. K.; Dallas, W. S.; Ferone, R.; Hanlon, M.; McKee, D. D.; Yates, B. B. Mode of Binding of Folate Analogs to Thymidylate Synthase. Evidence for Two

- Asymmetric but Interactive Substrate Binding Sites. *J. Biol. Chem.* **1994**, *269*, 1873-1882.
302. Pendergast, W.; Dickerson, S. H.; Dev, I. K.; Ferone, R.; Duch, D. S.; Smith, G. K. Benzo[f]quinazoline Inhibitors of Thymidylate Synthase: Methyleneamino-linked Arylglutamate Derivatives. *J Med Chem.* **1994**, *37*, 838-844.
303. Beutel, G.; Glen, H.; Schoffski, P.; Chick, J.; Gill, S.; Cassidy, J.; Twelves, C. Phase I Study of OSI-7904L, a Novel Liposomal Thymidylate Synthase Inhibitor in Patients with Refractory Solid Tumors. *Clin Cancer Res.* **2005**, *11*, 5487-5495.
304. Hooijberg, J. H.; Broxterman, H. J.; Kool, M.; Assaraf, Y. G.; Peters, G. J.; Noordhuis, P.; Scheper, R. J.; Borst, P.; Pinedo, H. M.; Jansen, G. Antifolate Resistance Mediated by the Multidrug Resistance Proteins MRP1 and MRP2. *Cancer Res.* **1999**, *59*, 2532-2535.
305. Montfort, W. R.; Weichsel, A. Thymidylate Synthase: Structure, Inhibition, and Strained Conformations During Catalysis. *Pharmacol. Ther.* **1997**, *76*, 29-43.
306. Zakrzewski, S. F.; Dave, C.; Rosen, F. Comparison of the Antitumor Activities and Toxicity of the 2,4-5(1-adamantyl)-6-methylpyrimidine and 2,4-Diamino-5-(1-adamantyl)6-ethyl-pyrimidine. *J. Natl. Cancer. Invest.* **1978**, *60*, 1029-1033.
307. Bliss, E. A.; Griffin, R. J.; Stevens, M. F. G. Structural Studies on Bioactive Compounds. Part 5. Synthesis and Properties of 2,4-Diaminopyrimidine DHFR Inhibitors Bearing Lipophilic Azido Groups. *J. Chem. Soc. Perkin Trans. I* **1987**, *1*, 2217- 2228.
308. Seage, G. R.; Losina, E.; Goldie, S. J.; Paltiel, A. D.; Kimmel, A. D.; Freedberg, K. A. The Relationship of Preventable Opportunistic Infections, HIV-1 RNA, and

- CD4 Cell Counts to Chronic Mortality. *JAIDS, J. Acquired Immune Defic. Syndr.* **2002**, *30*, 421-428.
309. Klepser, M. E.; Klepser, T. B. Drug Treatment of HIV-Related Opportunistic Infections. *Drugs* **1997**, *53*, 40–73.
310. DeClercq, E. Toward Improved Anti-HIV Chemotherapy: Therapeutic Strategies for Intervention with HIV Infections. *J. Med. Chem.* **1995**, *38*, 2491–2517.
311. Masur, H.; Polis, M. A.; Tuazon, C. V.; Ogota-Arakaki, D.; Kovacs, J. A.; Katz, D.; Hilt, D.; Simmons, T.; Feuerstein, I.; Lundgren, B.; Lane, H. C.; Chabner, B. A.; Allegra, C. J. Salvage Trial of Trimetrexate-Leucovorin for the Treatment of Cerebral Toxoplasmosis. *J. Infect. Dis.* **1993**, *167*, 1422-1426.
312. Gangjee, A.; Vasudevan, A.; Queener, S. F.; Kisliuk, R. L. 2,4-Diamino-5-Deaza-6-Substituted Pyrido[2,3-*d*]pyrimidine Antifolates as Potent and Selective Nonclassical Inhibitors of Dihydrofolate Reductases. *J. Med. Chem.* **1996**, *39*, 1438-1446.
313. News. FDA Approves Trimetrexate as Second line Therapy of *Pneumocystis carinii* Pneumonia *Am. J. Hosp. Pharm.* **1994**, *51*, 591-592.
314. Gangjee, A.; Li, W.; Kisliuk, R. L.; Cody, V.; Pace, J.; Piraino, J.; Makin, J. Design, Synthesis, and X-ray Crystal Structure of Classical and Nonclassical 2-Amino-4-oxo-5-substituted-6-ethylthieno[2,3-*d*]pyrimidines as Dual Thymidylate Synthase and Dihydrofolate Reductase Inhibitors and as Potential Antitumor Agents. *J. Med. Chem.* **2009**, *52*, 4892-4902.
315. Vainio, M. J.; Johnson, M. S. Generating conformer ensembles using a Multiobjective Genetic Algorithm. *J. Chem. Inf. Model.* **2007**, *47*, 2462-2474.

316. Stokstad, E. L. R. Historical Perspective On Key Advances in the Biochemistry and Physiology of Folates, in *Folic Acid Metabolism in Health and Disease*. M. F. Piccian, E. L. R. Stokstad and J. F. Gregory Eds., Wiley-Liss, New York, **1990**, pp 1-21.
317. Monahan, B. P. and Allegra, C. J. Antifolates. *Can. Chemother. Biother.*, **2006**, *4*, 91-124.
318. Chu, E.; Callender, M. A.; Farrell, M. P. and Schmitz, J. C. Thymidylate Synthase Inhibitors as Anticancer Agents: From Bench to Bedside. *Cancer Chemother. Pharmacol.*, **2003**, *52 Suppl. 1*, S80-89.
319. Hazarika, M.; White, R. M.; Johnson, J. R. and Pazdur, R. FDA Drug Approval Summaries: Pemetrexed (Alimta). *Oncologist*, **2004**, *9*, 482-488.
320. Cohen, M. H.; Johnson, J. R.; Wang, Y. C.; Sridhara, R. and Pazdur, R. FDA Drug Approval Summary: Pemetrexed for Injection (Alimta) for the Treatment of Non-Small Cell Lung Cancer. *Oncologist*, **2005**, *10*, 363-368.
321. Taylor, E. C.; Harrington, P. J.; Fletcher, S. R.; Beardsley, G. P. and Moran, R. G. Synthesis of the Antileukemic Agents 5,10-Dideazaaminopterin and 5,10-dideaza-5,6,7,8-tetrahydroaminopterin. *J. Med. Chem.*, **1985**, *28*, 914-921.
322. Stock, C. C.; Reilly, H. C.; Buckley, S. M.; Clarke, D. A. and Rhoads, C. P. Azaserine, a New Tumour-Inhibitory Substance; Studies with Crocker Mouse Sarcoma 180. *Nature*, **1954**, *173*, 71-72.
323. Lewis, L. R.; Robins, R. K. and Cheng, C. C. The Preparation and Antitumor Properties of Acylated Derivatives of 6-Thiopurine Ribosides. *J. Med. Chem*, **1964**, *7*, 200-204.

324. Hertz, R. and Tullner, W. W. Inhibition of Estrogen-induced Growth in the Genital Tract of the Female Chick by a Purine Antagonist; Reversal by Adenine. *Science*, **1949**, *109*, 539.
325. Jackson, R. C. and Harkrader, R. J. The Contributions of de novo and Salvage Pathways of Nucleotide Biosynthesis in Normal and Malignant Cells., in *Nucleosides and Cancer Treatment*. M. H. N. Tattersall and R. M. Fox Eds., Academic Press, Sydney, **1981**, pp 18-31.
326. Tonkinson, J. L.; Marder, P.; Andis, S. L.; Schultz, R. M.; Gossett, L. S.; Shih, C. and Mendelsohn, L. G. Cell Cycle Effects of Antifolate Antimetabolites: Implications for Cytotoxicity and Cytostasis. *Cancer Chemother. Pharmacol.*, **1997**, *39*, 521-531.
327. Smith, S. G.; Lehman, N. L. and Moran, R. G. Cytotoxicity of Antifolate Inhibitors of Thymidylate and Purine Synthesis to WiDr Colonic Carcinoma Cells. *Cancer Res.*, **1993**, *53*, 5697-5706.
328. Deng, Y.; Wang, Y.; Cherian, C.; Hou, Z.; Buck, S. A.; Matherly, L. H. and Gangjee, A. Synthesis and Discovery of High Affinity Folate Receptor-Specific Glycinamide Ribonucleotide Formyltransferase Inhibitors with Antitumor Activity. *J. Med. Chem.*, **2008**. *51*, 5052-5063.
328. Mauritz, R.; Peters, G. J.; Kathmann, I.; Teshale, H.; Noordhuis, P.; Comijn, E. M.; Pinedo, H. M. and Jansen, G. Dynamics of Antifolate Transport via the Reduced Folate Carrier and the Membrane Folate Receptor in Murine Leukaemia Cells in vitro and in vivo. *Cancer Chemother. Pharmacol.*, **2008**, *62*, 937-948.

329. Elnakat, H. and Ratnam, M. Distribution, Functionality and Gene Regulation of Folate Receptor Isoforms: Implications in Targeted Therapy. *Adv. Drug Deliv.*, **2004**, *56*, 1067-1084.
330. Salazar, M. D. and Ratnam, M. The Folate Receptor: What Does It Promise In Tissue-Targeted Therapeutics? *Cancer Metastasis Rev.*, **2007**, *26*, 141-152.
331. Leamon, C. P.; Reddy, J. A.; Vlahov, I. R.; Westrick, E.; Dawson, A.; Dorton, R.; Vetzal, M.; Santhapuram, H. K. and Wang, Y. Preclinical Antitumor Activity of a Novel Folate-Targeted Dual Drug Conjugate. *Mol. Pharm.*, **2007**, *4*, 659-667.
332. Lu, Y.; Wu, J.; Gonit, M.; Yang, X.; Lee, A.; Xiang, G.; Li, H.; Liu, S.; Marcucci, G.; Ratnam, M. and Lee, R. J. Role of Formulation Composition in Folate Receptor-Targeted Liposomal Doxorubicin Delivery to Acute Myelogenous Leukemia Cells. *Mol. Pharm.*, **2007**, *4*, 707-712.
333. Muller, C.; Forrer, F.; Schibli, R.; Krenning, E. P. and de Jong, M. SPECT Study of Folate Receptor-Positive Malignant and Normal Tissues in Mice Using a Novel ^{99m}Tc-Radiofolate. *J. Nucl. Med.*, **2008**, *49*, 310-317.
334. Jansen, G. Receptor- and Carrier-Mediated Transport Systems for Folates and Antifolates: Exploitation for Folate Chemotherapy and Immunotherapy, in *Anticancer Development Guide: Antifolate Drugs in Cancer Therapy*. A. L. Jackman Ed., Humana Press Inc., Totowa, NJ, **1999**, 293-321.
335. Ray, M. S.; Muggia, F. M.; Leichman, C. G.; Grunberg, S. M.; Nelson, R. L.; Dyke, R. W. and Moran, R. G. Phase I Study of (6R)-5,10-Dideazatetrahydrofolate: A Folate Antimetabolite Inhibitory to de novo Purine Synthesis. *J. Natl. Cancer Inst.*, **1993**, *85*, 1154-1159.

336. Deng, Y.; Zhou, X.; Desmoulin, S. K.; Wu, J.; Cherian, C.; Hou, Z.; Matherly, L. H Gangjee, A.; Lin, X.; Synthesis and Biological Activity of a Novel Series of 6-Substituted Thieno[2,3-d]pyrimidine Antifolate Inhibitors of Purine Biosynthesis with Selectivity for High Affinity Folate Receptors over the Reduced Folate Carrier and Proton-Coupled Folate Transporter for Cellular Entry. *J. Med. Chem.* **2009**, *52*, 2940-2951.
337. O'Connor, P. M.; Jackman, J.; Bae, I.; Myers, T. G.; Fan, S.; Mutoh, M.; Scudiero, D. A.; Monks, A.; Sausville, E. A.; Weinstein, J. N.; Friend, S.; Fornace, A. J. Jr. and Kohn, K. W. Characterization of the p53 Tumor Suppressor Pathway in Cell Lines of the National Cancer Institute Anticancer Drug Screen and Correlations with the Growth-inhibitory Potency of 123 Anticancer Agents. *Cancer Res.*, **1997**, *57*, 4285-4300.
338. Jordan, M. A. and Kamath, K. How do Microtubule-Targeted Drugs Work? An Overview. *Curr. Cancer Drug Targets*, **2007**, *7*, 730-742.
339. Lee, J. F. and Harris, L. N. Antimicrotubule Agents. In *Cancer: Principles & Practice of Oncology* 8th ED., V. T. DeVita, Jr., T. S. Lawrence and S. A. Rosenberg Eds., Lippincott Williams & Wilkins, **2008**, 447-456.
340. Löwe, J.; Li, H.; Downing, K. H. and Nogales, E. Refined Structure of $\alpha\beta$ -Tubulin at 3.5Å Resolution. *J. Mol. Biol.*, **2001**, *313*, 1045-1057.
341. Huey, R. M.; Calvo, E.; Barasoain, I.; Pineda, O.; Edler, M. C.; Matesanz, R.; Cerezo, G.; Vanderwal, C. D.; Day, B. W.; Sorensen, E. J.; Lopez, J. A.; Andreu, J. M.; Hamel, E. and Diaz, J. F. Cyclostreptin Binds Covalently to Microtubule Pores and Luminal Taxoid Binding Sites. *Nat. Chem. Biol.*, **2007**, *3*, 117-125.

342. Kanthou, C. and Tozer, M. T. Microtubule Depolymerizing Vascular Disrupting Agents: Novel Therapeutic Agents for Oncology and Other Pathologies. *Int. J. Exp. Path.*, 2009, *90*, 284-294.
343. Carlson, R. O. New Tubulin Targeting Agents Currently in Clinical Development. *Expert Opin. Investig. Drugs*, **2008**, *17*, 707-722.
344. Vos, J. W.; Dogterom, M.; Emons, A. M.. Microtubules Become More Dynamic but not Shorter During Preprophase Band Formation: A Possible ‘Search-and capture’ Mechanism for Microtubule translocation. *Cell Motil Cytoskeleton*, **2004**, *57*, 246-258.
345. Goldstein, L. J.; Galski, H.; Fojo, A.; Willingham, M.; Lai, S. L. ; et al. Expression of a Multidrug Resistance Gene in Human Cancers. *J. Natl. Cancer Inst.*, **1989**, *81*, 116-124.
346. Leonard, G. D.; Fojo, T. and Bates, S. E. The Role of ABC Transporters in Clinical Practice. *Oncologist*, **2003**, *8*, 411-424.
347. Yeh, J. J.; Hsu, W. H.; Wang, J. J.; Ho, S. T. and Kao, A. Predicting Chemotherapy Response to Taxol-based Therapy in Advanced Non-Small-Cell Lung Cancer with P-glycoprotein Expression. *Respiration*, **2003**, *70*, 32 – 35.
348. Chiou, J. F.; Liang, J. A.; Hsu, W. H.; Wang, J. J.; Ho, S. T. and Kao, A. Comparing the Relationship of Taxol-based Chemotherpay Response with P-glycoprotein and Lung Resistance-related Protein Expression in Non-Small Cell Lung Cancer. *Lung*, **2003**, *181*, 267 – 273.
349. Fojo, T. and Menefee, M. Mechanisms of Multidrug Resistance: The Potential Role of Microtubule-stabilizing Agents. *Ann. Oncol.*, **2007**, *18*, 3 – 8.

350. Rosell, R.; Scagliotti, G.; Danenberg, K. D.; Lord, R. V. N.; Bepler, G.; Novello, S.; Cooc, J.; Crino, L.; Sanchez, J. J.; Taron, M.; Boni, C.; De Marinis, F.; Tonato, M.; Marangolo, M.; Gozzelino, F.; Di Costanzo, F.; Rinaldi, M.; Salonga, D.; Stephens, C. Transcripts in Pretreatment Biopsies From A Three-Arm Randomized Trial In Metastatic Non-Small-Cell Lung Cancer. *Oncogene*, **2003**, *22*, 3548 – 3553.
351. Dumontet, C.; Isaac, S.; Souquet, P.-J.; Bejui-Thivolet, F.; Pacheco, Y.; Peloux, N.; Frankfurter, A.; Luduena, R.; Perol, M. Expression of Class III Beta Tubulin In Non-Small Cell Lung Cancer Is Correlated With Resistance To Taxane Chemotherapy. *Bull. Cancer*, **2005**, *92*, 25 – 30.
352. Seve, P.; Isaac, S.; Tredan, O.; Souquet, P.-J.; Pacheco, Y.; Perol, M.; Lafanechere, L.; Penet, A.; Peiller, E.-L.; Dumontet, C. Expression of Class III β - Tubulin Is Predictive of Patient Outcome in Patients with Non-Small Cell Lung Cancer Receiving Vinorelbine-Based Chemotherapy *Clin. Cancer Res.*, **2005**, *11*, 5481 – 5486.
353. Tommasi S.; Mangia A.; Lacalamita R.; Bellizzi A.; Fedele V.; Chiriatti A.; Thomssen C.; Kendzierski N.; Latorre A.; Lorusso V.; Schittulli F.; Zito F.; Kavallaris M.; Paradiso A. Cytoskeleton and Paclitaxel Sensitivity In Breast Cancer: The Role Of Beta-Tubulins. *Int. J. Cancer*, **2007**, *120*, 2078 – 2085.
354. Mozzetti, S.; Ferlini, C.; Concolino, P.; Filippetti, F.; Raspaglio, G.; Prislei, S.; Gallo, D.; Martinelli, E.; Ranelletti, F. O.; Ferrandina, G.; Scambia, G. Class III β -tubulin Overexpression Is A Prominent Mechanism Of Paclitaxel Resistance In Ovarian Cancer Patients. *Clin. Cancer Res.* **2005**, *11*, 298 – 305.

355. Ferrandina, G.; Zannoni, G. F.; Martinelli, E.; Paglia, A.; Gallotta, V.; Mozzetti, S.; Scambia, G.; Ferlini, C. Class III β -Tubulin Overexpression Is A Marker Of Poor Clinical Outcome In Advanced Ovarian Cancer Patients. *Clin. Cancer Res.*, **2006**, *12*, 2774 – 2779.
356. Strengel, C.; Newman, S. P.; Lesse, M. P.; Potter, B. V. L.; Reed, M. J. and Purohit, A. Class III Beta- Tubulin Expression and in vitro Resistance To Microtubule Targeting Agents. *Brit. J. Cancer*, **2010**, *102*, 316 – 324.
357. Lee L., Robb L.M., Lee M., Davis R., Mackay, H., Chavda, S., O'Brien, E.L., Risinger, AL, Mooberry, SL, Lee, M. Design, Synthesis and Biological Evaluations of 2,5-Diaryl-2,3-dihydro-1,3,4-oxadiazoline Analogs of Combretastatin-A4. *J. Med. Chem.* **2010**, *53*, 325 – 334.
358. Gewalt K.; Schinke E.; Böttcher H., Heterocyclen aus CH-aciden nitrilen. VII. 2-Aminothiophene aus oxo-Mercaptanen und Methylenaktiven Nitrilen. *Chem. Ber.* **1966**, *99*, 94-100.
359. Zhang, M.; Harper, R. W. A Concise Synthetic Entry to Substituted 2-Aminothieno[2,3-*d*]pyrimidines via a Gewalt Precursor. *Bioorg. Med. Chem. Lett.* **1997**, *7*, 1629-1634.
360. Gangjee, A.; Mavandadi, F.; Kisliuk, R. L.; McGuire, J. J.; Queener, S. F. 2-Amino-4-oxo-5-substituted-pyrrolo[2,3-*d*]pyrimidines as Nonclassical Antifolate Inhibitors of Thymidylate Synthase. *J. Med. Chem.* **1996**, *39*, 4563-4568.
361. Rosowsky, A.; Forsch, R. A.; Null, A.; Moran, R. G., 5-Deazafolate Analogues

- with a Rotationally Restricted Glutamate or Ornithine Side Chain: Synthesis and Binding Interaction with Folylpolyglutamate Synthetase. *J. Med. Chem.* **1999**, *42*, 3510-3519.
362. Rosowsky, A.; Chen, K. K.; Lin, M., 2,4-Diaminothieno[2,3-d]pyrimidines as Antifolates and Antimalarials. 3. Synthesis of 5,6-Disubstituted Derivatives and Related Tetracyclic Analogs. *J. Med. Chem.* **1973**, *16*, 191-194.
363. Gangjee, A.; Yu, J. M.; Copper, J. E.; Smith, C. D., Discovery of Novel Antitumor Antimitotic Agents that also Reverse Tumor Resistance. *J. Med. Chem.* **2007**, *50*, 3290-3301.
364. Sengupta, S. K.; Chatterjee, S.; Protopapa, H. K.; Modeat, E. J., 2,3-Diaminopyrimidines from Dicyandiamide. IV. Condensation with Bicyclic Aromatic Ketones. *J. Org. Chem* **1972**, *37*, 1323-1328.
365. Wartenberg, F. H.; Koppe, T.; Wetzal, W.; Wydra, M.; Benz, A., Method for Producing Benzo Annelated Heterocycles. PCT Int. Appl.(2001), CODEN: PIXXD2 WO 01/77099 A1 19980305
366. Grossman, R. B. Transition-Metal-Catalyzed and -Mediated Reactions. In *The art of writing reasonable organic reaction mechanisms*. Grossman, R. B. 2nd Ed. Springer Press: New York, **2003**, pp 285.
367. Marsham, P. R.; Jackman, A. L.; Hayter, A. J.; Daw, M. R.; Snowden, J. L.; O'Connor, B. M.; Bishop, J. A.; Calvert, A. H.; Hughes, L. R., Quinazoline Antifolate Thymidylate Synthase Inhibitors: Bridge Modifications and Conformationally Restricted Analogues in the C2-methyl Series. *J. Med. Chem.* **1991**, *34*, 2209-2218.

368. Gangjee, A.; Devraj, R.; McGuire, J. J.; Kisliuk, R. L. 5-Arylthio Substituted 2-Amino-4-oxo-6-methylpyrrolo[2,3-*d*]pyrimidine Antifolates as Thymidylate Synthase Inhibitors and Antitumor Agents. *J. Med. Chem.* **1995**, *38*, 4495-4502.
369. Gangjee, A.; Qiu, Y.; Li, W.; Kisliuk, R. L., Potent Dual Thymidylate Synthase and Dihydrofolate Reductase Inhibitors: Classical and Nonclassical 2-amino-4-oxo-5-arylthio-substituted-6-methylthieno[2,3-*d*]pyrimidine Antifolates. *J. Med. Chem.* **2008**, *51*, 5789-5797.
370. Taylor, E. C.; Young, W. B.; Chaudhari, R.; Patel, M. Synthesis of a Regioisomer of N-{4-[2-(2-amino-4(3*H*)-oxo-7*H*-pyrrolo[2,3-*d*]pyrimidin-5-yl)ethyl]benzoyl}-L-glutamic Acid (LY231514), an Active Thymidylate Synthase Inhibitor and Antitumor Agent. *Heterocycles* **1993**, *36*, 1897-1908.
371. Itoh, T.; Mase, T., A general palladium-catalyzed coupling of aryl bromides/triflates and thiols. *Org. Lett.* **2004**, *6*, 4587-4590.
372. Cherng, Y. H., Efficient nucleophilic substitution reactions of pyrimidyl and pyrazyl halides with nucleophiles, under focused microwave irradiation. *Tetrahedron.* **2002**, *58*, 887-890.
373. Larock, C. R.; Leung, W.; Stolz-Dunn, S. Synthesis of Aryl-substituted Aldehydes and Ketones via Palladium-Catalyzed Coupling of Aryl Halides and Non-Allylic Unsaturated Alcohols. *Tetrahedron Lett.* **1989**, *30*, 6629-6632.
374. Gangjee, A.; Zhou, X.; Zhang, X.; Kisliuk, R. L., Classical and Nonclassical 2-Amino-4-oxo-5-arylthio-substituted-6-isopropyl thieno[2,3-*d*]pyrimidine Antifolates as Potent Thymidylate Synthase Inhibitors. Presented at the 237th American

Chemical Society (ACS) National Meeting, Salt Lake City, UT, March 22-26, 2009,
MEDI 095.

Appendix

The biological evaluations of the analogs listed in the following tables were performed by Dr. Roy L. Kisliuk (Department of Biochemistry, Tufts University School of Medicine) against rhTS, rhDHFR, *E. coli* TS and *E. coli* DHFR; Dr. Sherry F. Queener (Department of Pharmacology and Toxicology, Indiana University School of Medicine) against rat liver (rl)DHFR, *P. carinii* DHFR, *T. gondii* DHFR, and *M. avium* DHFR; Dr. Vivian Cody (Hauptman-Woodward Medical Research Institute).

Table 13. Inhibition concentration (IC₅₀, μM) against isolated TS and DHFR ^a of **285-294**

Compound	TS (μM)			DHFR (μM)		
	human ^b	<i>E. coli</i> ^b	<i>T. gondii</i> ^c	human ^d	<i>E. coli</i> ^e	<i>T. gondii</i> ^c
285	>29(0)	>29(0)	>29(0)	35	0.035	1.4
286	>24(0)	>24(0)	>24(0)	>29(38)	0.044	1.5
287	>25(19)	>25(0)	>25(0)	30	0.18	0.13
288	>25(10)	>25(10)	>25(0)	>30(25)	0.09	0.2
289	>22(7)	>22(0)	>22(0)	10	0.09	0.29
290	>23(38)	>23(0)	>23(0)	27	0.081	1.3
291	22	>22(15)	>22(0)	>26(39)	0.16	2.1
292	>24(31)	>24(0)	>24(0)	>29(17)	0.044	2.9
293	>23(41)	>23(24)	>23(33)	>28(10)	0.084	0.34
294	>2.4(0)	>2.4(0)	>2.4(0)	>29(40)	0.0087	0.26
Pemetrexed^g	9.5	76	2.8	6.6	230	0.43
MTX	nd	nd	nd	0.022	0.0045	0.025
PDDF^h	0.085	0.017	0.17	2.1	63	0.11
Raltitrexed	0.17	1.9	0.36	11	22	2.2
Trimethoprim	nd	nd	nd	>50	0.01	6.8

^a The percent inhibition was determined at a minimum of four inhibitor concentrations within 20% of the

50% point. The standard deviations for determination of 50% points were within ± 10% of the value given.

^b Kindly provided by Dr. Frank Maley, New York State Department of Health. ^c Kindly provided by Dr.

Karen Anderson, Yale University, New Haven CT. ^d Kindly provided by Dr. J. H. Freisheim, Medical

College of Ohio, Toledo, OH. ^e Kindly provided by Dr. R. L. Blakley, St. Jude Children's hospital, Memphis TN. nd = not determined. ^g Kindly provided by Dr. Chuan Shih, Eli Lilly and Co. ^h Kindly provided by Dr. M. G. Nair, University of South Alabama.

Table 14. Inhibitory concentrations (IC₅₀, μM) against isolated DHFR^a and selectivity ratios^b of **285-294**

Compound	Inhibition concentration (IC ₅₀ , μM)				Selectivity ratio (IC ₅₀ /IC ₅₀)		
	<i>P. carinii</i>	<i>T. gondii</i>	<i>M. avium</i>	rat liver	rl/pc	rl/tg	rl/ma
285	6.7	2.7	0.11	1.4	0.21	0.52	12.73
286	7.3	3.2	0.086	8.6	1.18	2.69	100
287	1.9	0.63	0.15	0.88	0.46	1.4	5.87
288	5.2	2.4	0.24	4.9	0.94	2.04	20.42
289	1.7	0.25	0.23	0.33	0.19	1.32	1.43
290	1.63	0.282	0.022	1.64	1	5.82	73.80
291	5.9	0.99	0.43	1.8	0.31	1.85	4.19
292	4.9	3.4	0.09	7.1	1.45	2.09	78.89
293	4.4	5.1	0.41	5	1.14	0.98	12.2
294	10.2	2.99	1.35	3	0.29	1	2.22
TMQ	0.042	0.01	0.0015	0.003	0.07	0.3	2
TMP	12	2.8	0.3	180	14	65	610

^a These assays were carried out at 37 °C under conditions of substrate (90 μM dihydrofolic acid) and

cofactor (119 μM NADPH) in the presence of 150 mM KCl.⁹ ^b Selectivity Ratios [(IC₅₀ rIDHFR)/(IC₅₀ pcDHFR), (IC₅₀ rIDHFR)/(IC₅₀ tgDHFR), and (IC₅₀ rIDHFR)/(IC₅₀ maDHFR)]

Table 15. Inhibitory Concentrations of **301** (IC₅₀ in μM) against TS and DHFR.^a

compound	TS(μM)			DHFR(μM)		
	human ^b	<i>E. coli</i> ^b	<i>T. gondii</i> ^c	human ^d	<i>E. coli</i> ^e	<i>T. gondii</i> ^c
PDDF ^f	0.072	0.027	0.09	nd	Nd	nd
296 ^g	0.085	0.085	nd	nd	Nd	nd
297 ^h	0.042	nd	nd	2.2	Nd	nd
298	0.26	0.82	1.7	>20(35)	15	1.4
299	0.8	0.85	3.7	>20(24)	>20(38)	1.8
300	0.068	0.017	0.14	0.09	0.4	0.02
301	0.034	0.05	0.17	0.1	0.4	0.01
PMX ⁱ	9.5	76	2.8	6.6	2300	0.43
MTX	Nd	nd	nd	0.022	0.0066	0.022

^a The percent inhibition was determined at a minimum of four inhibitor concentrations within 20% of the 50% point. The standard deviations for determination of 50% points were within ± 10% of the value given.

^b Kindly provided by Dr. Frank Maley, New York State Department of Health. ^c Kindly provided by Dr. Karen Anderson, Yale Univerisy, New Haven CT. ^d Kindly provided by Dr. J. H. Freisheim, Medical College of Ohio, Toledo, OH. ^e Kindly provided by Dr. R. L. Blakley, St. Jude Children's hospital, Memphis TN. ^f Kindly provided by Dr. M. G. Nair, University of South Alabama. ^g Kindly provided by Dr. J. J. McGuire, Roswell Park Cancer Institute, Buffalo, NY. ^h Data derived from ref 20. ⁱ Kindly provided by Dr. Chuan Shih, Eli Lilly and Co. nd = not determined

Table 16. Inhibition concentration (IC₅₀, μM) against isolated TS and DHFR ^a of 304-

311

compound	TS (μM)			DHFR (μM)		
	human ^b	<i>E. coli</i> ^b	<i>T.gondi</i> ^c	human ^d	<i>E. coli</i> ^e	<i>T.gondii</i> ^c
304	0.08	0.06	0.096	0.95	>19 (43)	0.19
305	3.8	22	14	>32 (12)	>3.2 (0)	>3.2 (41)
306	0.32	1.2	1.2	> 2.8 (0)	> 2.8 (0)	> 2.8 (44)
307	1.1	2.1	1.9	>2.5 (0)	>2.5 (0)	1.8
308	12	> 23(38)	> 38 (21)	> 2.7 (0)	> 2.7 (0)	2.1
309	0.46	2.3	2.1	> 2.7 (0)	> 2.7 (0)	2.2
310	1.3	10	6.3	> 30 (23)	> 3.0 (0)	3.0
311	0.35	2.3	2.5	> 28 (0)	> 2.8 (0)	> 2.8 (44)
Pemetrexed^g	9.5	76	2.8	6.6	230	0.43
PDDF^j	0.085	0.019	0.43	1.9	23	0.22
MTX	nd	nd	nd	0.02	0.0088	0.033
Trimethoprim	nd	nd	nd	>340 (22)	0.01	6.8

^a The percent inhibition was determined at a minimum of four inhibitor concentrations within 20% of the 50% point. The standard deviations for determination of 50% points were within ± 10% of the value given.

^b Kindly provided by Dr. Frank Maley, New York State Department of Health. ^c Kindly provided by Dr. Karen Anderson, Yale University, New Haven CT. ^d Kindly provided by Dr. J. H. Freisheim, Medical College of Ohio, Toledo, OH. ^e Kindly provided by Dr. R. L. Blakley, St. Jude Children's hospital, Memphis TN. nd = not determined. ^g Kindly provided by Dr. Chuan Shih, Eli Lilly and Co. ^j Kindly provided by Dr. M. G. Nair, University of South Alabama.

Table 17. Inhibition concentration (IC₅₀, μM) against isolated TS and DHFR ^a of **317-319**.

Compound	TS (μM)			DHFR (μM)			
	huma ^b	<i>E. coli</i> ^b	<i>T. gondii</i> ^c	huma ^d	<i>E. coli</i> ^e	<i>T. gondii</i> ^c	DHFR Selectivity (rh/tg)
317	>1.4 (16)	>1.4 (24)	>1.4 (15)	17.0	> 17 (0)	0.017	1000
318	0.21	2.3	1.8	> 2.6 (0)	> 2.6 (0)	0.023	>113
319	0.23	>2.1 (25)	1.1	2.2	> 25 (17)	0.02	110
PMX ⁱ	9.5	76	2.8	6.6	230	0.43	15
PDDF ^j	0.085	0.019	0.43	1.9	23	0.22	8.6
MTX	nd	Nd	nd	0.02	0.0088	0.033	0.6
Trimethop rim	nd	Nd	nd	>340 (22)	0.01	6.8	>50

^aThe percent inhibition was determined at a minimum of four inhibitor concentrations within 20% of the 50% point. The standard deviations for determination of 50% points were within ± 10% of the value given.

^b Kindly provided by Dr. Frank Maley, New York State Department of Health. ^c Kindly provided by Dr. Karen Anderson, Yale Univerisy, New Haven CT. ^d Kindly provided by Dr. J. H. Freisheim, Medical College of Ohio, Toledo, OH. ^e Kindly provided by Dr. R. L. Blakley, St. Jude Children's hospital, Memphis TN. nd = not determined. ⁱ Kindly provided by Dr. Chuan Shih, Eli Lilly and Co. ^j Kindly provided by Dr. M. G. Nair, University of South Alabama.

Table 18. Inhibition concentration (IC₅₀ in μM) against TS and DHFR^a of 324-330

compound	TS (μM)			DHFR(μ M)		
	human ^b	<i>E. coli</i> ^b	<i>T. gondii</i> ^c	human ^d	<i>E. coli</i> ^e	<i>T. gondii</i> ^c
324	>18(4 2)	>18(32)	>18(24)	0.44	>22(15)	0.11
325	>18(1 4)	>18(9)	>18(14)	21	>210(24)	1.7
326	>17(3 1)	>17(3)	>17(16)	2.1	>21(0)	0.17
327	>17(3 6)	>17(17)	>17(33)	2.0	>20(0)	0.14
328	>17(3 8)	>17(17)	>17(22)	1.0	>20(0)	0.01
329	14	>16(17)	0.16	0.24	>19(21)	0.019
330	7.0	15	5.0	0.23	>19 (30)	0.019
MTX	20	>18(12)	27	0.022	0.0066	0.019
Pemetrexed^f	9.5	76	2.8	6.6	230	0.43
PDDF^g	0.085	0.019	0.43	1.9	23	0.22
Pyrimethamine	nd	nd	nd	6.0	2.0	0.2
Trimethoprim	nd	nd	nd	0.038	0.02	2.9

^a The percent inhibition was determined at a minimum of four inhibitor concentrations within 20% of the 50% point. The standard deviations for determination of 50% points were within ± 10% of the value given. nd = not determined. Numbers in parentheses indicate the % inhibition at the concentration tested. ^b Kindly provided by Dr. Frank Maley, New York State Department of Health. ^c Kindly provided by Dr. Karen Anderson, Yale University, New Haven CT. ^d Kindly provided by Dr. J. H. Freisheim, Medical College of Ohio, Toledo, OH. ^e Kindly provided by Dr. R. L. Blakley, St. Jude Children's hospital, Memphis TN. ^f Kindly provided by Dr. Chuan Shih, Eli Lilly and Co. ^g Kindly provided by Dr. M. G. Nair, University of South Alabama

Table 19. IC₅₀s (nM) for thienopyrimidine compounds **324** to **330** in cell proliferation inhibition of RFC- and FR-expressing cell lines.

Antifolate (number CH ₂ , n)	hRFC		hFR α		hFR β		hRFC/ FR α		hRFC/ FR α	
	PC43-10	R2	RT16	RT16 (+FA)	D4	D4 (+FA)	KB	KB (+FA)	IGROV1	IGROV1 (+FA)
324 (n=2)	>1000	>1000	>1000	>1000	>1000	>1000	>1000	>1000	>1000	>1000
325 (n=3)	>1000	>1000	13(3.4)	>1000	112(12)	>1000	23(5.5)	>1000	4.7(1.9)	>1000
326 (n=4)	>1000	>1000	9(2.9)	>1000	20(3.9)	>1000	4.9(1.3)	>1000	5.9(1.9)	>1000
327 (n=5)	>1000	>1000	56(9.8)	>1000	56(13)	>1000	132(23)	>1000	25(1.7)	>1000
328 (n=6)	>1000	>1000	108(17)	>1000	364(46)	>1000	310(54)	>1000	334(59)	>1000
329 (n=7)	>1000	>1000	>1000	>1000	>1000	>1000	>1000	>1000	>1000	>1000
330 (n=8)	>1000	>1000	>1000	>1000	>1000	>1000	>1000	>1000	>1000	>1000
Methotrexate	12(1.1)	216(8.7)	114(31)	461(62)	106(11)	211(43)	6.0(0.6)	20(2.4)	21(3.4)	22(2.1)
Pemetrexed	138(13)	894(93)	42(9)	388(68)	60(8)	254(78)	68(12)	327(103)	102(25)	200(18)
Raltitrexed	6.3(1.3)	>1000	15(5)	>1000	22(10)	746(138)	5.9(2.2)	22(5)	12.6(3.3)	20(4.3)
Lometrexol	12(2.3)	>1000	12(8)	188(41)	2.6(1.0)	275(101)	1.2(0.6)	31(7)	3.1(0.9)	16(6)
Trimetrexate	25(7.3)	6.7(1.3)	13(1)	4.1(1)	11(4.2)	6.1(1.9)	58(18)	155(38)	12(4)	8.6(1.9)
OSI-7904	11(3.3)	>1000	277(81)	>1000	52(12)	>1000	5.8(3.5)	32(15)	5.2(1.7)	6.9(1.6)

Table 20. Inhibition concentration (IC₅₀ in μM) against TS and DHFR^a of **335-38**.

compound	TS (μM)			DHFR(μM)		
	human ^b	<i>E. coli</i> ^b	<i>T. gondii</i> ^c	human ^d	<i>E. coli</i> ^e	<i>T. gondii</i> ^c
335	>19(27)	>19(0)	>19(0)	2.3	>23(0)	0.046
336	>18(21)	>18(10)	>18(0)	4.0	>22(0)	0.15
337	>19(19)	>19(19)	>19(0)	2.3	>23(14)	0.046
338	>19(35)	>19(20)	>19(16)	2.3	>23(19)	0.046
MTX	20	>18(12)	27	0.02	0.0073	0.022
Pemetrexed^f	9.5	76	2.8	6.6	230	0.43
PDDF^g	0.085	0.019	0.018	1.9	23	0.22
Pyrimethamine	nd	nd	nd	6.0	2.0	0.2
Trimethoprim	nd	nd	nd	0.038	0.02	2.9

^a The percent inhibition was determined at a minimum of four inhibitor concentrations within 20% of the 50% point. The standard deviations for determination of 50% points were within ± 10% of the value given. nd = not determined. Numbers in parentheses indicate the % inhibition at the concentration tested. ^b Kindly provided by Dr. Frank Maley, New York State Department of Health. ^c Kindly provided by Dr. Karen Anderson, Yale University, New Haven CT. ^d Kindly provided by Dr. J. H. Freisheim, Medical College of Ohio, Toledo, OH. ^e Kindly provided by Dr. R. L. Blakley, St. Jude Children's hospital, Memphis TN. ^f Kindly provided by Dr. Chuan Shih, Eli Lilly and Co. ^g Kindly provided by Dr. M. G. Nair, University of South Alabama

Table 21. FRα binding percentages and IC₅₀s (nM) for thienopyrimidine compounds **335-338** in cell proliferation inhibition of RFC-, PCFT- and FR-expressing cell lines.

Antifolate	FR α binding %	RFC		hFR α		RFC/ FR α		RFC/ FR α		PCFT	
		PC43-10	R2	RT16	RT16 (+FA)	KB	KB (+FA)	IGROV 1	IGROV1 (+FA)	R2/PCFT4	R2/VC
335	19.4	N	N	25	N	N	nd	nd	nd	>1000	>1000
336	16.7	N	N	13	N	N	nd	nd	nd	>1000	>1000
337	35.2	N	N	66	N	N	nd	nd	nd	>1000	>1000
338	36.1	N	N	60	N	N	nd	nd	nd	>1000	>1000
Methotrexate	nd	12(1.1)	216 (8.7)	114 (31)	461(62)	6.0 (0.6)	20(2.4)	21(3.4)	22(2.1)	120.5(16.8)	>1000
Pemetrexed	nd	138(13)	894 (93)	42(9)	388(68)	68(12)	327 (103)	102(25)	200(18)	13.2(2.4)	974.0(18.1)
Raltitrexed	nd	6.3(1.3)	>1000	15(5)	>1000	5.9 (2.2)	22(5)	12.6 (3.3)	20(4.3)	99.5(11.4)	>1000
Lometrexol	nd	12(2.3)	>1000	12(8)	188(41)	1.2 (0.6)	31(7)	3.1(0.9)	16(6)	248.0(18.2)	>1000nM
Trimetrexate	nd	25(7.3)	6.7 (1.3)	13(1)	4.1(1)	58(18)	155(38)	12(4)	8.6(1.9)	nd	nd

FR experiments, cytotoxicity assays were performed in the absence and presence of 200 nM folic acid (FA). The data shown are mean values from three experiments (plus/minus SEM in parentheses). N = not active. nd = not determined. IC₅₀ data of classical antifolate compounds, methotrexate, pemetrexed, raltitrexed, lometrexol, trimetrexate were previously published from our laboratory. For the FR α binding experiments, 250 nM of unlabeled ligand was used as competitor with ³H-folic acid (50 nM) for binding. The numbers shown represent the percent of ³H-bound normalized to cell number. The protocol is based on our previous publications.

Table 22. Inhibition concentration (IC₅₀ in μM) against TS and DHFR^a of **333**.

compound	TS (μM)			DHFR(μM)		
	human ^b	<i>E. coli</i> ^b	<i>T. gondii</i> ^c	human ^d	<i>E. coli</i> ^e	<i>T. gondii</i> ^c
333	6.8	>17 (23)	17	2.0	>20 (14)	0.063
MTX	20	>18(12)	27	0.02	0.0073	0.022
Pemetrexed^f	9.5	76	2.8	6.6	230	0.43
PDDF^g	0.085	0.019	0.018	1.9	23	0.22
Pyrimethamine	nd	nd	nd	6.0	2.0	0.2
Trimethoprim	nd	nd	nd	0.038	0.02	2.9

^a The percent inhibition was determined at a minimum of four inhibitor concentrations within 20% of the 50% point. The standard deviations for determination of 50% points were within ± 10% of the value given. nd = not determined. Numbers in parentheses indicate the % inhibition at the concentration tested. ^b Kindly provided by Dr. Frank Maley, New York State Department of Health. ^c Kindly provided by Dr. Karen Anderson, Yale University, New Haven CT. ^d Kindly provided by Dr. J. H. Freisheim, Medical College of Ohio, Toledo, OH. ^e Kindly provided by Dr. R. L. Blakley, St. Jude Children's hospital, Memphis TN. ^f Kindly provided by Dr. Chuan Shih, Eli Lilly and Co. ^g Kindly provided by Dr. M. G. Nair, University of South Alabama

Table 23. FR α binding percentages and IC₅₀s (nM) for thienopyrimidine compounds **333** in cell proliferation inhibition of RFC-, PCFT- and FR-expressing cell lines.

Antifolate	FR α binding %	RFC		hFR α		RFC/ FR α		RFC/ FR α		PCFT	
		PC43-10	R2	RT16	RT16 (+FA)	KB	KB (+FA)	IGROV1	IGROV1 (+FA)	R2/PCFT4	R2/VC
333	nd	>1000	>1000	3.1	nd	2.1	nd	12.8	nd	>1000	>1000
Methotrexate	nd	12 (1.1)	216 (8.7)	114 (31)	461(62)	6.0 (0.6)	20 (2.4)	21 (3.4)	22 (2.1)	120.5 (16.8)	>1000
Pemetrexed	nd	138 (13)	894 (93)	42 (9)	388(68)	68 (12)	327 (103)	102 (25)	200 (18)	13.2 (2.4)	974.0 (18.1)
Raltitrexed	nd	6.3 (1.3)	>1000	15 (5)	>1000	5.9 (2.2)	22(5)	12.6 (3.3)	20 (4.3)	99.5 (11.4)	>1000
Lometrexol	nd	12 (2.3)	>1000	12 (8)	188(41)	1.2 (0.6)	31(7)	3.1 (0.9)	16(6)	248.0 (18.2)	>1000nM
Trimetrexate	nd	25 (7.3)	6.7 (1.3)	13 (1)	4.1(1)	58 (18)	155 (38)	12 (4)	8.6 (1.9)	nd	nd

FR experiments, cytotoxicity assays were performed in the absence and presence of 200 nM folic acid (FA). The data shown are mean values from three experiments (plus/minus SEM in parentheses). N = not active. nd = not determined. IC₅₀ data of classical antifolate compounds, methotrexate, pemetrexed, raltitrexed, lometrexol, trimetrexate, **2 and 3**, were previously published from our laboratory.⁹ For the FR α binding experiments, 250 nM of unlabeled ligand was used as competitor with ³H-folic acid (50 nM) for binding. The numbers shown represent the percent of ³H-bound normalized to cell numbr. The protocol is based on our previous publications.